Publ. Astron. Soc. Japan (2019) 71(SP2), 1–124
doi: 10.1093/pasj/xxx000

CO Multi-line Imaging of Nearby Galaxies (COMING) IV. Overview of the Project

Kazuo SORAI, Nario KUNO, Kazuyuki MURAOKA, Yusuke MIYAMOTO, Hiroyuki KANEKO, Hiroyuki NAKANISHI, Naomasa NAKAI, Kazuki YANAGITANI, Takahiro TANAKA, Yuya SATO, Dragan SALAK, Michiko UMEI, Kana MOROKUMA-MATSUI, Naoko MATSUMOTO, Saeko UENO, Hsi-An PAN, Yuto NOMA, Tsutomu, T. TAKEUCHI, Moe YODA, Mayu KURODA, Atsushi YASUDA, Yoshiyuki YAJIMA, Nagisa OI, Shugo SHIBATA, Masumichi SETA, Yoshimasa WATANABE, Shoichiro KITA, Ryusei KOMATSUZAKI, Ayumi KAJIKAWA, Yu YASHIMA, Suchetha COORAY, Hiroyuki BAJI, Yoko SEGAWA, Takami TASHIRO, Miho TAKEDA, Nozomi KISHIDA, Takuya HATAKEYAMA, Yuto TOMIYASU and Chey SAITA

*E-mail: sorai@astro1.sci.hokudai.ac.jp

Received 2018 December 17; Accepted 2019 September 18

Supplementary data

Supplementary figures 1 – 134 show the background-subtracted infrared image in WISE $3.4\mu\mathrm{m}$ (a), integrated intensity map (b), first-degree moment map (c), and second-degree moment map (d) of $^{12}\mathrm{CO}\ (J=1-0)$, (e) integrated intensity map of $^{13}\mathrm{CO}\ (J=1-0)$, and (f) integrated intensity map of $\mathrm{C}^{18}\mathrm{O}\ (J=1-0)$ of all the observed galaxies. Panels (c) and (d) were not presented in 17 figures (for 19 galaxies), as described in subsection 6.1. Panel (e) is presented in 52 figures (for 54 galaxies), while panel (f) is only presented in three figures (for three galaxies), as also discussed in subsection 6.1. The observation beam size is shown in the bottom right or left corner of panels (b), (e), and (f). The white contours overlaid on panels (b), (e), and (f) depict the integrated intensity of $^{12}\mathrm{CO}\ (J=1-0)$. The magenta contours overlaid on panels (e) and (f) are the integrated intensity of $^{13}\mathrm{CO}\ (J=1-0)$ and $\mathrm{C}^{18}\mathrm{O}\ (J=1-0)$, respectively. The contours levels are indicated in each figure caption. The galaxies are shown in the order listed in table 1.

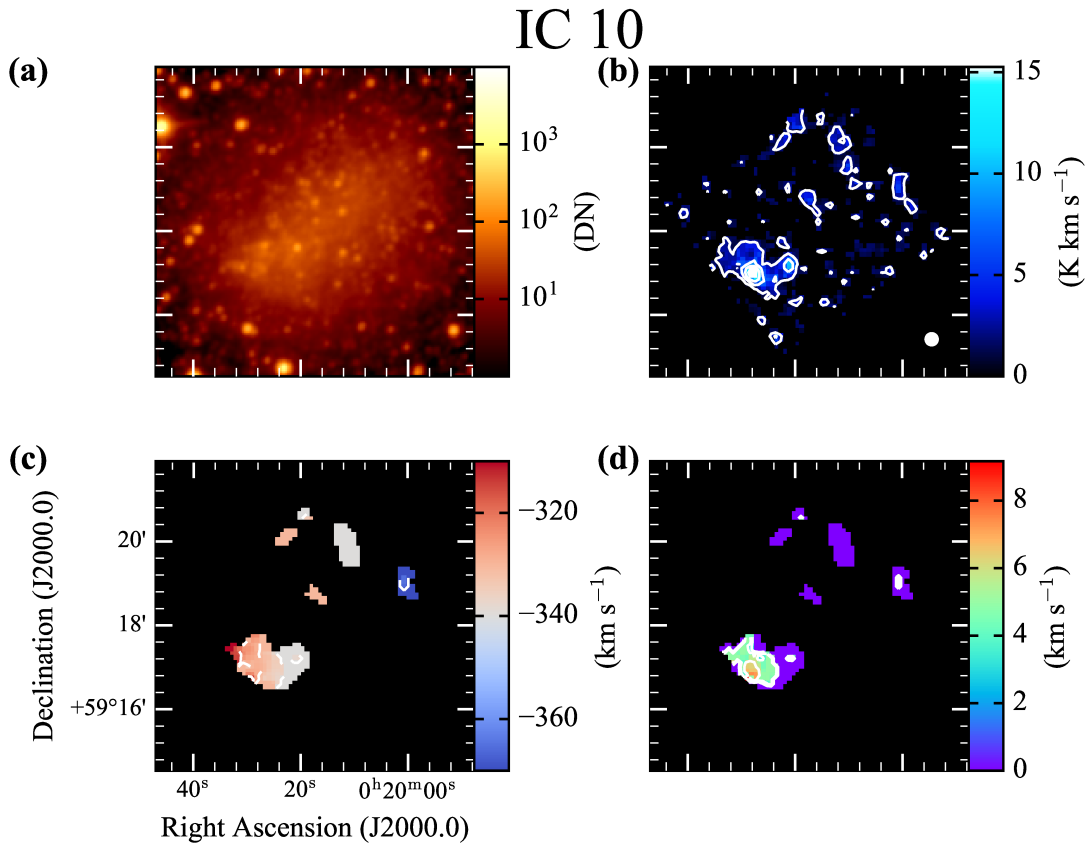

Supplementary fig. 1. Same as figure 12, but for IC 10. The contours are plotted at 10 %, 35 %, 60 %, and 85 % of the maximum intensity of $20.12\,\mathrm{K\,km\,s^{-1}}$ in (b) and in steps of $10\,\mathrm{km\,s^{-1}}$ in (c) and in steps of $2\,\mathrm{km\,s^{-1}}$ in (d).

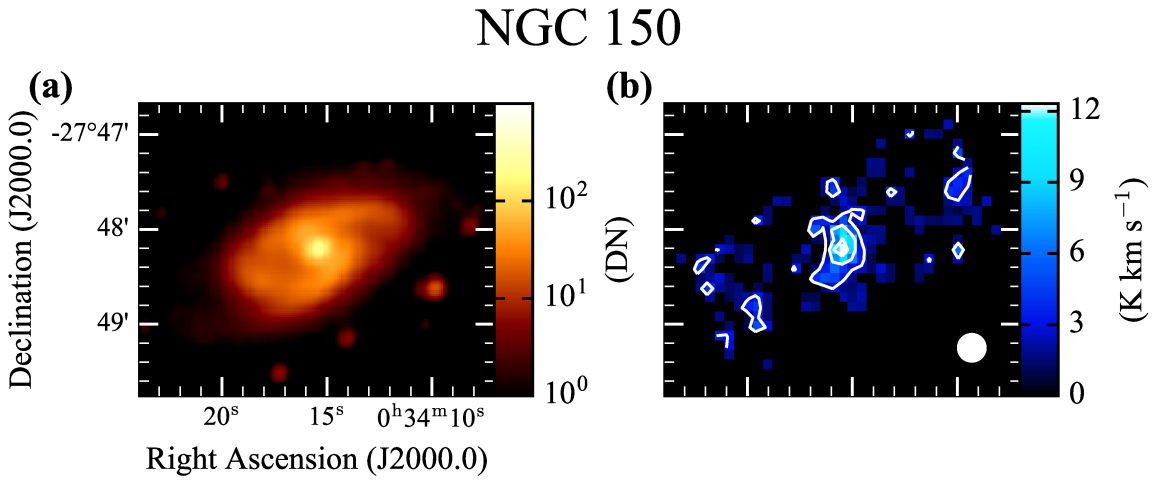

Supplementary fig. 2. Same as figure 12, but for NGC 150. The contours are plotted at 20 %, 50 %, and 80 % of the maximum intensity of $13.79\,\mathrm{K\,km\,s^{-1}}$ in (b). First- and second-degree moment maps are not presented, since no significant emission is detected after masking (see subsection 6.1).

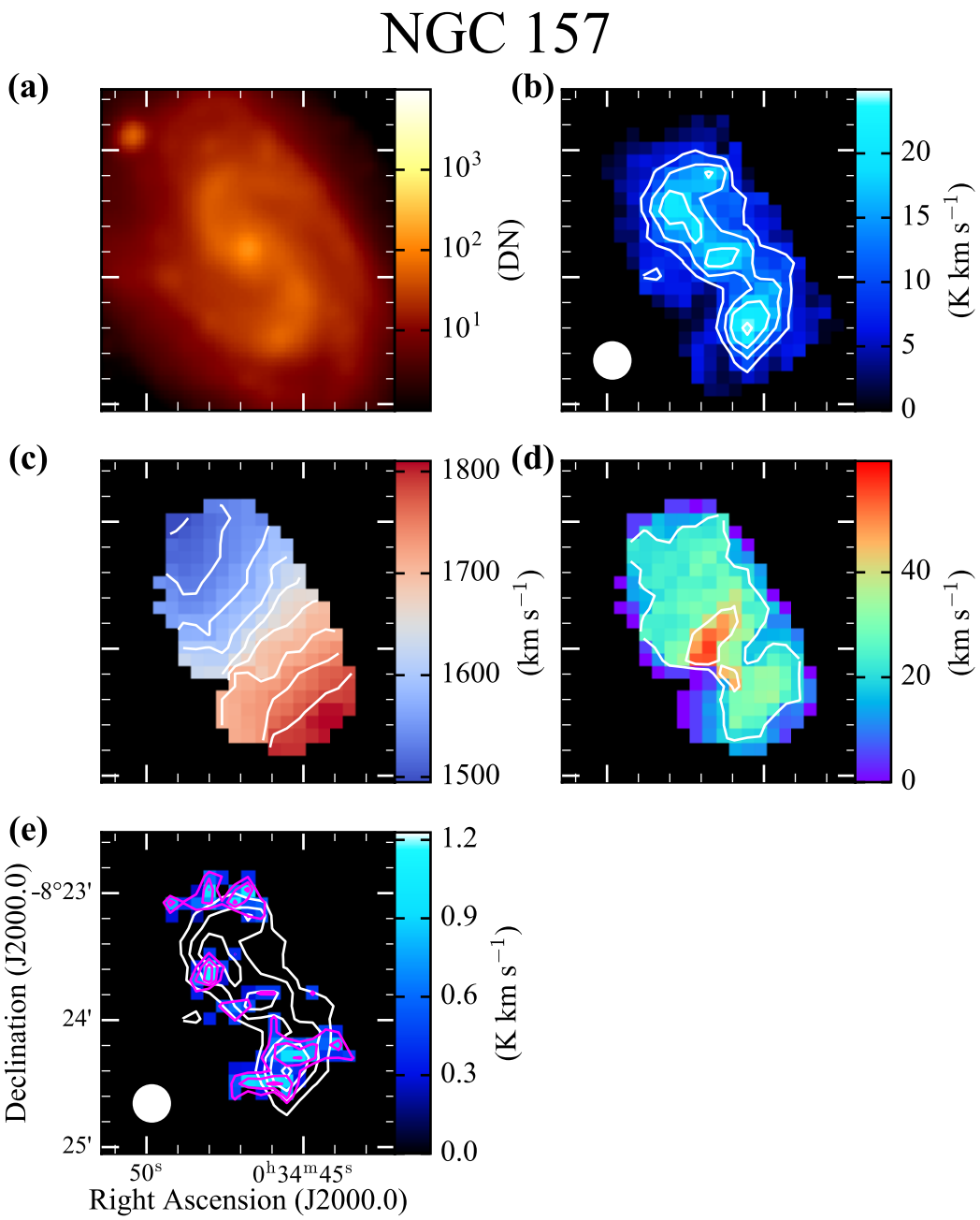

Supplementary fig. 3. Same as figure 12, but for NGC 157 and the OTF beam size is indicated as a white filled circle in the bottom left corner in panel (b). The contours are plotted at 35 %, 55 %, 75 %, and 95 % of the maximum intensity of $24.13\,\mathrm{K\,km\,s^{-1}}$ in (b) and (e) (*white*), in steps of $35\,\mathrm{km\,s^{-1}}$ in (c), in steps of $20\,\mathrm{km\,s^{-1}}$ in (d), and 35 %, 60 %, and 85 % of the maximum intensity of $1.13\,\mathrm{K\,km\,s^{-1}}$ in (e) (*magenta*).

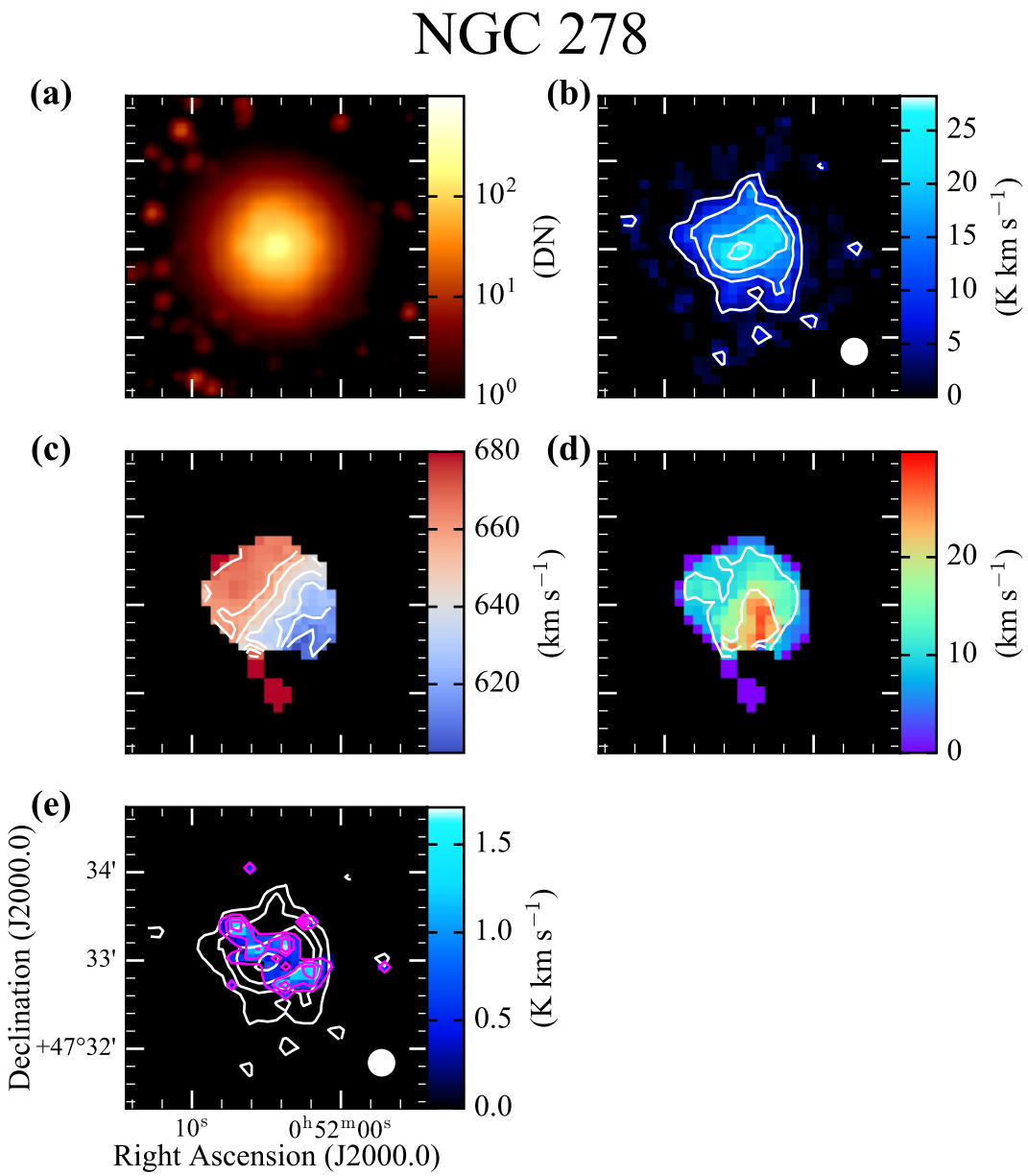

Supplementary fig. 4. Same as figure 12, but for NGC 278. The contours are plotted at 15 %, 40 %, 65 %, and 90 % of the maximum intensity of $27.24\,\mathrm{K\,km\,s^{-1}}$ in (b) and (e) (*white*), in steps of $10\,\mathrm{km\,s^{-1}}$ in (c) and (d), and at 15 %, 45 %, and 75 % of the maximum intensity of $1.67\,\mathrm{K\,km\,s^{-1}}$ in (e) (*magenta*).

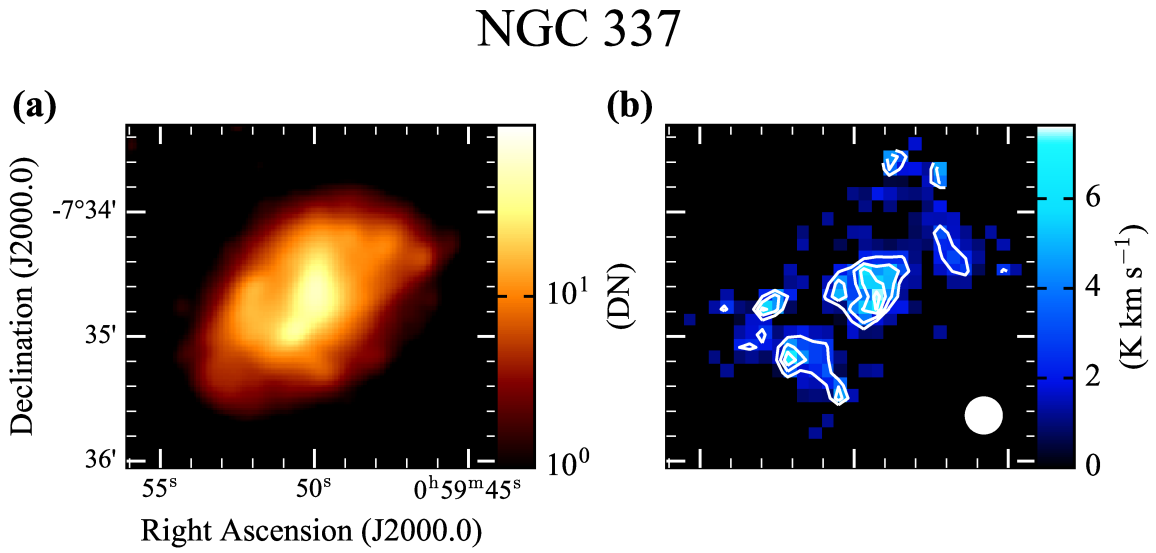

Supplementary fig. 5. Same as figure 12, but for NGC 337. The contours are plotted at 30 %, 50 %, 70 %, and 90 % of the maximum intensity of $7.46\,\mathrm{K\,km\,s^{-1}}$ in (b).

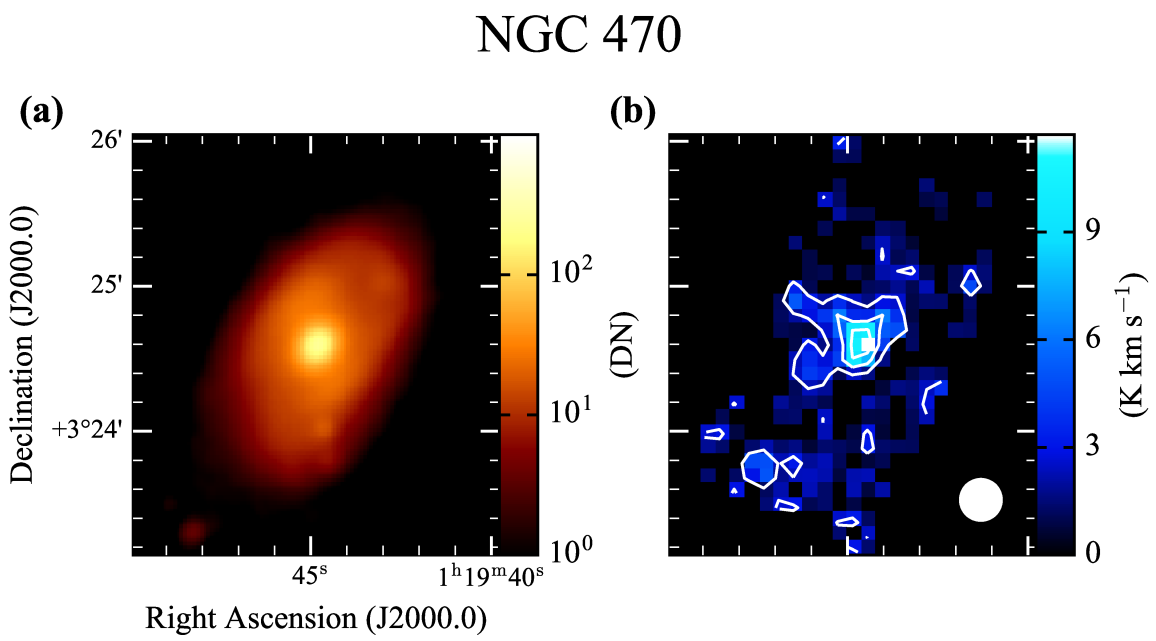

Supplementary fig. 6. Same as figure 12, but for NGC 470. The contours are plotted at 20 %, 50 %, and 80 % of the maximum intensity of $12.26\,\mathrm{K\,km\,s^{-1}}$ in (b).

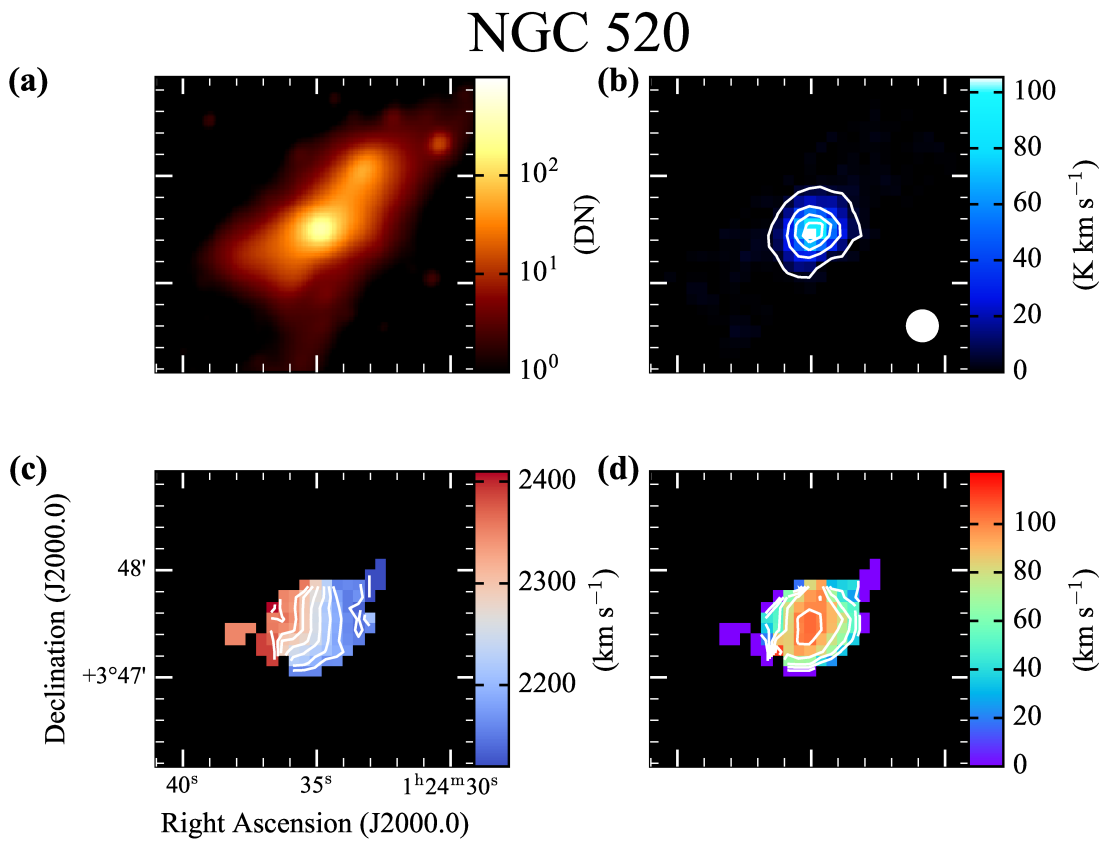

Supplementary fig. 7. Same as figure 12, but for NGC 520. The contours are plotted at 5 %, 30 %, 55 %, and 80 % of the maximum intensity of $105.56\,\mathrm{K\,km\,s^{-1}}$ in (b), in steps of $30\,\mathrm{km\,s^{-1}}$ in (c), and in steps of $20\,\mathrm{km\,s^{-1}}$ in (d).

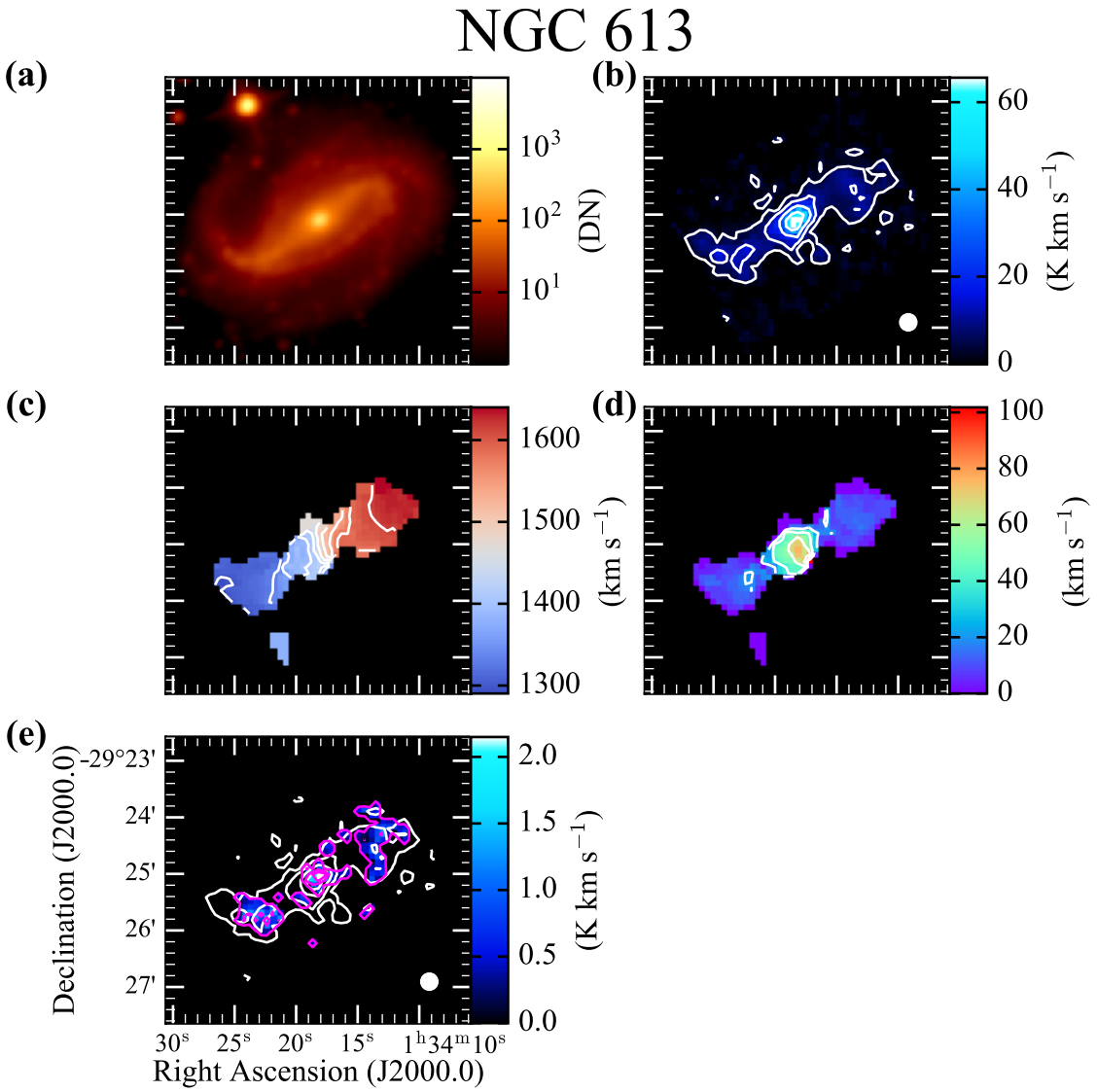

Supplementary fig. 8. Same as figure 12, but for NGC 613. The contours are plotted at 5 %, 15 %, 35 %, and 65 % of the maximum intensity of $78.03\,\mathrm{K\,km\,s^{-1}}$ in (b) and (e) (*white*), in steps of $35\,\mathrm{km\,s^{-1}}$ in (c), in steps of $20\,\mathrm{km\,s^{-1}}$ in (d), and at 5 %, 45 %, and 75 % of the maximum intensity of $2.62\,\mathrm{K\,km\,s^{-1}}$ in (e) (*magenta*).

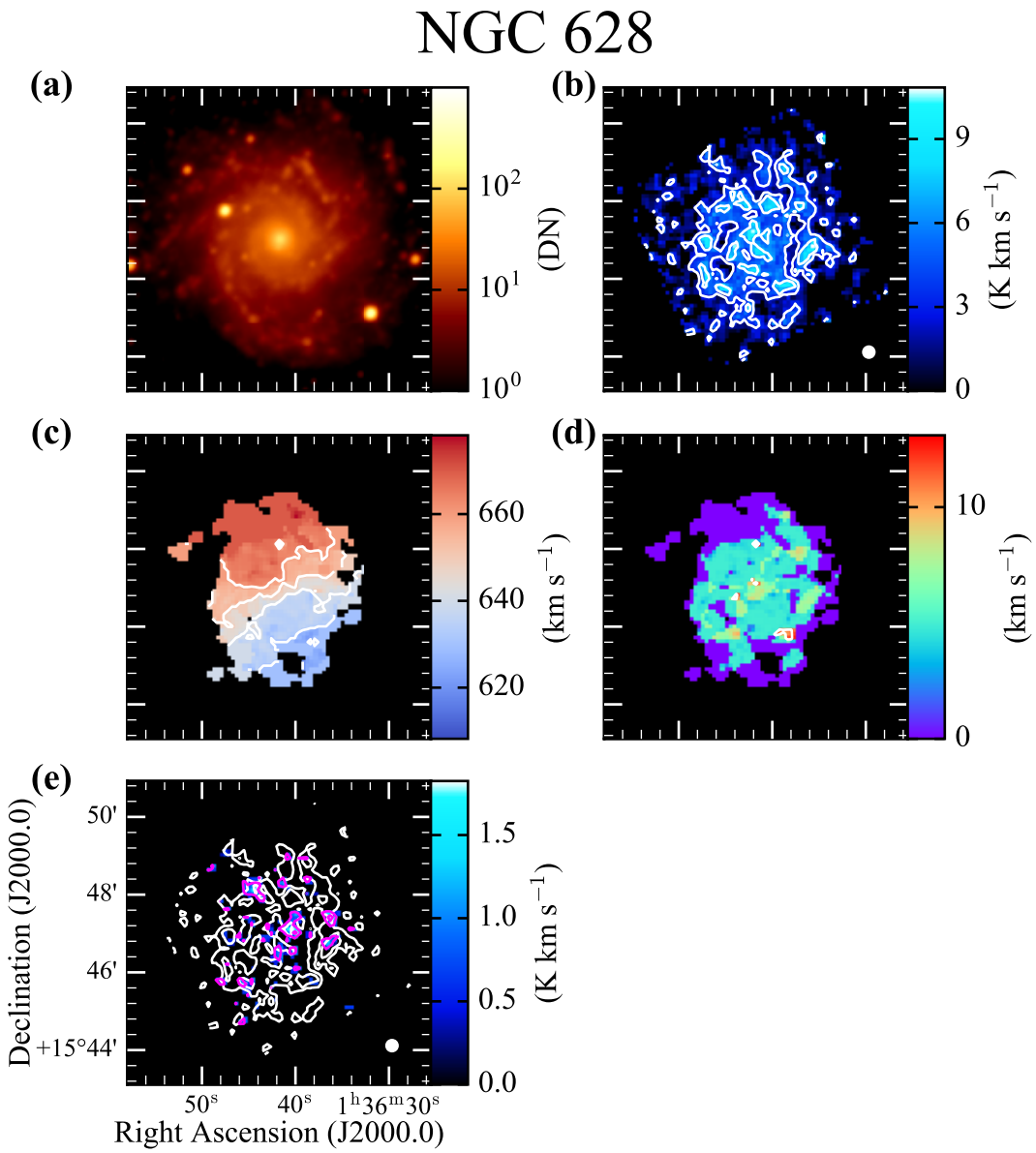

Supplementary fig. 9. Same as figure 12, but for NGC 628. The contours are plotted at 30 %and 60 %of the maximum intensity of $11.00\,\mathrm{K\,km\,s^{-1}}$ in (b) and (e) (*white*), in steps of $10\,\mathrm{km\,s^{-1}}$ in (c) and (d), and at 30 % and 80 % of the maximum intensity of $2.46\,\mathrm{K\,km\,s^{-1}}$ in (e) (*magenta*).

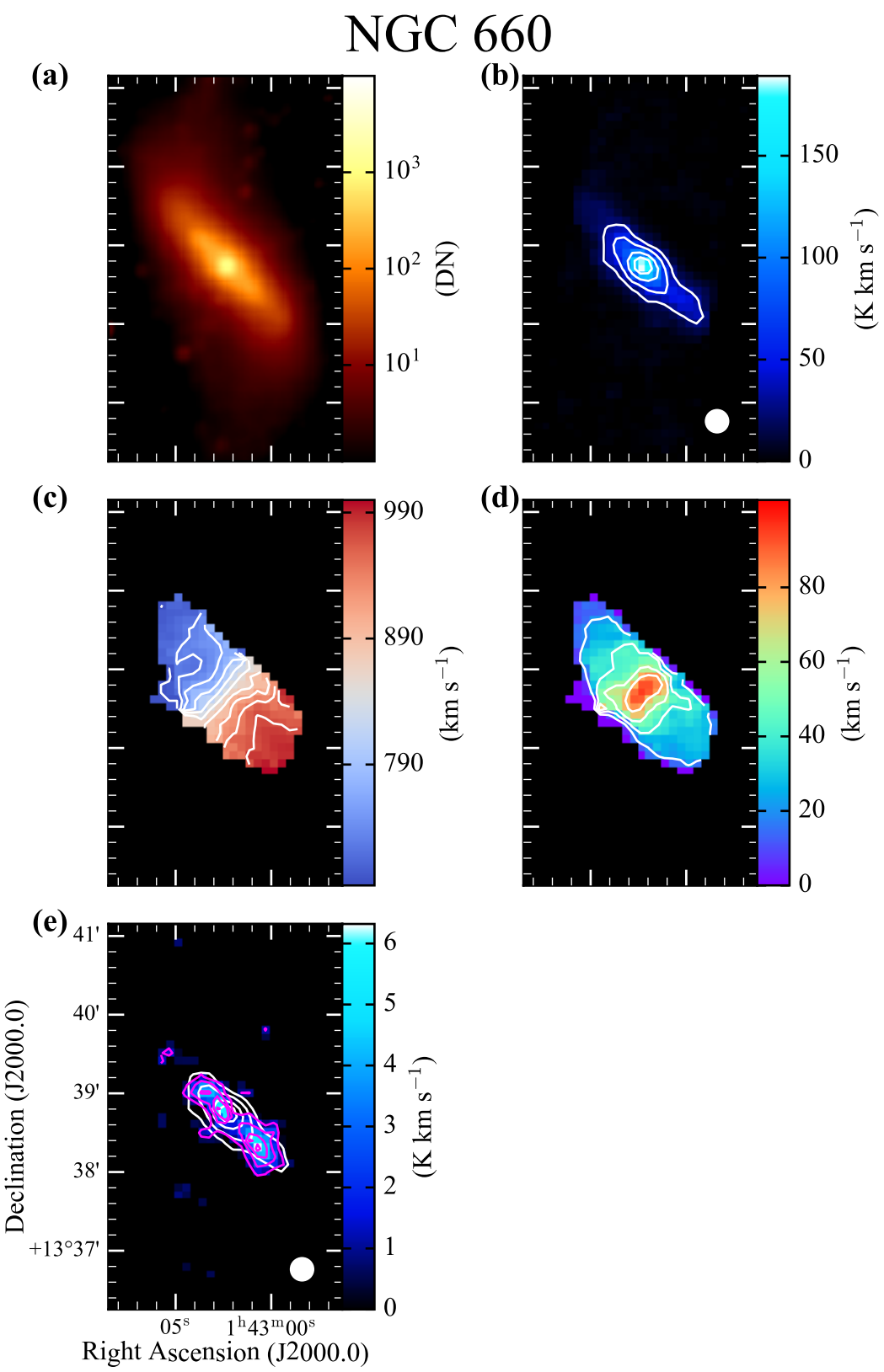

Supplementary fig. 10. Same as figure 12, but for NGC 660. The contours are plotted at 15 %, 30 %, 55 %, and 80 % of the maximum intensity of 187.78 K km s^{-1} in (b) and (e) (*white*), in steps of 30 km s^{-1} in (c), in steps of 20 km s^{-1} in (d), and at 15 %, 40 %, 65 %, and 90 % of the maximum intensity of 6.28 K km s^{-1} in (e) (*magenta*).

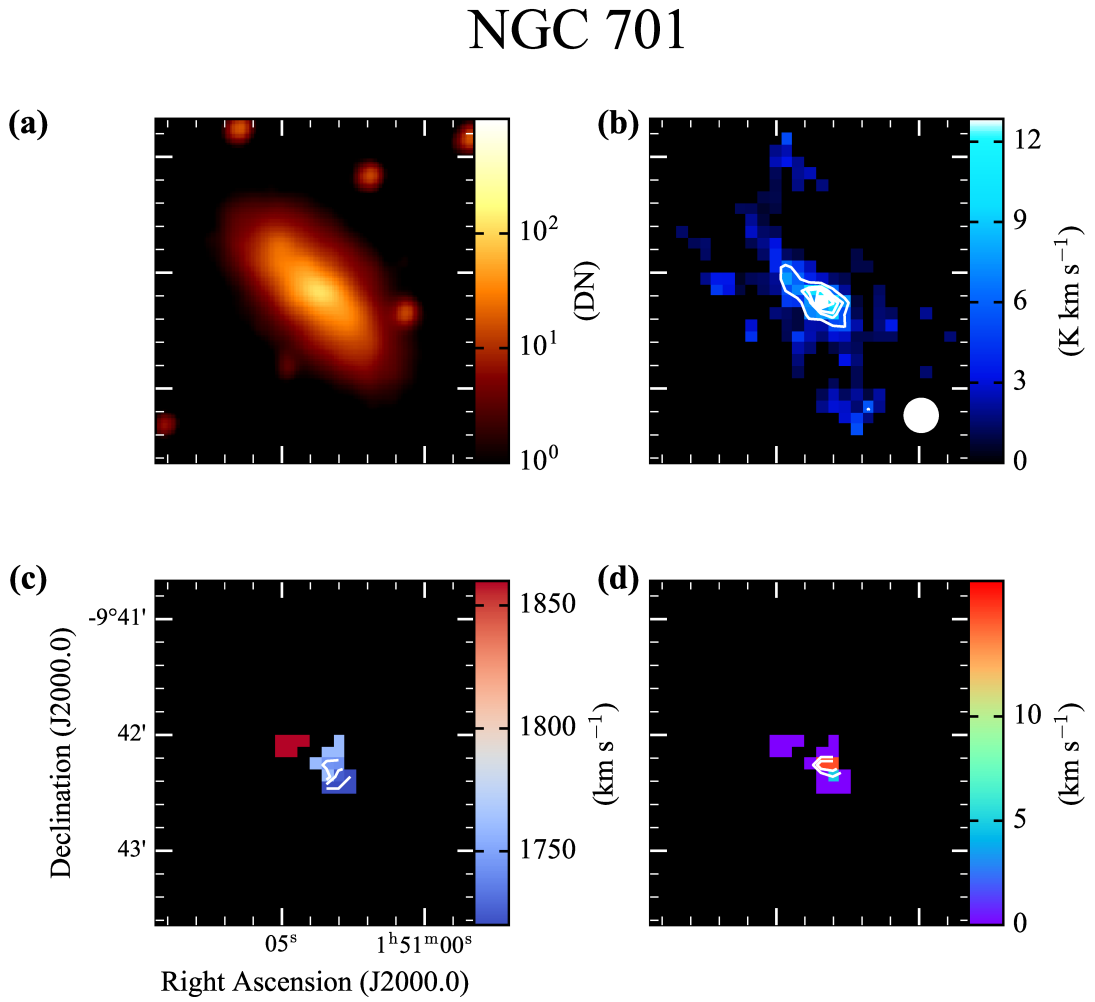

Supplementary fig. 11. Same as figure 12, but for NGC 701. The contours are plotted at 40 %, 60 %, 70 %, and 80 % of the maximum intensity of $13.63\,\mathrm{K\,km\,s^{-1}}$ in (b), in steps of $15\,\mathrm{km\,s^{-1}}$ in (c), and in steps of $5\,\mathrm{km\,s^{-1}}$ in (d).

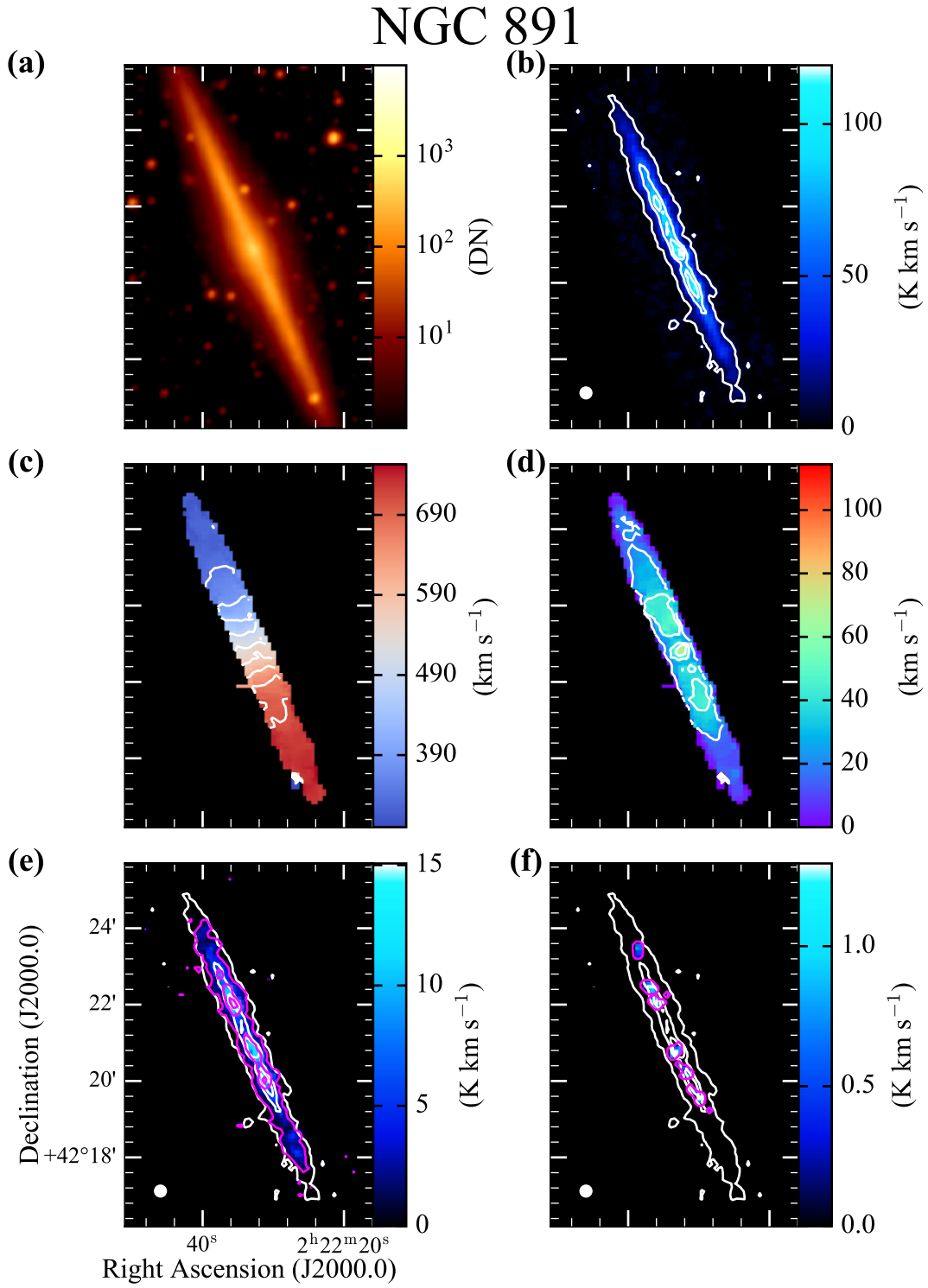

Supplementary fig. 12. Same as figure 12 (NGC 891). The contours are plotted at 5 %, 40 %, and 60 % of the maximum intensity of 152.45 K km s^{-1} in (b), (e), and (f) (*white*), in steps of 45 km s^{-1} in (c), in steps of 20 km s^{-1} in (d), at 5 %, 45 %, and 85 % of the maximum intensity of 16.53 K km s^{-1} in (e) (*magenta*), and at 5 % of the maximum intensity of 2.26 K km s^{-1} in ($C^{18}O$)f) (*magenta*).

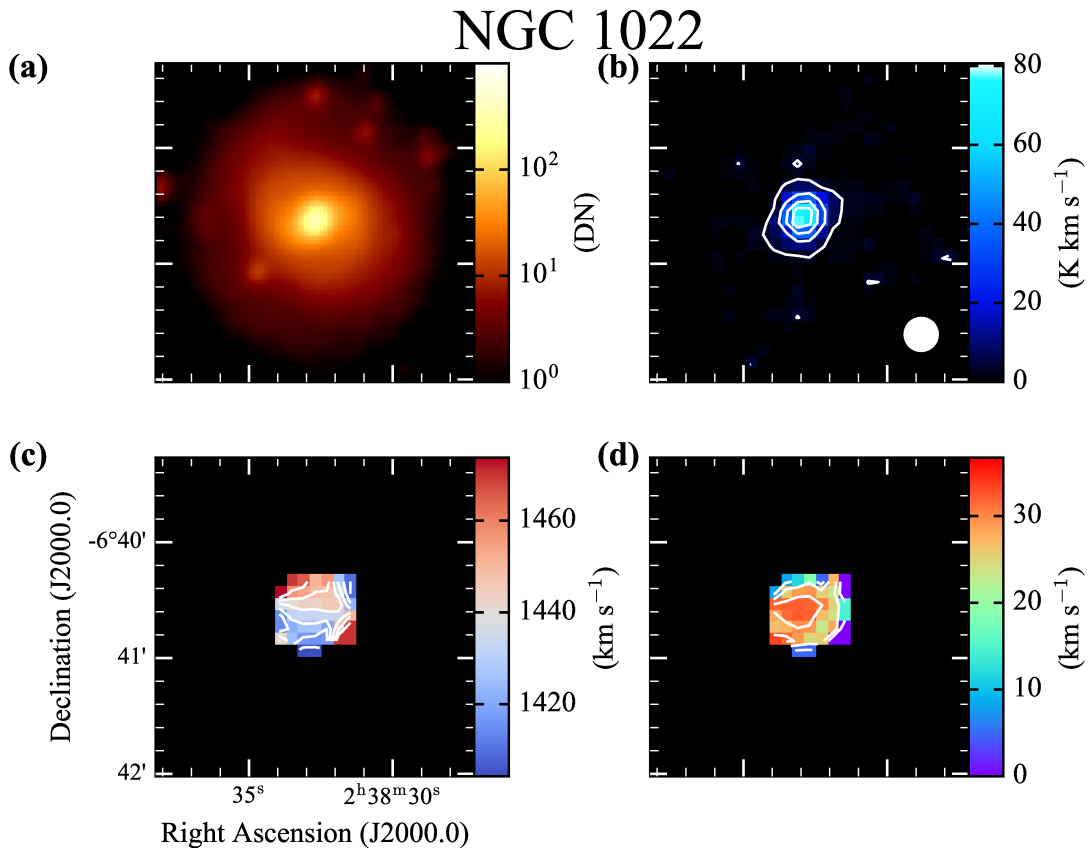

Supplementary fig. 13. Same as figure 12, but for NGC 1022. The contours are plotted at 5 %, 30 %, 55 %, and 80 % of the maximum intensity of $77.55\,\mathrm{K\,km\,s^{-1}}$ in (b) and in steps of $10\,\mathrm{km\,s^{-1}}$ in (c) and (d).

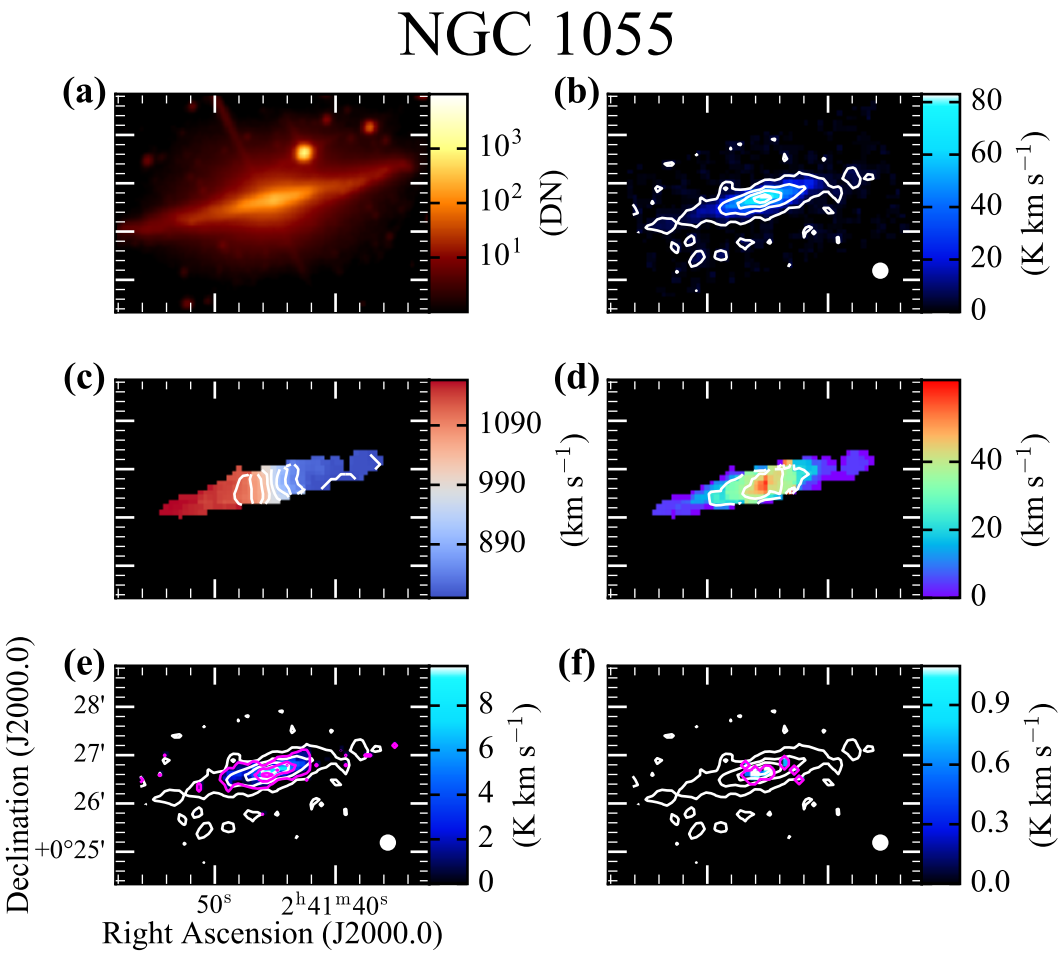

Supplementary fig. 14. Same as figure 12, but for NGC 1055. The contours are plotted at 5 %, 30 %, 55 %, and 80 % of the maximum intensity of $94.59\,\mathrm{K\,km\,s^{-1}}$ in (b), (e), and (f) (*white*), in steps of $40\,\mathrm{km\,s^{-1}}$ in (c), in steps of $20\,\mathrm{km\,s^{-1}}$ in (d), at 5 %, 45 %, and 85 % of the maximum intensity of $10.35\,\mathrm{K\,km\,s^{-1}}$ in (e) (*magenta*), and at 5 % of the maximum intensity of $1.59\,\mathrm{K\,km\,s^{-1}}$ in (f) (*magenta*).

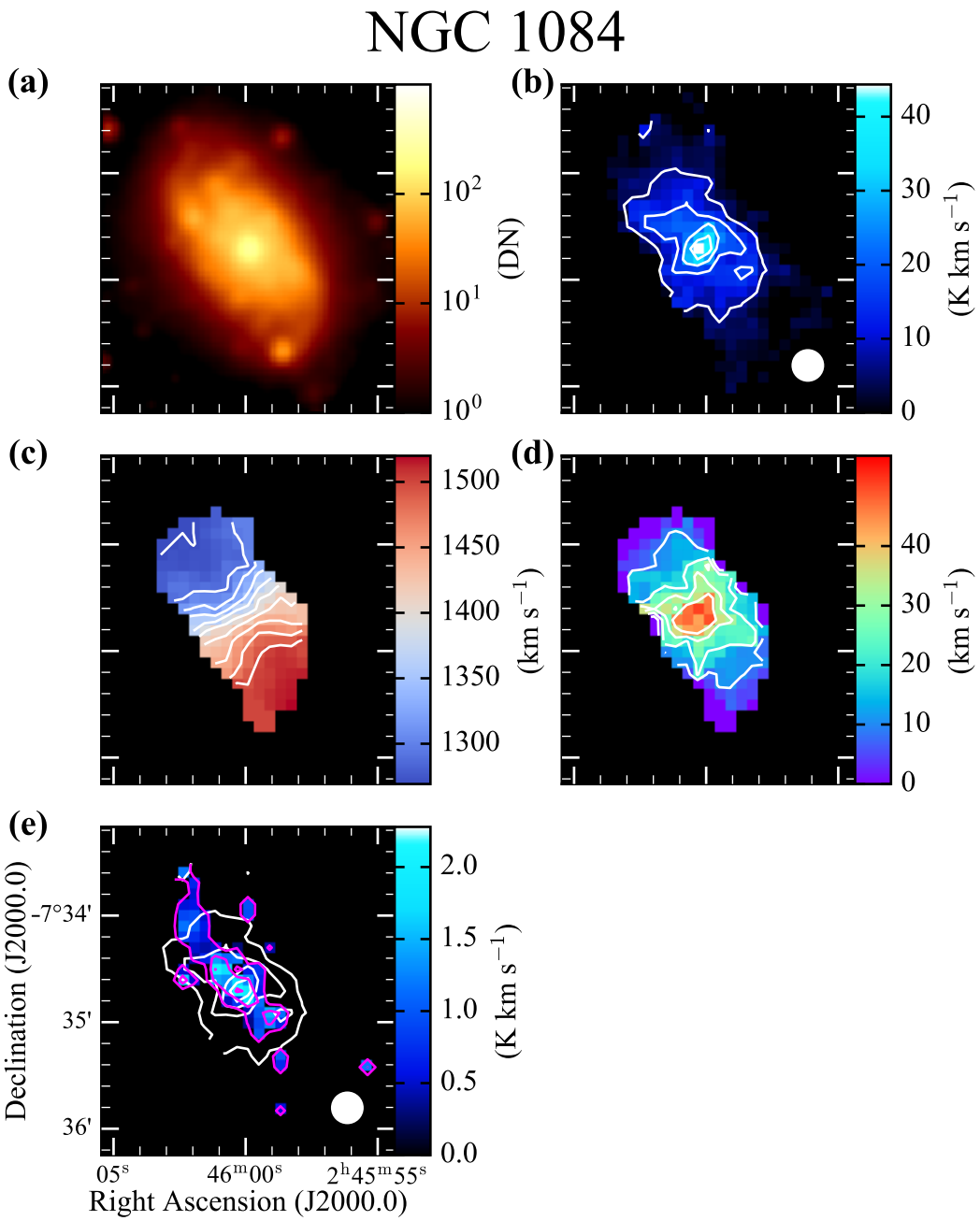

Supplementary fig. 15. Same as figure 12, but for NGC 1084. The contours are plotted at 15 %, 35 %, 55 %, and 75 % of the maximum intensity of 45.15 K km s^{-1} in (b) and (e) (*white*), in steps of 25 km s^{-1} in (c), in steps of 10 km s^{-1} in (d), and at 15 %, 55 %, and 95 % of the maximum intensity of 2.14 K km s^{-1} in (e) (*magenta*).

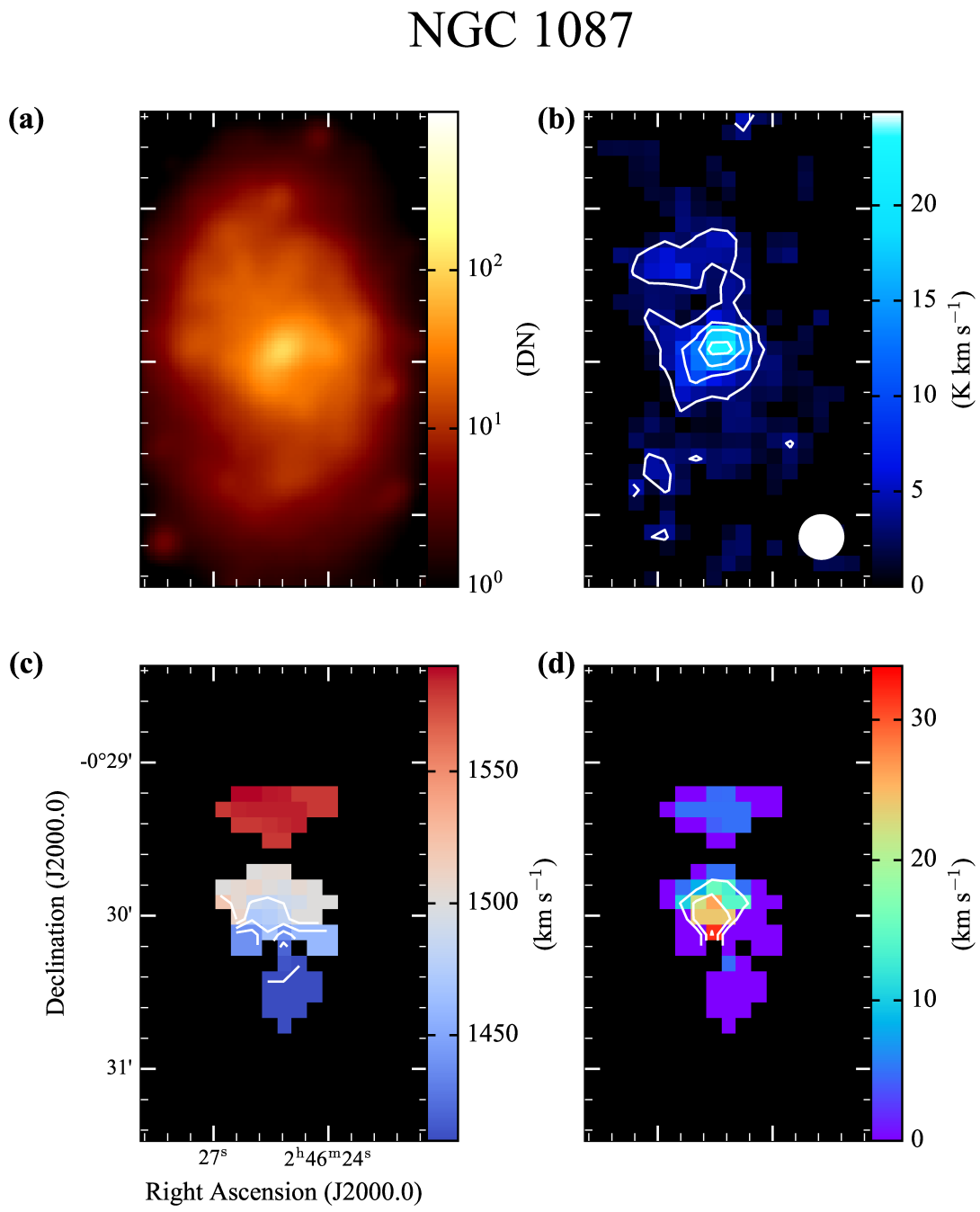

Supplementary fig. 16. Same as figure 12, but for NGC 1087. The contours are plotted at 15 %, 40 %, 65 %, and 90 % of the maximum intensity of 22.93 K km s^{-1} in (b), in steps of 20 km s^{-1} in (c), and in steps of 10 km s^{-1} in (d).

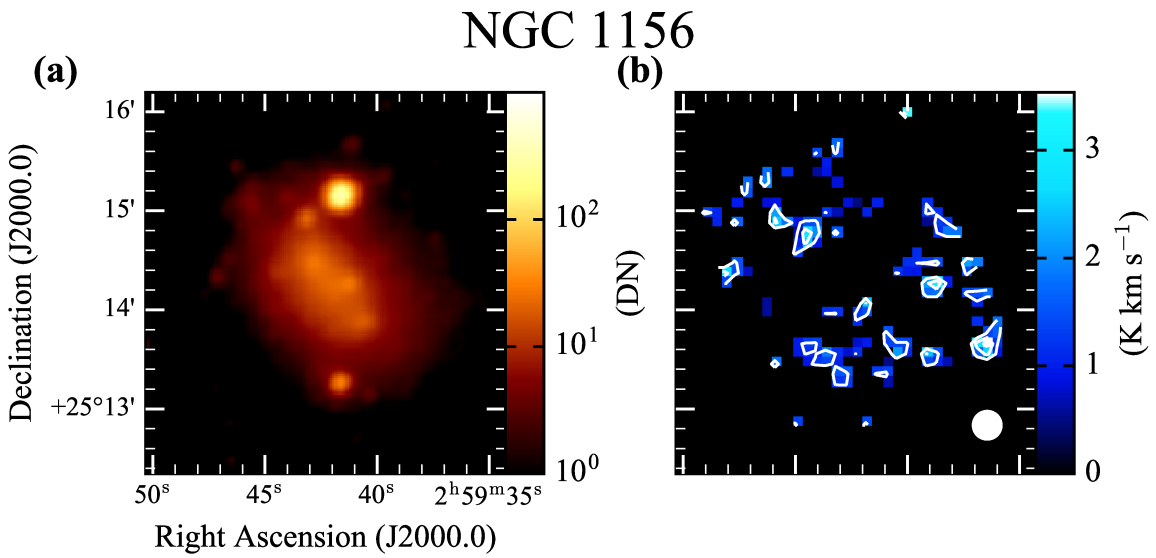

Supplementary fig. 17. Same as figure 12, but for NGC 1156. The contours are plotted at 30 %, 60 %, and 90 % of the maximum intensity of $3.88\,\mathrm{K\,km\,s^{-1}}$ in (b).

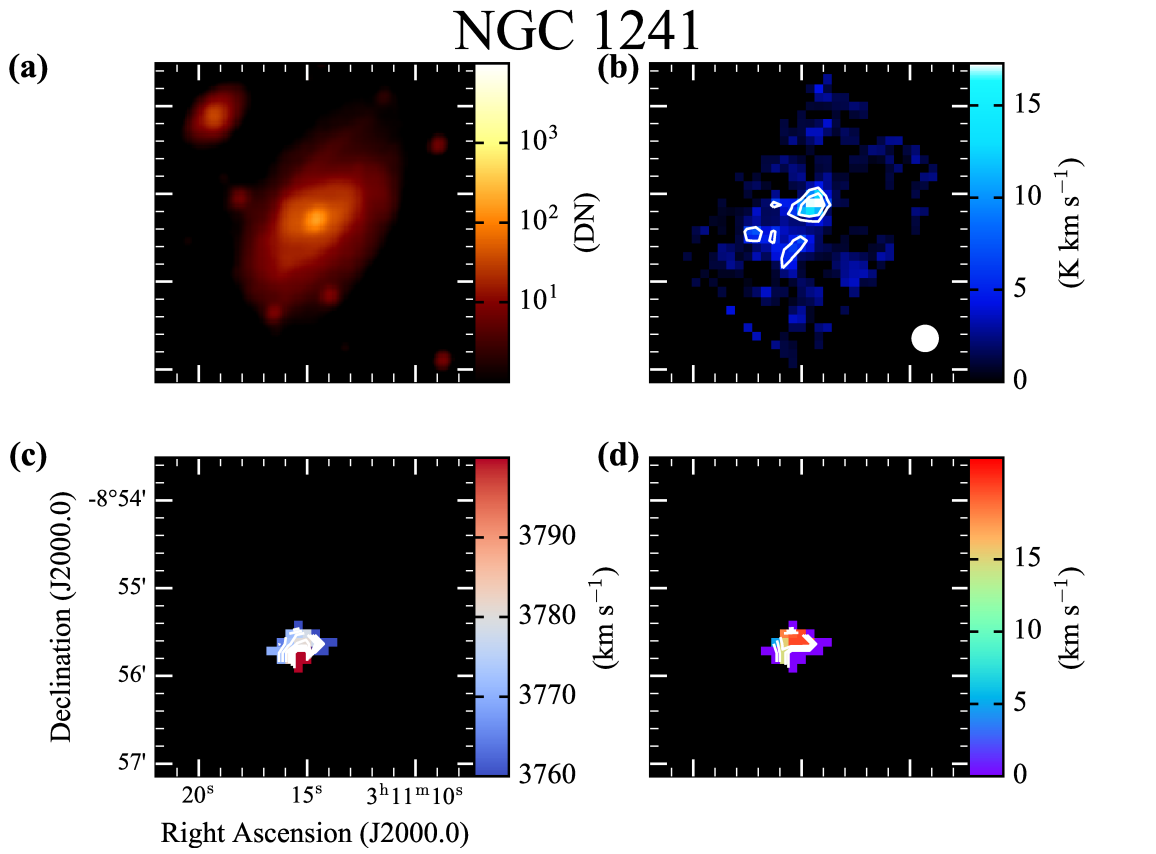

Supplementary fig. 18. Same as figure 12, but for NGC 1241. The contours are plotted at 30 % and 60 % of the maximum intensity of $17.33\,\mathrm{K\,km\,s^{-1}}$ in (b) and in steps of $5\,\mathrm{km\,s^{-1}}$ in (c) and (d).

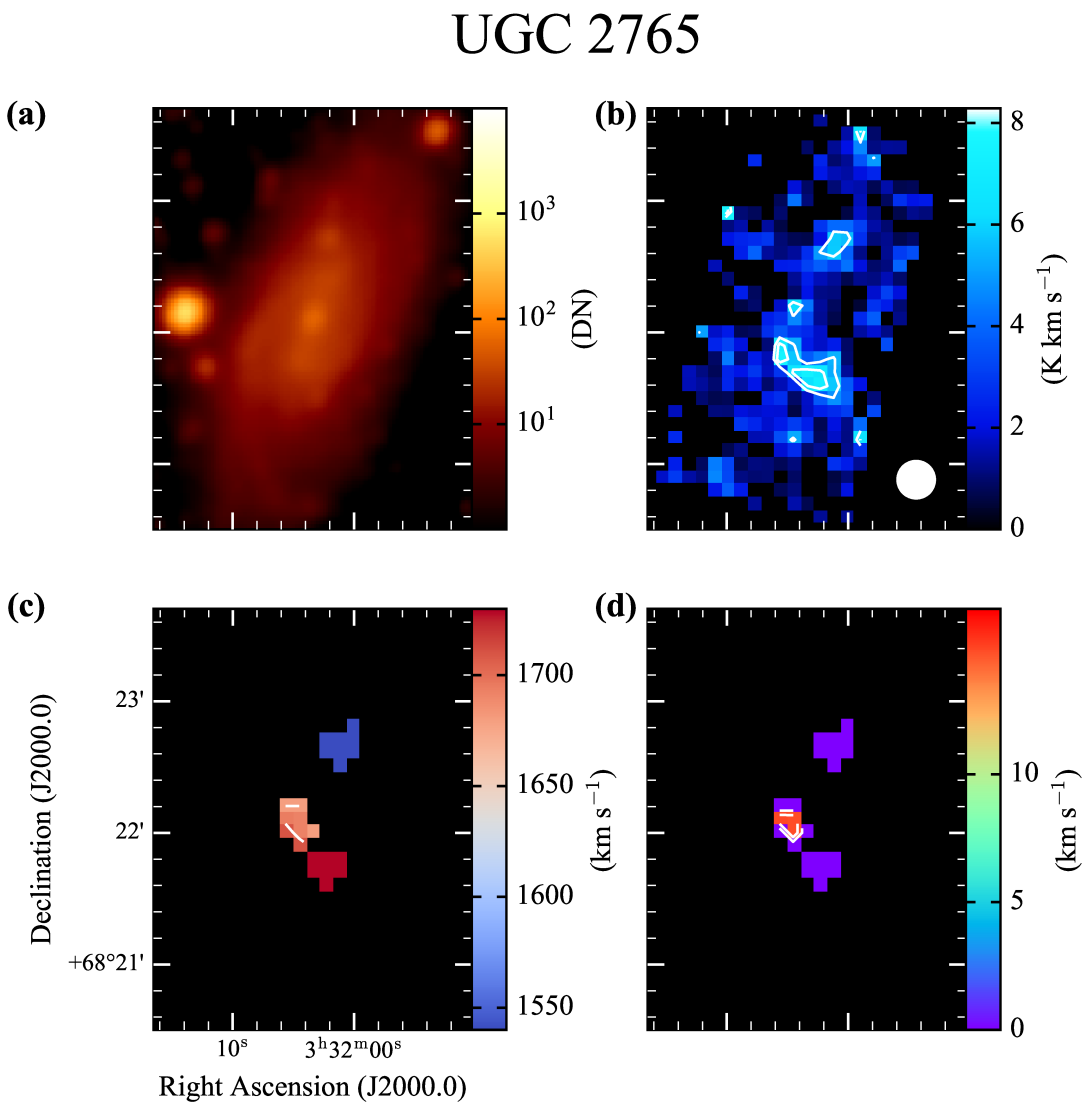

Supplementary fig. 19. Same as figure 12, but for UGC 2765. The contours are plotted at 65 % and 85 % of the maximum intensity of $7.56\,\mathrm{K\,km\,s^{-1}}$ in (b), in steps of $20\,\mathrm{km\,s^{-1}}$ in (c), and in steps of $5\,\mathrm{km\,s^{-1}}$ in (d).

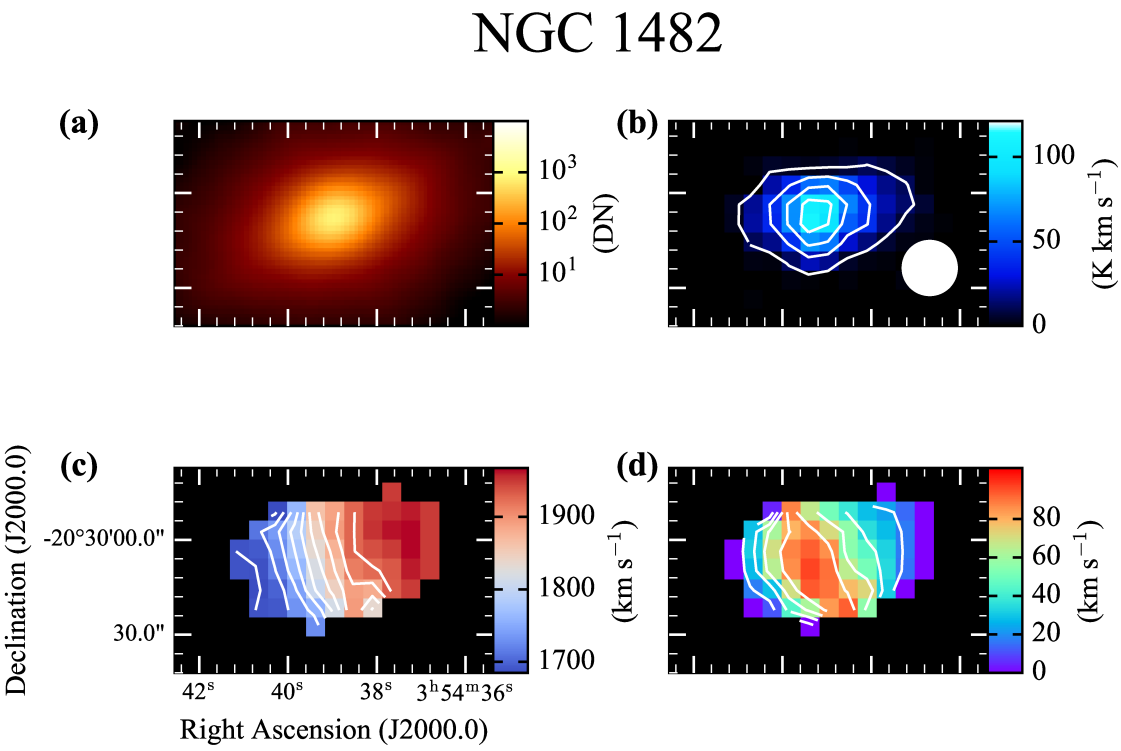

Supplementary fig. 20. Same as figure 12, but for NGC 1482. The contours are plotted at 10 %, 35 %, 60 %, and 85 % of the maximum intensity of 111.32 K km s^{-1} in (b), in steps of 30 km s^{-1} in (c), and in steps of 20 km s^{-1} in (d).

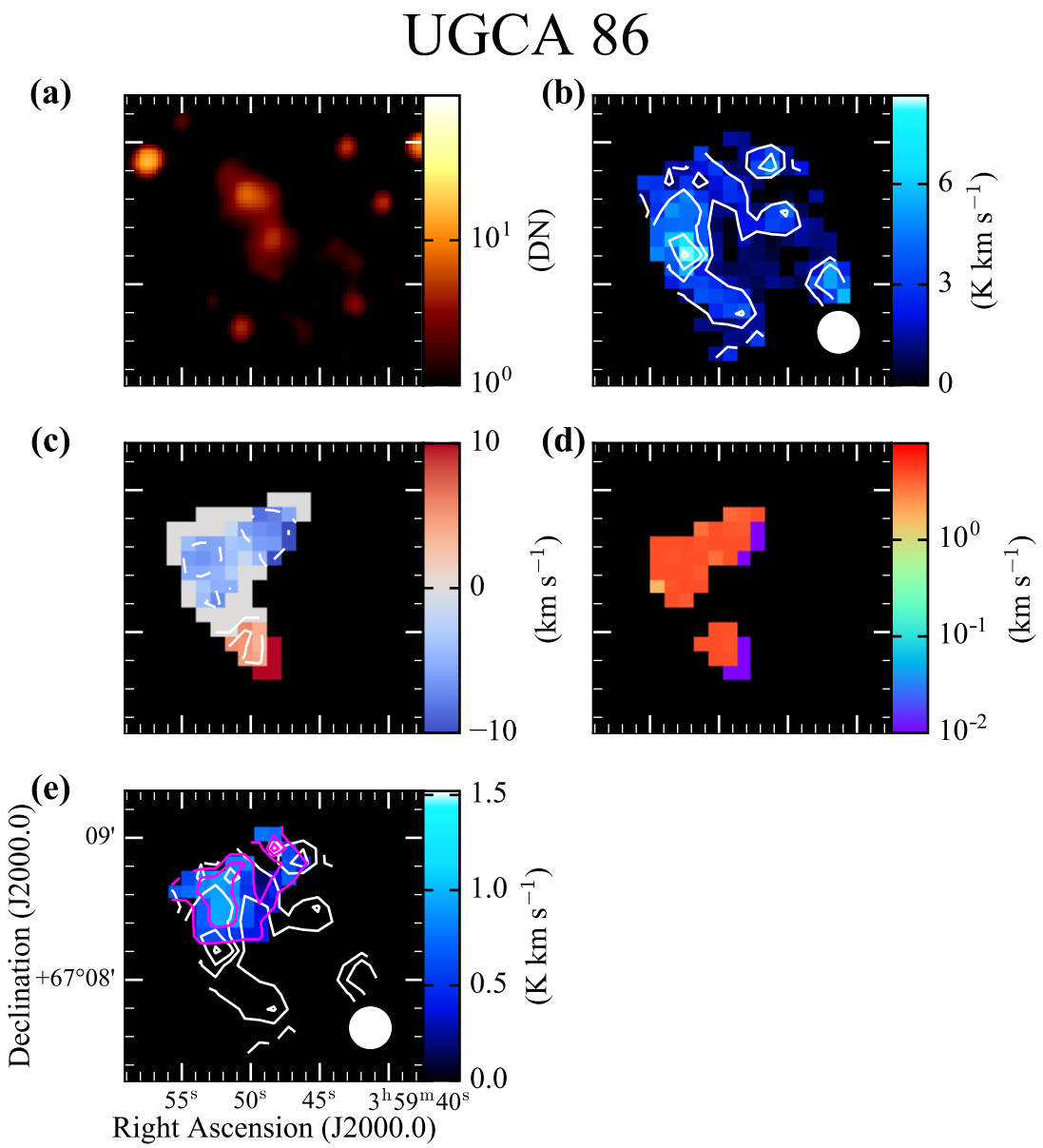

Supplementary fig. 21. Same as figure 12, but for UGCA 86. The contours are plotted at 20 %, 45 %, 70 %, and 95 % of the maximum intensity of $8.40\,\mathrm{K\,km\,s^{-1}}$ in (b) and (e) (*white*), in steps of $5\,\mathrm{km\,s^{-1}}$ in (c) (dashed contours indicate negative velocities), and at 20 %, 50 %, and 80 % of the maximum intensity of $1.67\,\mathrm{K\,km\,s^{-1}}$ in (e) (*magenta*).

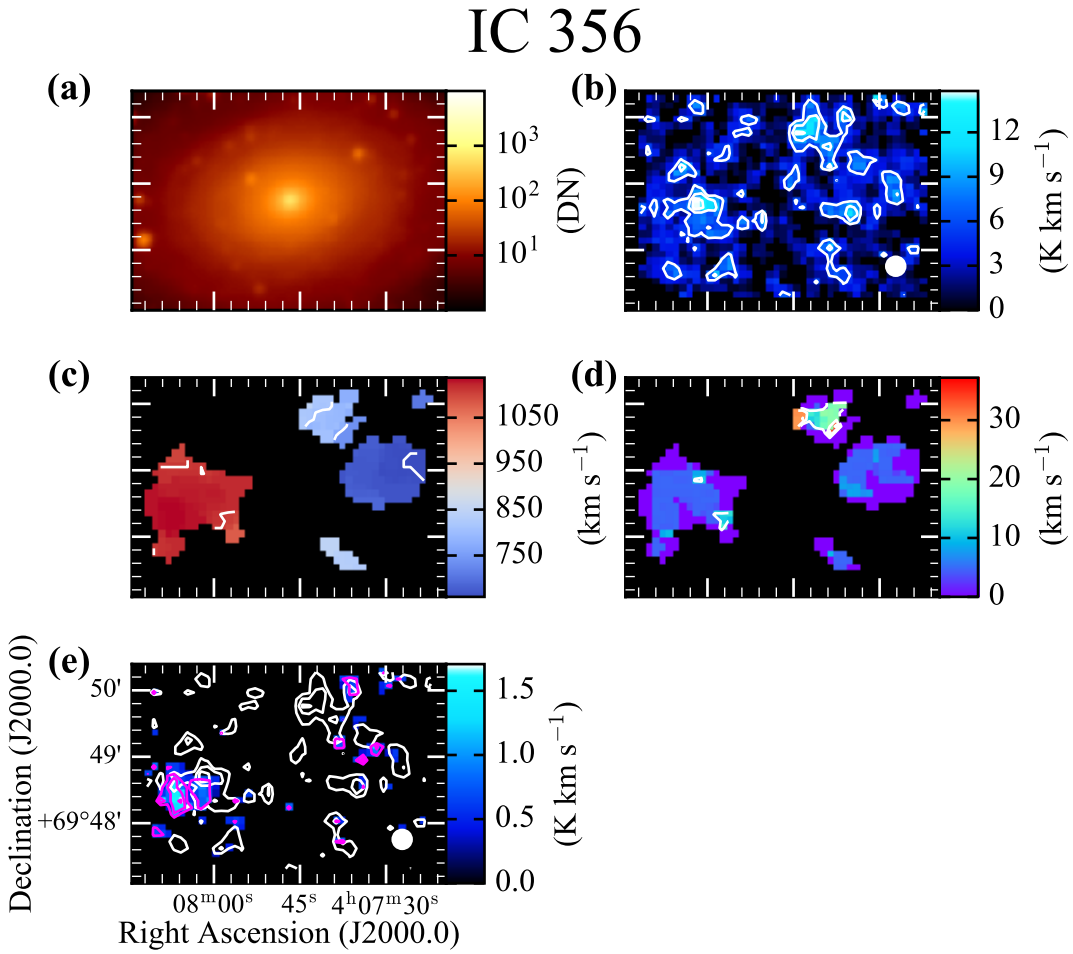

Supplementary fig. 22. Same as figure 12, but for IC 356. The contours are plotted at 35 %, 60 %, and 85 % of the maximum intensity of $15.13\,\mathrm{K\,km\,s^{-1}}$ in (b) and (e) (*white*), in steps of $50\,\mathrm{km\,s^{-1}}$ in (c), in steps of $10\,\mathrm{km\,s^{-1}}$ in (d), and at 35 %, 65 %, and 95 % of the maximum intensity of $1.81\,\mathrm{K\,km\,s^{-1}}$ in (e) (*magenta*).

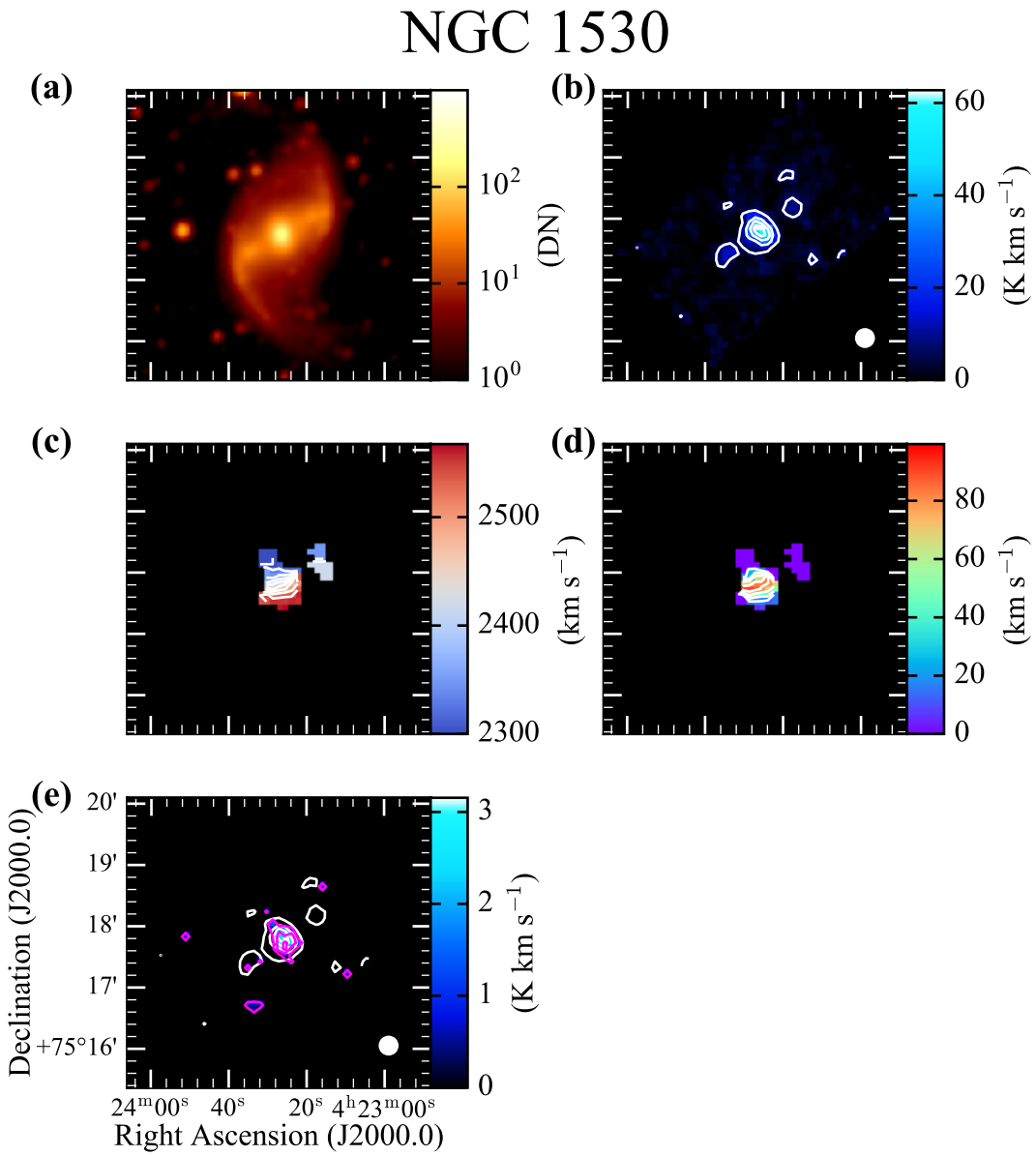

Supplementary fig. 23. Same as figure 12, but for NGC 1530. The contours are plotted at 10 %, 35 %, 60 %, and 85 % of the maximum intensity of 63.97 K km s^{-1} in (b) and (e) (*white*), in steps of 30 km s^{-1} in (c), in steps of 20 km s^{-1} in (d), and at 10 %, 50 %, and 90 % of the maximum intensity of 3.49 K km s^{-1} in (e) (*magenta*).

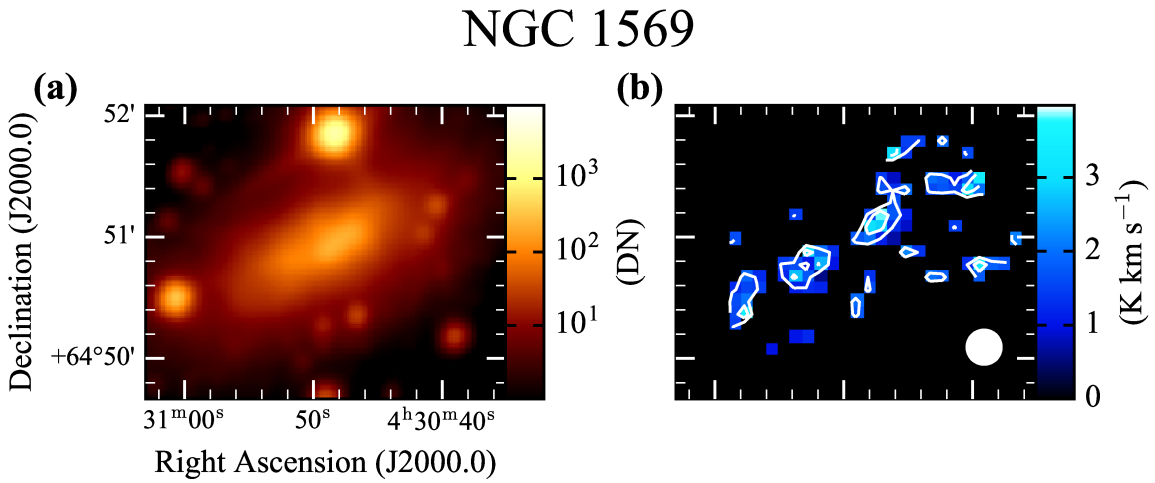

Supplementary fig. 24. Same as figure 12, but for NGC 1569. The contours are plotted at 35 % and 65 % of the maximum intensity of $3.84\,\mathrm{K\,km\,s^{-1}}$ in (b).

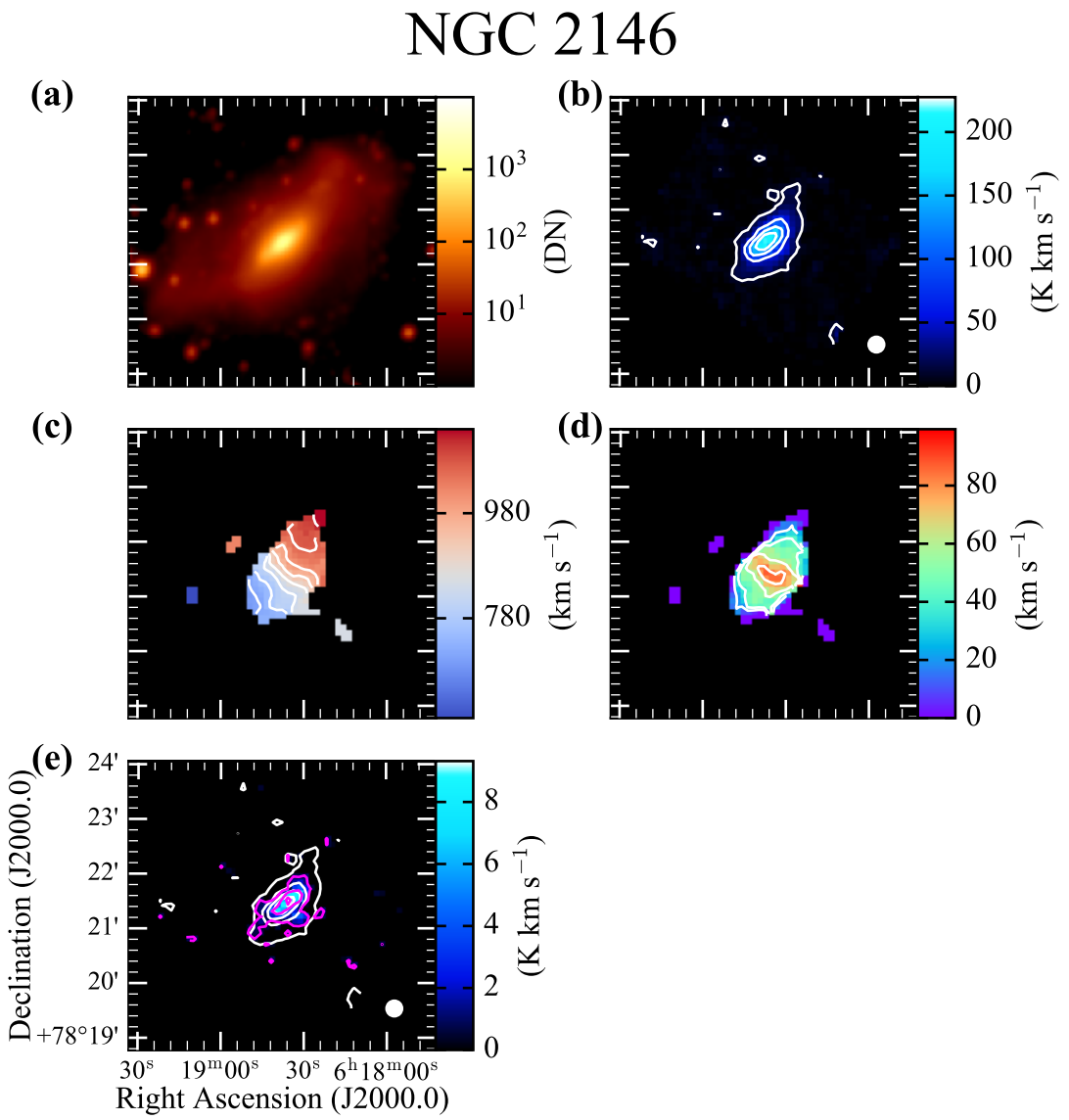

Supplementary fig. 25. Same as figure 12, but for NGC 2146. The contours are plotted at 5 %, 30 %, 55 %, and 80 % of the maximum intensity of 217.12 K km s^{-1} in (b) and (e) (*white*), in steps of 60 km s^{-1} in (c), in steps of 20 km s^{-1} in (d), and at 5 %, 45 %, and 85 % of the maximum intensity of 11.75 K km s^{-1} in (e) (*magenta*).

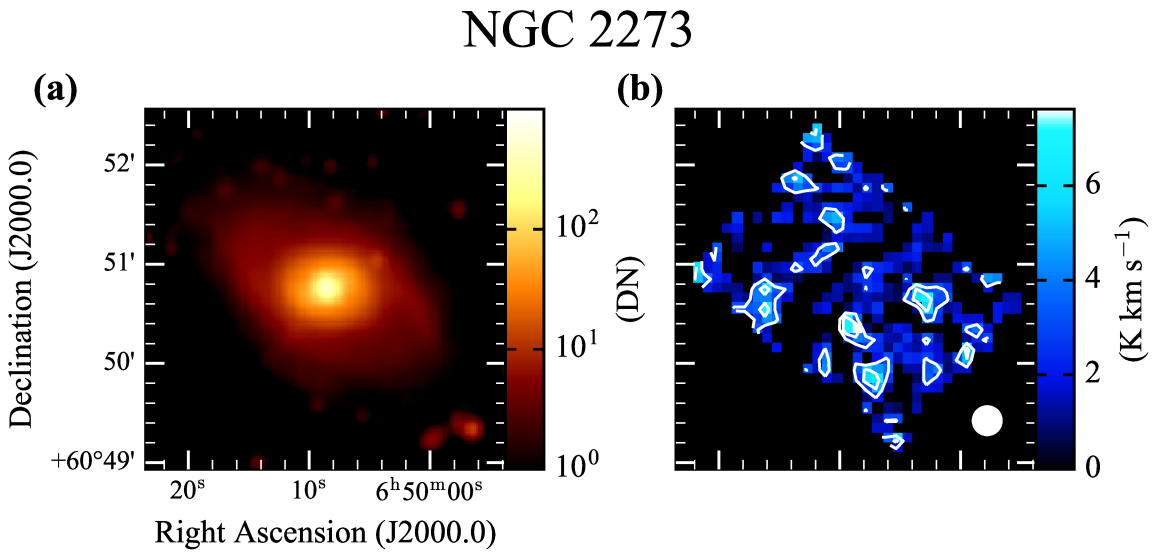

Supplementary fig. 26. Same as figure 12, but for NGC 2273. The contours are plotted at 35 % and 65 % of the maximum intensity of $7.83\,\mathrm{K\,km\,s^{-1}}$ in (b).

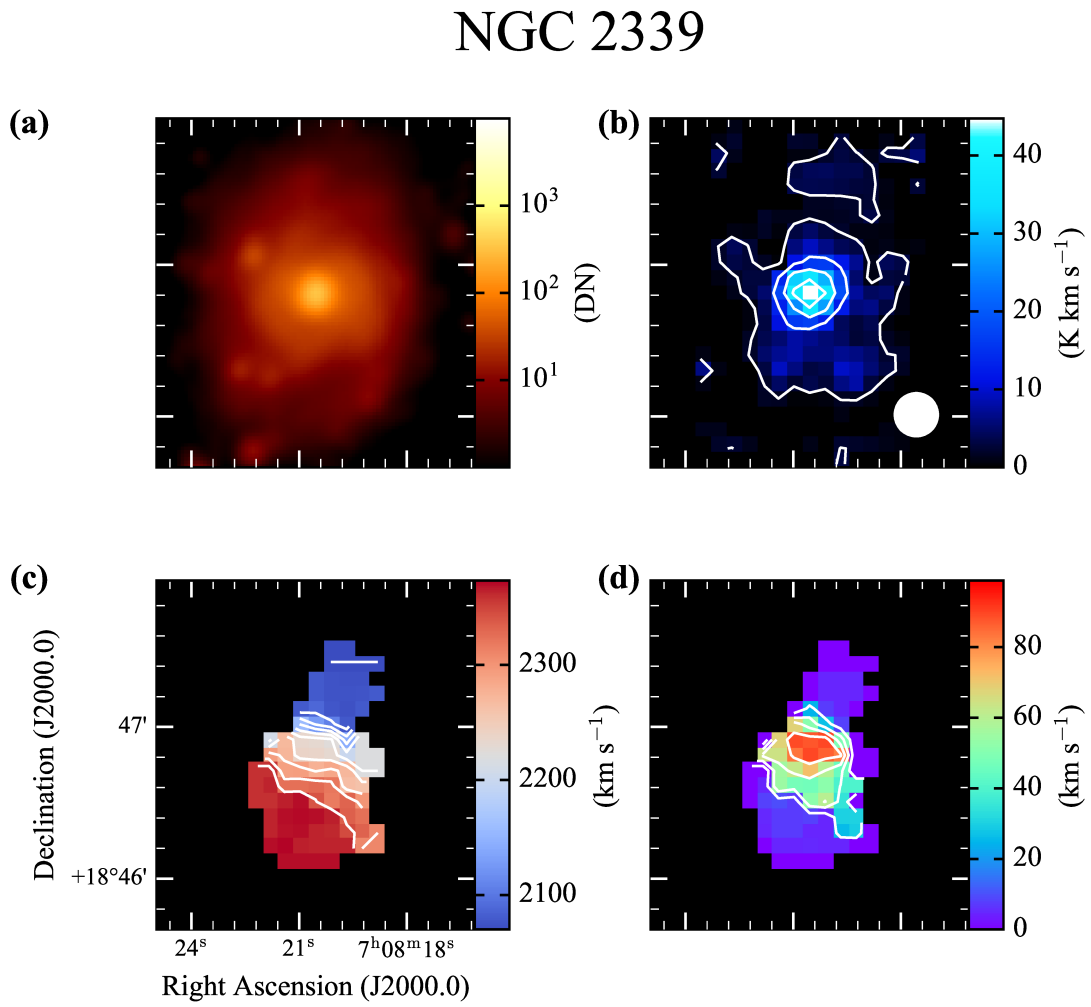

Supplementary fig. 27. Same as figure 12, but for NGC 2339. The contours are plotted at 5 %, 30 %, 55 %, and 80 % of the maximum intensity of $46.34\,\mathrm{K\,km\,s^{-1}}$ in (b), in steps of $30\,\mathrm{km\,s^{-1}}$ in (c), and in steps of $20\,\mathrm{km\,s^{-1}}$ in (d).

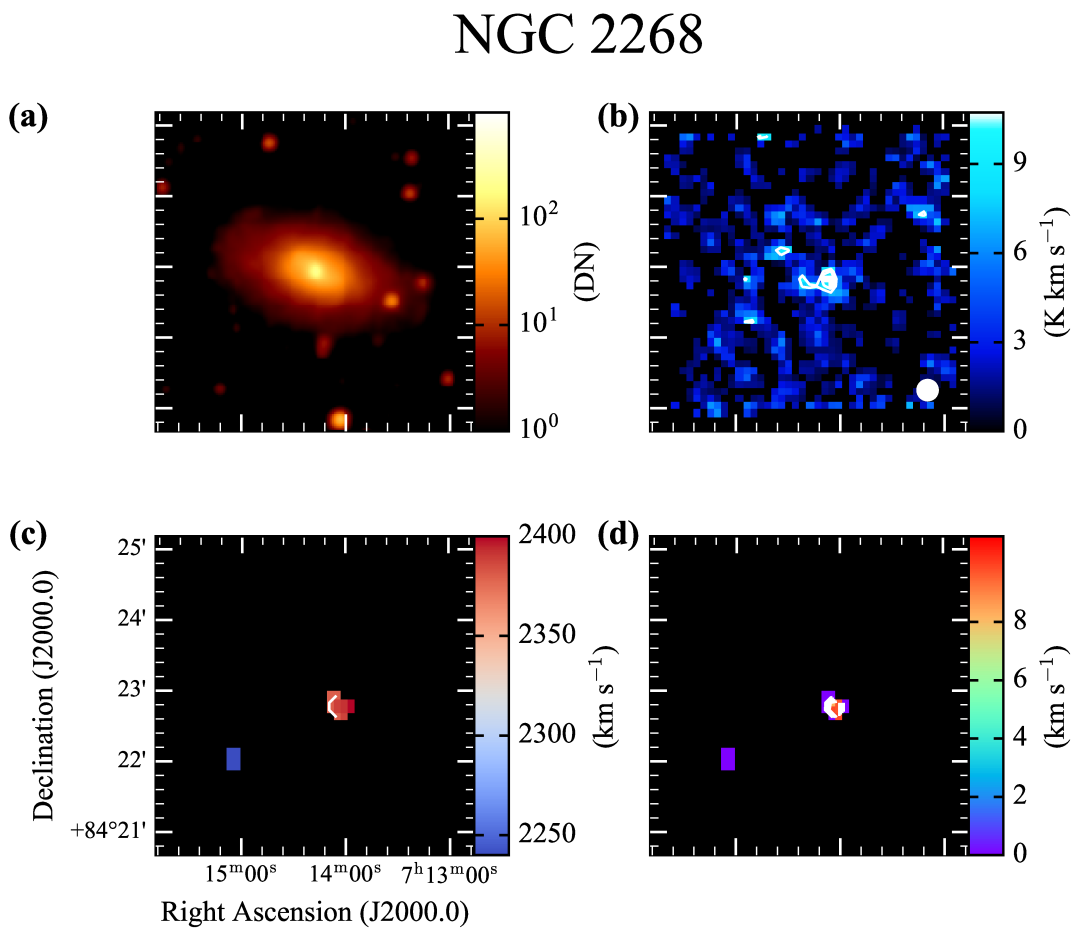

Supplementary fig. 28. Same as figure 12, but for NGC 2268. The contours are plotted at 55 % and 70 % of the maximum intensity of $13.53\,\mathrm{K\,km\,s^{-1}}$ in (b), in steps of $20\,\mathrm{km\,s^{-1}}$ step in (c), and in steps of $2\,\mathrm{km\,s^{-1}}$ in (d).

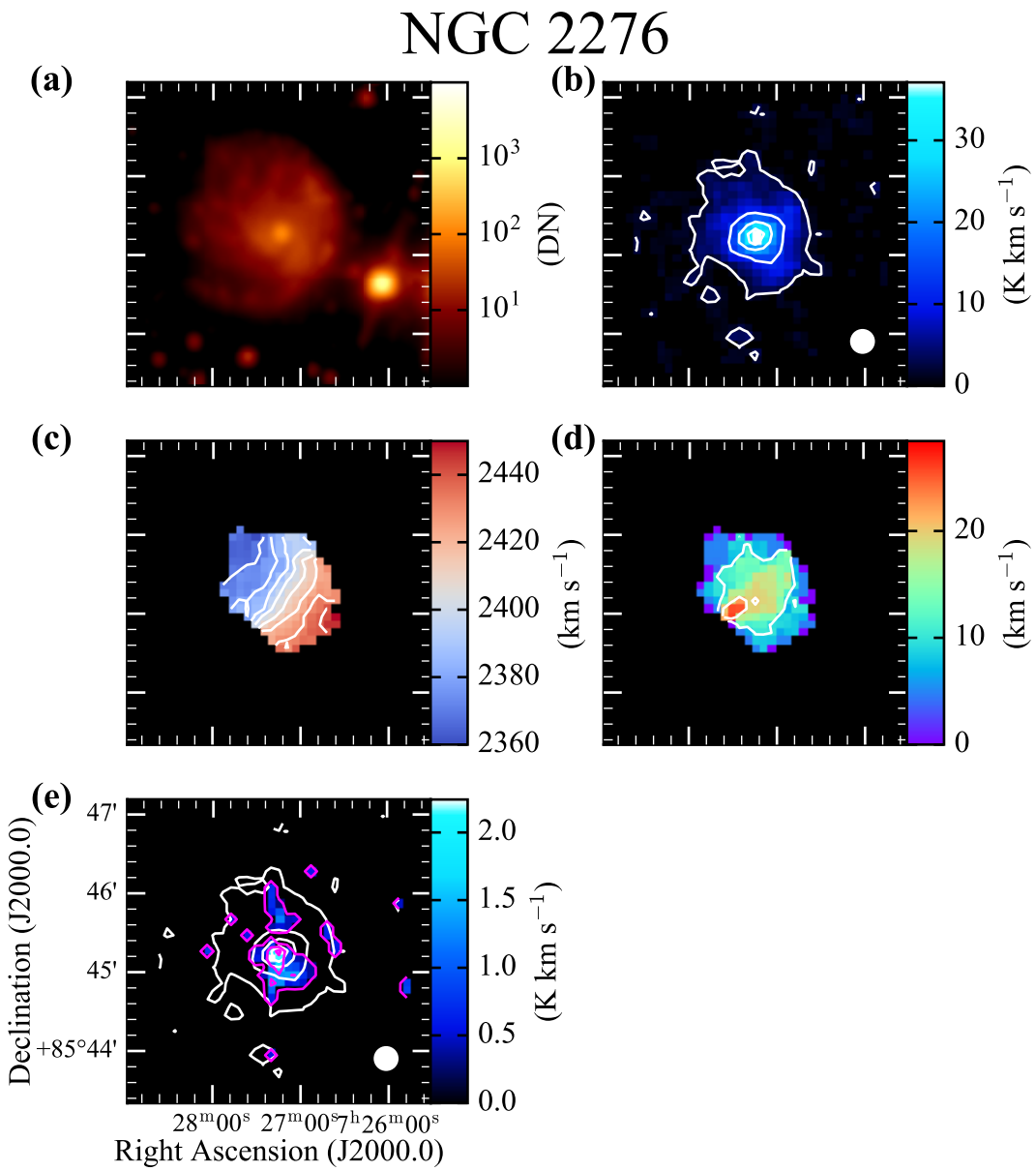

Supplementary fig. 29. Same as figure 12, but for NGC 2276. The contours are plotted at 5 %, 30 %, 55 %, and 80 % of the maximum intensity of $41.92\,\mathrm{K\,km\,s^{-1}}$ in (b) and (e) (*white*), in steps of $10\,\mathrm{km\,s^{-1}}$ in (c) and (d), and at 5 %, 45 %, and 85 % of the maximum intensity of $3.09\,\mathrm{K\,km\,s^{-1}}$ in (e) (*magenta*).

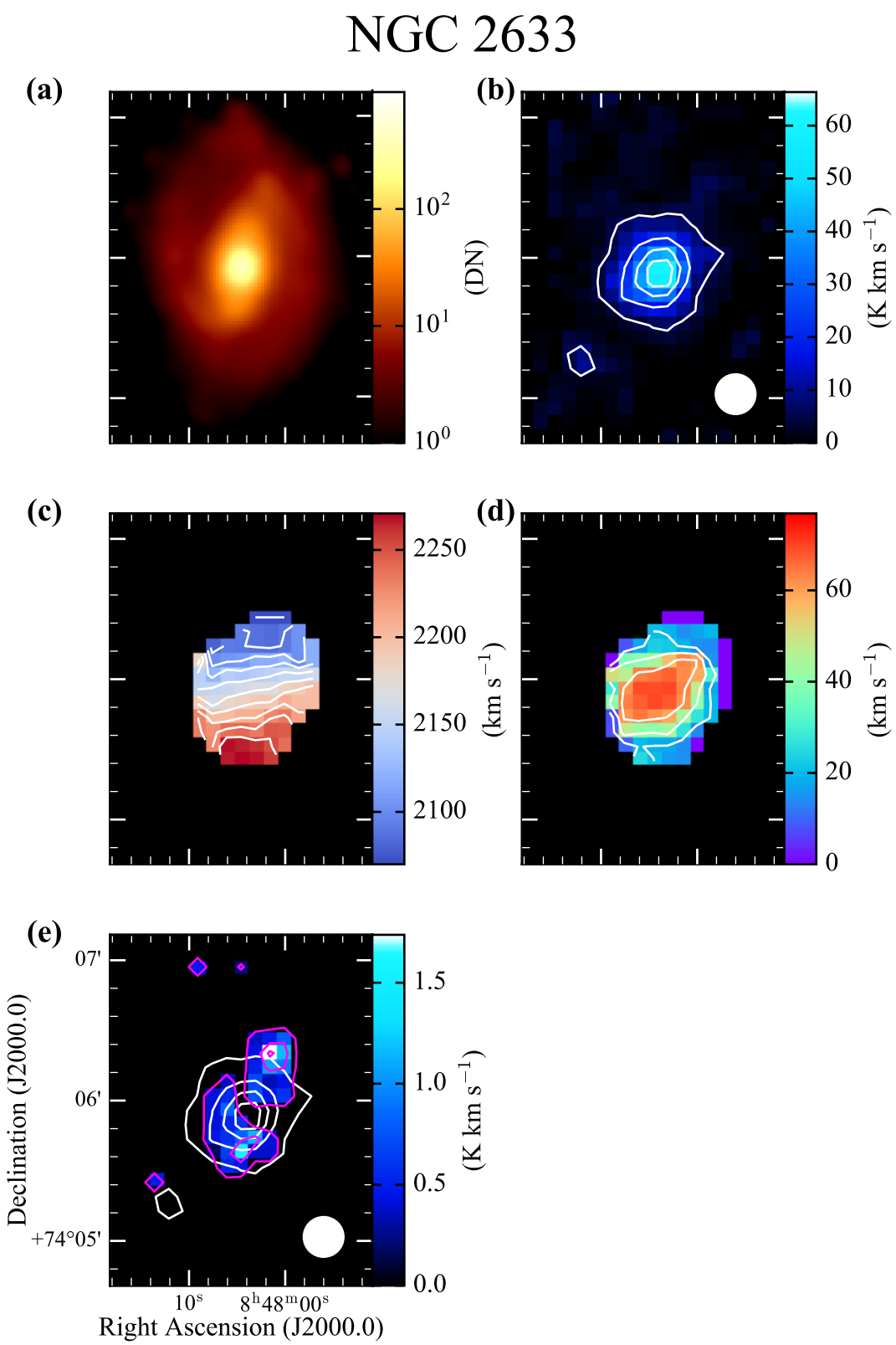

Supplementary fig. 30. Same as figure 12, but for NGC 2633. The contours are plotted at 10 %, 35 %, 60 %, and 85 % of the maximum intensity of $60.58\,\mathrm{K\,km\,s^{-1}}$ in (b) and (e) (*white*), in steps of $20\,\mathrm{km\,s^{-1}}$ in (c) and (d), and at 10 %, 50 %, and 90 % of the maximum intensity of $1.80\,\mathrm{K\,km\,s^{-1}}$ in (e) (*magenta*).

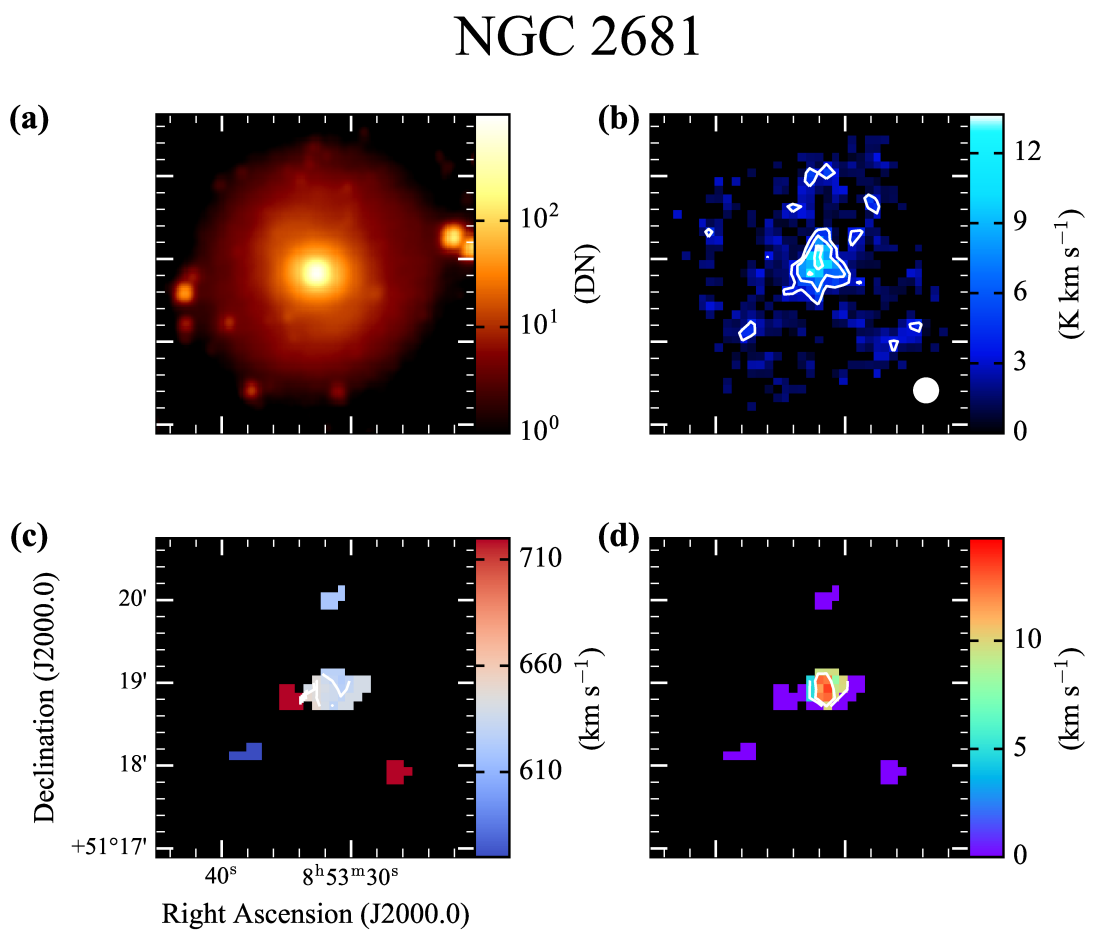

Supplementary fig. 31. Same as figure 12, but for NGC 2681. The contours are plotted at 25 %, 45 %, and 85 % of the maximum intensity of $13.50\,\mathrm{K\,km\,s^{-1}}$ in (b), in steps of $15\,\mathrm{km\,s^{-1}}$ in (c), and in steps of $5\,\mathrm{km\,s^{-1}}$ in (d).

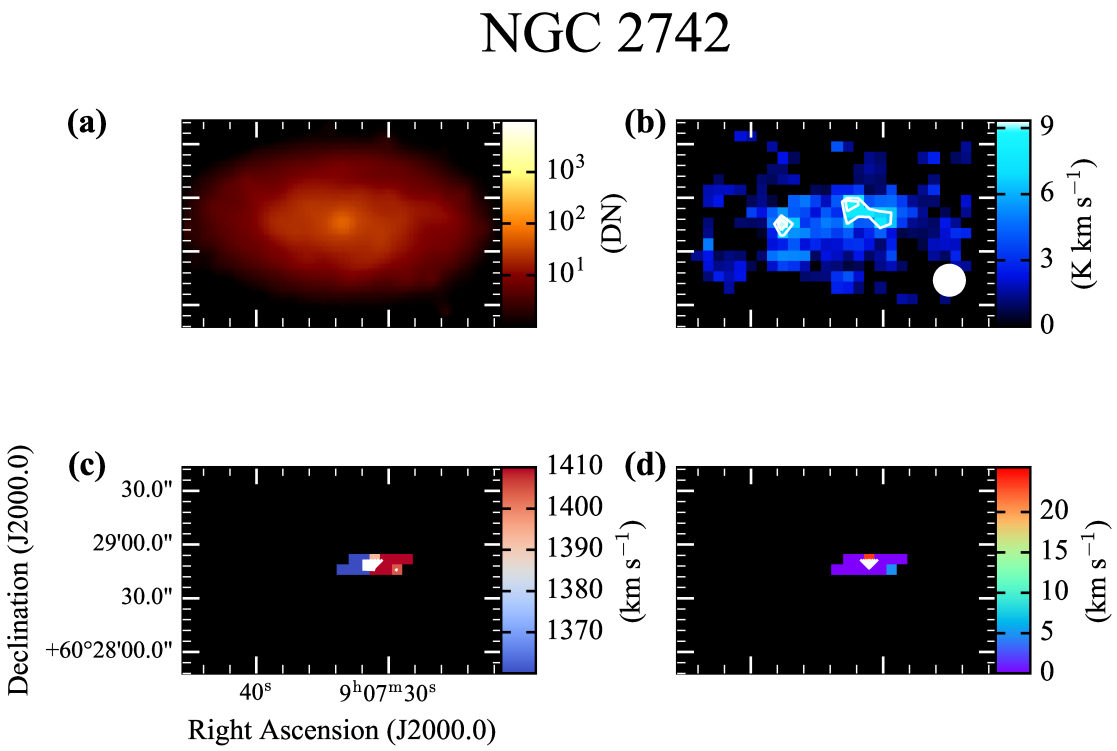

Supplementary fig. 32. Same as figure 12, but for NGC 2742. The contours are plotted at 70 % and 85 % of the maximum intensity of $9.21\,\mathrm{K\,km\,s^{-1}}$ in (b) and in steps of $5\,\mathrm{km\,s^{-1}}$ in (c) and (d).

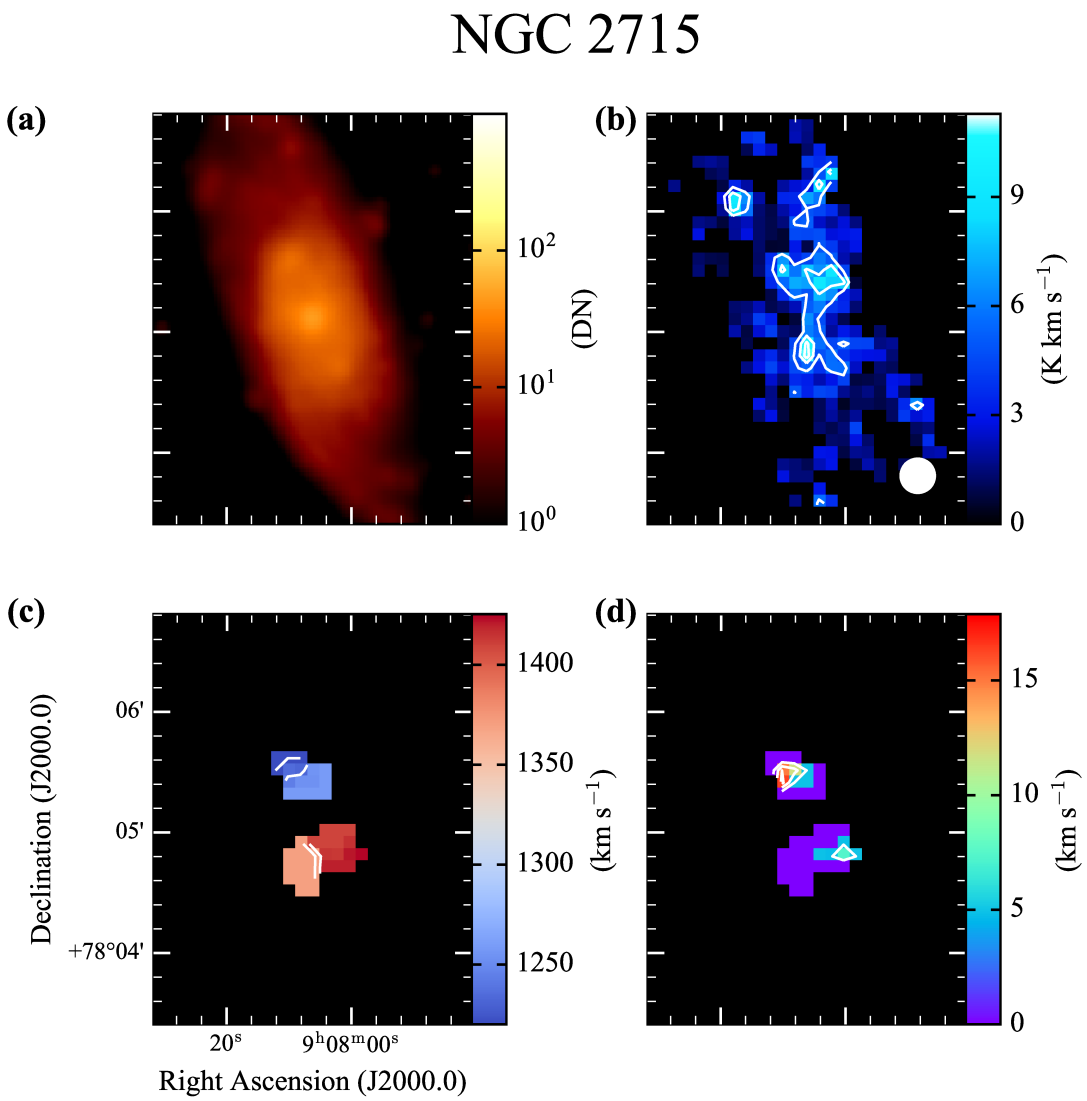

Supplementary fig. 33. Same as figure 12, but for NGC 2715. The contours are plotted at 45 %, 70 %, and 90 % of the maximum intensity of $10.81\,\mathrm{K\,km\,s^{-1}}$ in (b), in steps of $20\,\mathrm{km\,s^{-1}}$ in (c), and in steps of $5\,\mathrm{km\,s^{-1}}$ in (d).

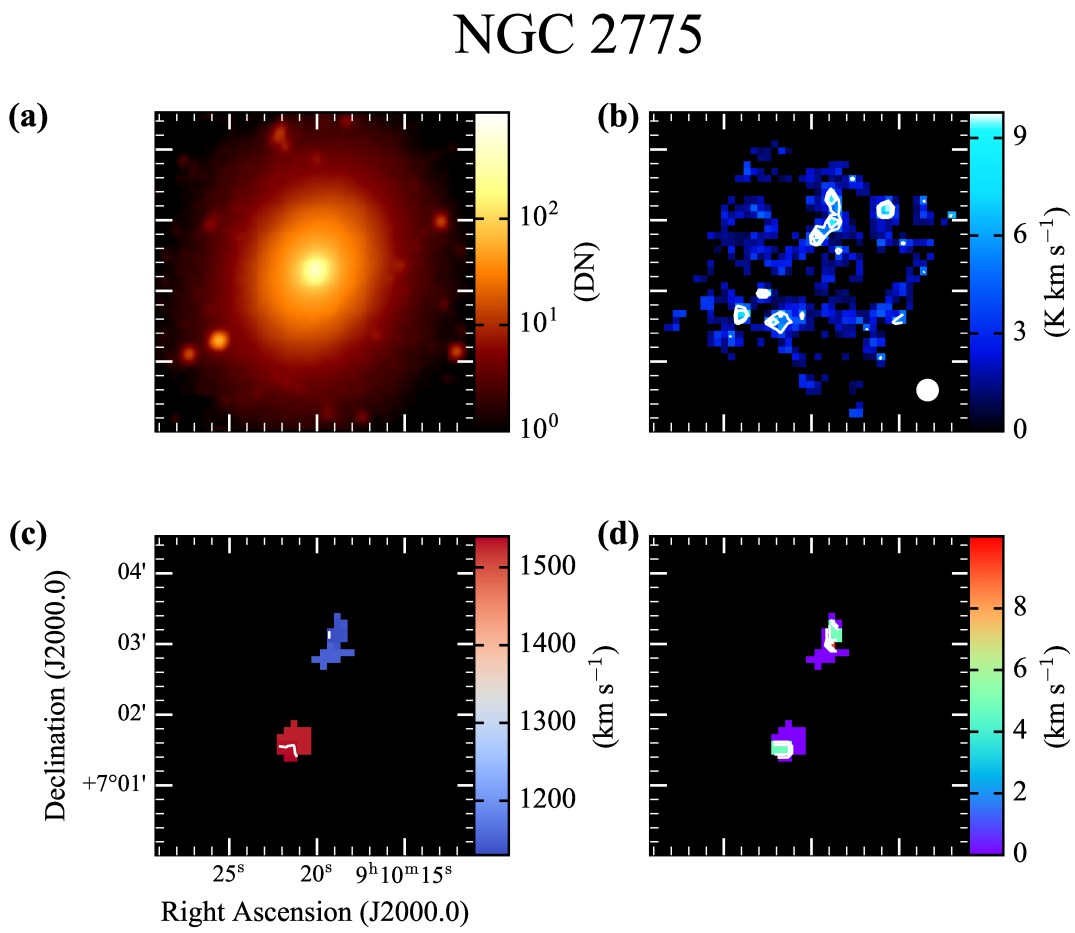

Supplementary fig. 34. Same as figure 12, but for NGC 2775. The contours are plotted at 45 % and 60 % of the maximum intensity of $10.23\,\mathrm{K\,km\,s^{-1}}$ in (b), in steps of $45\,\mathrm{km\,s^{-1}}$ in (c), and in steps of $2\,\mathrm{km\,s^{-1}}$ in (d).

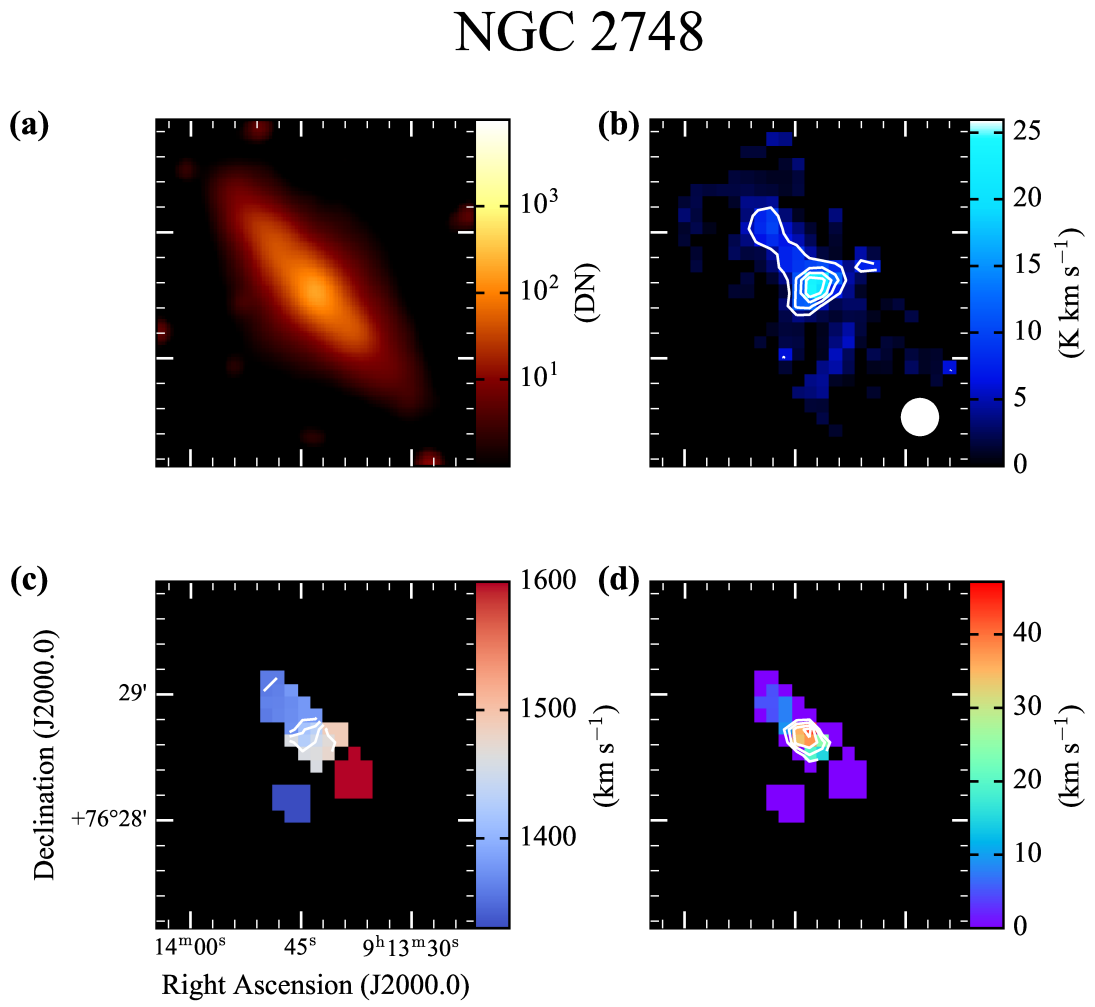

Supplementary fig. 35. Same as figure 12, but for NGC 2748. The contours are plotted at 25 %, 45 %, 65 %, and 85 % of the maximum intensity of $24.06\,\mathrm{K\,km\,s^{-1}}$ in (b), in steps of $30\,\mathrm{km\,s^{-1}}$ in (c), and in steps of $10\,\mathrm{km\,s^{-1}}$ in (d).

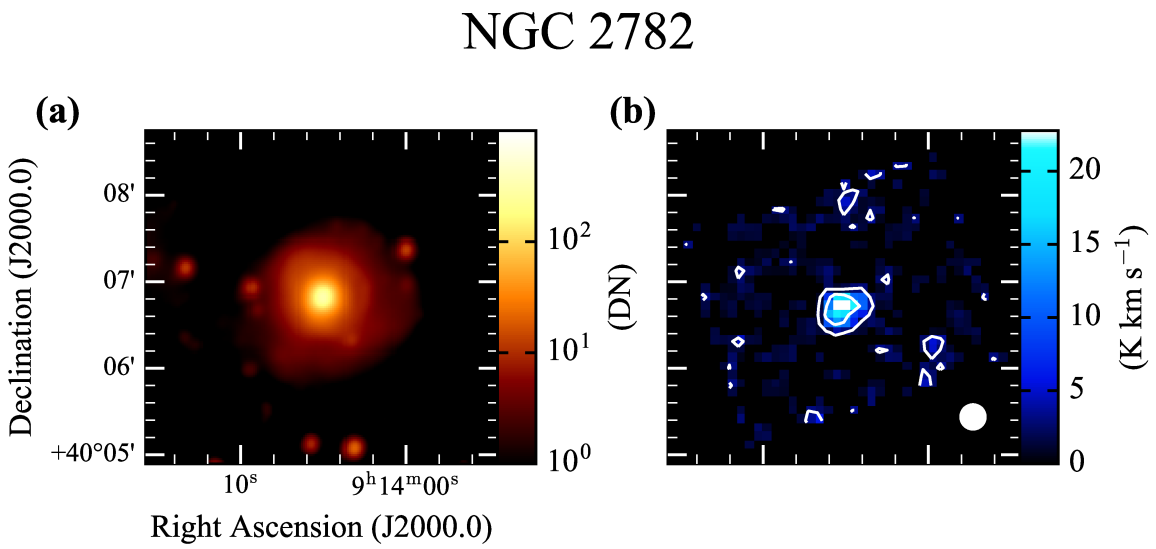

Supplementary fig. 36. Same as figure 12, but for NGC 2782. The contours are plotted at 10 % and 45 % of the maximum intensity of $28.37\,\mathrm{K\,km\,s^{-1}}$ in (b).

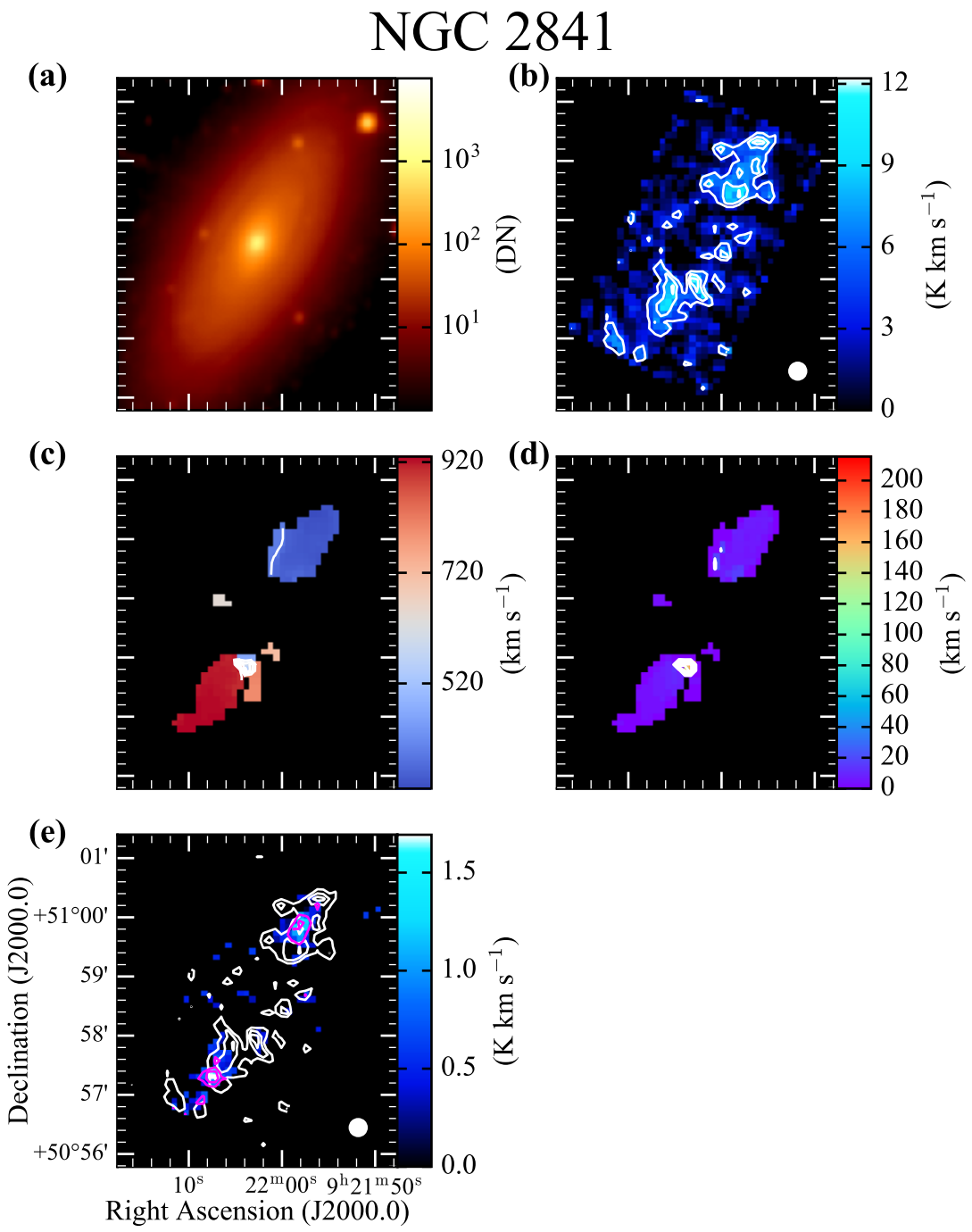

Supplementary fig. 37. Same as figure 12, but for NGC 2841. The contours are plotted at 35 %, 60 %, and 85 % of the maximum intensity of $11.90\,\mathrm{K\,km\,s^{-1}}$ in (b) and (e) (*white*), in steps of $60\,\mathrm{km\,s^{-1}}$ in (c), in steps of $20\,\mathrm{km\,s^{-1}}$ in (d), and at 35 % and 70 % of the maximum intensity of $1.88\,\mathrm{K\,km\,s^{-1}}$ in (e) (*magenta*).

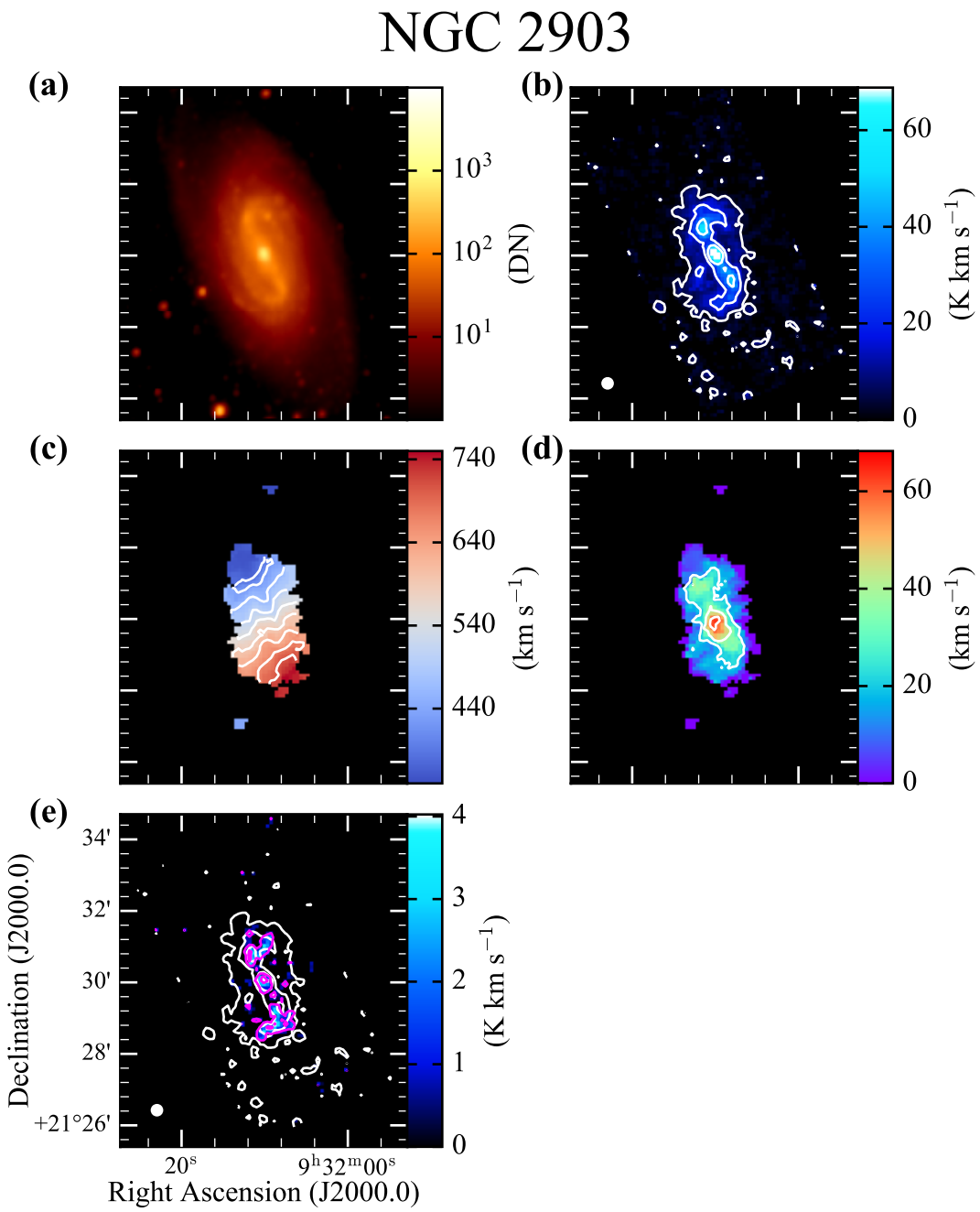

Supplementary fig. 38. Same as figure 12, but for NGC 2903. The contours are plotted at 5 %, 20 %, and 45 % of the maximum intensity of $97.00\,\mathrm{K\,km\,s^{-1}}$ in (b) and (e) (*white*), in steps of $40\,\mathrm{km\,s^{-1}}$ in (c), in steps of $20\,\mathrm{km\,s^{-1}}$ in (d), and at 15 % and 65 % of the maximum intensity of $5.93\,\mathrm{K\,km\,s^{-1}}$ in (e) (*magenta*).

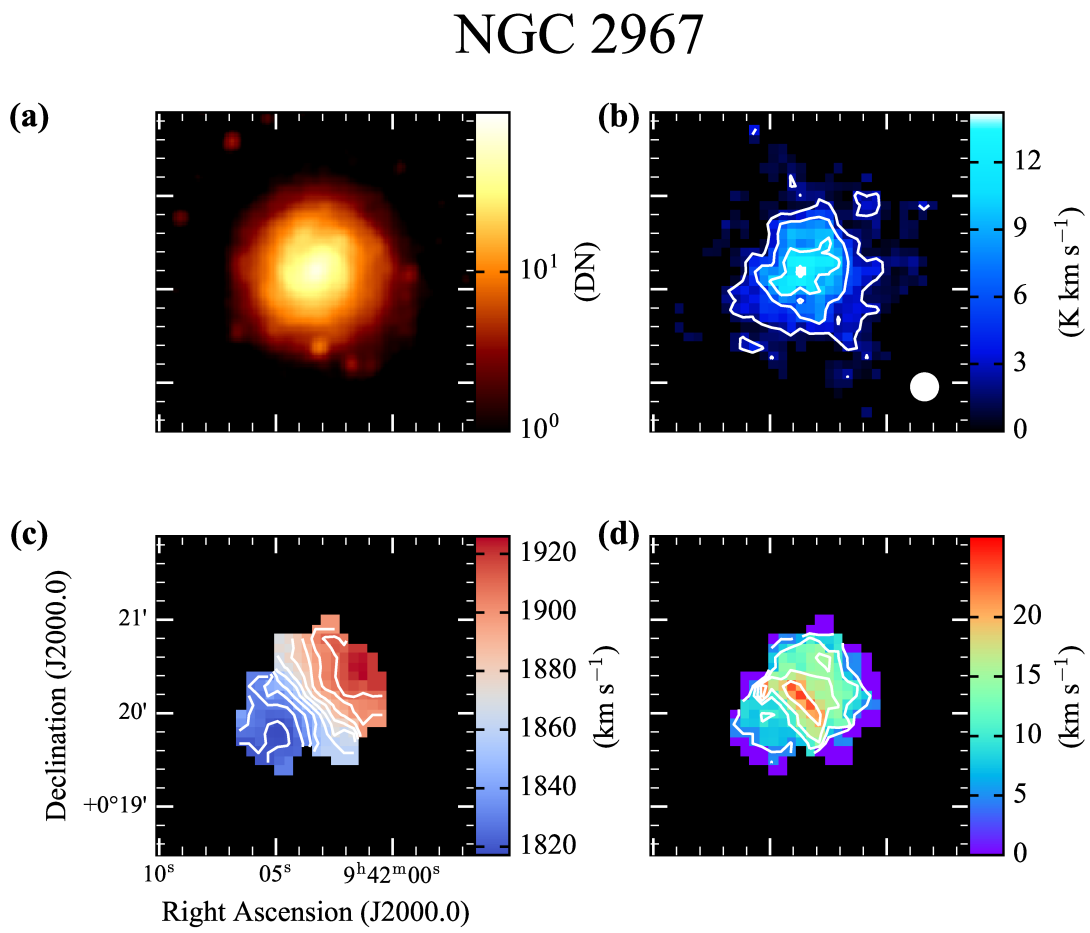

Supplementary fig. 39. Same as figure 12, but for NGC 2967. The contours are plotted at 15 %, 40 %, 65 %, and 90 % of the maximum intensity of $15.42\,\mathrm{K\,km\,s^{-1}}$ in (b), in steps of $10\,\mathrm{km\,s^{-1}}$ in (c), and in steps of $5\,\mathrm{km\,s^{-1}}$ in (d).

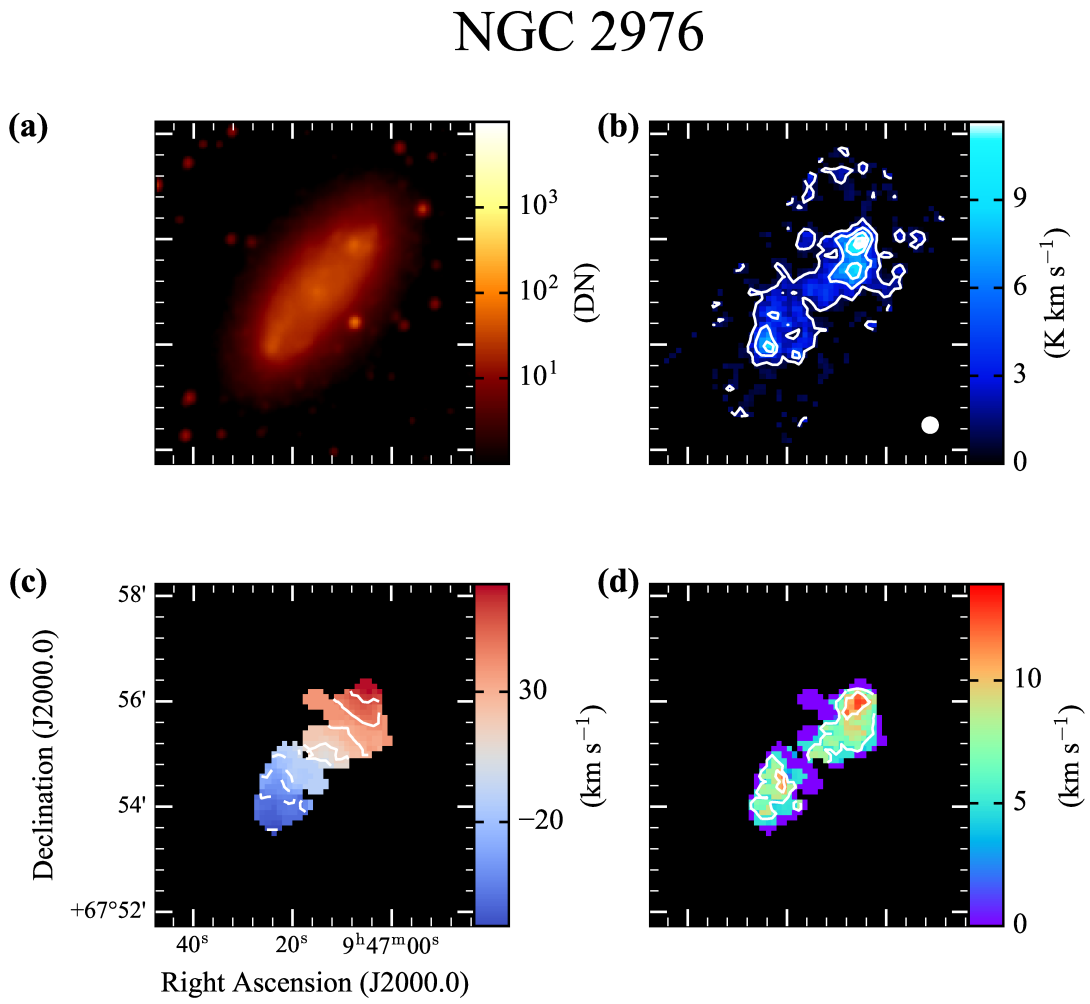

Supplementary fig. 40. Same as figure 12, but for NGC 2976. The contours are plotted at 10 %, 35 %, 60 %, and 85 % of the maximum intensity of $13.04\,\mathrm{K\,km\,s^{-1}}$ in (b), in steps of $15\,\mathrm{km\,s^{-1}}$ in (c) (dashed contours indicate negative velocity), and in steps of $5\,\mathrm{km\,s^{-1}}$ in (d).

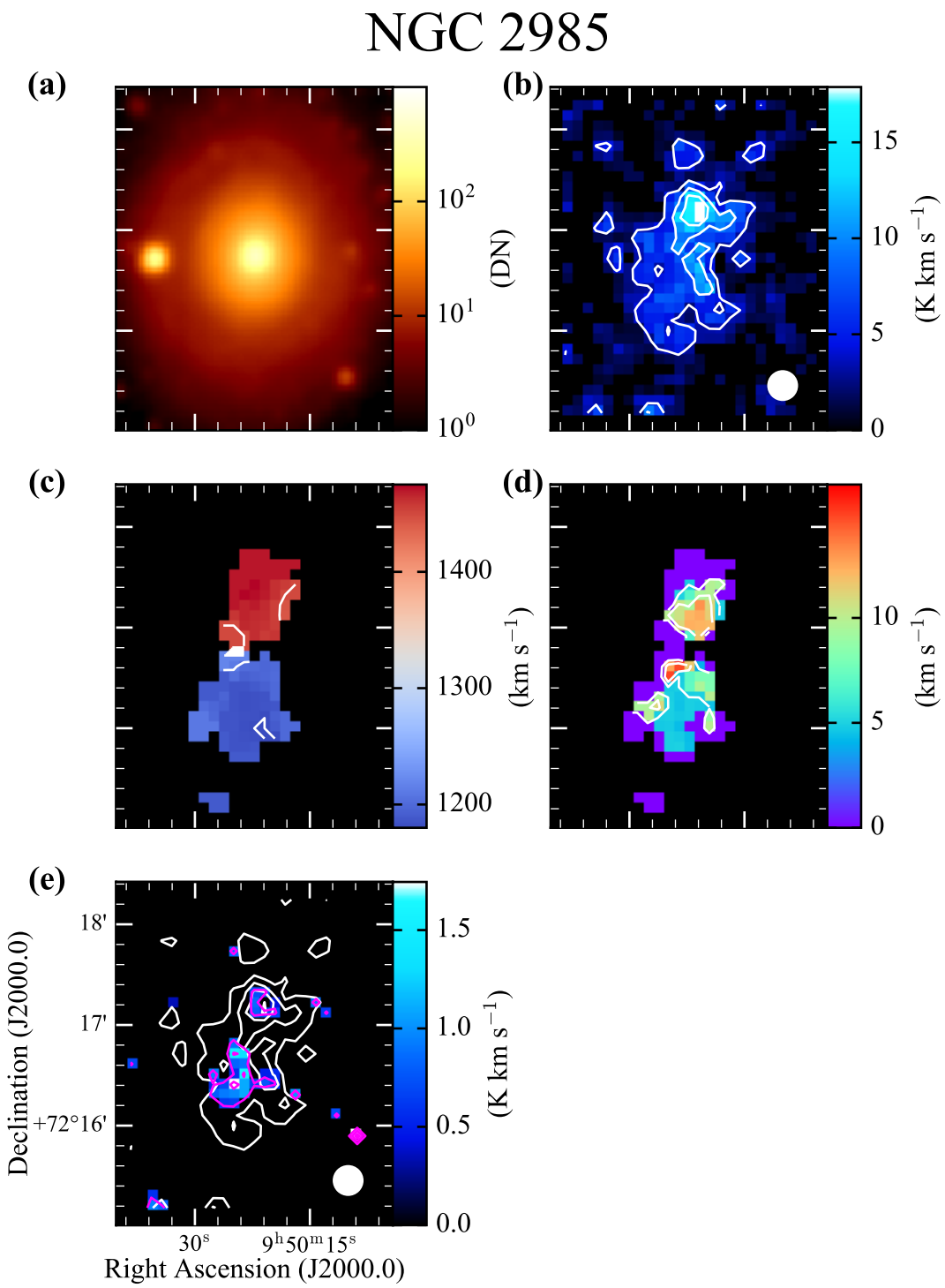

Supplementary fig. 41. Same as figure 12, but for NGC 2985. The contours are plotted at 20 %, 45 %, 70 %, and 95 % of the maximum intensity of 19.76 K km s^{-1} in (b) and (e) (*white*), in steps of 30 km s^{-1} in (c), in steps of 5 km s^{-1} in (d), and at 20 %, 50 %, and 80 % of the maximum intensity of 2.90 K km s^{-1} in (e) (*magenta*).

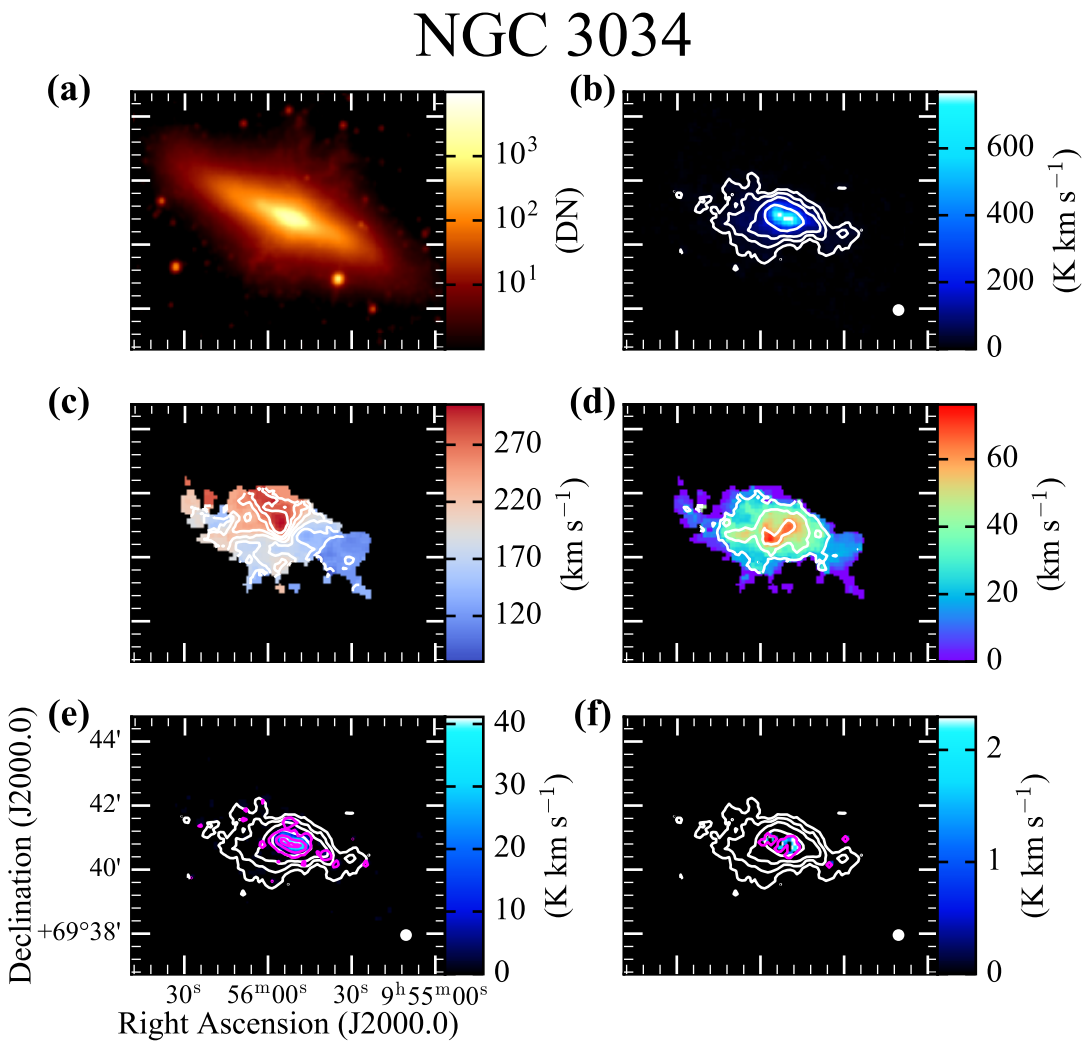

Supplementary fig. 42. Same as figure 12, but for NGC 3034. The contours are plotted at 2 %, 5 %, 10 %, and 30 % of the maximum intensity of 826.48 K km s^{-1} in (b), (e), and (f) (*white*), and (f) (*white*), in steps of 25 km s^{-1} in (c), in steps of 20 km s^{-1} in (d), at 4 %, 44 %, and 84 % of the maximum intensity of 45.83 K km s^{-1} in (e) (*magenta*), and at 4 % of the maximum intensity of 3.58 K km s^{-1} in (f) (*magenta*).

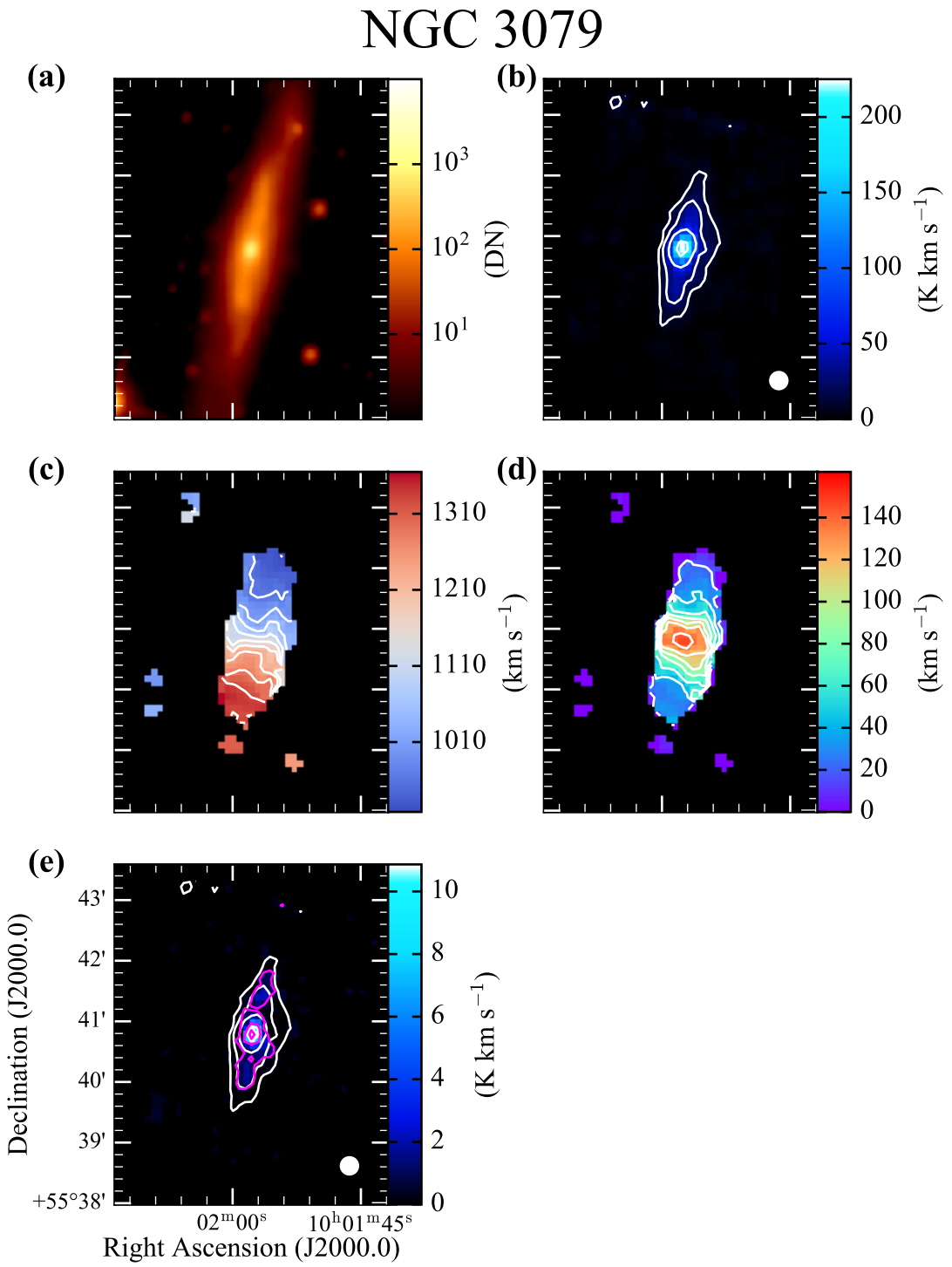

Supplementary fig. 43. Same as figure 12, but for NGC 3079. The contours are plotted at 4 %, 10 %, 30 %, and 80 % of the maximum intensity of 250.49 K km s^{-1} in (b) and (e) (*white*), in steps of 45 km s^{-1} in (c), in steps of 20 km s^{-1} in (d), and at 4 %, 44 %, and 84 % of the maximum intensity of 15.72 K km s^{-1} in (e) (*magenta*).

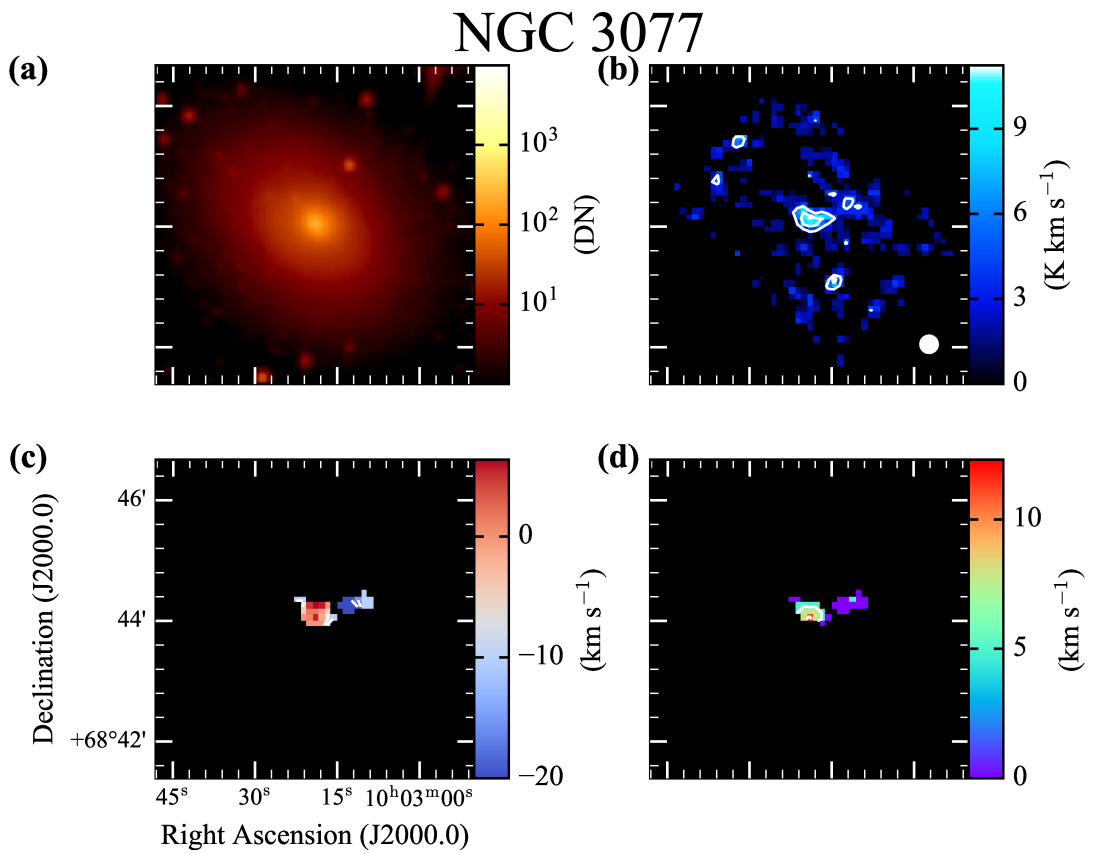

Supplementary fig. 44. Same as figure 12, but for NGC 3077. The contours are plotted at 35 % and 75 % of the maximum intensity of $11.72\,\mathrm{K\,km\,s^{-1}}$ in (b) and in steps of $5\,\mathrm{km\,s^{-1}}$ in (c) and (d).

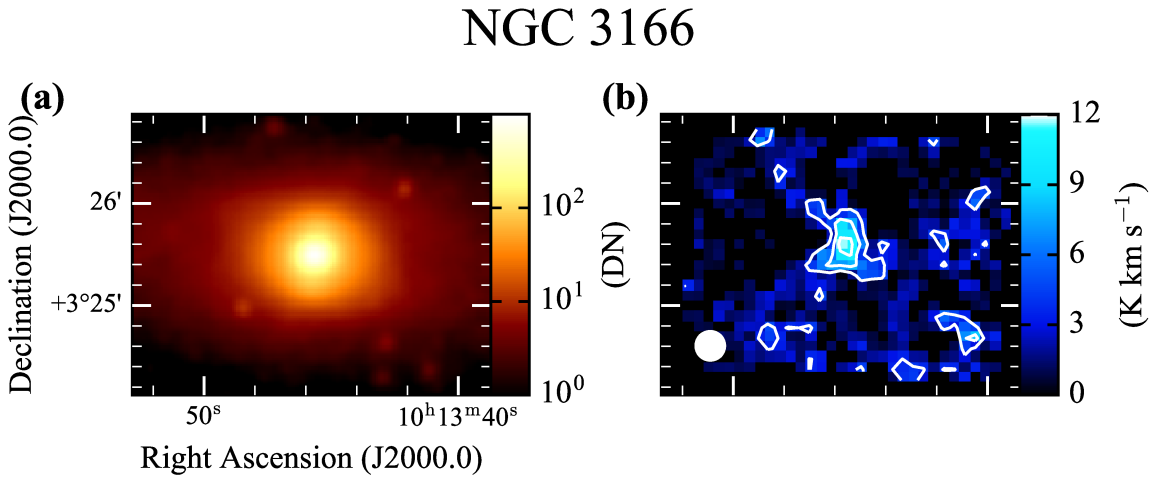

Supplementary fig. 45. Same as figure 12, but for NGC 3166 and the OTF beam size is indicated in the bottom left corner in panel (b). The contours are plotted at 30 %, 60 %, and 90 % of the maximum intensity of $11.77\,\mathrm{K\,km\,s^{-1}}$ in (b).

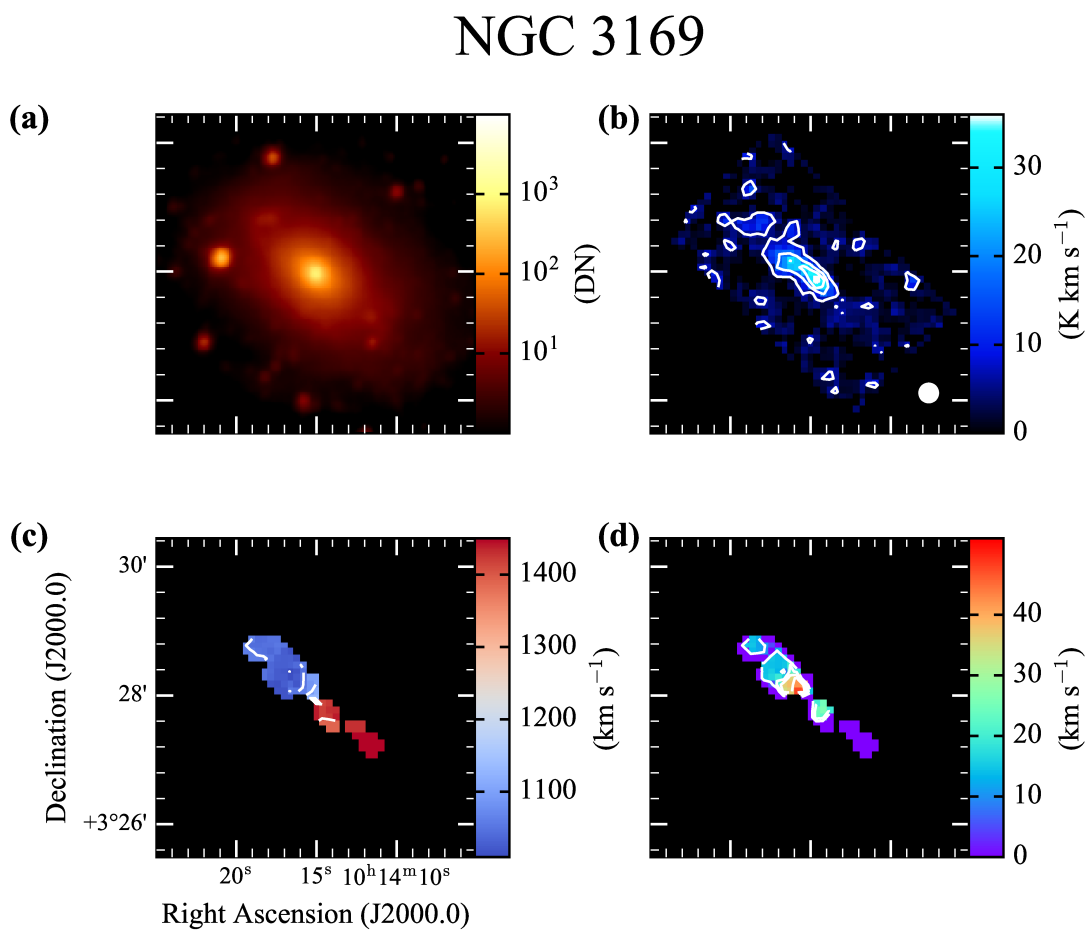

Supplementary fig. 46. Same as figure 12, but for NGC 3169. The contours are plotted at 15 %, 40 %, 65 %, and 90 % of the maximum intensity of $42.89\,\mathrm{K\,km\,s^{-1}}$ in (b), in steps of $45\,\mathrm{km\,s^{-1}}$ in (c), and in steps of $10\,\mathrm{km\,s^{-1}}$ in (d).

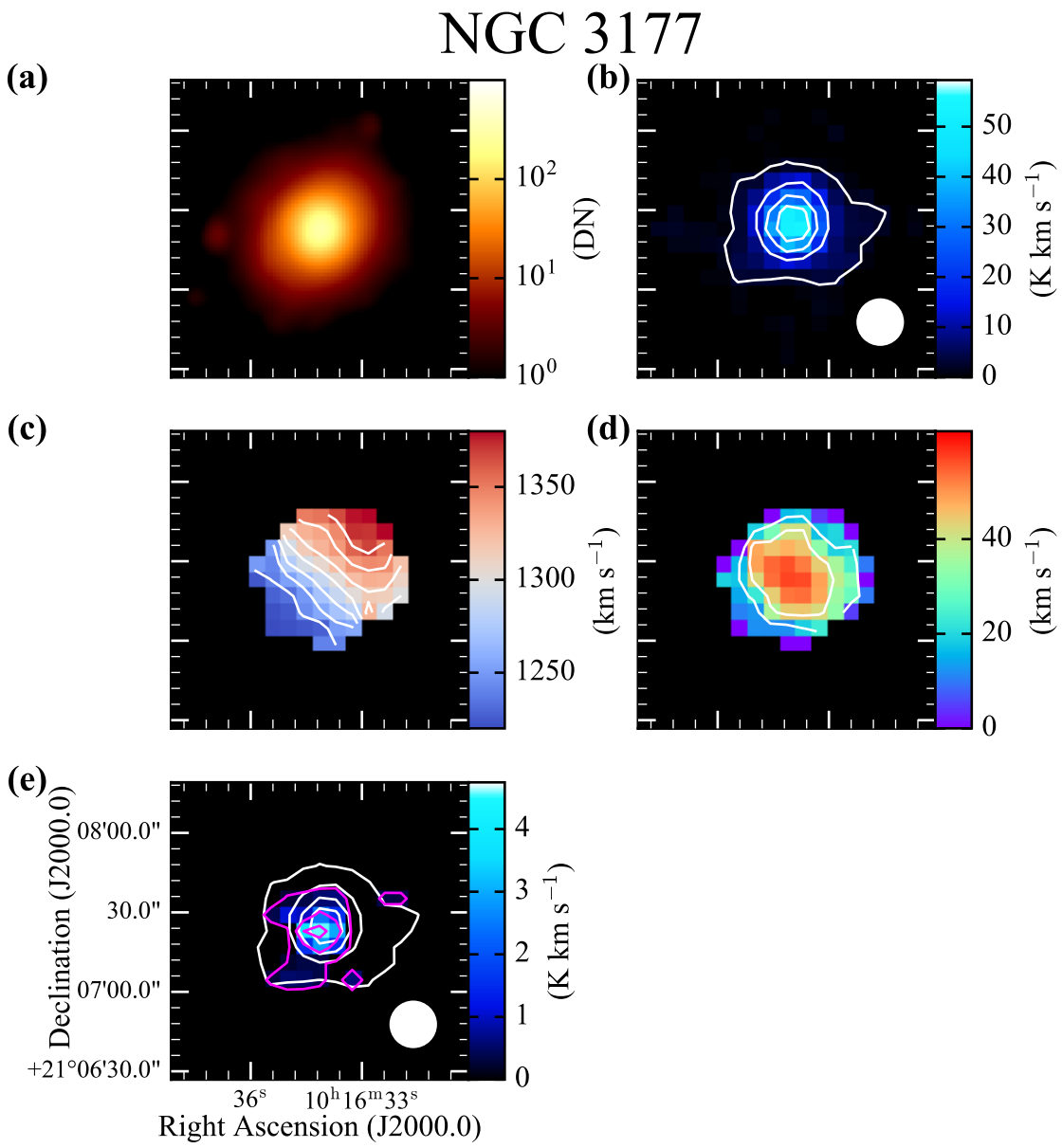

Supplementary fig. 47. Same as figure 12, but for NGC 3177. The contours are plotted at 5 %, 30 %, 55 %, and 80 % of the maximum intensity of 54.35 K km s^{-1} in (b) and (e) (*white*), in steps of 20 km s^{-1} in (c) and (d), and at 5 %, 45 %, and 85 % of the maximum intensity of 4.58 K km s^{-1} in (e) (*magenta*).

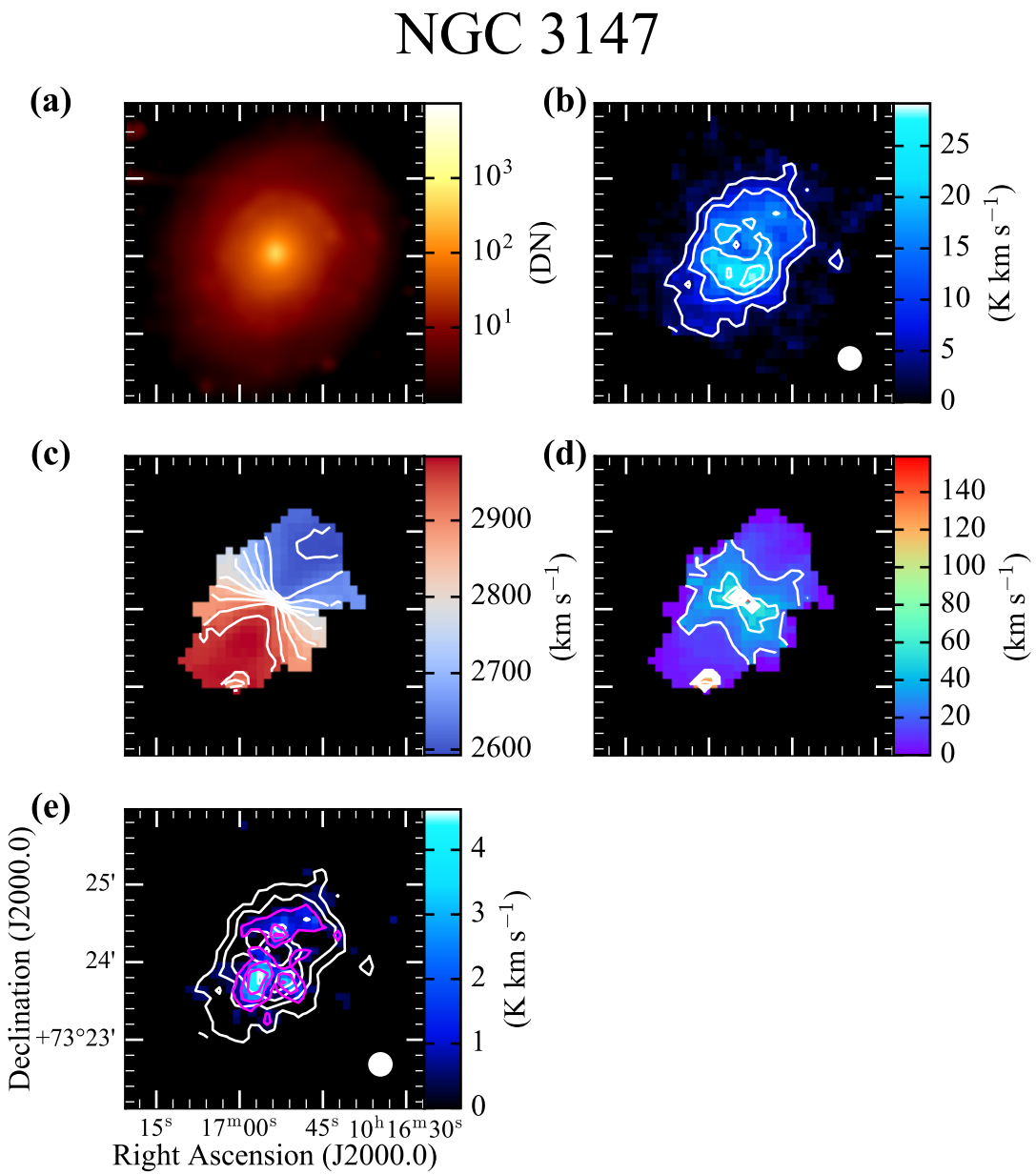

Supplementary fig. 48. Same as figure 12, but for NGC 3147. The contours are plotted at 15 %, 35 %, 60 %, and 85 % of the maximum intensity of 28.43 K km s^{-1} in (b) and (e) (*white*), in steps of 40 km s^{-1} in (c), in steps of 20 km s^{-1} in (d), and at 15 %, 45 %, and 75 % of the maximum intensity of 4.57 K km s^{-1} in (e) (*magenta*).

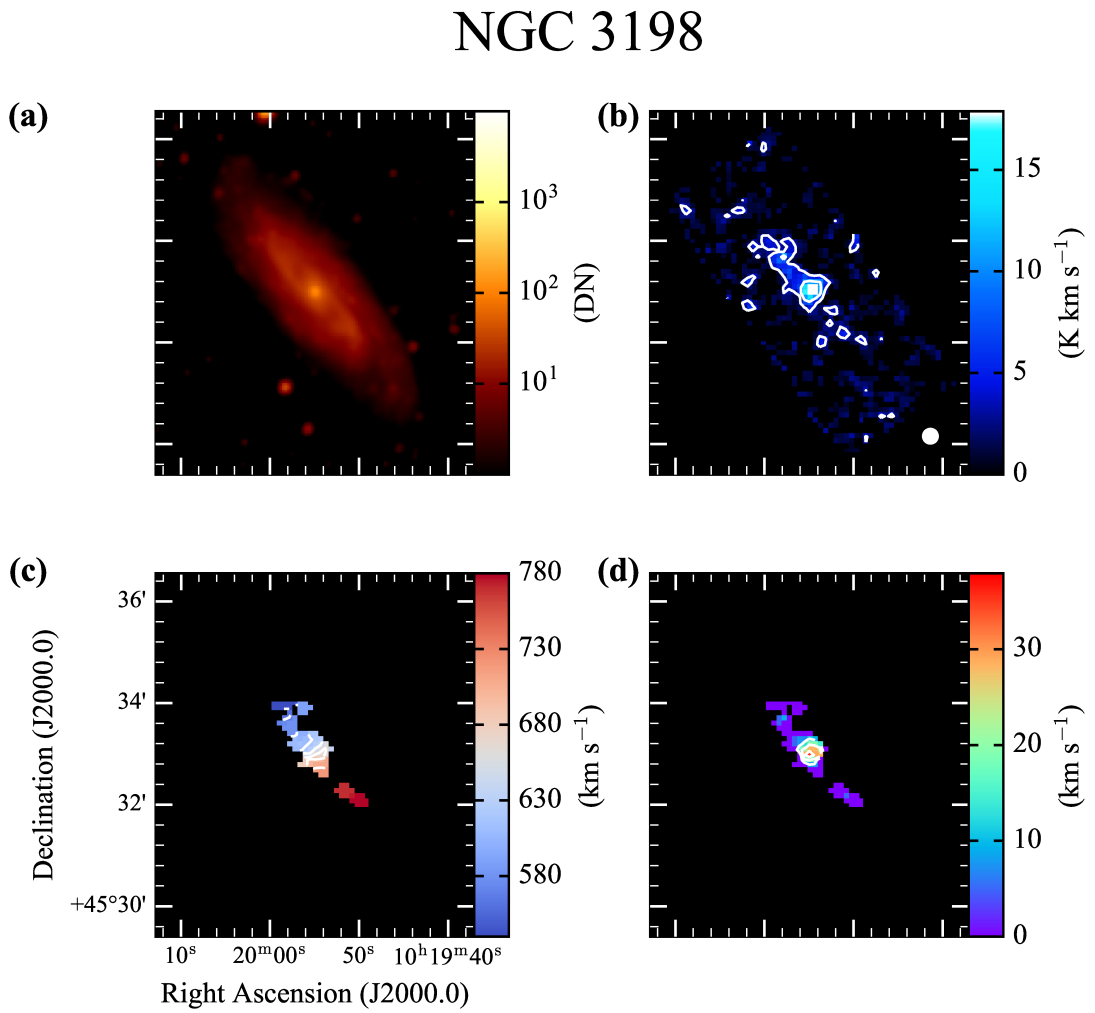

Supplementary fig. 49. Same as figure 12, but for NGC 3198. The contours are plotted at 15 % and 45 % of the maximum intensity of $20.87\,\mathrm{K\,km\,s^{-1}}$ in (b), in steps of $25\,\mathrm{km\,s^{-1}}$ step in (c), and in steps of $10\,\mathrm{km\,s^{-1}}$ in (d).

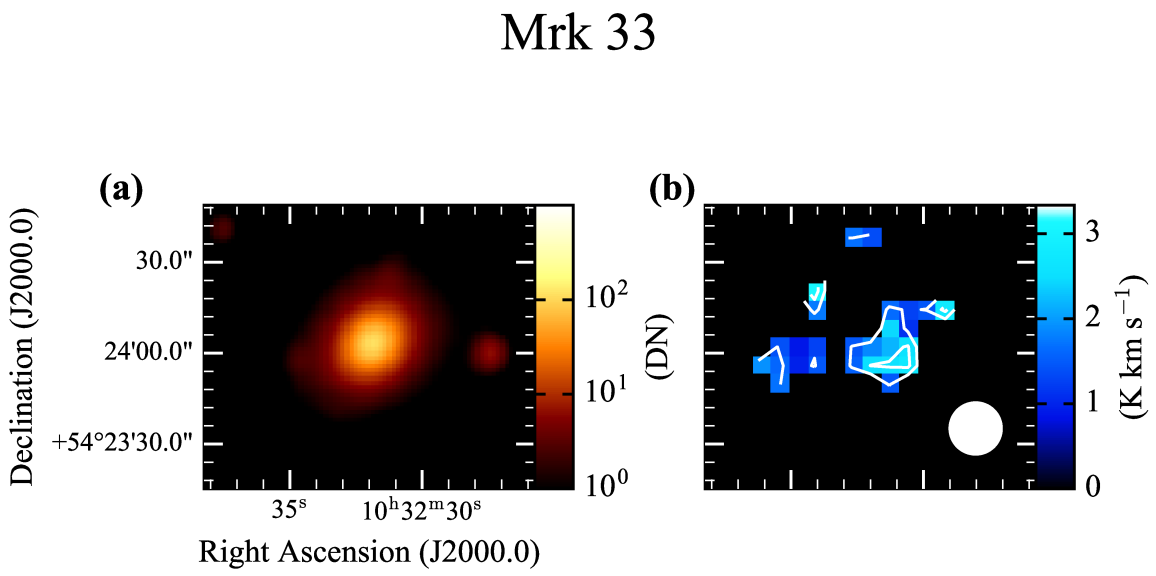

Supplementary fig. 50. Same as figure 12, but for Mrk 33. The contours are plotted at 45 % and 80 % of the maximum intensity of $3.11\,\mathrm{K\,km\,s^{-1}}$ in (b).

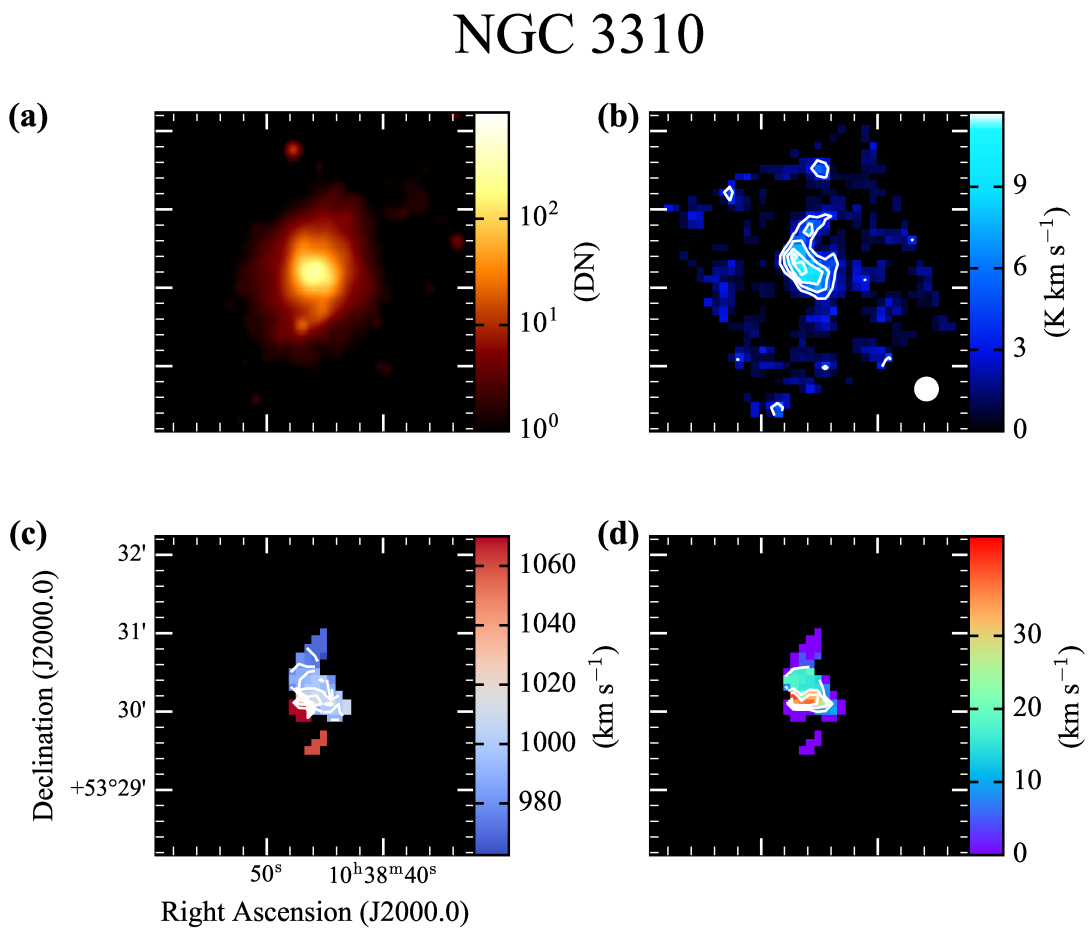

Supplementary fig. 51. Same as figure 12, but for NGC 3310. The contours are plotted at 30 %, 50 %, 70 %, and 90 % of the maximum intensity of $11.34\,\mathrm{K\,km\,s^{-1}}$ in (b) and in steps of $10\,\mathrm{km\,s^{-1}}$ in (c) and (d).

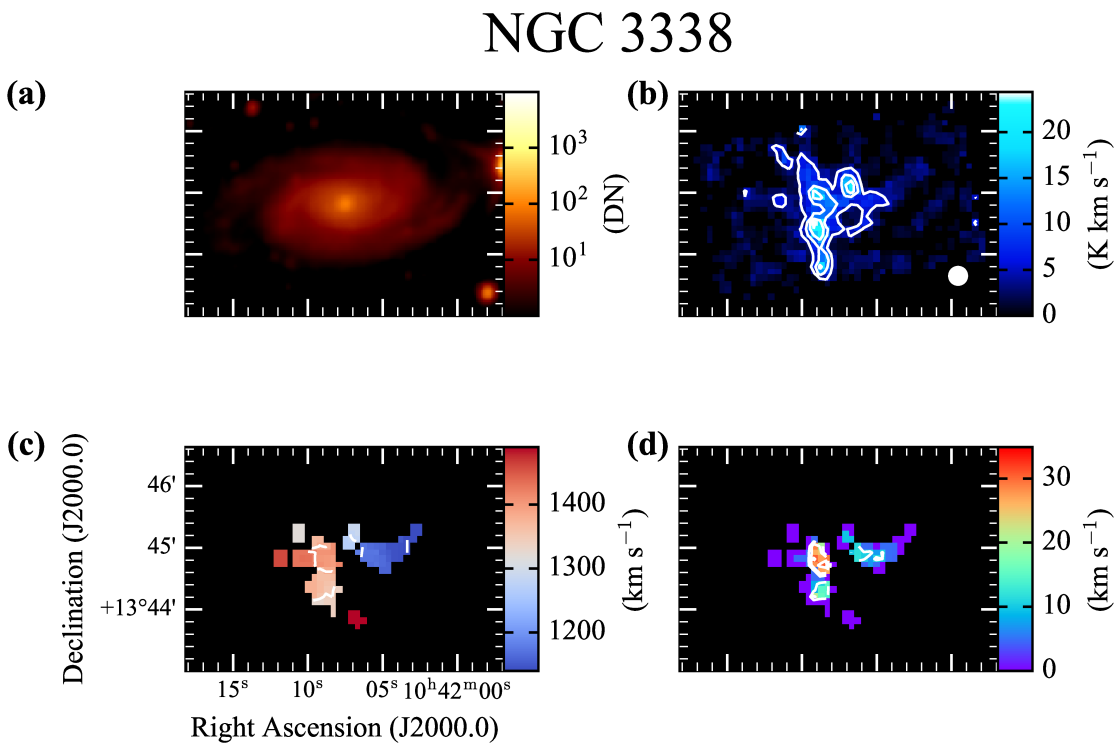

Supplementary fig. 52. Same as figure 12, but for NGC 3338. The contours are plotted at 20 %, 45 %, 70 %, and 95 % of the maximum intensity of $24.19\,\mathrm{K\,km\,s^{-1}}$ in (b), in steps of $35\,\mathrm{km\,s^{-1}}$ in (c), and in steps of $10\,\mathrm{km\,s^{-1}}$ in (d).

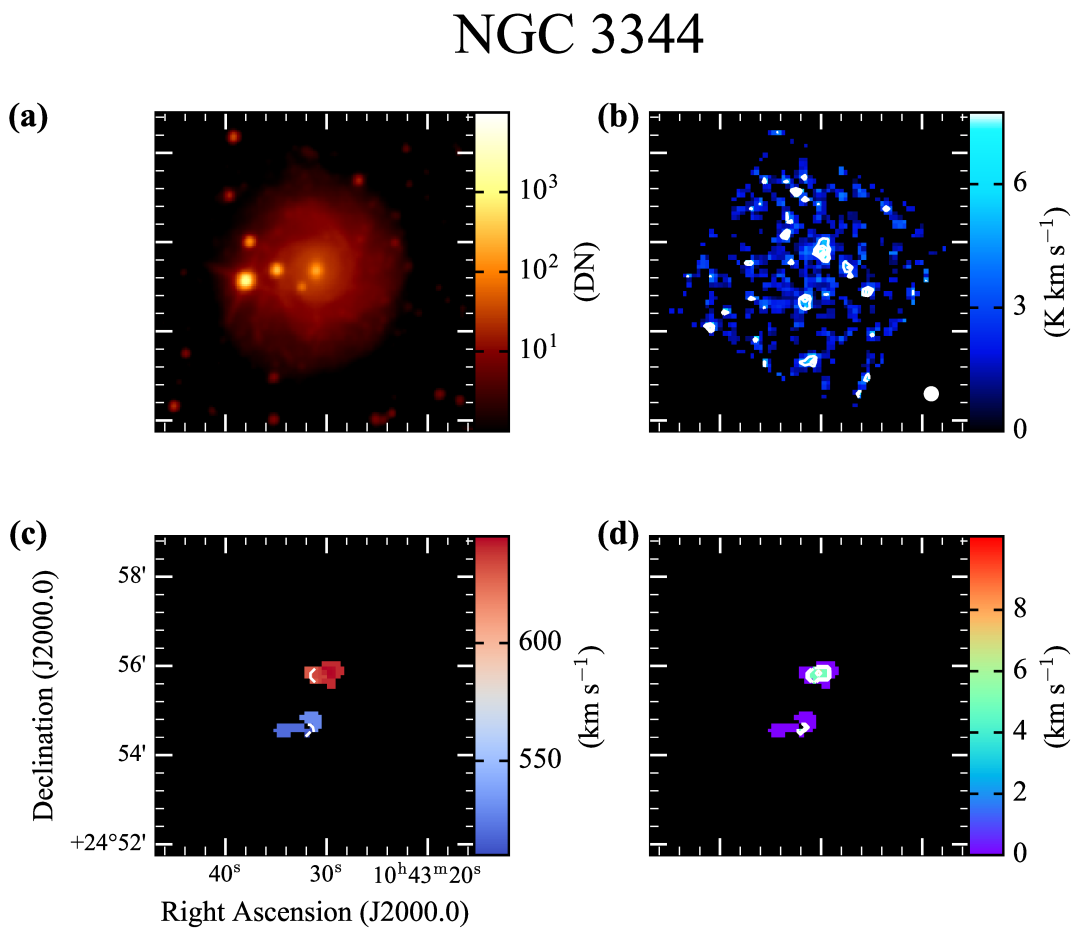

Supplementary fig. 53. Same as figure 12, but for NGC 3344. The contours are plotted at 45 %, 60 %, 75 %, and 90 % of the maximum intensity of $9.28\,\mathrm{K\,km\,s^{-1}}$ in (b), in steps of $15\,\mathrm{km\,s^{-1}}$ in (c), and in steps of $2\,\mathrm{km\,s^{-1}}$ in (d).

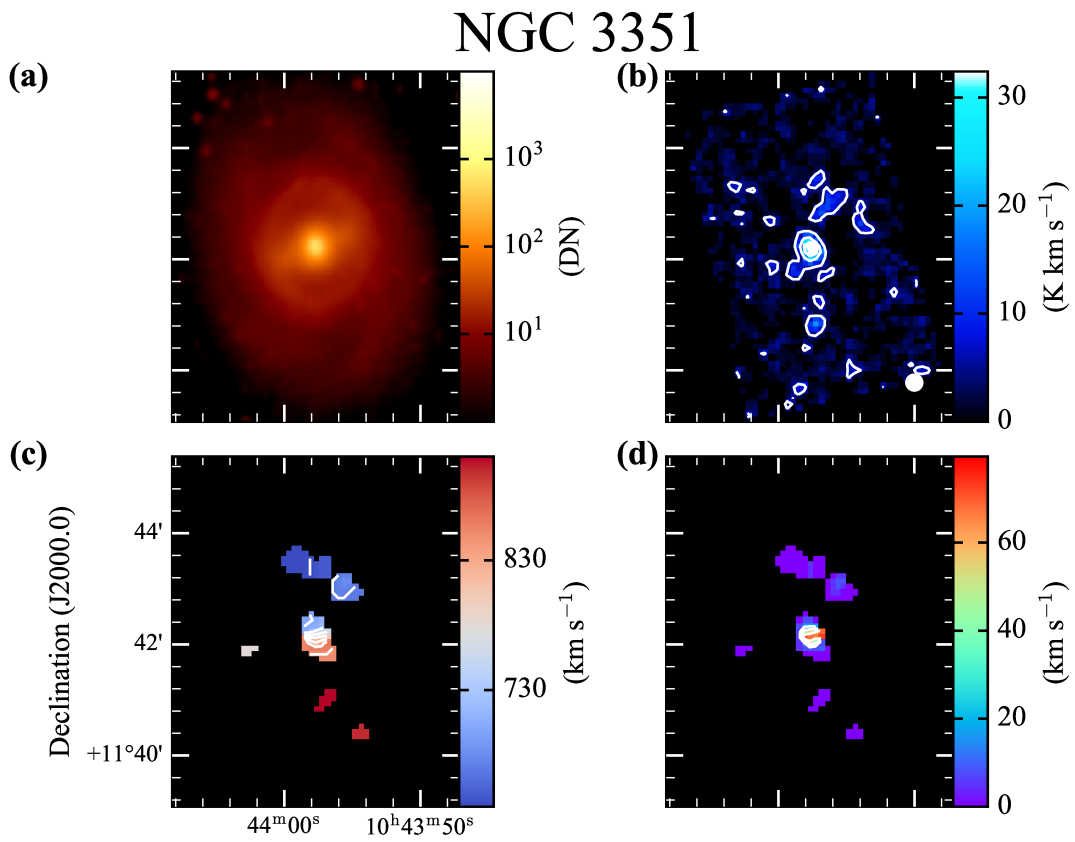

Supplementary fig. 54. Same as figure 12, but for NGC 3351. The contours are plotted at 10 %, 35 %, 60 %, and 85 % of the maximum intensity of $55.17\,\mathrm{K\,km\,s^{-1}}$ in (b), in steps of $30\,\mathrm{km\,s^{-1}}$ in (c), and in steps of $20\,\mathrm{km\,s^{-1}}$ in (d).

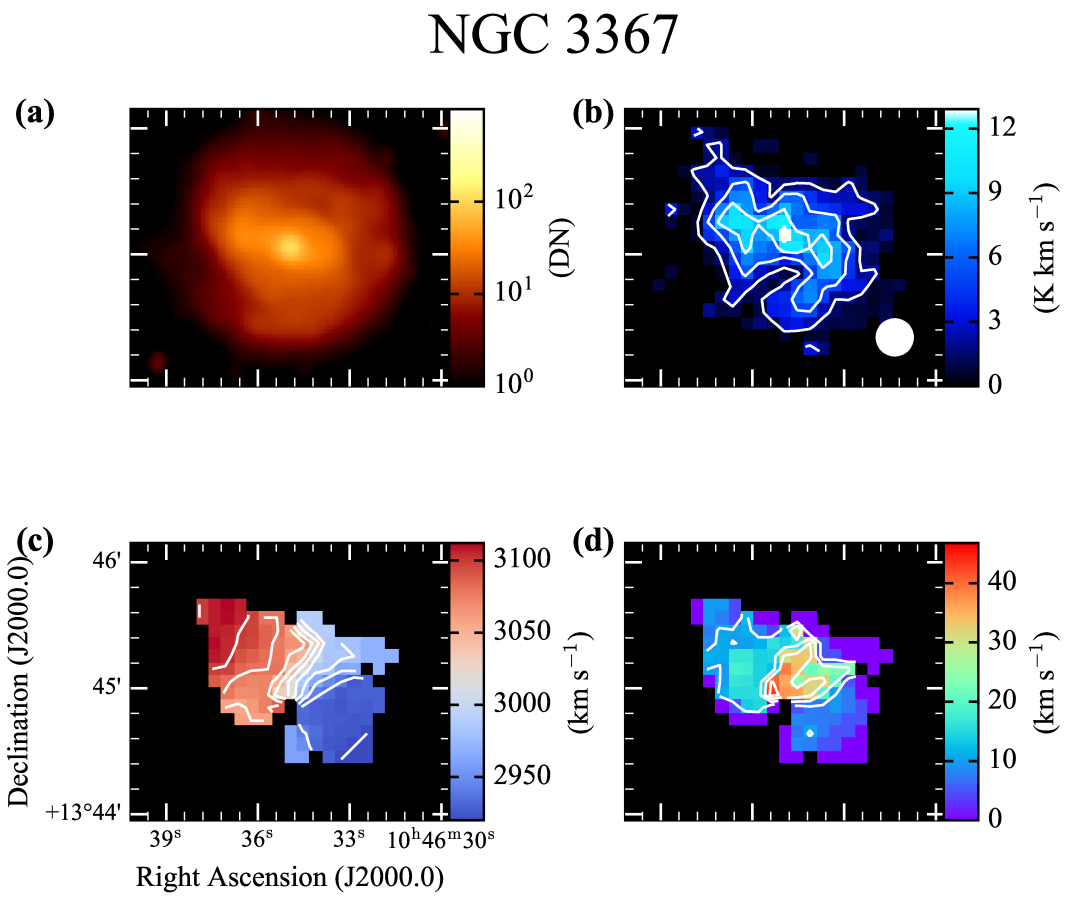

Supplementary fig. 55. Same as figure 12, but for NGC 3367. The contours are plotted at 15 %, 40 %, 65 %, and 90 % of the maximum intensity of $13.14\,\mathrm{K\,km\,s^{-1}}$ in (b), in steps of $20\,\mathrm{km\,s^{-1}}$ in (c), and in steps of $10\,\mathrm{km\,s^{-1}}$ in (d).

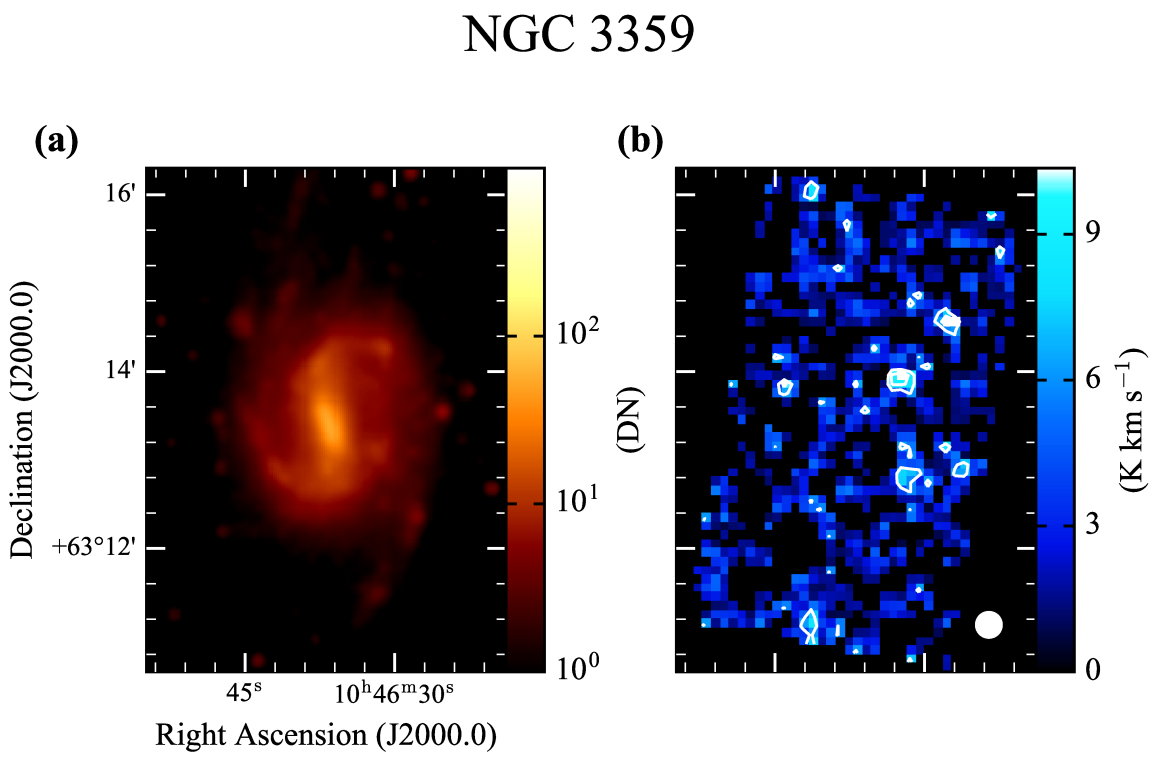

Supplementary fig. 56. Same as figure 12, but for NGC 3359. The contours are plotted at 50 % and 80 % of the maximum intensity of $11.02\,\mathrm{K\,km\,s^{-1}}$ in (b).

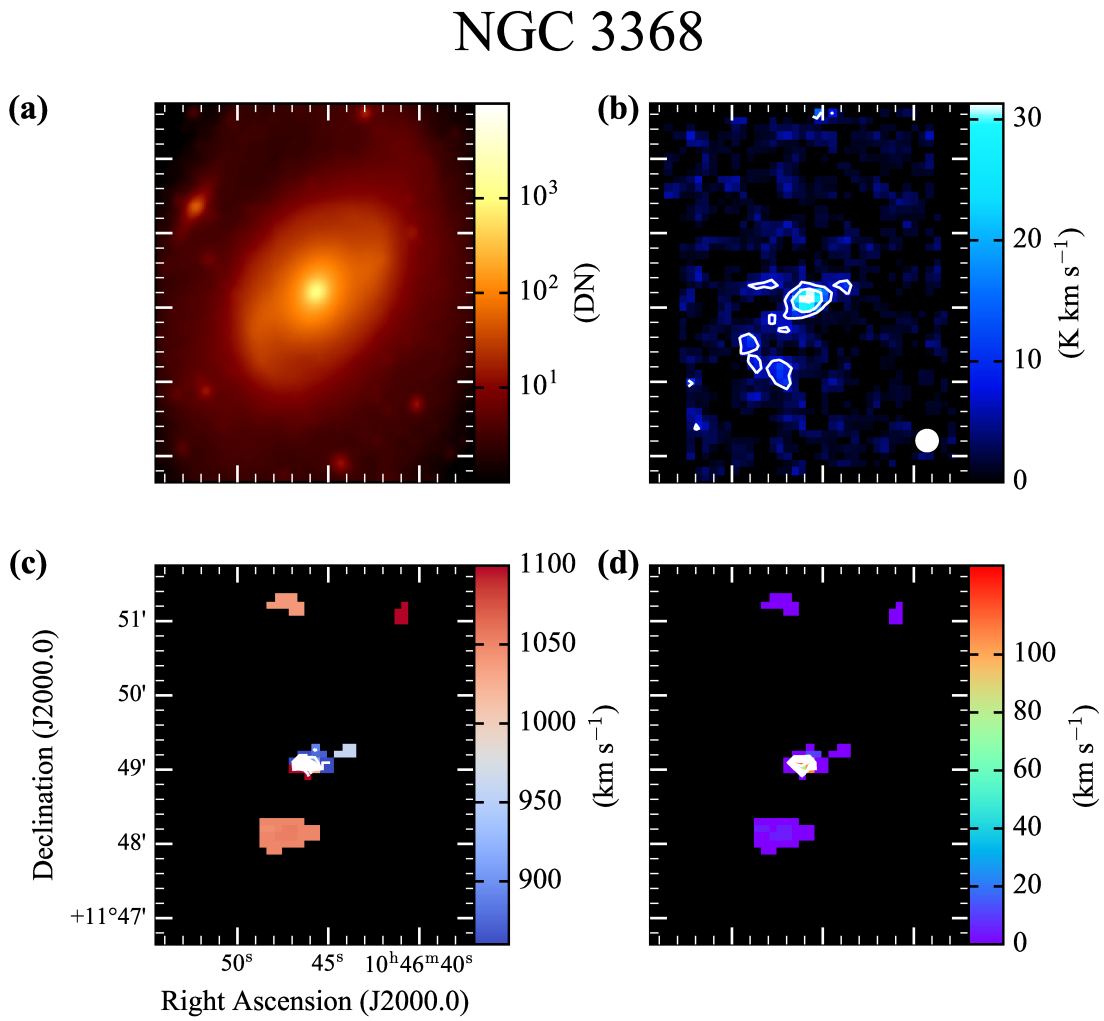

Supplementary fig. 57. Same as figure 12, but for NGC 3368. The contours are plotted at 15 %, 40 %, and 90 % of the maximum intensity of $47.27\,\mathrm{K\,km\,s^{-1}}$ in (b), in steps of $25\,\mathrm{km\,s^{-1}}$ in (c), and in steps of $20\,\mathrm{km\,s^{-1}}$ in (d).

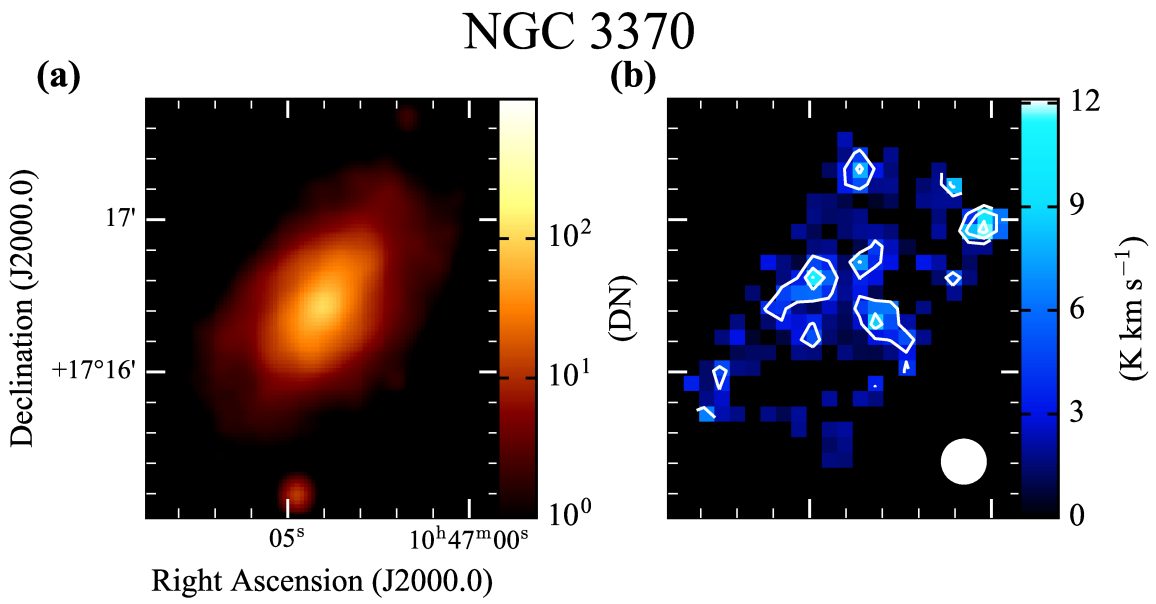

Supplementary fig. 58. Same as figure 12, but for NGC 3370. The contours are plotted at 30 %, 60 %, and 90 % of the maximum intensity of $11.70\,\mathrm{K\,km\,s^{-1}}$ in (b).

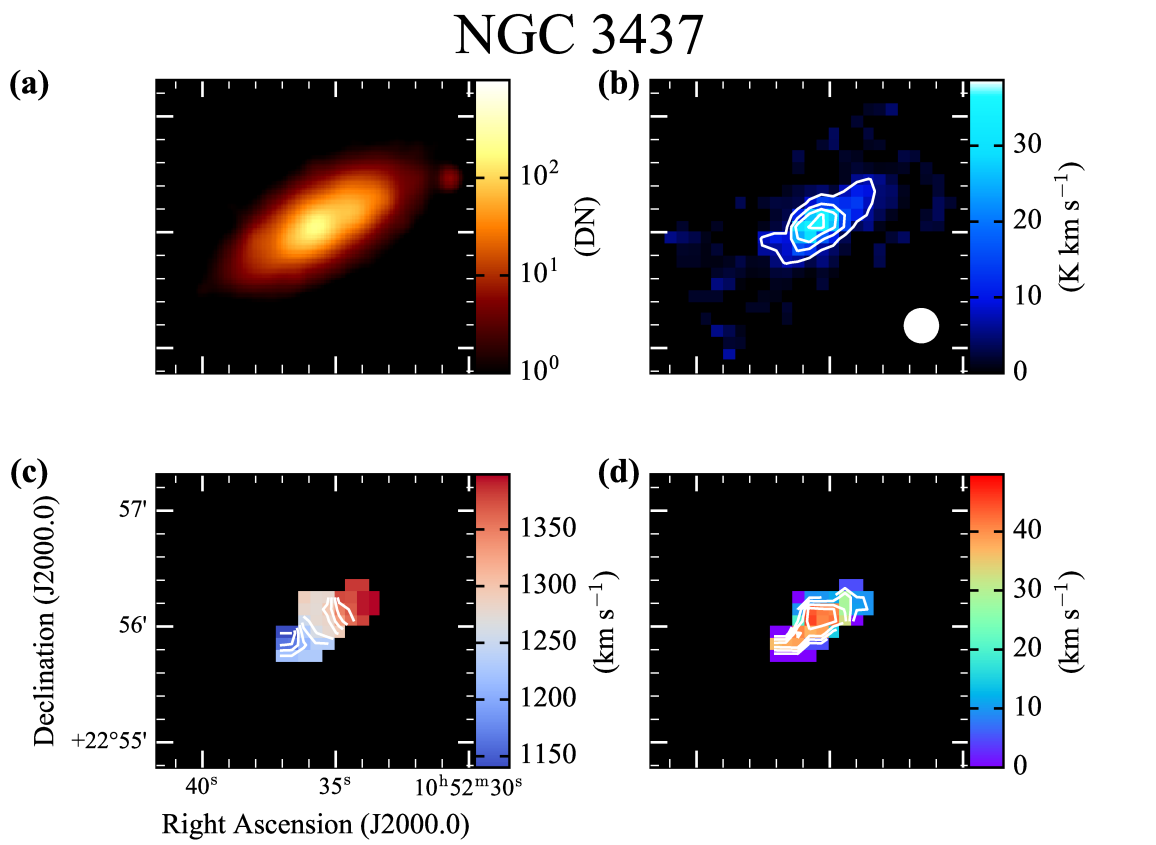

Supplementary fig. 59. Same as figure 12, but for NGC 3437. The contours are plotted at 20 %, 45 %, 70 %, and 95 % of the maximum intensity of $35.56\,\mathrm{K\,km\,s^{-1}}$ in (b), in steps of $25\,\mathrm{km\,s^{-1}}$ in (c), and in steps of $10\,\mathrm{km\,s^{-1}}$ in (d).

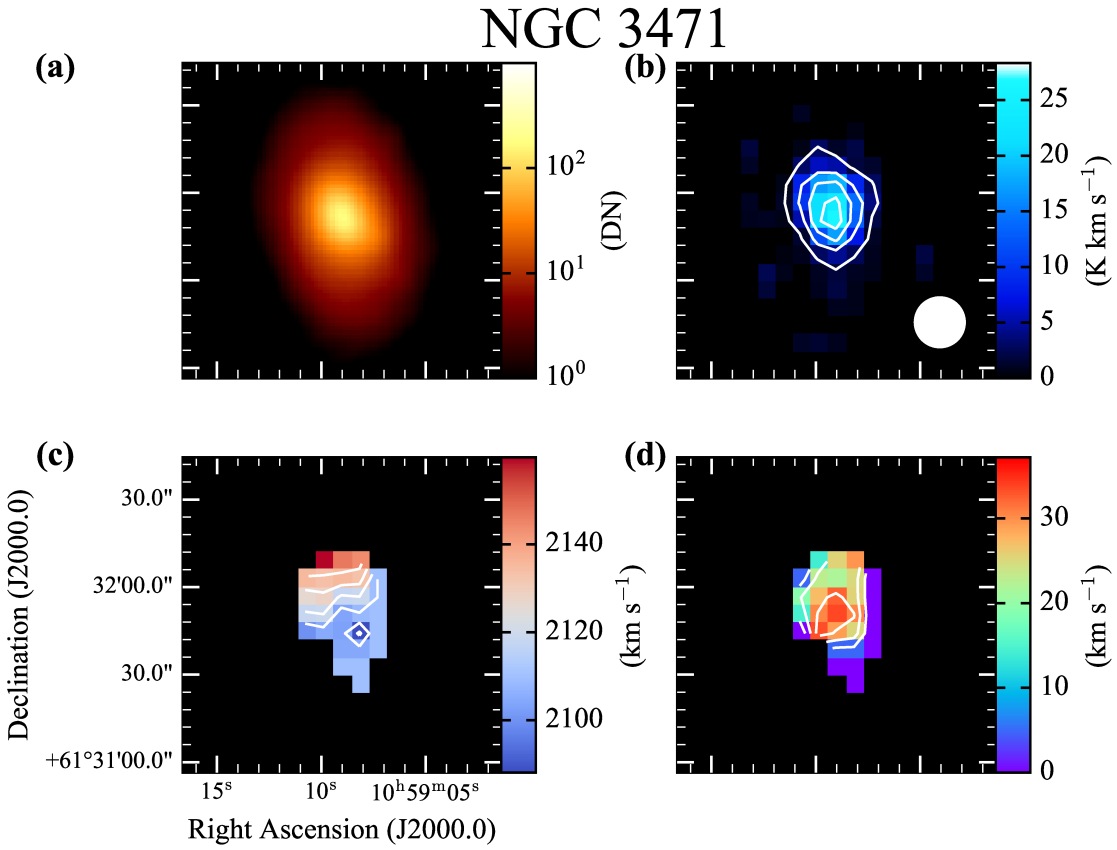

Supplementary fig. 60. Same as figure 12, but for NGC 3471. The contours are plotted at 10 %, 35 %, 60 %, and 85 % of the maximum intensity of $26.48\,\mathrm{K\,km\,s^{-1}}$ in (b) and in steps of $10\,\mathrm{km\,s^{-1}}$ in (c) and (d).

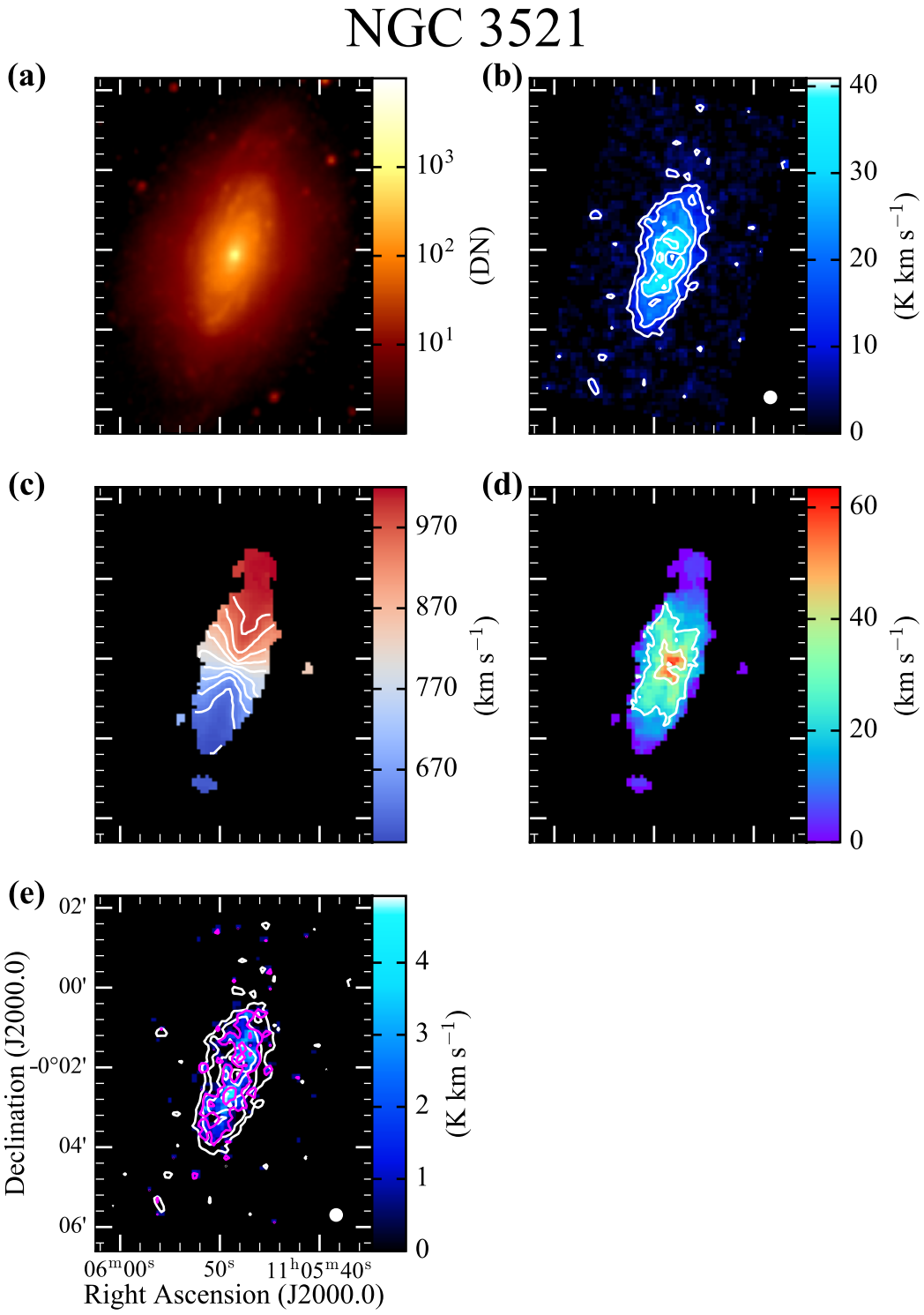

Supplementary fig. 61. Same as figure 12, but for NGC 3521. The contours are plotted at 15 %, 35 %, 60 %, and 80 % of the maximum intensity of $45.62\,\mathrm{K\,km\,s^{-1}}$ in (b) and (e) (*white*), in steps of $45\,\mathrm{km\,s^{-1}}$ in (c), in steps of $20\,\mathrm{km\,s^{-1}}$ in (d), and at 15 % and 65 % of the maximum intensity of $5.51\,\mathrm{K\,km\,s^{-1}}$ in (e) (*magenta*).

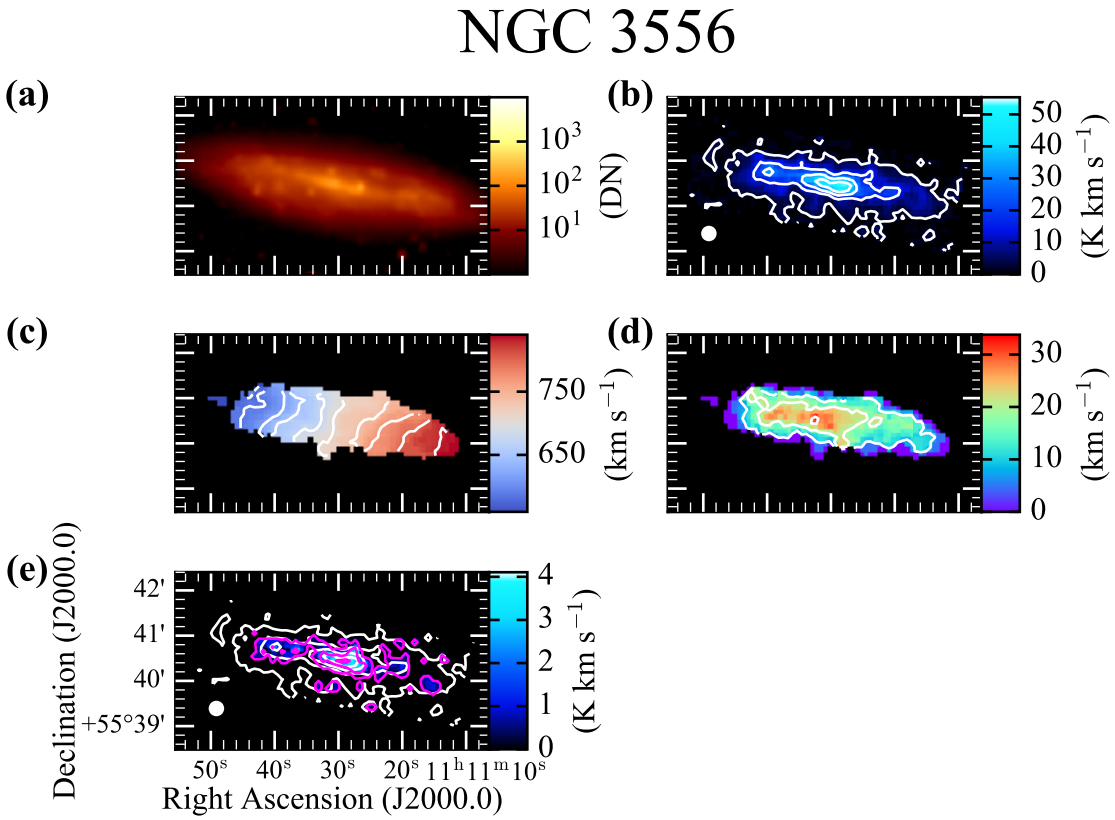

Supplementary fig. 62. Same as figure 12, but for NGC 3556. The contours are plotted at 5 %, 30 %, 55 %, and 80 % of the maximum intensity of 53.23 K km s^{-1} in (b) and (e) (*white*), in steps of 30 km s^{-1} in (c), in steps of 10 km s^{-1} in (d), and at 5 %, 45 %, and 85 % of the maximum intensity of 4.56 K km s^{-1} in (e) (*magenta*).

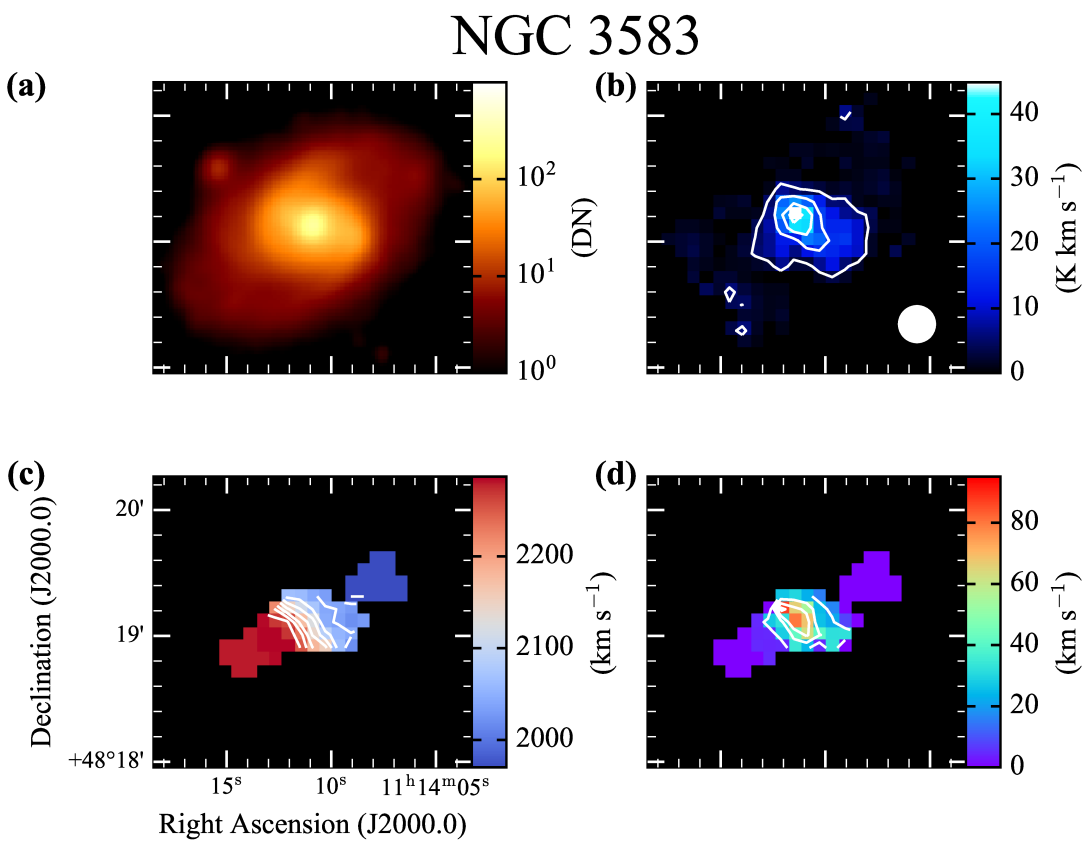

Supplementary fig. 63. Same as figure 12, but for NGC 3583. The contours are plotted at 10 %, 35 %, 60 %, and 85 % of the maximum intensity of $46.82\,\mathrm{K\,km\,s^{-1}}$ in (b), in steps of $35\,\mathrm{km\,s^{-1}}$ in (c), and in steps of $20\,\mathrm{km\,s^{-1}}$ in (d).

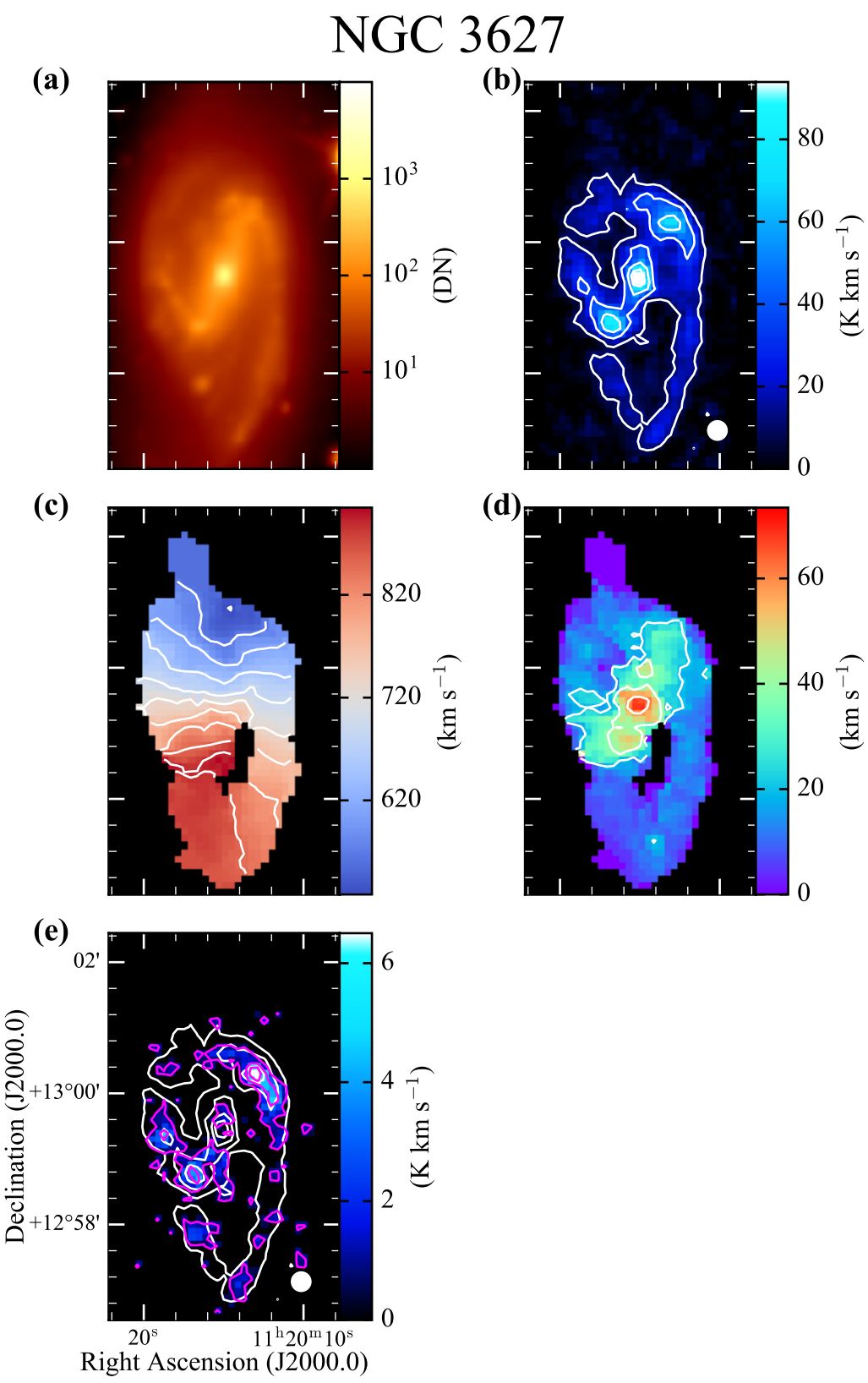

Supplementary fig. 64. Same as figure 12, but for NGC 3627. The contours are plotted at 10 %, 30 %, 55 %, and 80 % of the maximum intensity of 109.87 K km s^{-1} in (b) and (e) (*white*), in steps of 40 km s^{-1} in (c), in steps of 20 km s^{-1} in (d), and at 10 %, 45 %, and 80 % of the maximum intensity of 7.88 K km s^{-1} in (e) (*magenta*).

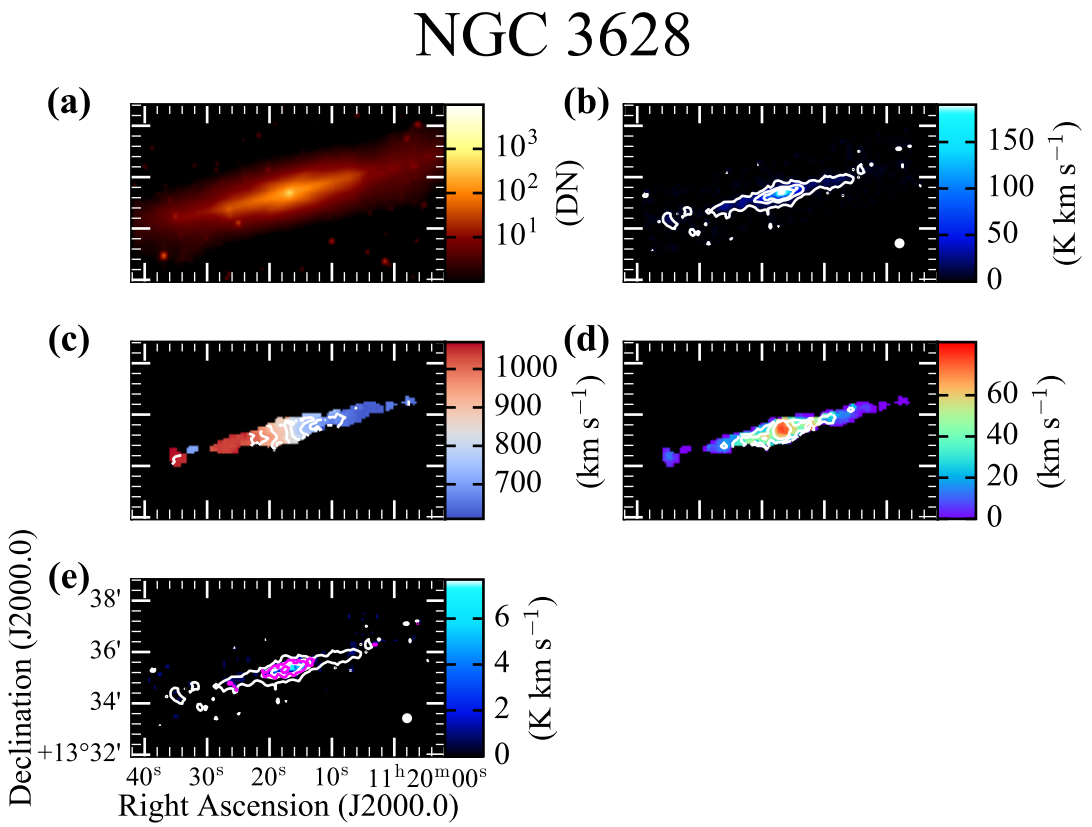

Supplementary fig. 65. Same as figure 12, but for NGC 3628. The contours are plotted at 3 %, 15 %, and 30 % of the maximum intensity of $248.31\,\mathrm{K\,km\,s^{-1}}$ in (b) and (e) (*white*), in steps of $50\,\mathrm{km\,s^{-1}}$ in (c), in steps of $20\,\mathrm{km\,s^{-1}}$ in (d), and at 10 % and 60 % of the maximum intensity of $14.57\,\mathrm{K\,km\,s^{-1}}$ in (e) (*magenta*).

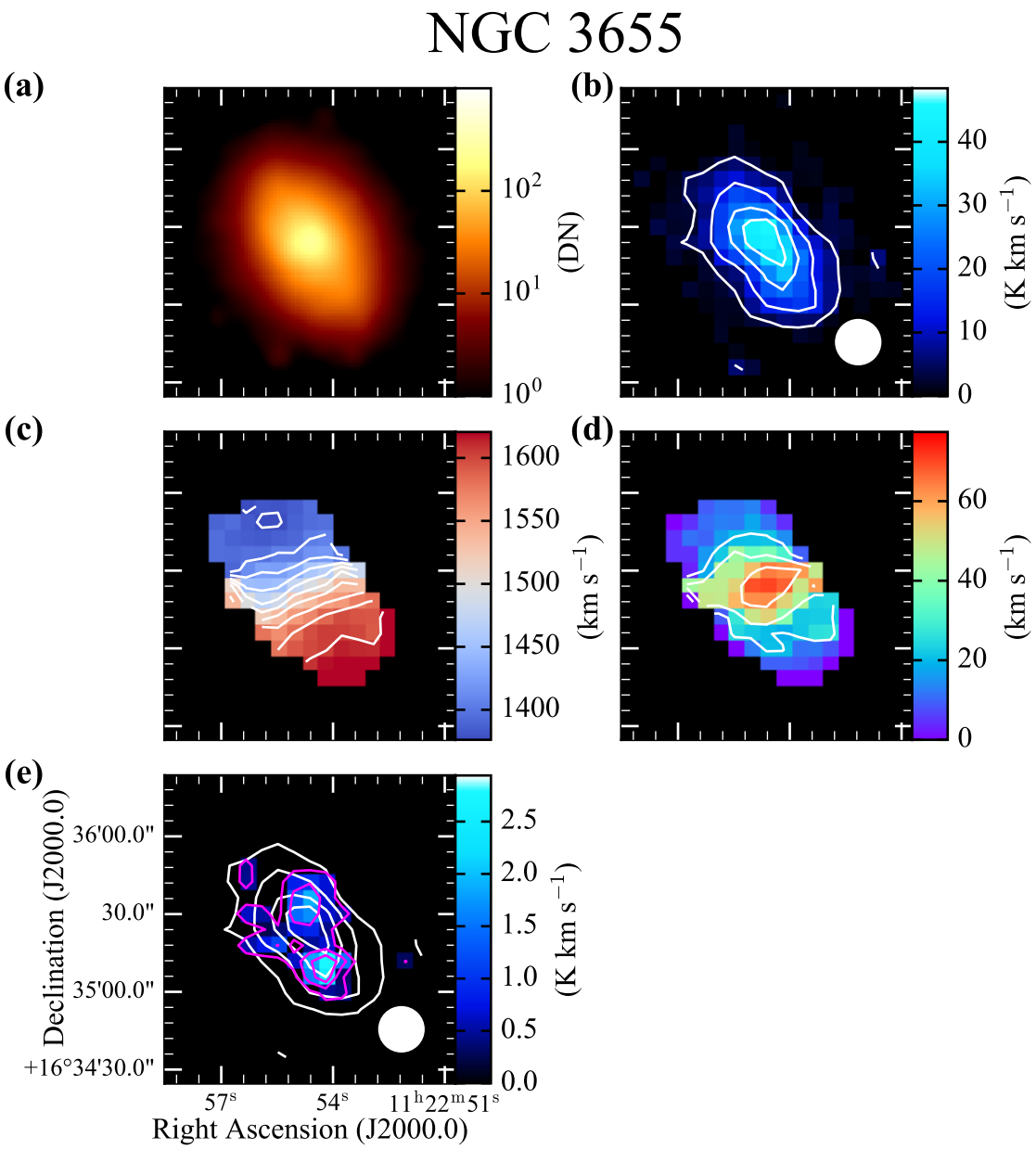

Supplementary fig. 66. Same as figure 12, but for NGC 3655. The contours are plotted at 10 %, 30 %, 55 %, and 80 % of the maximum intensity of 45.22 K km s^{-1} in (b) and (e) (*white*), in steps of 25 km s^{-1} in (c), in steps of 20 km s^{-1} in (d), and at 10 %, 40 %, and 70 % of the maximum intensity of 2.77 K km s^{-1} in (e) (*magenta*).

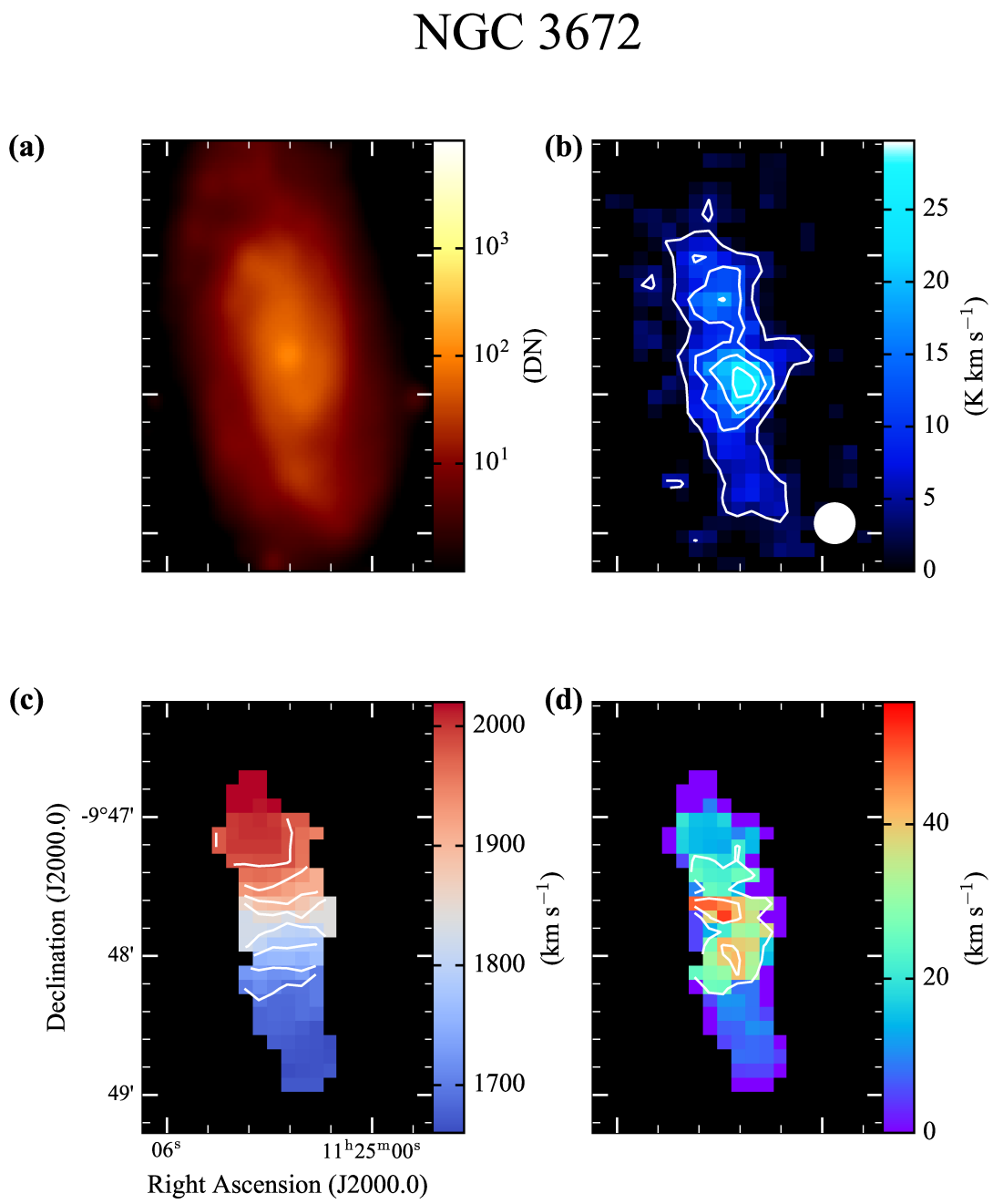

Supplementary fig. 67. Same as figure 12, but for NGC 3672. The contours are plotted at 15 %, 40 %, 65 %, and 90 % of the maximum intensity of 27.12 K km s^{-1} in (b), in steps of 40 km s^{-1} in (c), and in steps of 20 km s^{-1} in (d).

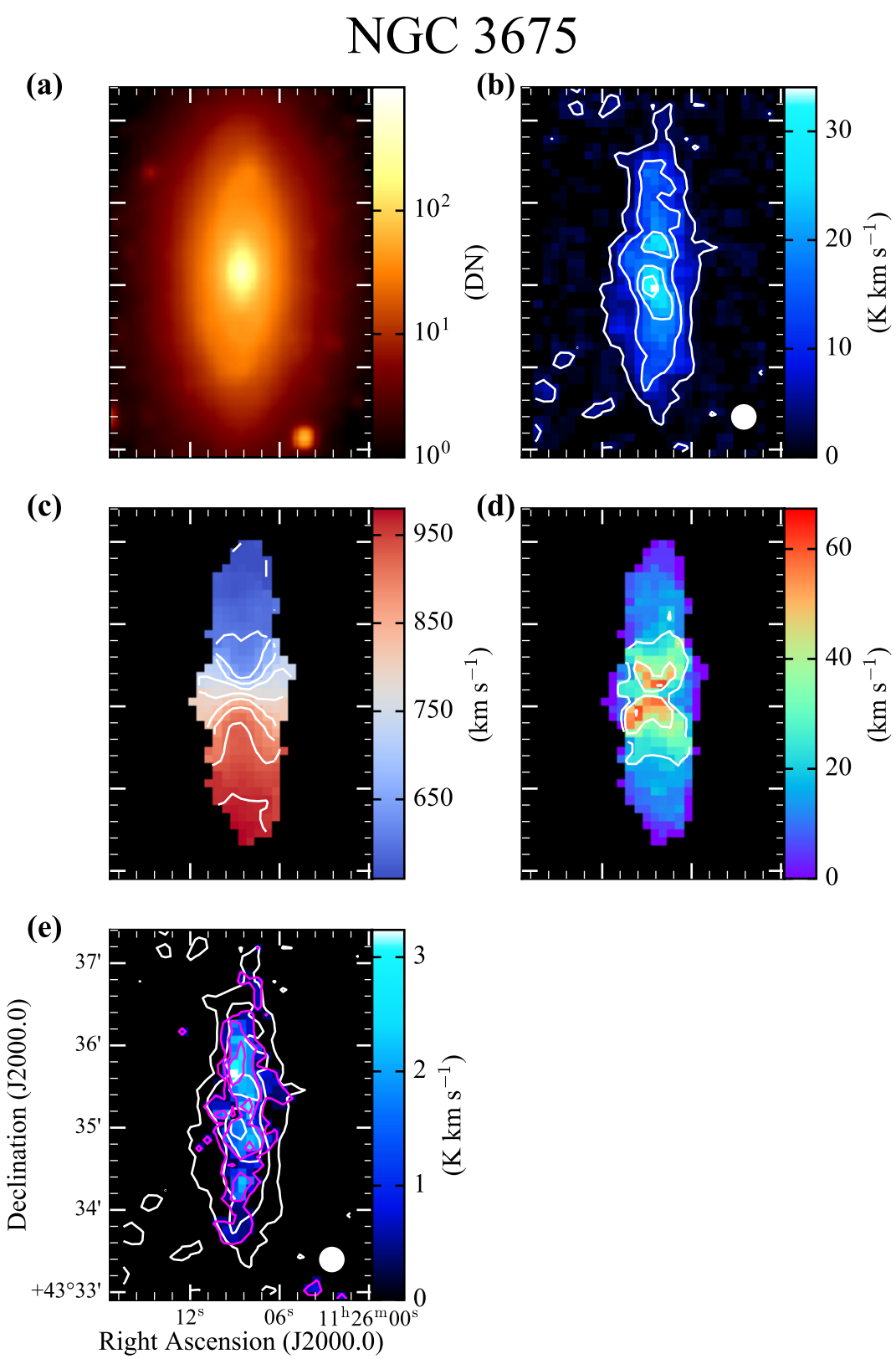

Supplementary fig. 68. Same as figure 12, but for NGC 3675. The contours are plotted at 10 %, 35 %, 60 %, and 85 % of the maximum intensity of 33.93 K km s^{-1} in (b) and (e) (*white*), in steps of 45 km s^{-1} in (c), in steps of 20 km s^{-1} in (d), and at 10 %, 40 %, and 70 % of the maximum intensity of 3.35 K km s^{-1} in (e) (*magenta*).

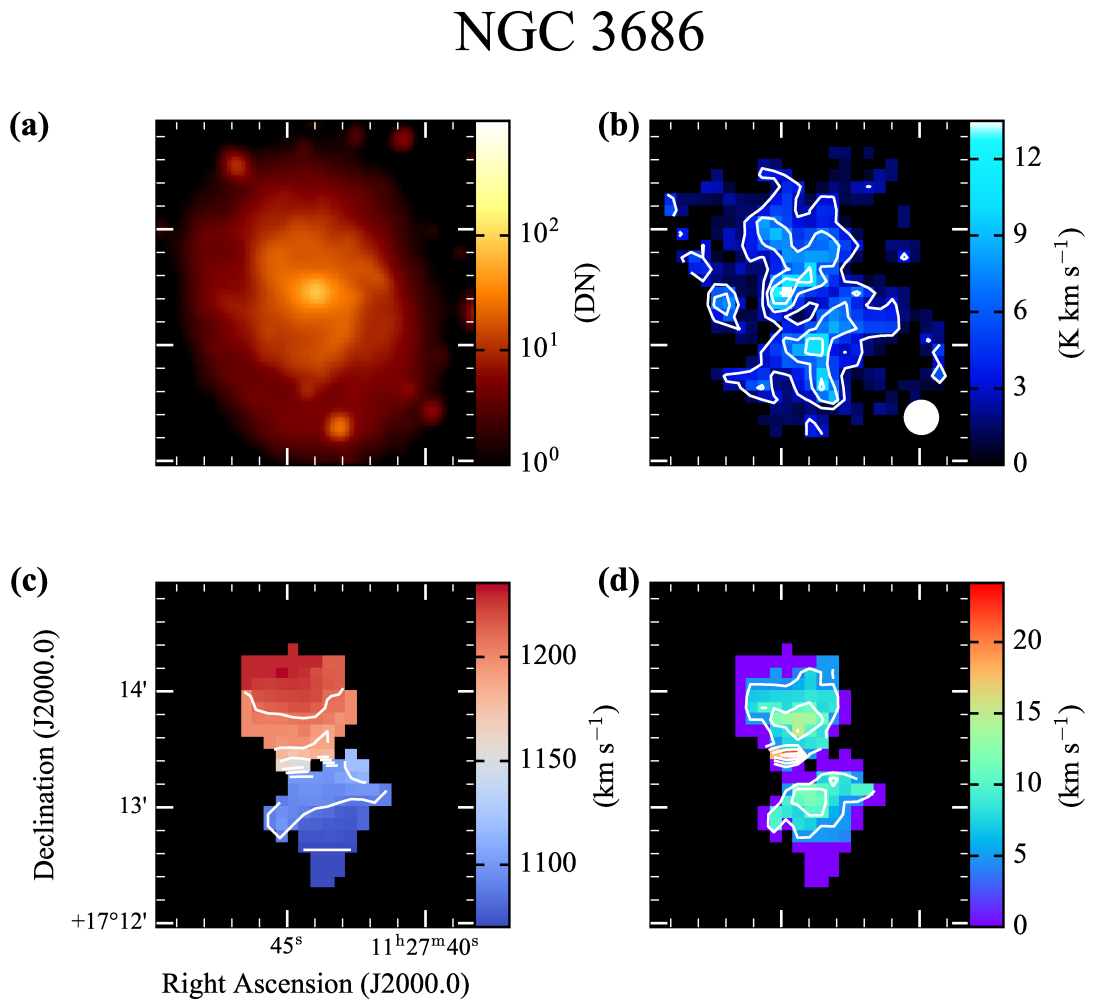

Supplementary fig. 69. Same as figure 12, but for NGC 3686. The contours are plotted at 20 %, 45 %, 70 %, and 95 % of the maximum intensity of $14.12\,\mathrm{K\,km\,s^{-1}}$ in (b), in steps of $20\,\mathrm{km\,s^{-1}}$ in (c), and in steps of $5\,\mathrm{km\,s^{-1}}$ in (d).

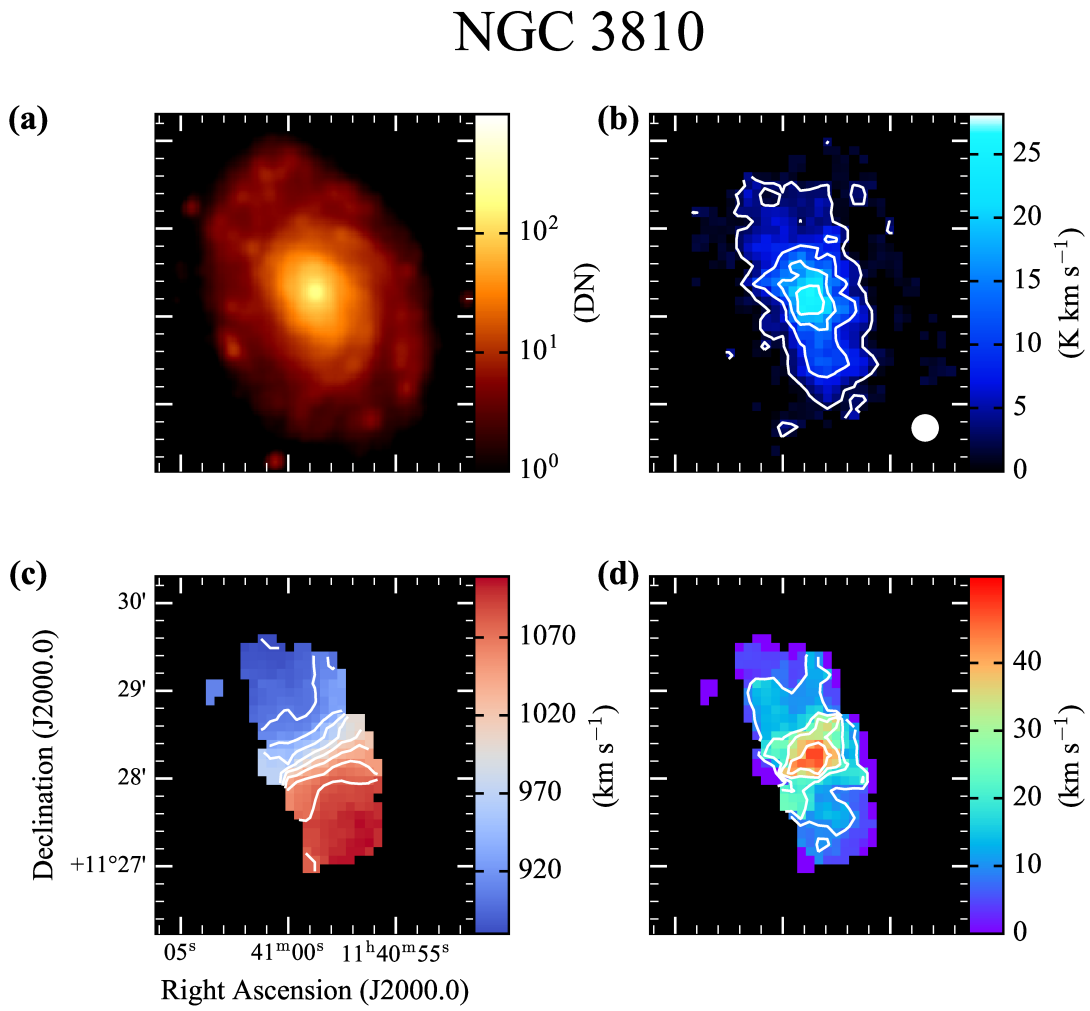

Supplementary fig. 70. Same as figure 12, but for NGC 3810. The contours are plotted at 10 %, 35 %, 60 %, and 85 % of the maximum intensity of 26.68 K km s^{-1} in (b), in steps of 25 km s^{-1} in (c), and in steps of 10 km s^{-1} in (d).

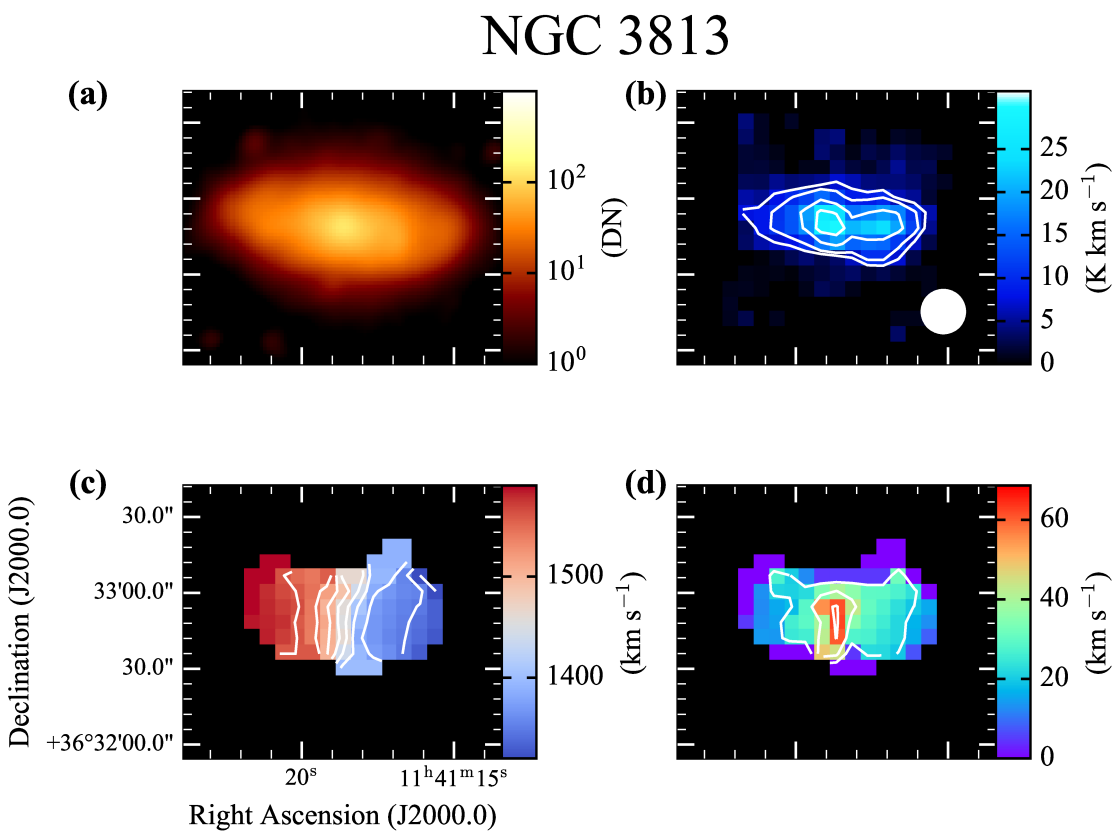

Supplementary fig. 71. Same as figure 12, but for NGC 3813. The contours are plotted at 25 %, 35 %, 60 %, and 85 % of the maximum intensity of $29.56\,\mathrm{K\,km\,s^{-1}}$ in (b), in steps of $30\,\mathrm{km\,s^{-1}}$ in (c), and in steps of $20\,\mathrm{km\,s^{-1}}$ in (d).

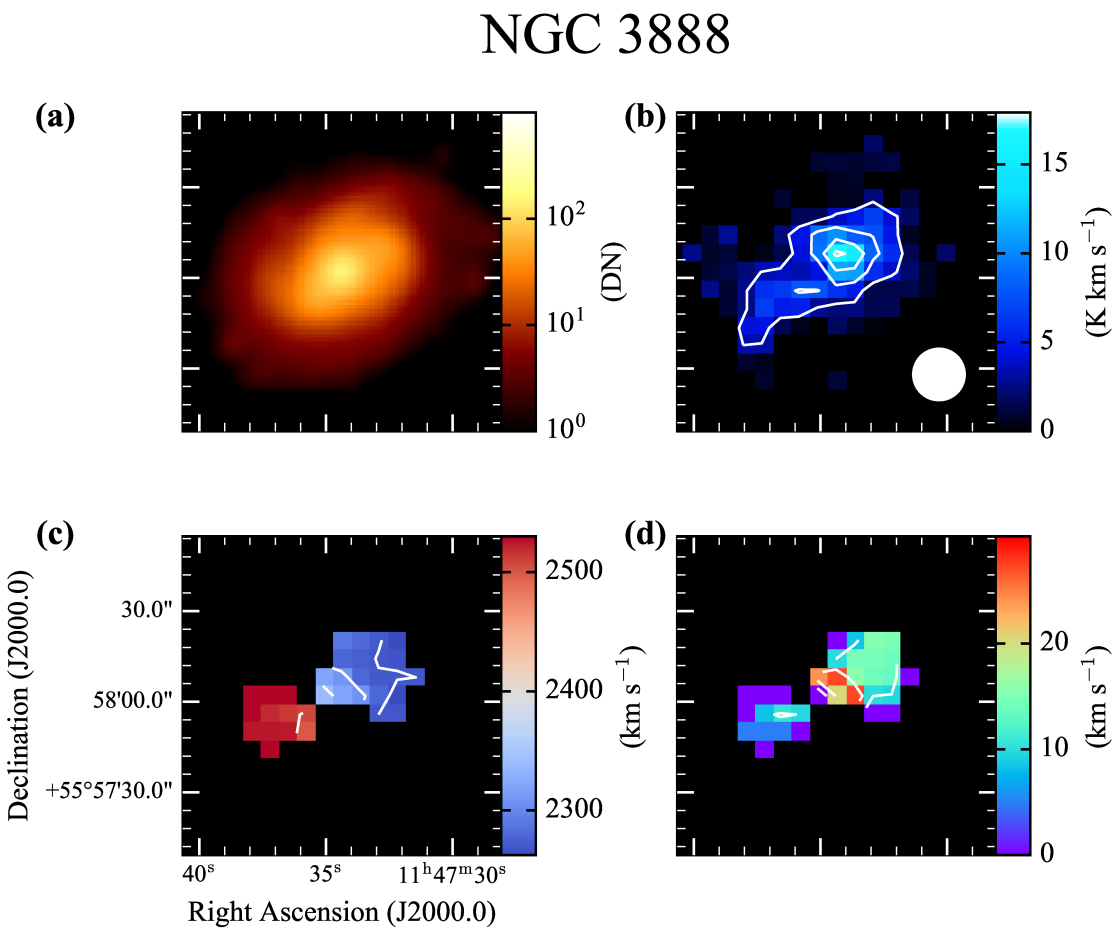

Supplementary fig. 72. Same as figure 12, but for NGC 3888. The contours are plotted at 20 %, 45 %, 70 %, and 95 % of the maximum intensity of $16.93\,\mathrm{K\,km\,s^{-1}}$ in (b), in steps of $30\,\mathrm{km\,s^{-1}}$ in (c), and in steps of $10\,\mathrm{km\,s^{-1}}$ in (d).

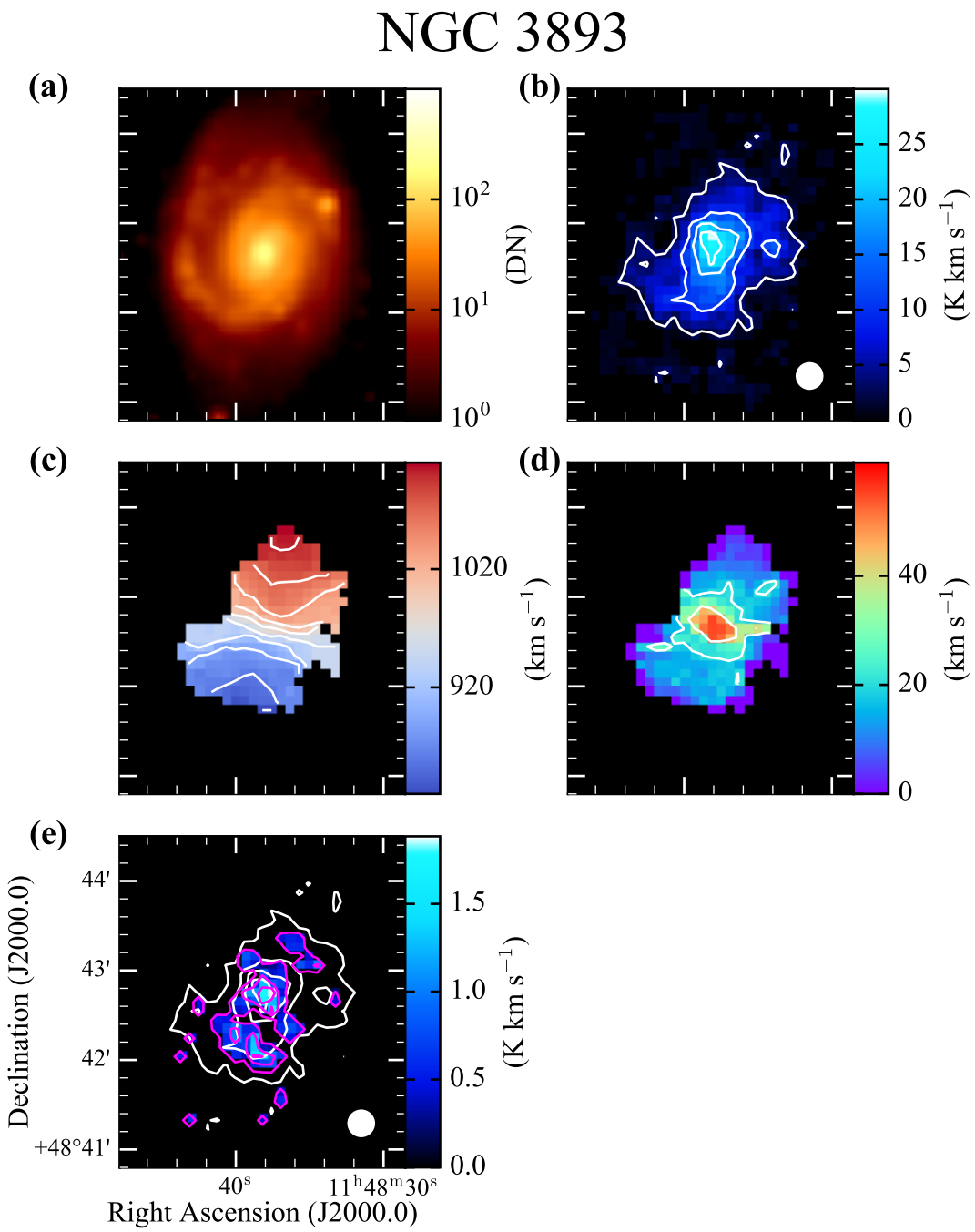

Supplementary fig. 73. Same as figure 12, but for NGC 3893. The contours are plotted at 10 %, 35 %, 60 %, and 85 % of the maximum intensity of 29.76 K km s^{-1} in (b) and (e) (*white*), in steps of 30 km s^{-1} in (c), in steps of 20 km s^{-1} in (d), and at 10 %, 40 %, and 70 % of the maximum intensity of 2.12 K km s^{-1} in (e) (*magenta*).

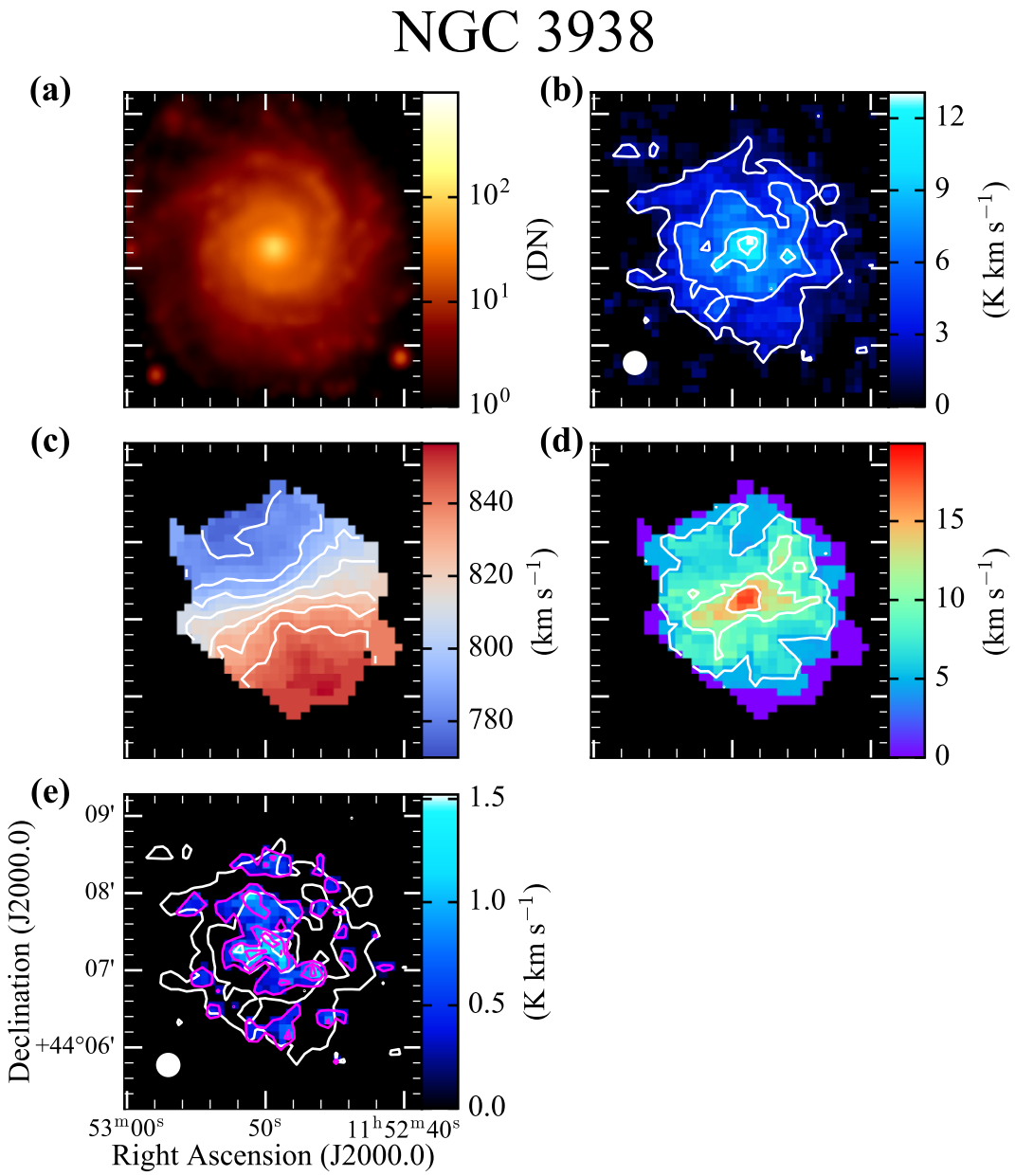

Supplementary fig. 74. Same as figure 12, but for NGC 3938. The contours are plotted at 15 %, 35 %, 60 %, and 85 % of the maximum intensity of 13.70 K km s^{-1} in (b) and (e) (*white*), in steps of 10 km s^{-1} in (c), in steps of 5 km s^{-1} in (d), and at 15 %, 45 %, and 75 % of the maximum intensity of 1.69 K km s^{-1} in (e) (*magenta*).

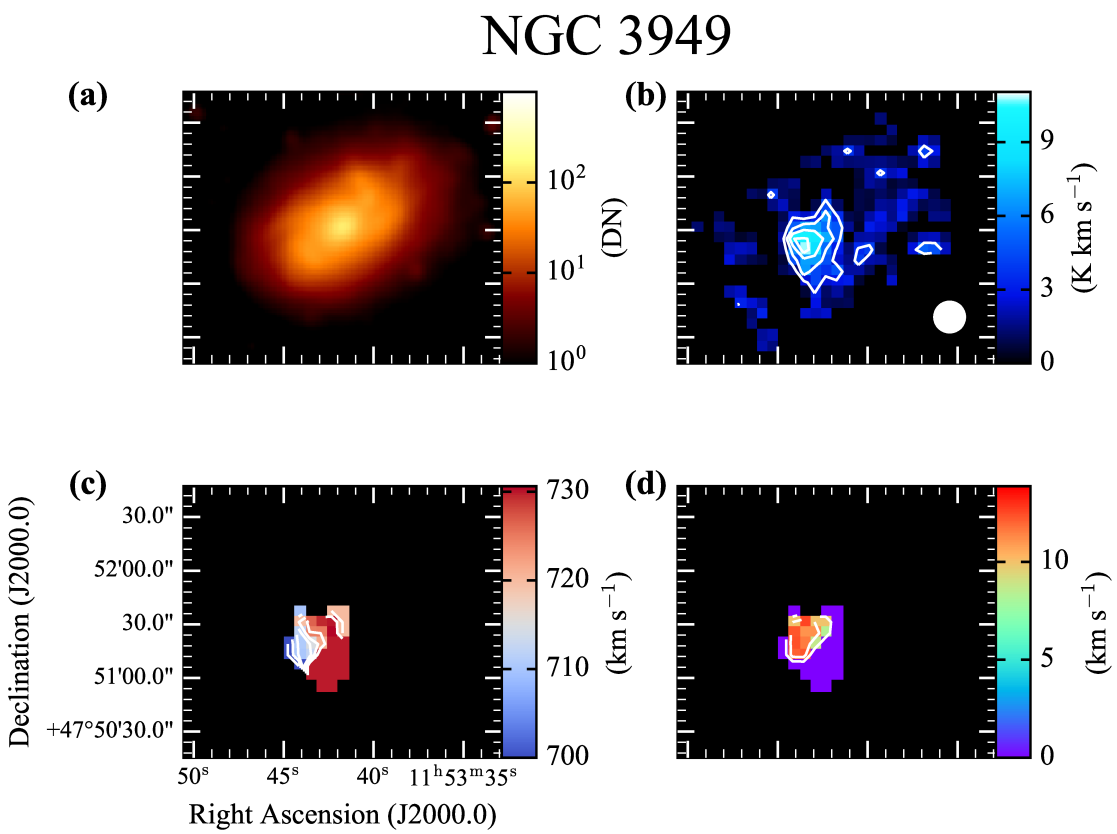

Supplementary fig. 75. Same as figure 12, but for NGC 3949. The contours are plotted at 30 %, 50 %, 70 %, and 90 % of the maximum intensity of $10.79\,\mathrm{K\,km\,s^{-1}}$ in (b) and in steps of $5\,\mathrm{km\,s^{-1}}$ in (c) and (d).

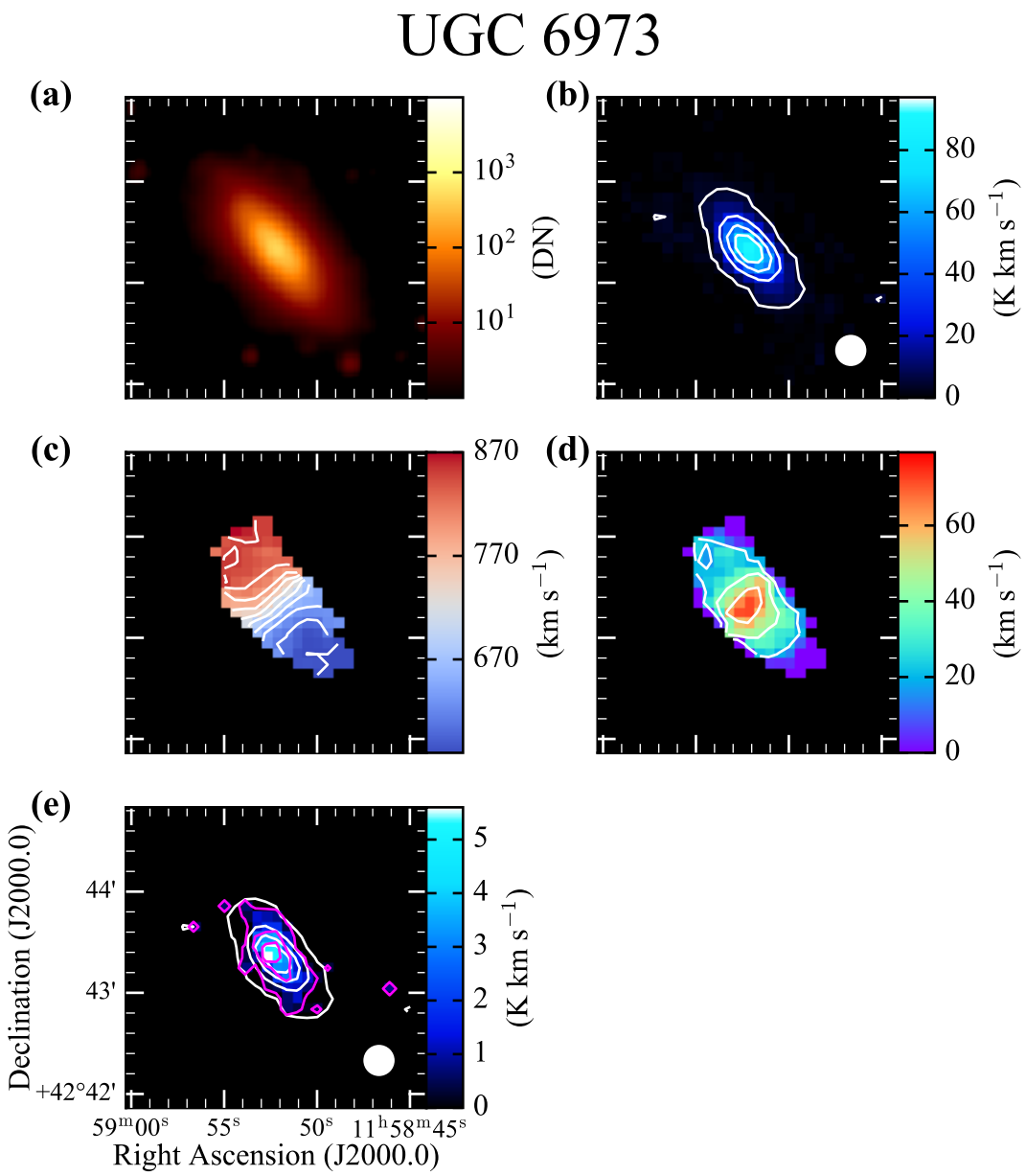

Supplementary fig. 76. Same as figure 12, but for UGC 6973. The contours are plotted at 5 %, 30 %, 55 %, and 80 % of the maximum intensity of 90.78 K km s^{-1} in (b) and (e) (*white*), in steps of 30 km s^{-1} in (c), in steps of 20 km s^{-1} in (d), and at 5 %, 45 %, and 75 % of the maximum intensity of 5.71 K km s^{-1} in (e) (*magenta*).

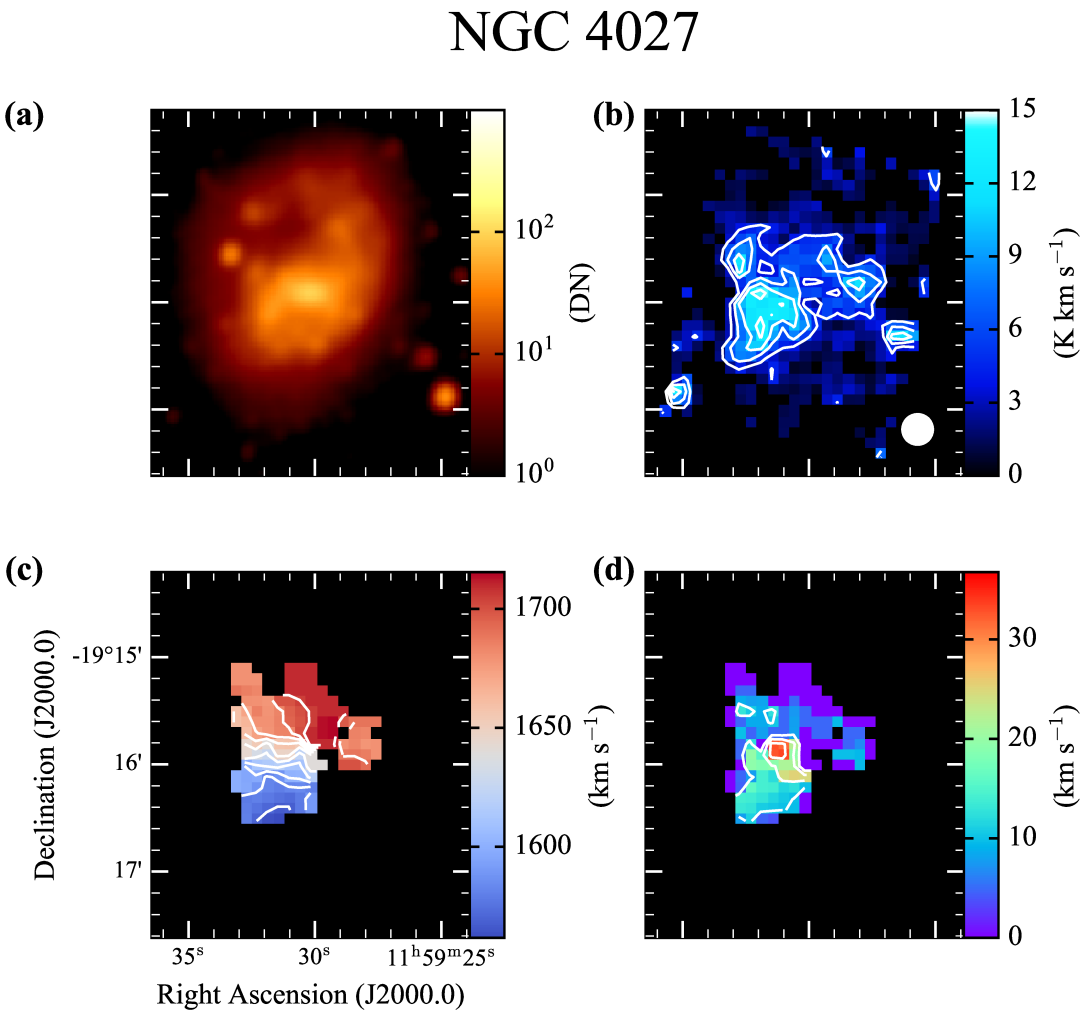

Supplementary fig. 77. Same as figure 12, but for NGC 4027. The contours are plotted at 30 %, 50 %, 70 %, and 90 % of the maximum intensity of $14.37\,\mathrm{K\,km\,s^{-1}}$ in (b), in steps of $15\,\mathrm{km\,s^{-1}}$ in (c), and in steps of $10\,\mathrm{km\,s^{-1}}$ in (d).

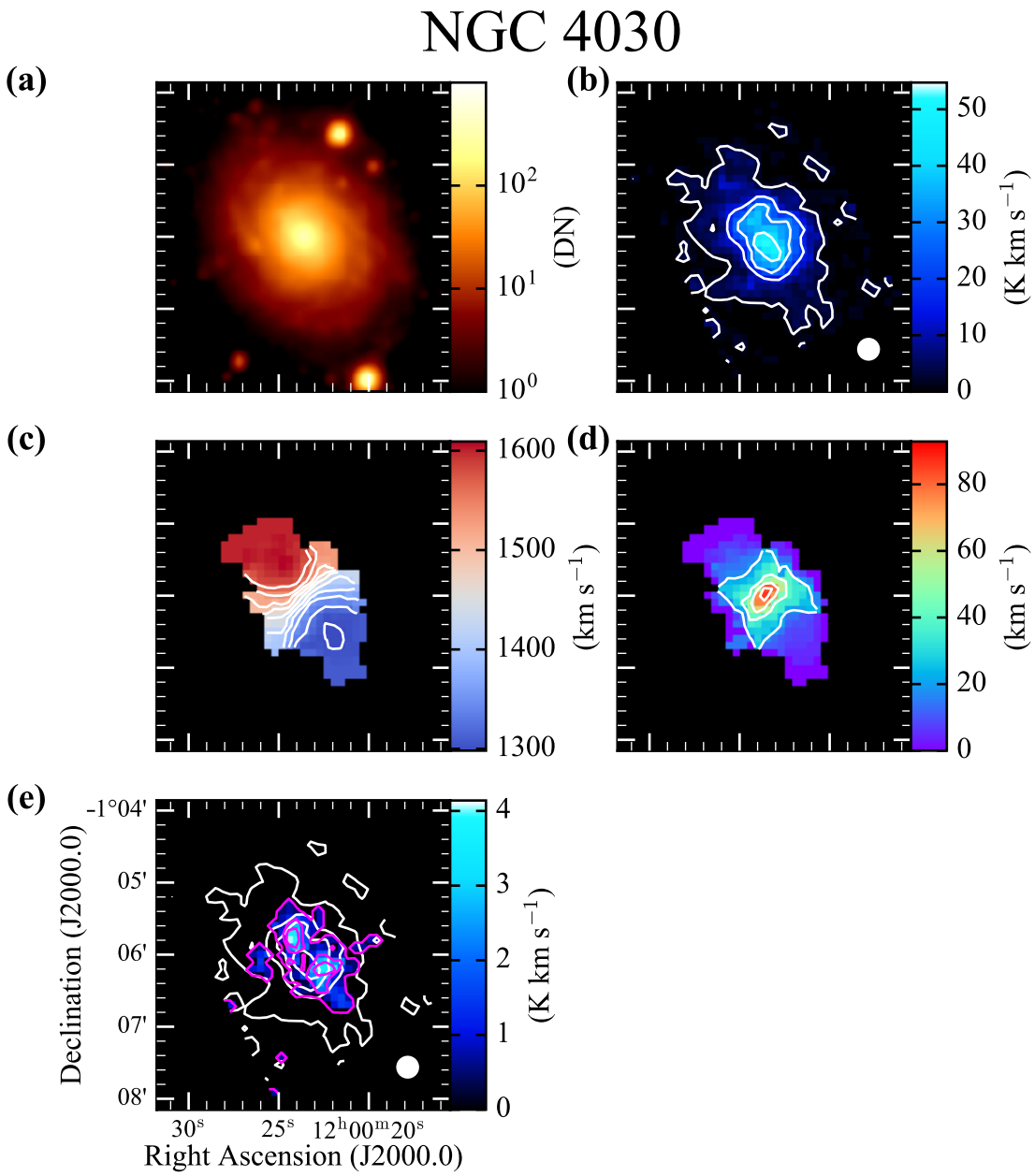

Supplementary fig. 78. Same as figure 12, but for NGC 4030. The contours are plotted at 5 %, 30 %, 55 %, and 80 % of the maximum intensity of 51.99 K km s^{-1} in (b) and (e) (*white*), in steps of 30 km s^{-1} in (c), in steps of 20 km s^{-1} in (d), and at 5 %, 45 %, and 75 % of the maximum intensity of 4.07 K km s^{-1} in (e) (*magenta*).

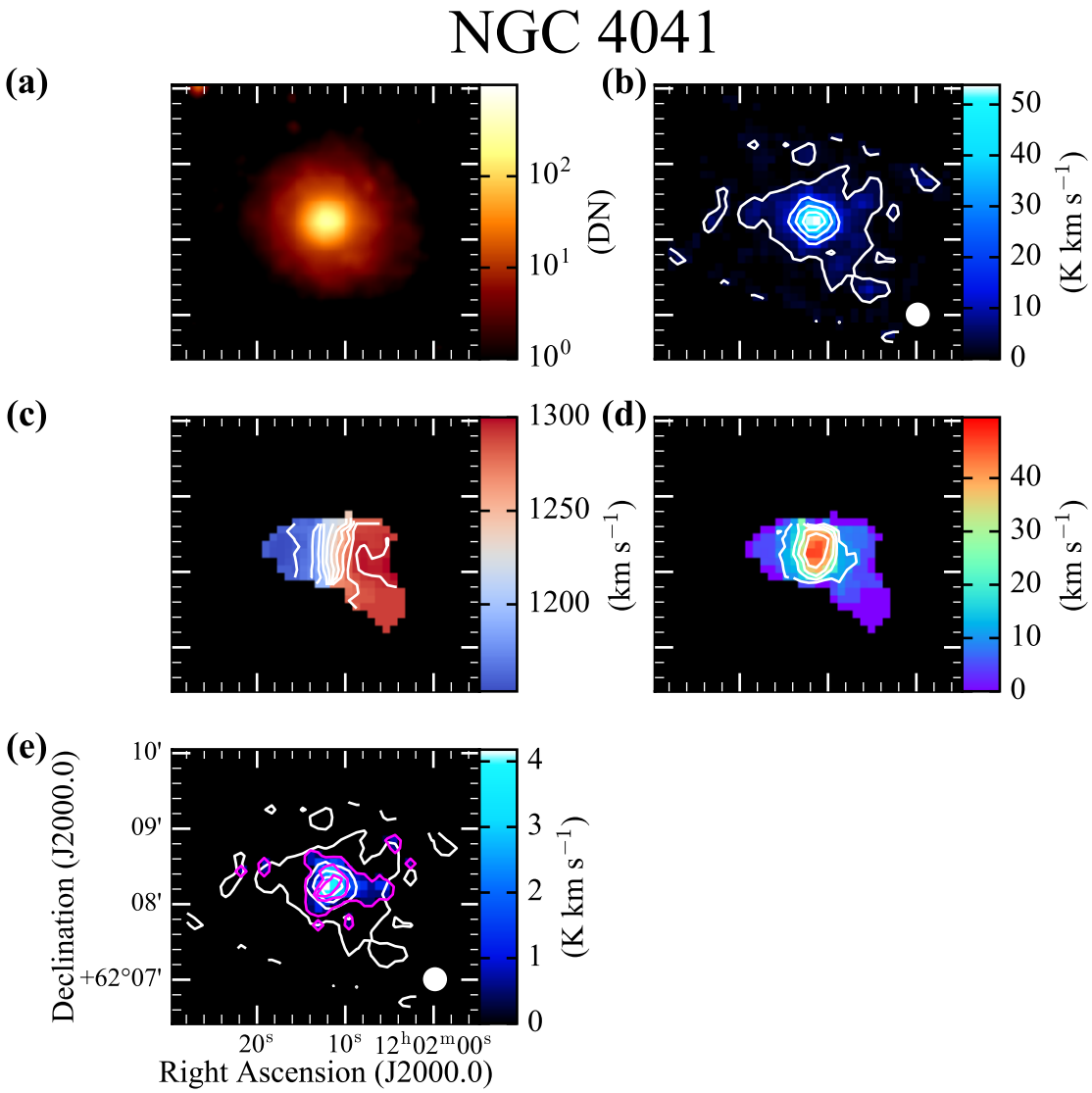

Supplementary fig. 79. Same as figure 12, but for NGC 4041. The contours are plotted at 5 %, 30 %, 55 %, and 80 % of the maximum intensity of 54.66 K km s^{-1} in (b) and (e) (*white*), in steps of 15 km s^{-1} in (c), in steps of 10 km s^{-1} in (d), and at 5 %, 45 %, and 75 % of the maximum intensity of 4.36 K km s^{-1} in (e) (*magenta*).

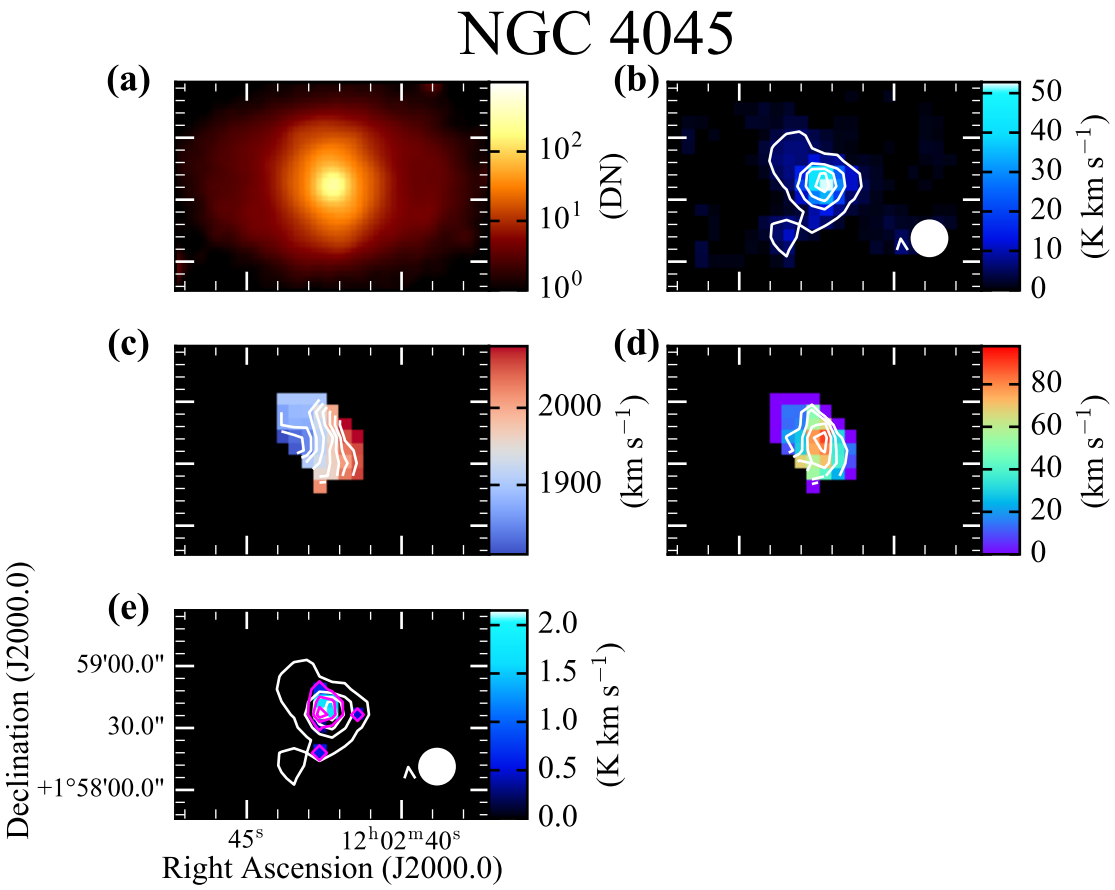

Supplementary fig. 80. Same as figure 12, but for NGC 4045. The contours are plotted at 10 %, 35 %, 60 %, and 85 % of the maximum intensity of 52.37 K km s^{-1} in (b) and (e) (*white*), in steps of 30 km s^{-1} in (c), in steps of 20 km s^{-1} in (d), and at 10 %, 50 %, and 80 % of the maximum intensity of 2.52 K km s^{-1} in (e) (*magenta*).

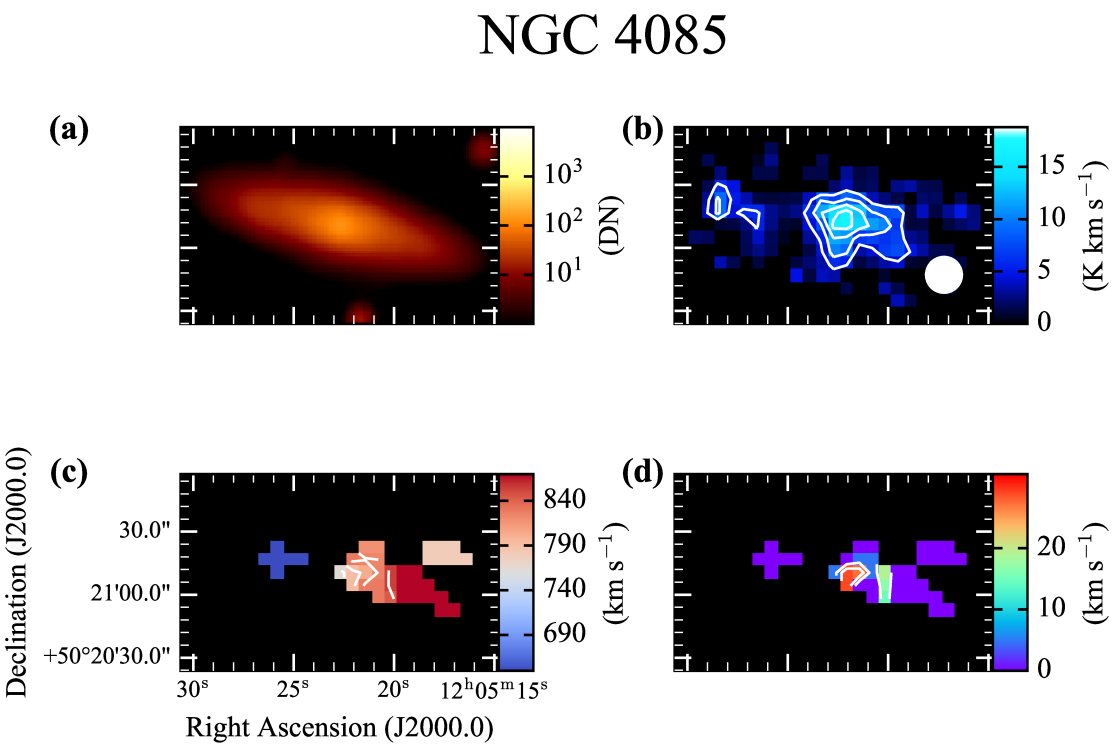

Supplementary fig. 81. Same as figure 12, but for NGC 4085. The contours are plotted at 30 %, 50 %, 70 %, and 90 % of the maximum intensity of $17.27\,\mathrm{K\,km\,s^{-1}}$ in (b), in steps of $25\,\mathrm{km\,s^{-1}}$ in (c), and in steps of $10\,\mathrm{km\,s^{-1}}$ in (d).

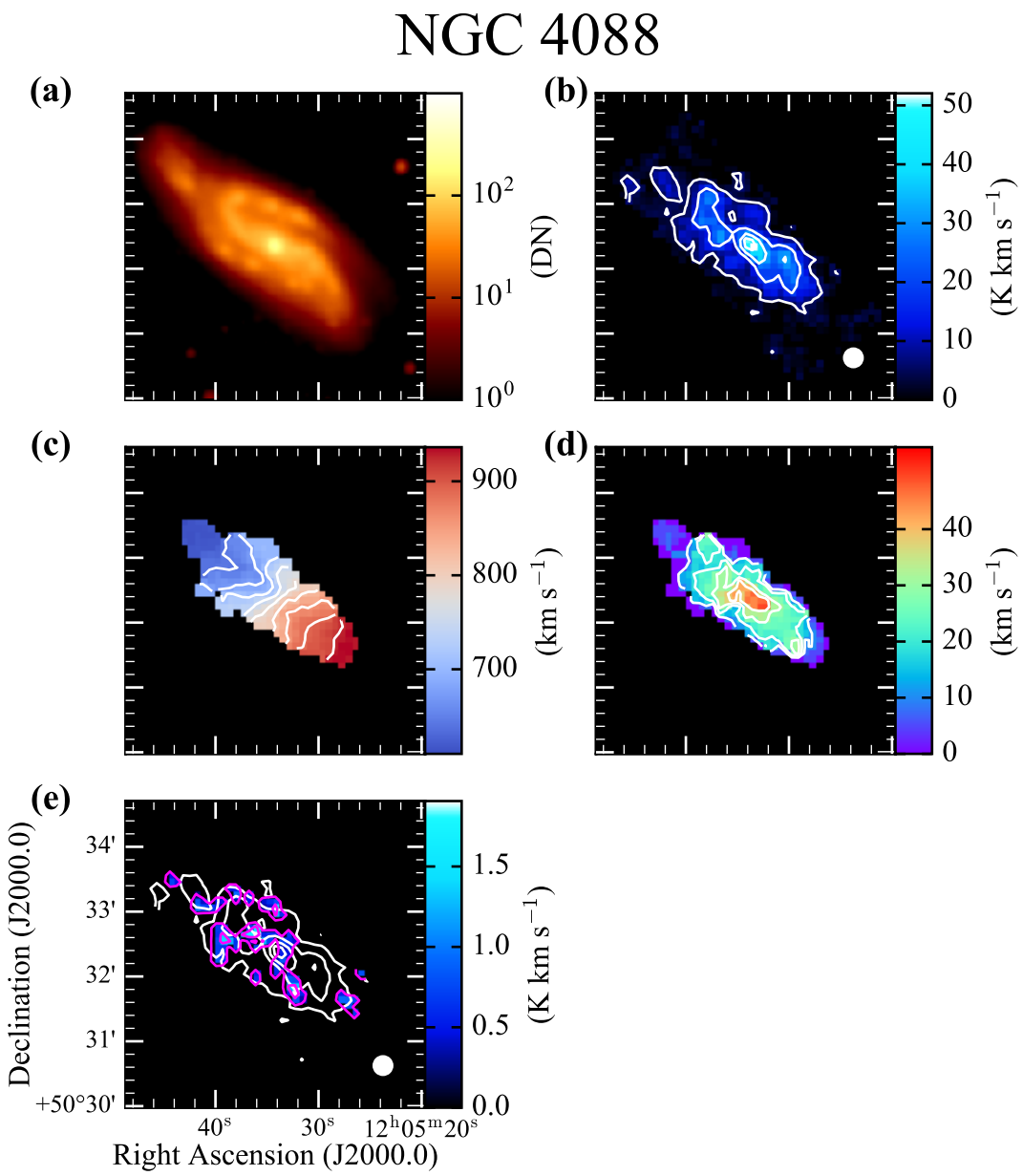

Supplementary fig. 82. Same as figure 12, but for NGC 4088. The contours are plotted at 10 %, 35 %, 60 %, and 85 % of the maximum intensity of $53.05\,\mathrm{K\,km\,s^{-1}}$ in (b) and (e) (*white*), in steps of $35\,\mathrm{km\,s^{-1}}$ in (c), in steps of $10\,\mathrm{km\,s^{-1}}$ in (d), and at 10 % and 60 % of the maximum intensity of $1.95\,\mathrm{K\,km\,s^{-1}}$ in (e) (*magenta*).

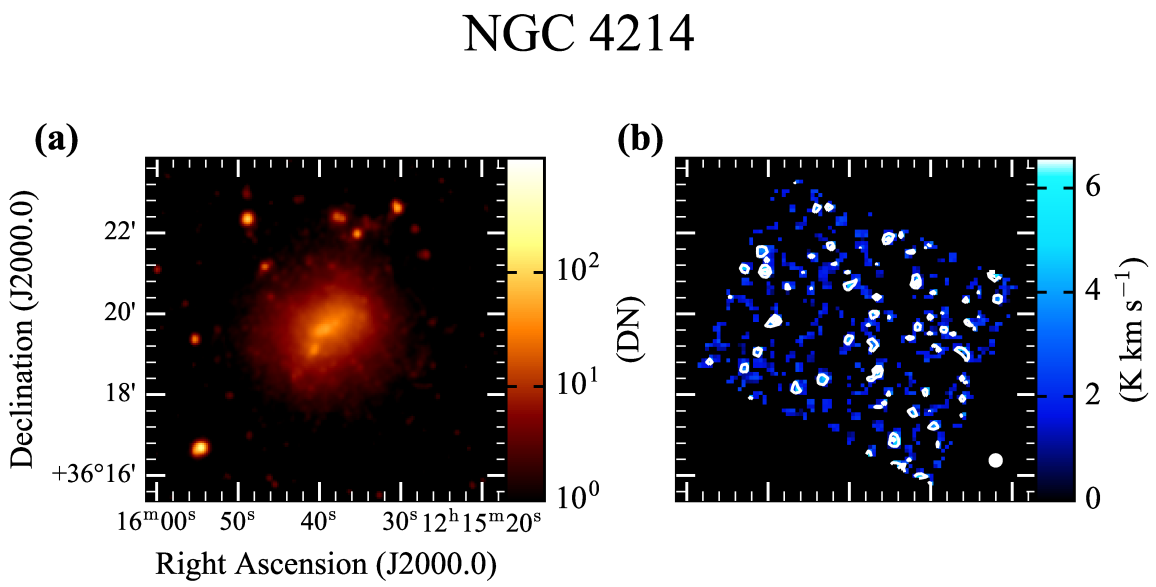

Supplementary fig. 83. Same as figure 12, but for NGC 4214. The contours are plotted at 30 % and 60 % of the maximum intensity of $8.85\,\mathrm{K\,km\,s^{-1}}$ in (b).

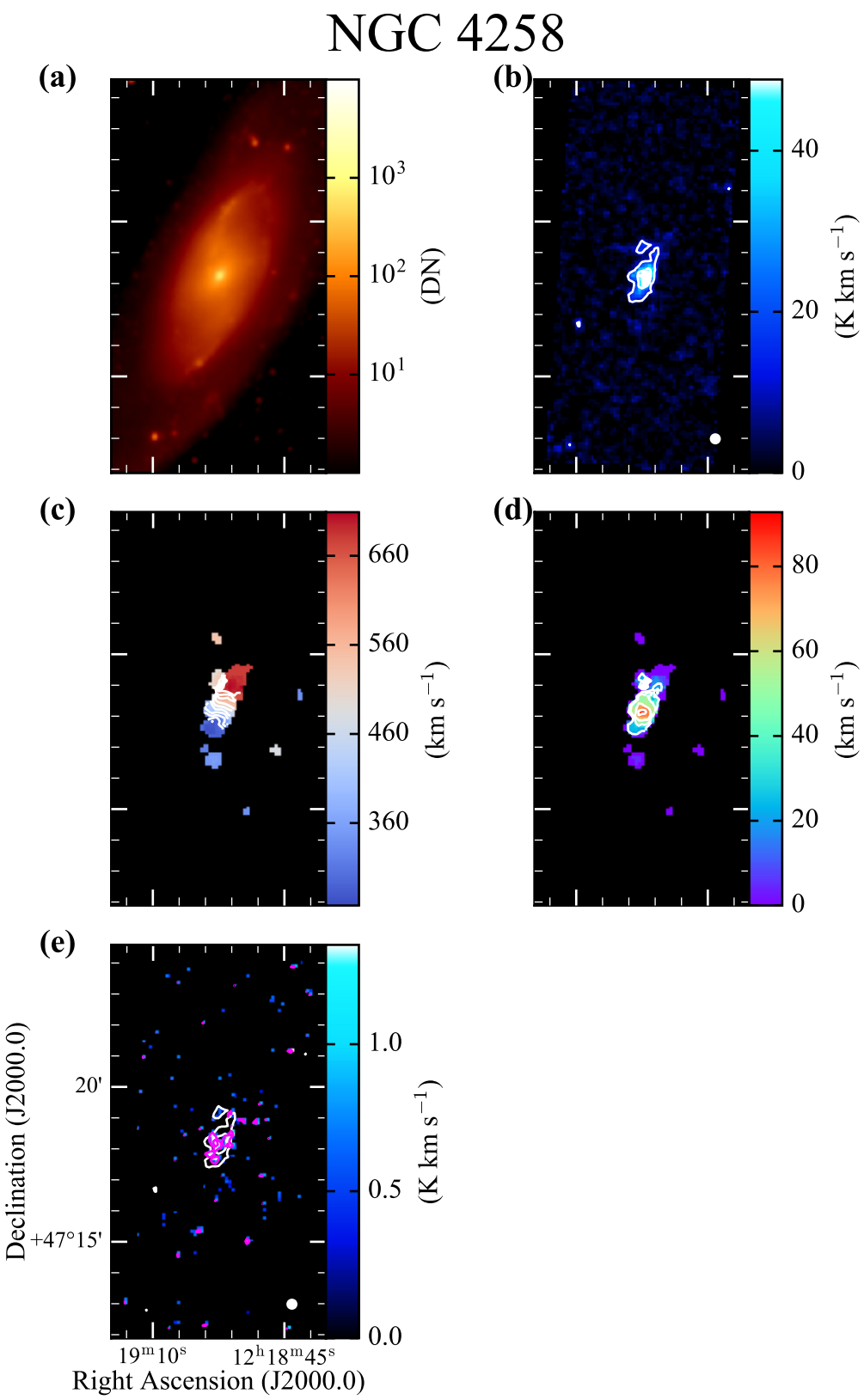

Supplementary fig. 84. Same as figure 12, but for NGC 4258. The contours are plotted at 15 % and 50 % of the maximum intensity of 79.77 K km s^{-1} in (b) and (e) (*white*), in steps of 45 km s^{-1} in (c), in steps of 20 km s^{-1} in (d), and at 30 % and 70 % of the maximum intensity of 2.32 K km s^{-1} in (e) (*magenta*).

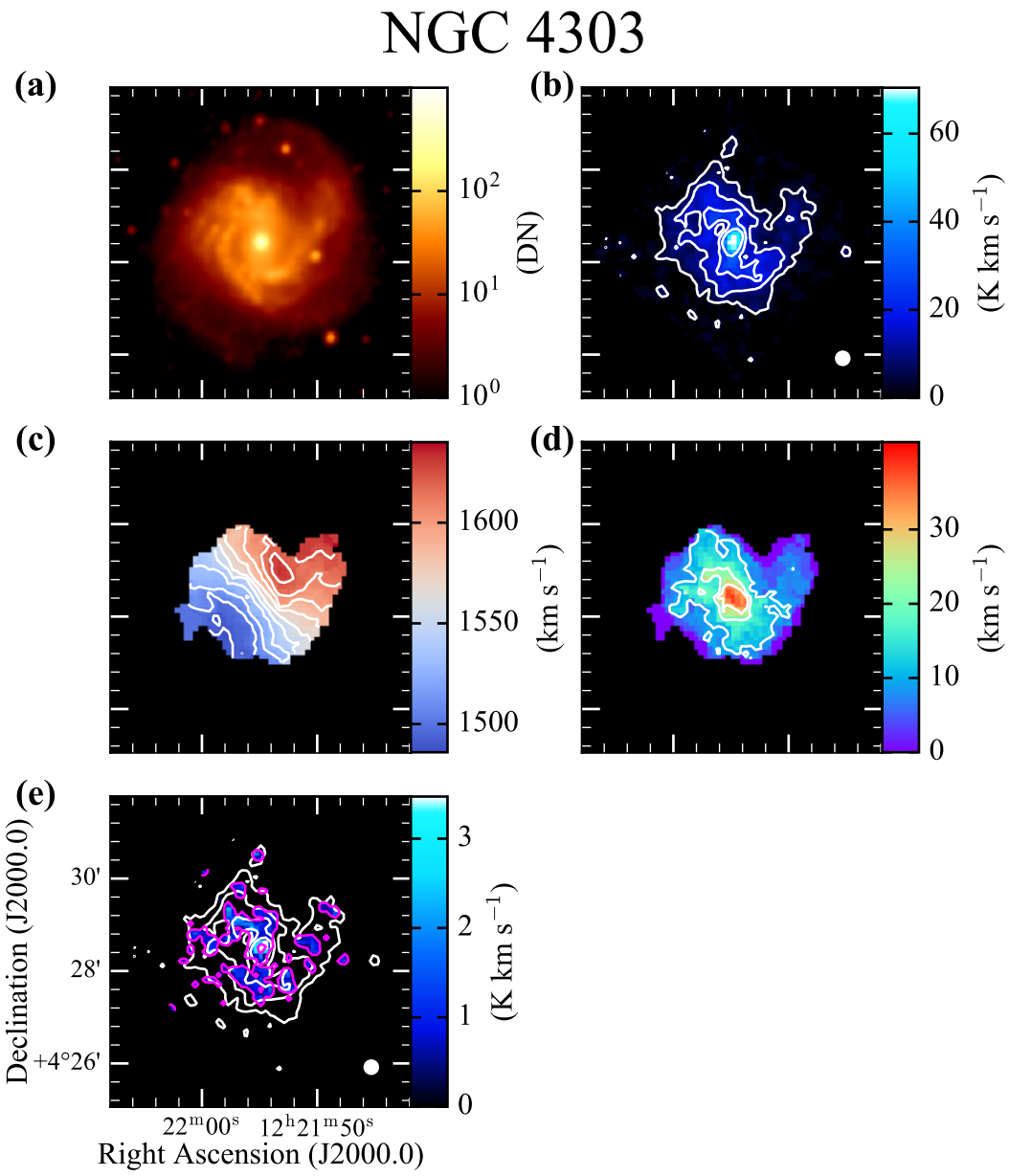

Supplementary fig. 85. Same as figure 12, but for NGC 4303. The contours are plotted at 5 %, 15 %, 25 %, and 45 % of the maximum intensity of 79.23 K km s^{-1} in (b) and (e) (*white*), in steps of 15 km s^{-1} in (c), in steps of 10 km s^{-1} in (d), and at 5 % and 65 % of the maximum intensity of 6.82 K km s^{-1} in (e) (*magenta*).

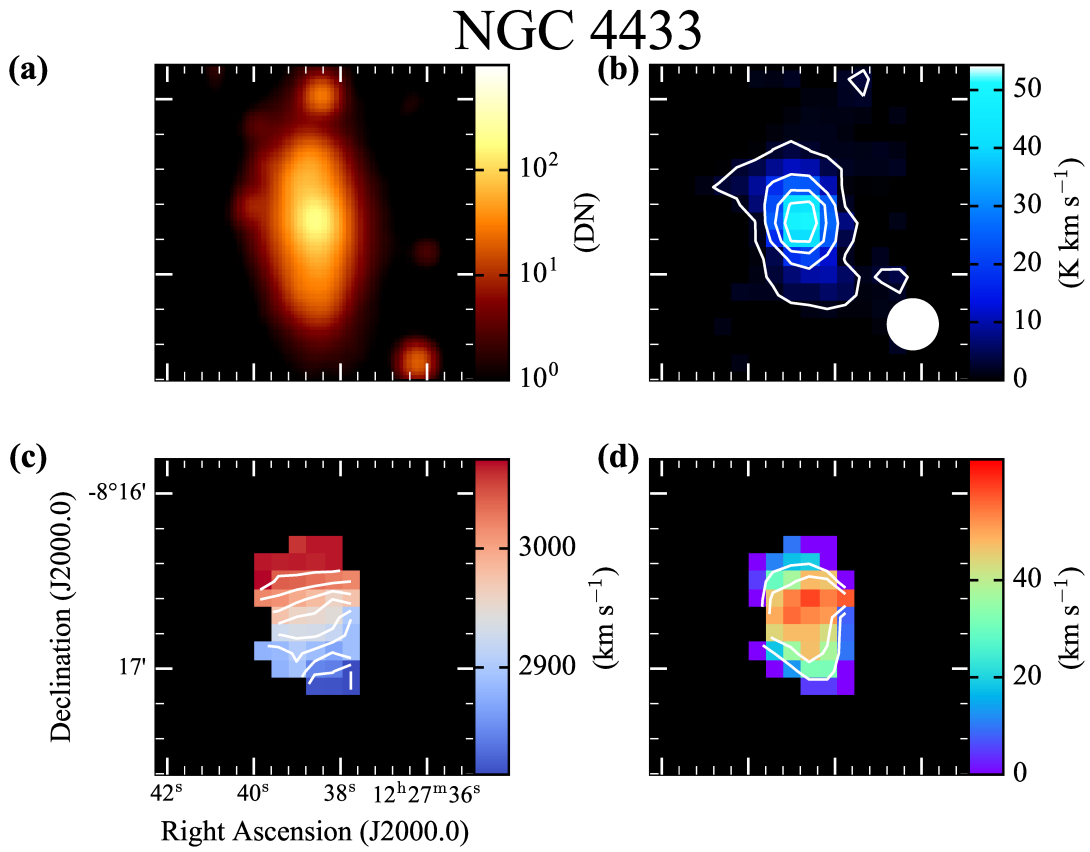

Supplementary fig. 86. Same as figure 12, but for NGC 4433. The contours are plotted at 5 %, 30 %, 55 %, and 80 % of the maximum intensity of $50.36\,\mathrm{K\,km\,s^{-1}}$ in (b), in steps of $30\,\mathrm{km\,s^{-1}}$ in (c), and in steps of $20\,\mathrm{km\,s^{-1}}$ in (d).

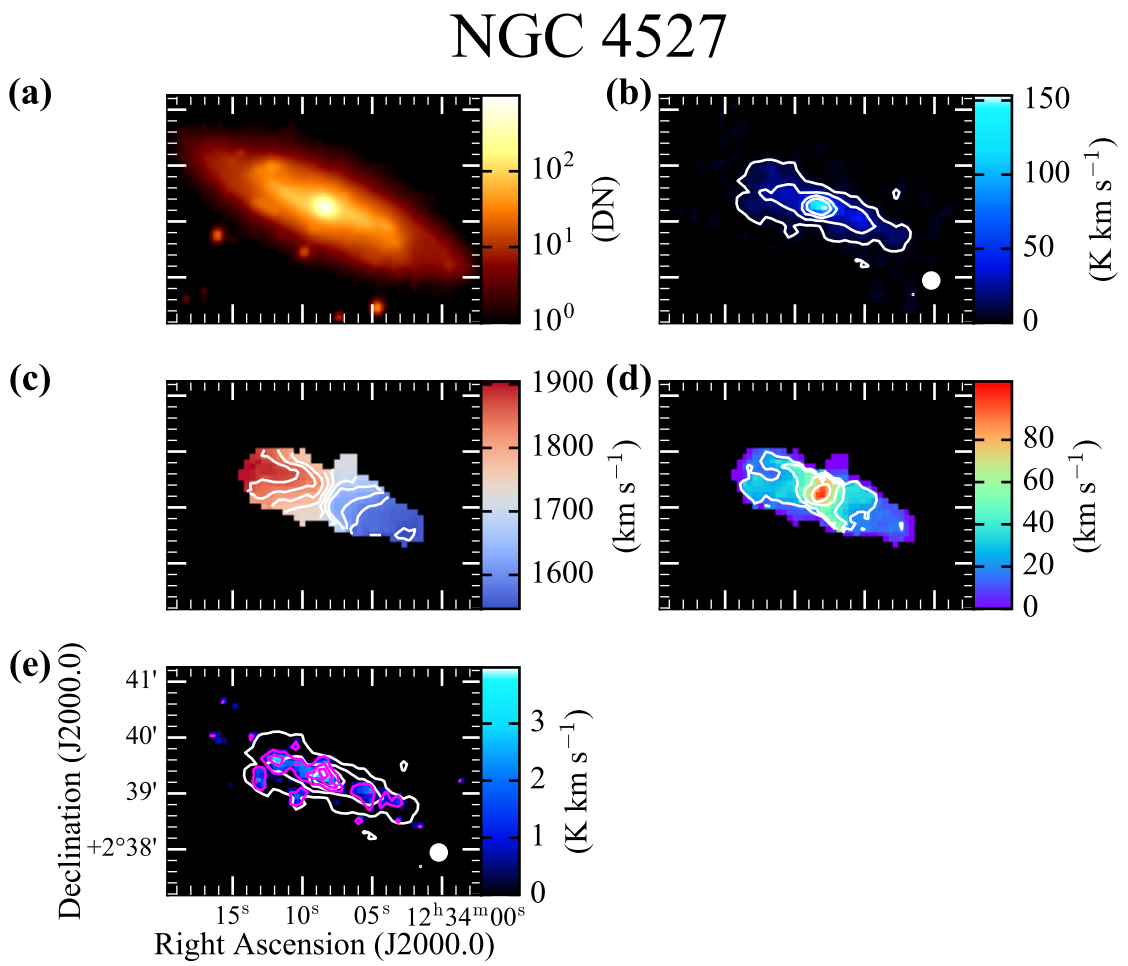

Supplementary fig. 87. Same as figure 12, but for NGC 4527. The contours are plotted at 5 %, 15 %, 35 %, and 55 % of the maximum intensity of 155.25 K km s^{-1} in (b) and (e) (*white*), in steps of 35 km s^{-1} in (c), in steps of 20 km s^{-1} in (d), and at 15 %, 45 %, and 75 % of the maximum intensity of 5.20 K km s^{-1} in (e) (*magenta*).

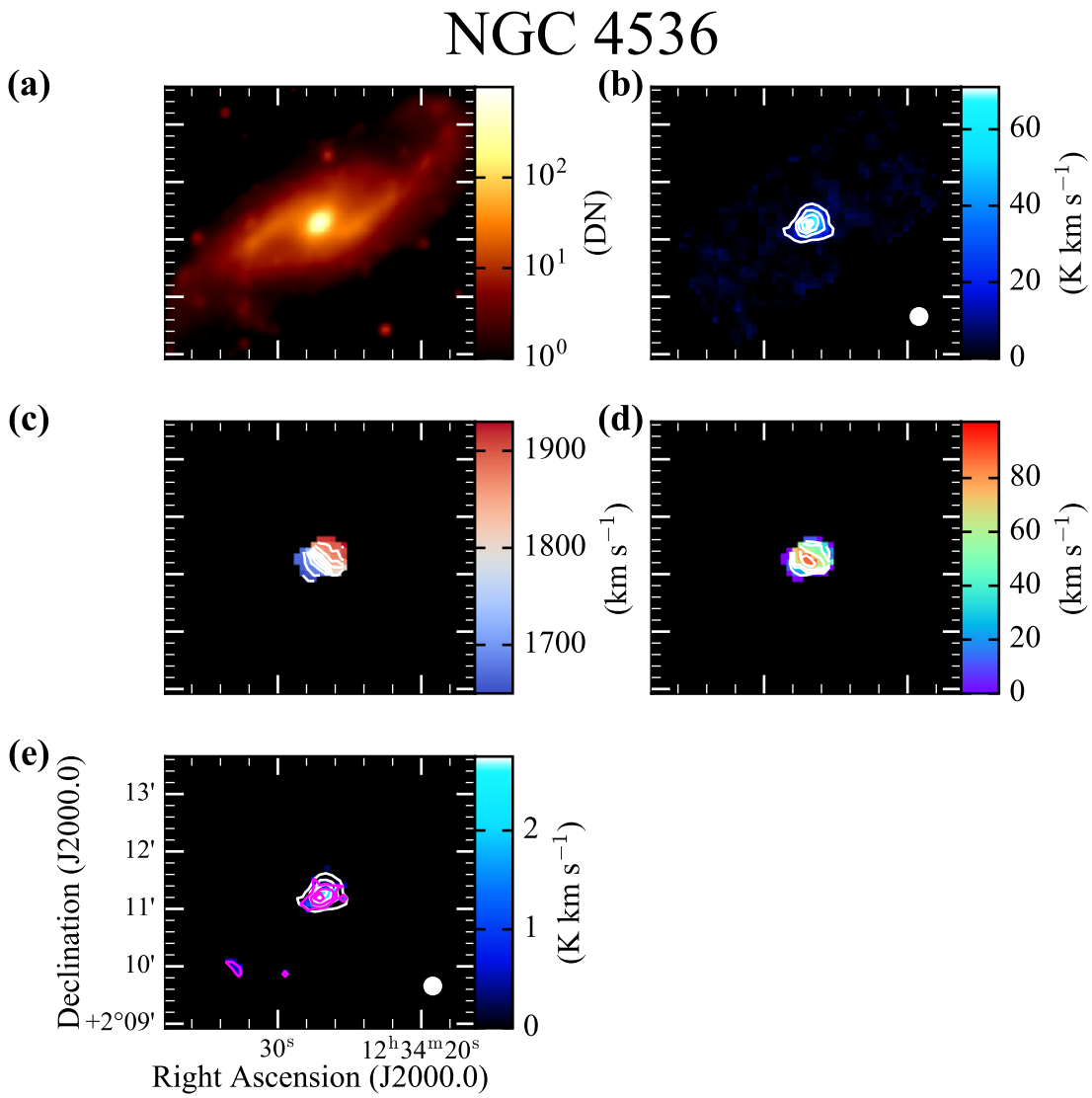

Supplementary fig. 88. Same as figure 12, but for NGC 4536. The contours are plotted at 10 %, 35 %, 60 %, and 85 % of the maximum intensity of 75.99 K km s^{-1} in (b) and (e) (*white*), in steps of 30 km s^{-1} in (c), in steps of 20 km s^{-1} in (d), and at 15 %, 45 %, and 75 % of the maximum intensity of 3.40 K km s^{-1} in (e) (*magenta*).

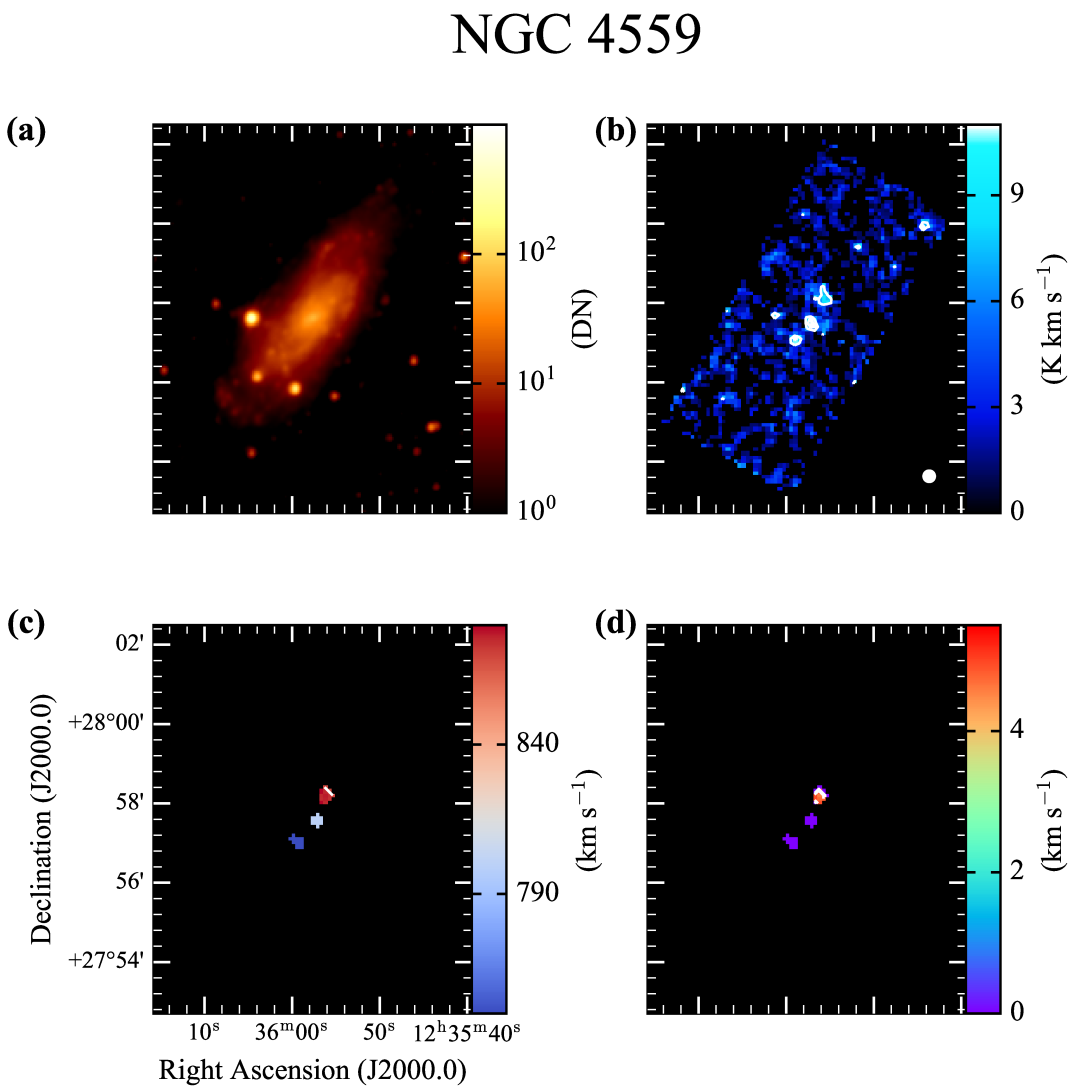

Supplementary fig. 89. Same as figure 12, but for NGC 4559. The contours are plotted at 45 % and 75 % of the maximum intensity of $15.32\,\mathrm{K\,km\,s^{-1}}$ in (b), in steps of $15\,\mathrm{km\,s^{-1}}$ in (c), and in steps of $2\,\mathrm{km\,s^{-1}}$ in (d).

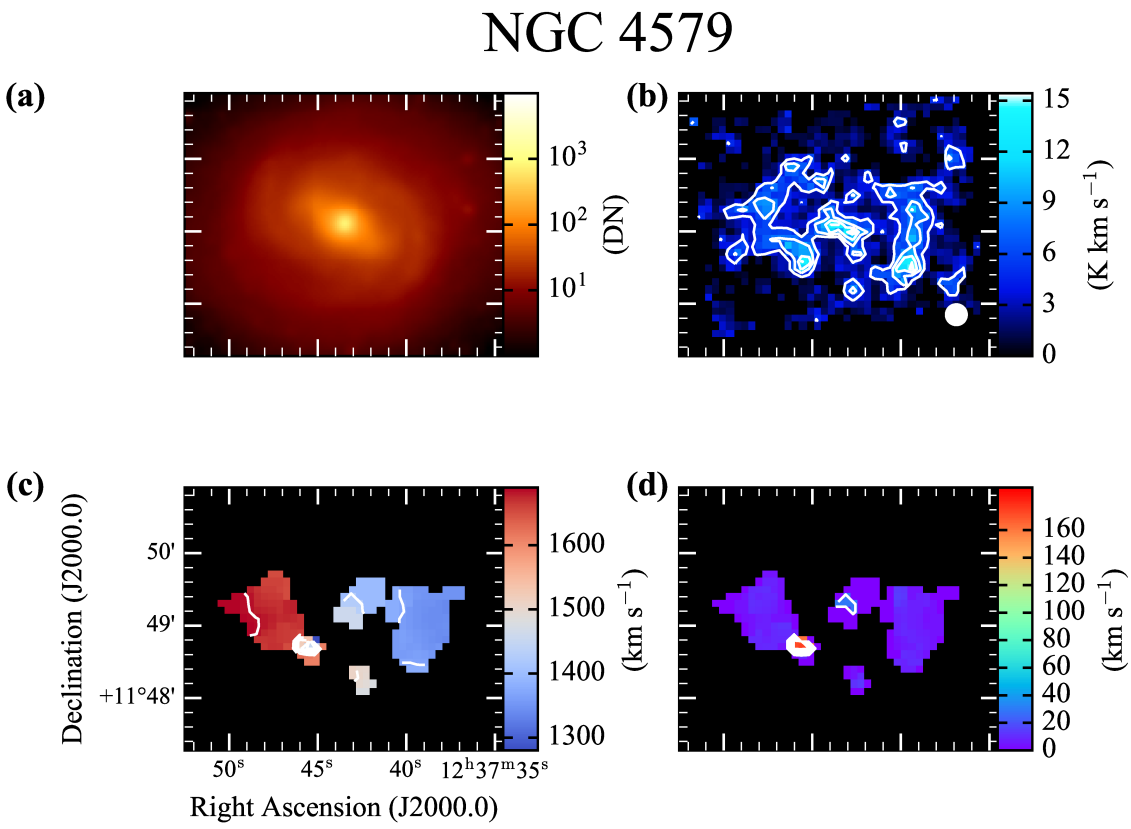

Supplementary fig. 90. Same as figure 12, but for NGC 4579. The contours are plotted at 30 %, 50 %, 70 %, and 90 % of the maximum intensity of $15.41\,\mathrm{K\,km\,s^{-1}}$ in (b), in steps of $45\,\mathrm{km\,s^{-1}}$ in (c), and in steps of $20\,\mathrm{km\,s^{-1}}$ in (d).

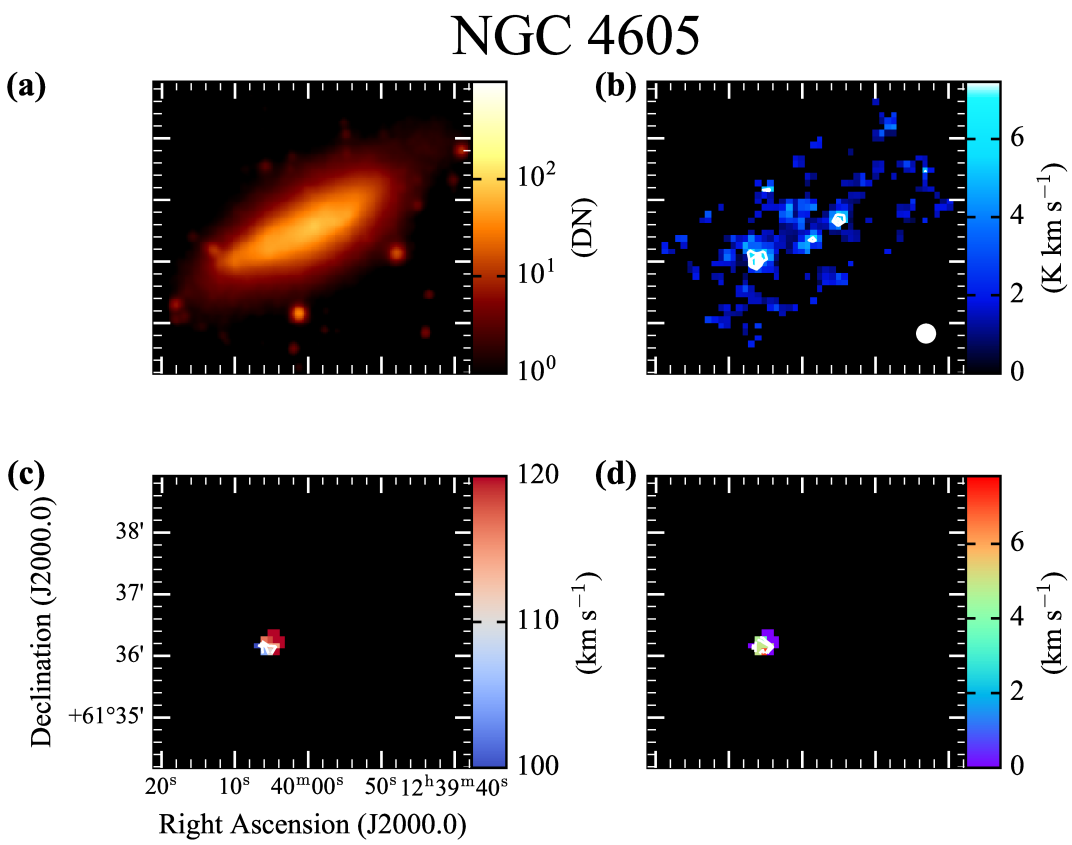

Supplementary fig. 91. Same as figure 12, but for NGC 4605. The contours are plotted at 55 % and 70 % of the maximum intensity of $9.00\,\mathrm{K\,km\,s^{-1}}$ in (b), in steps of $5\,\mathrm{km\,s^{-1}}$ in (c), and in steps of $2\,\mathrm{km\,s^{-1}}$ in (d).

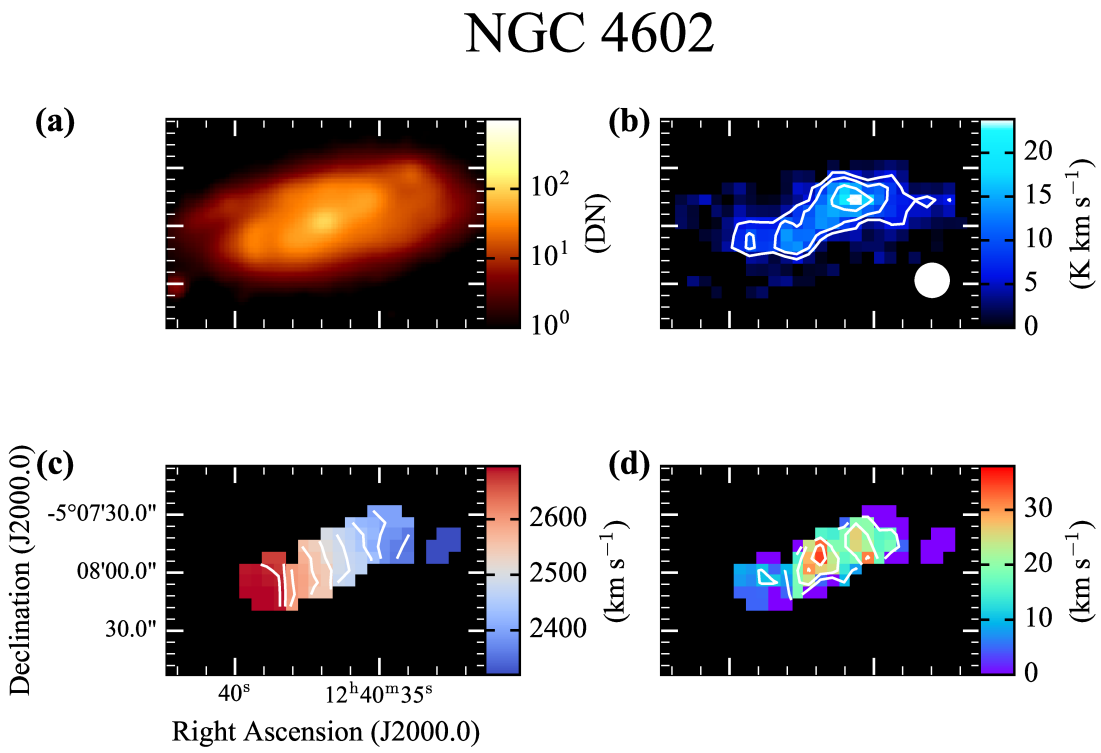

Supplementary fig. 92. Same as figure 12, but for NGC 4602. The contours are plotted at 25 %, 40 %, 65 %, and 90 % of the maximum intensity of $23.64\,\mathrm{K\,km\,s^{-1}}$ in (b), in steps of $40\,\mathrm{km\,s^{-1}}$ in (c), and in steps of $10\,\mathrm{km\,s^{-1}}$ in (d).

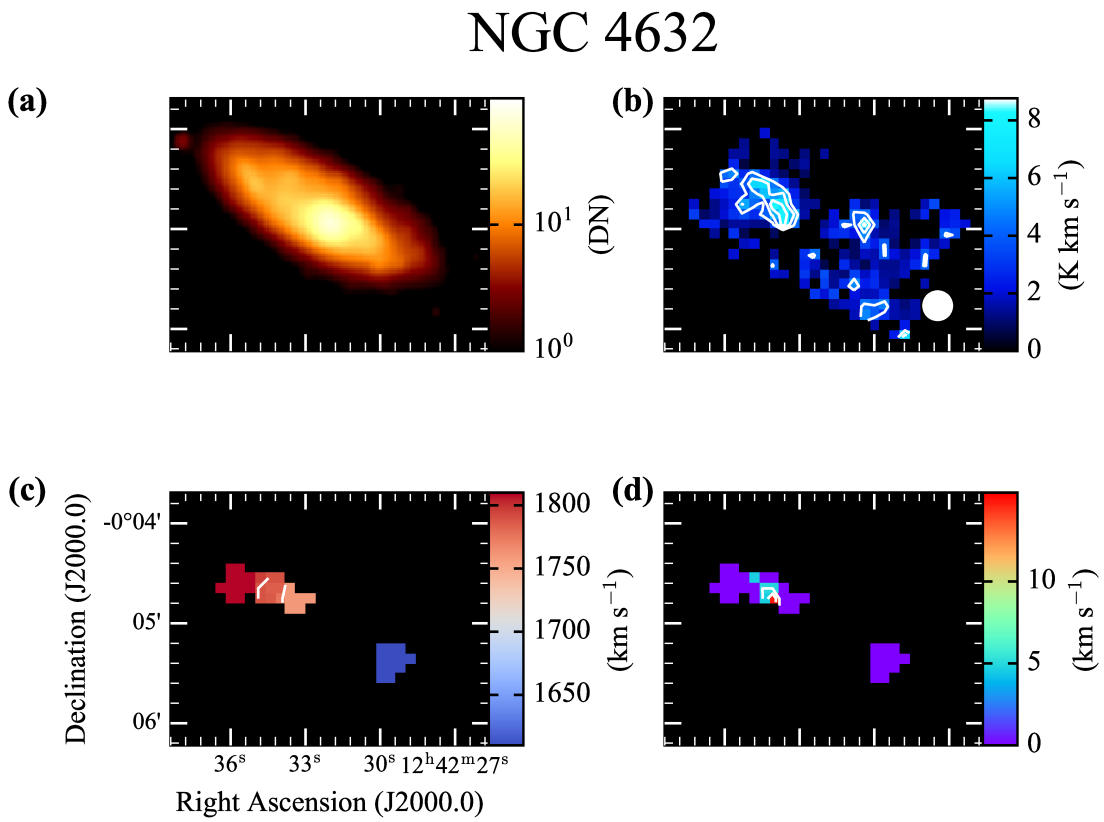

Supplementary fig. 93. Same as figure 12, but for NGC 4632. The contours are plotted at 45 %, 65 %, and 85 % of the maximum intensity of $8.31\,\mathrm{K\,km\,s^{-1}}$ in (b), in steps of $20\,\mathrm{km\,s^{-1}}$ in (c), and in steps of $5\,\mathrm{km\,s^{-1}}$ in (d).

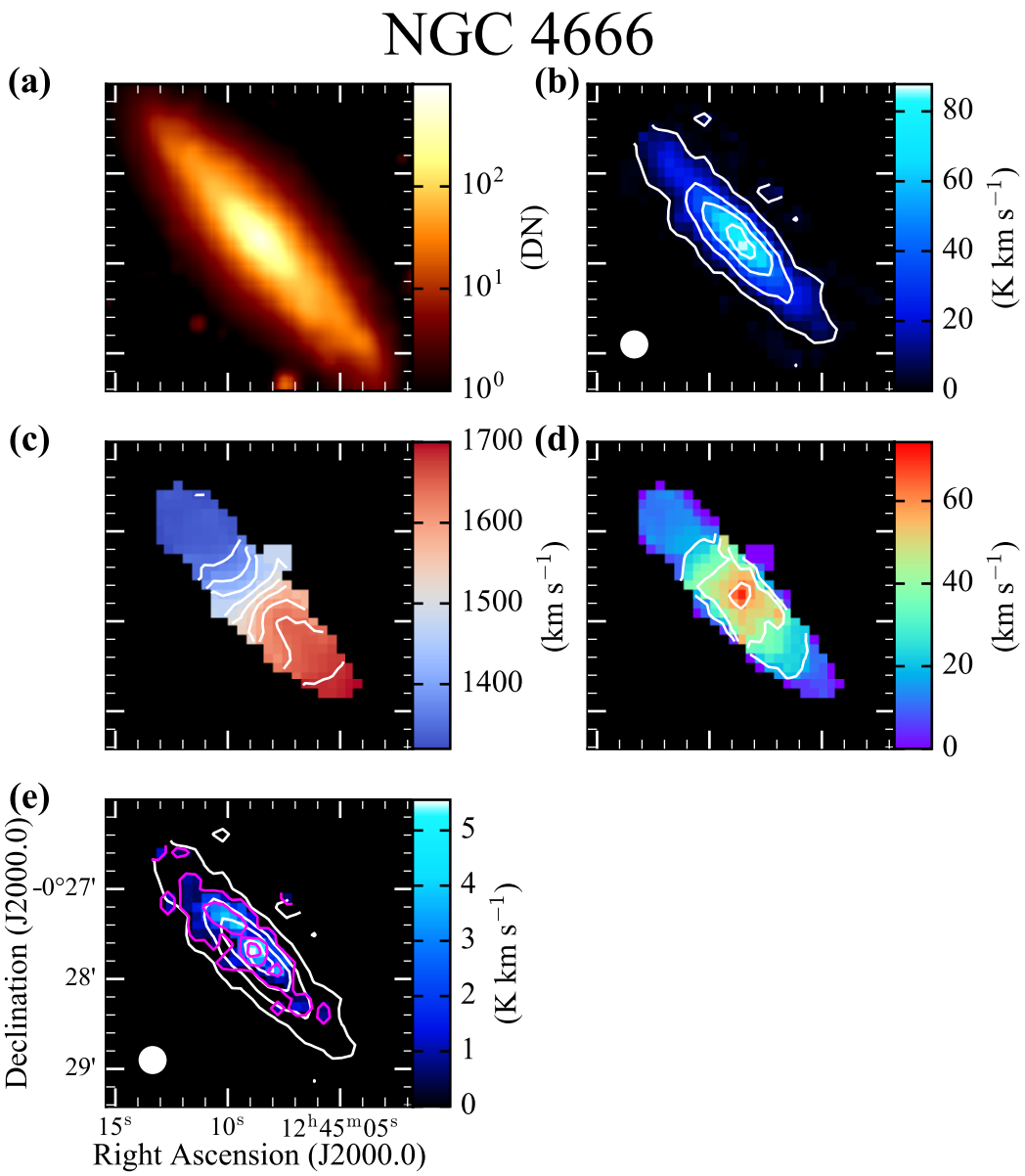

Supplementary fig. 94. Same as figure 12, but for NGC 4666. The contours are plotted at 5 %, 30 %, 55 %, and 80 % of the maximum intensity of 86.52 K km s^{-1} in (b) and (e) (*white*), in steps of 40 km s^{-1} in (c), in steps of 20 km s^{-1} in (d), and at 5 %, 45 %, and 85 % of the maximum intensity of 5.51 K km s^{-1} in (e) (*magenta*).

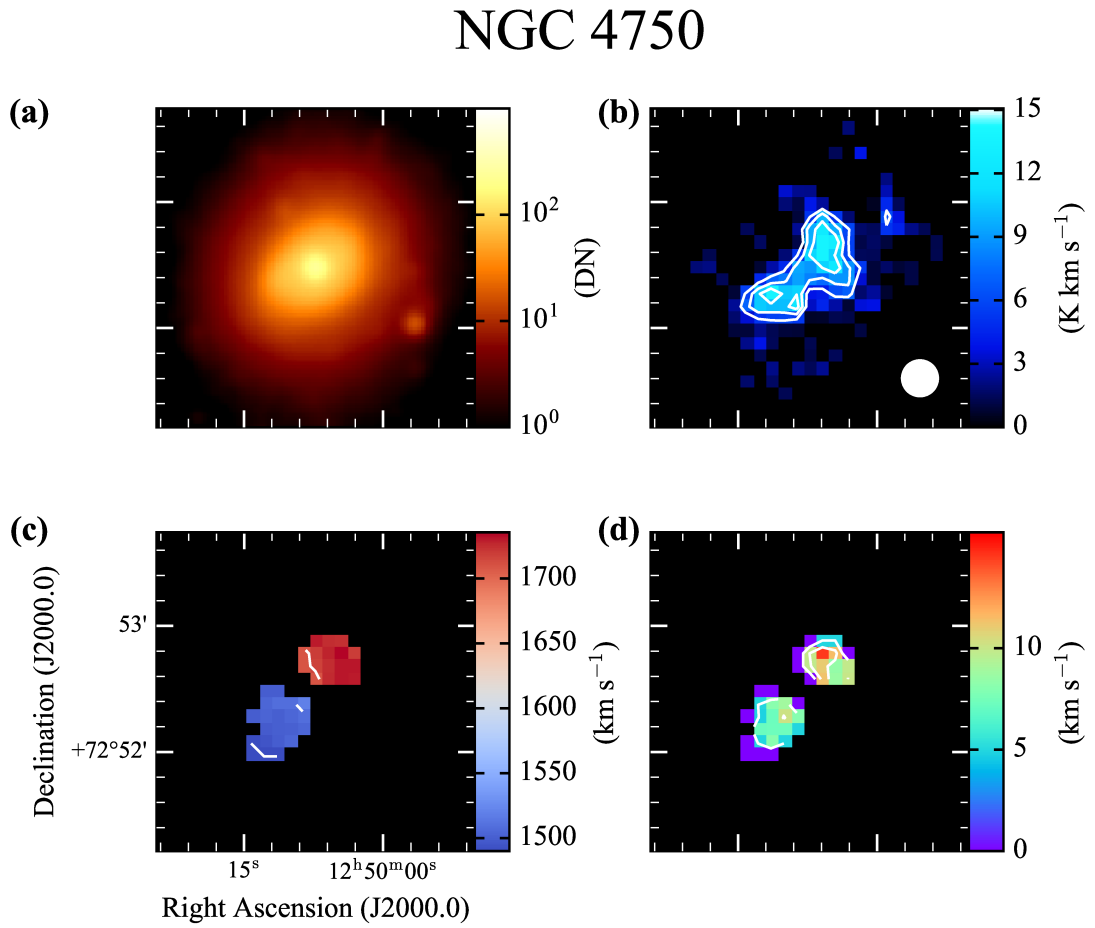

Supplementary fig. 95. Same as figure 12, but for NGC 4750. The contours are plotted at 40 %, 60 %, and 80 % of the maximum intensity of $13.75\,\mathrm{K\,km\,s^{-1}}$ in (b), in steps of $25\,\mathrm{km\,s^{-1}}$ in (c), and in steps of $5\,\mathrm{km\,s^{-1}}$ in (d).

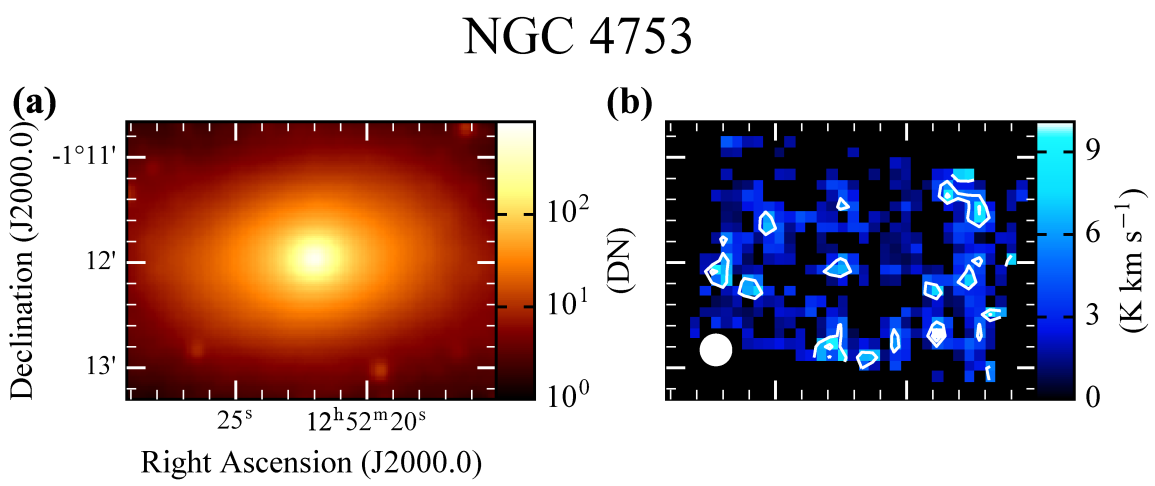

Supplementary fig. 96. Same as figure 12, but for NGC 4753. The contours are plotted at 40 % and 70 % of the maximum intensity of $11.57\,\mathrm{K\,km\,s^{-1}}$ in (b).

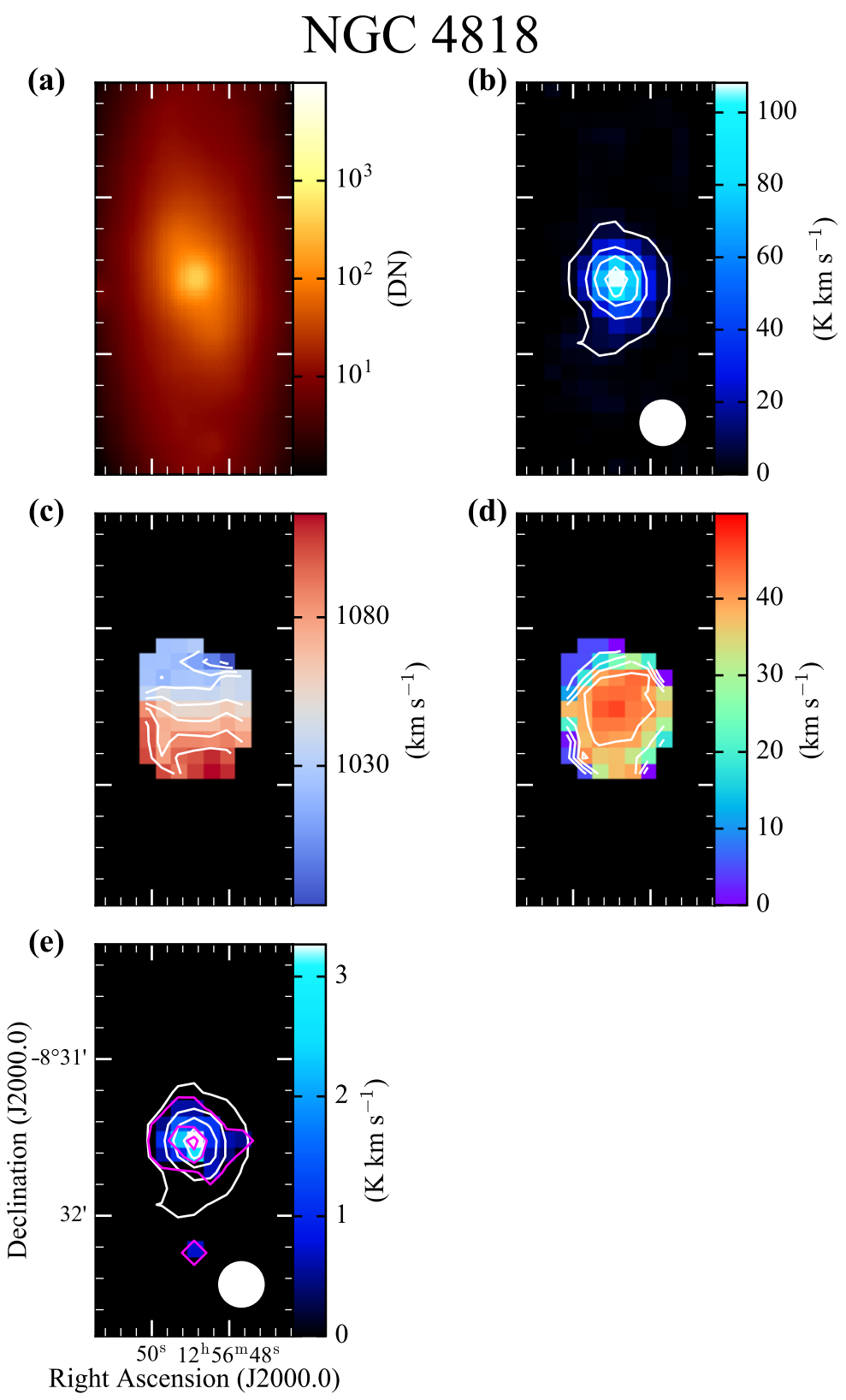

Supplementary fig. 97. Same as figure 12, but for NGC 4818. The contours are plotted at 5 %, 30 %, 55 %, and 80 % of the maximum intensity of 107.46 K km s^{-1} in (b) and (e) (*white*), in steps of 15 km s^{-1} in (c), in steps of 10 km s^{-1} in (d), and at 5 %, 45 %, and 85 % of the maximum intensity of 3.50 K km s^{-1} in (e) (*magenta*).

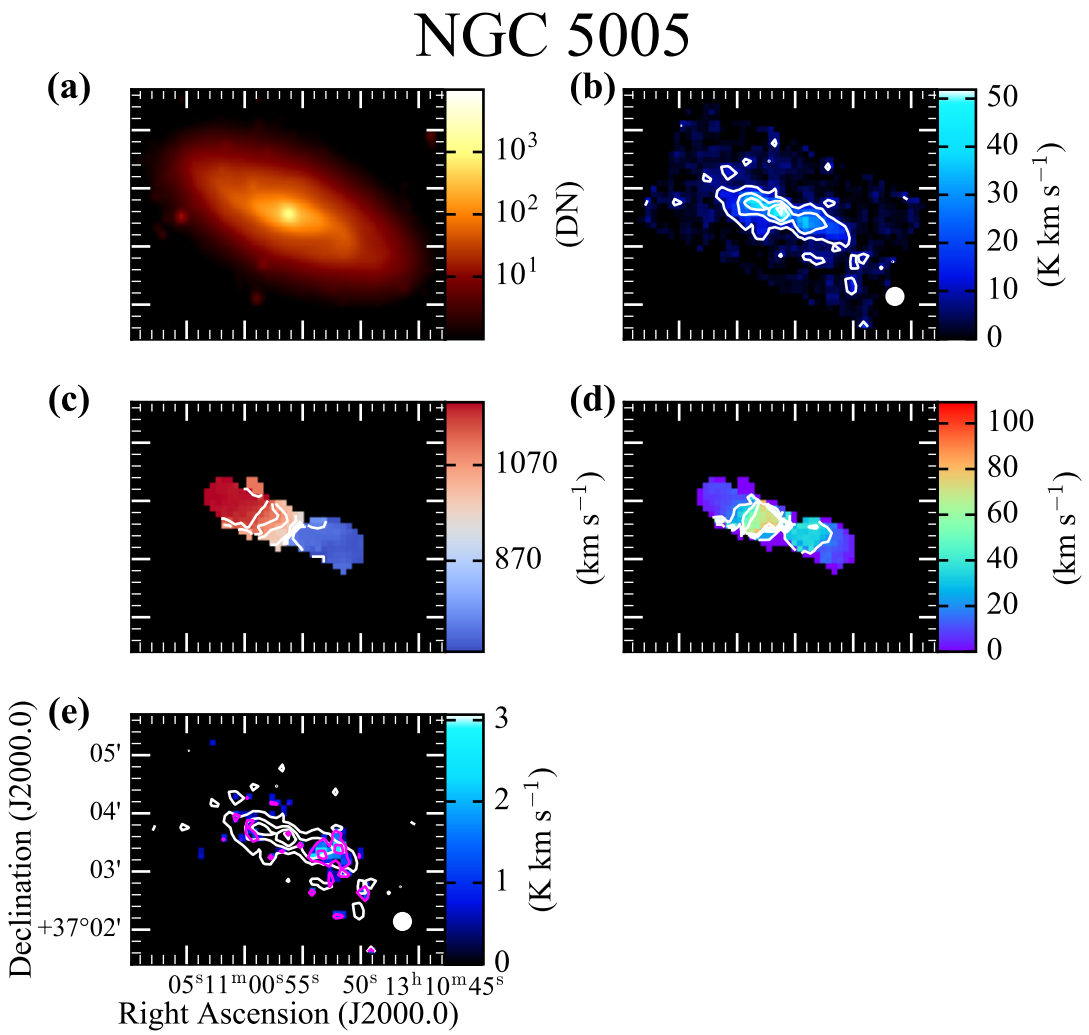

Supplementary fig. 98. Same as figure 12, but for NGC 5005. The contours are plotted at 15 %, 40 %, 65 %, and 90 % of the maximum intensity of $56.29\,\mathrm{K\,km\,s^{-1}}$ in (b) and (e) (*white*), in steps of $60\,\mathrm{km\,s^{-1}}$ in (c), in steps of $20\,\mathrm{km\,s^{-1}}$ in (d), and at 20 % and 70 % of the maximum intensity of $3.76\,\mathrm{K\,km\,s^{-1}}$ in (e) (*magenta*).

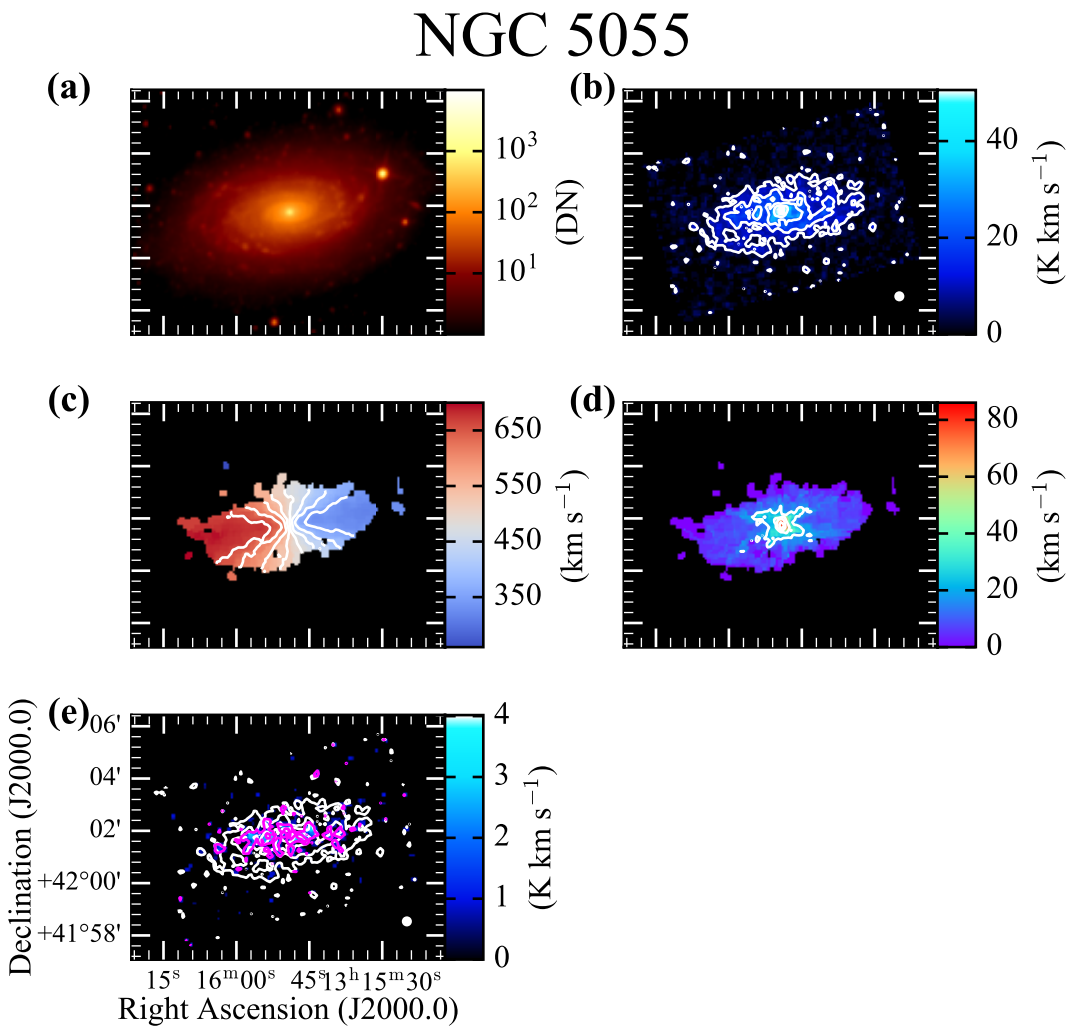

Supplementary fig. 99. Same as figure 12, but for NGC 5055. The contours are plotted at 7%, 15%, 25%, and 45% of the maximum intensity of $91.35\,\mathrm{K\,km\,s^{-1}}$ in (b) and (e) (*white*), in steps of $45\,\mathrm{km\,s^{-1}}$ in (c), in steps of $20\,\mathrm{km\,s^{-1}}$ in (d), and at 20% and 70% of the maximum intensity of $5.03\,\mathrm{K\,km\,s^{-1}}$ in (e) (*magenta*).

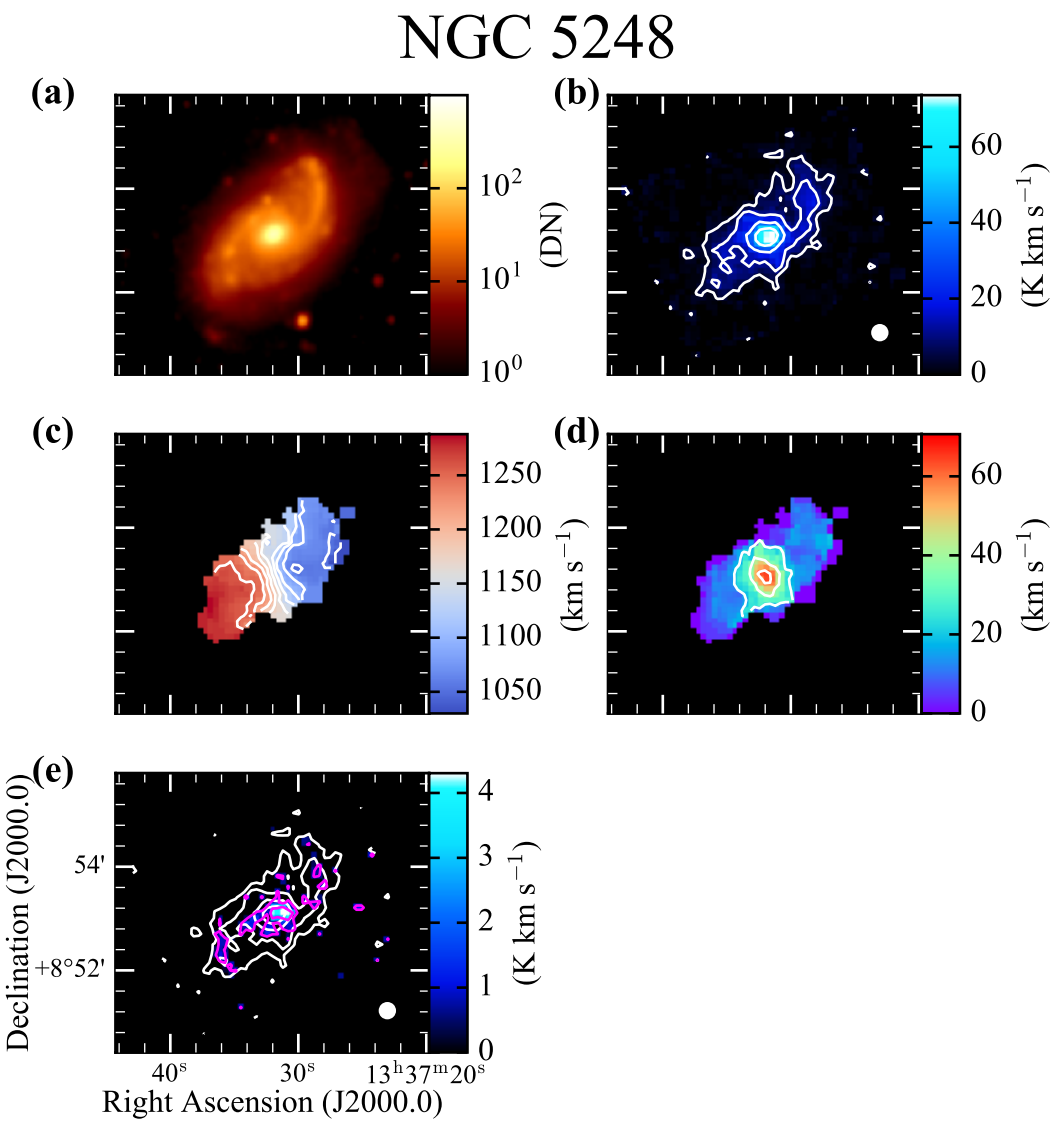

Supplementary fig. 100. Same as figure 12, but for NGC 5248. The contours are plotted at 5 %, 15 %, 35 %, and 65 % of the maximum intensity of $83.84\,\mathrm{K\,km\,s^{-1}}$ in (b) and (e) (*white*), in steps of $25\,\mathrm{km\,s^{-1}}$ in (c), in steps of $20\,\mathrm{km\,s^{-1}}$ in (d), and at 15 % and 65 % of the maximum intensity of $4.46\,\mathrm{K\,km\,s^{-1}}$ in (e) (*magenta*).

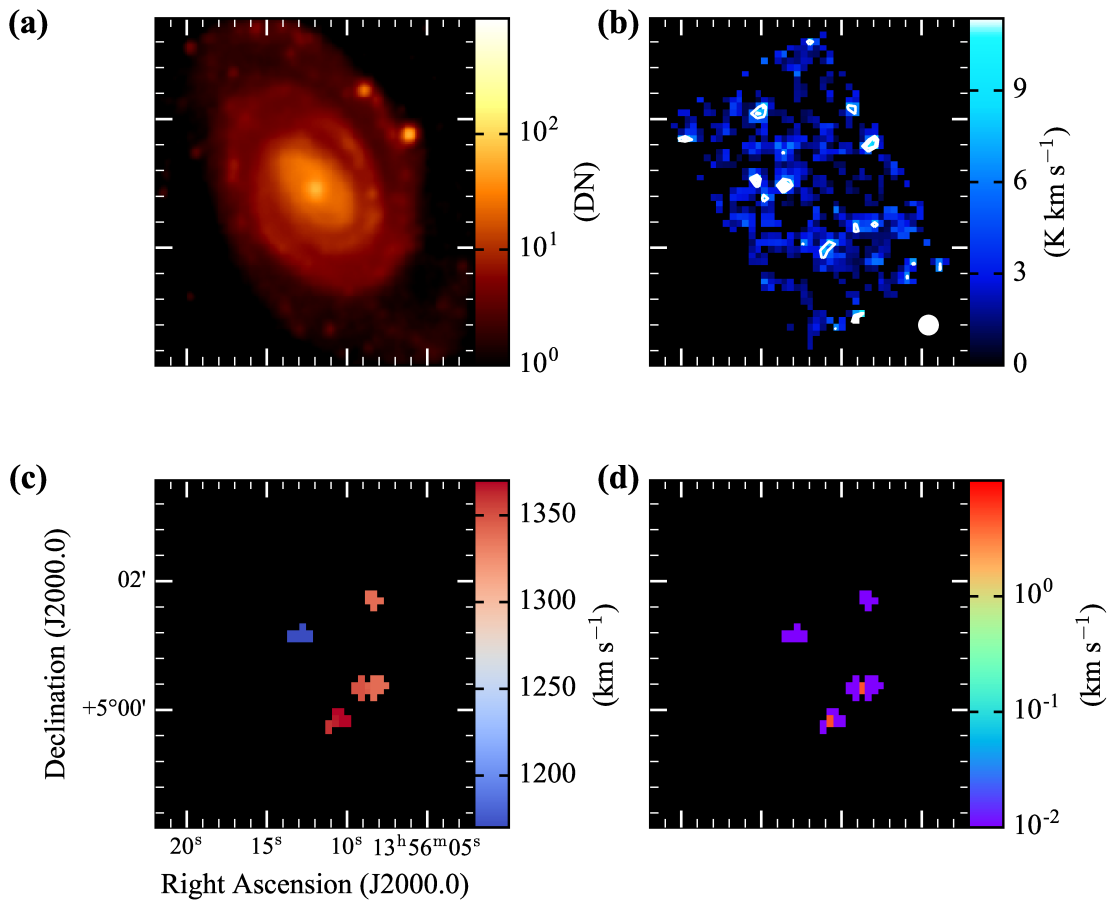

Supplementary fig. 101. Same as figure 12, but for NGC 5364. The contours are plotted at 50 %, 65 %, 80 %, and 95 % of the maximum intensity of 11.83 K km s^{-1} in (b).

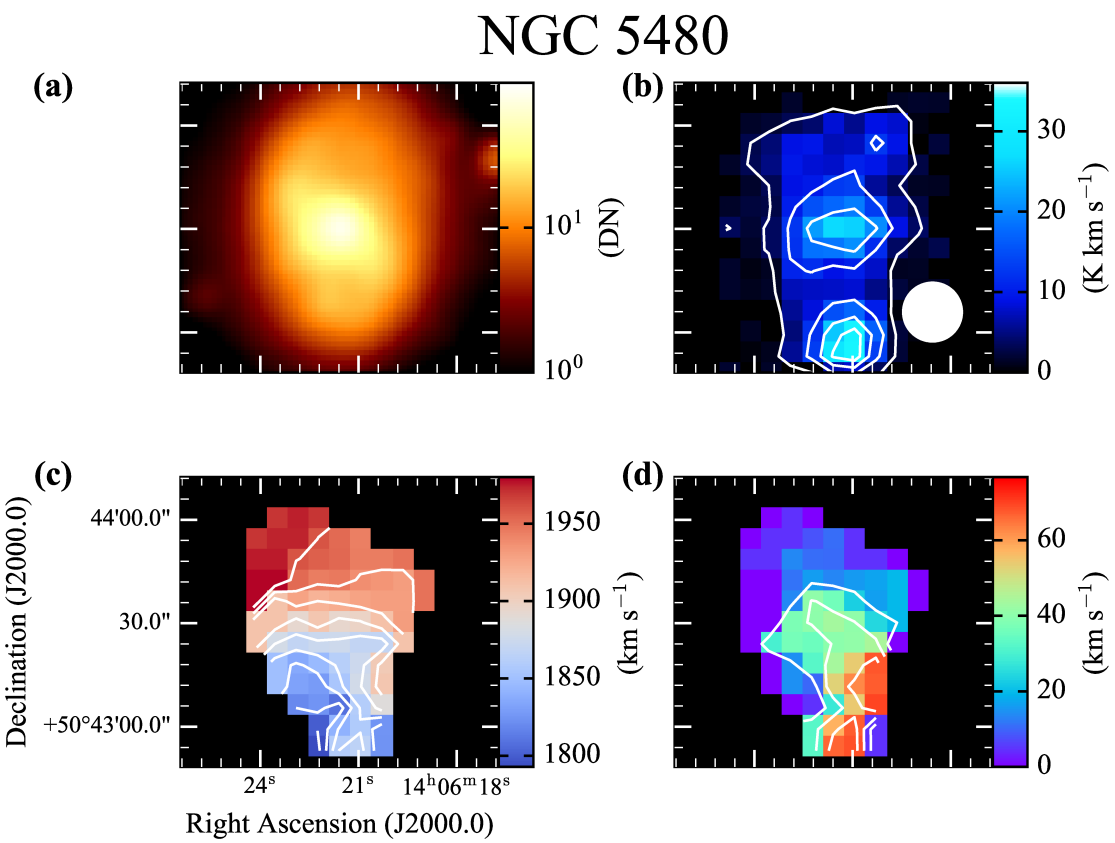

Supplementary fig. 102. Same as figure 12, but for NGC 5480. The contours are plotted at 10 %, 35 %, 60 %, and 85 % of the maximum intensity of $32.94\,\mathrm{K\,km\,s^{-1}}$ in (b) and in steps of $20\,\mathrm{km\,s^{-1}}$ in (c) and (d).

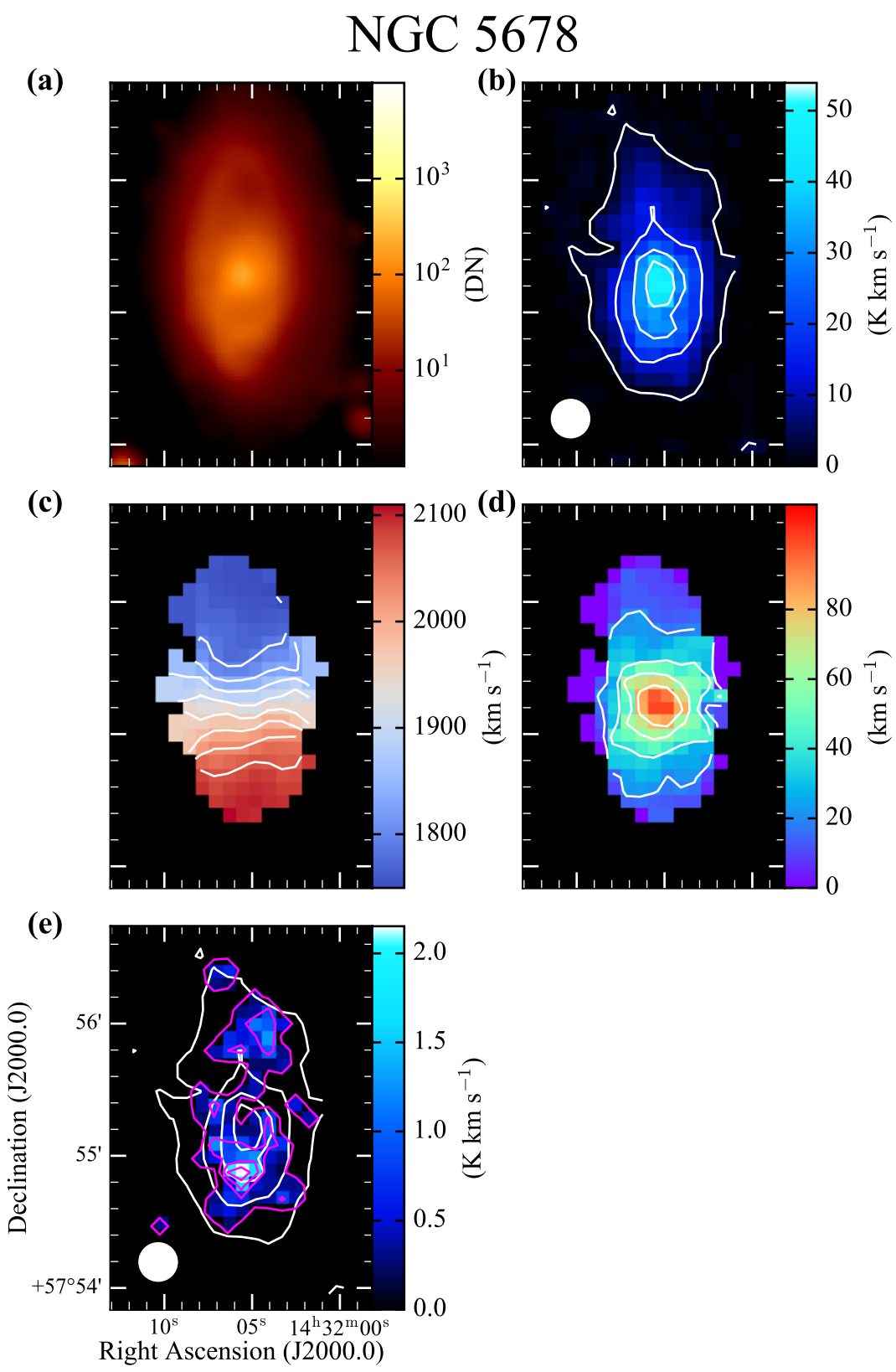

Supplementary fig. 103. Same as figure 12, but for NGC 5678. The contours are plotted at 5 %, 30 %, 55 %, and 80 % of the maximum intensity of 49.72 K km s^{-1} in (b) and (e) (*white*), in steps of 40 km s^{-1} in (c), in steps of 20 km s^{-1} in (d), and at 5 %, 30 %, 55 %, and 80 % of the maximum intensity of 2.44 K km s^{-1} in (e) (*magenta*).

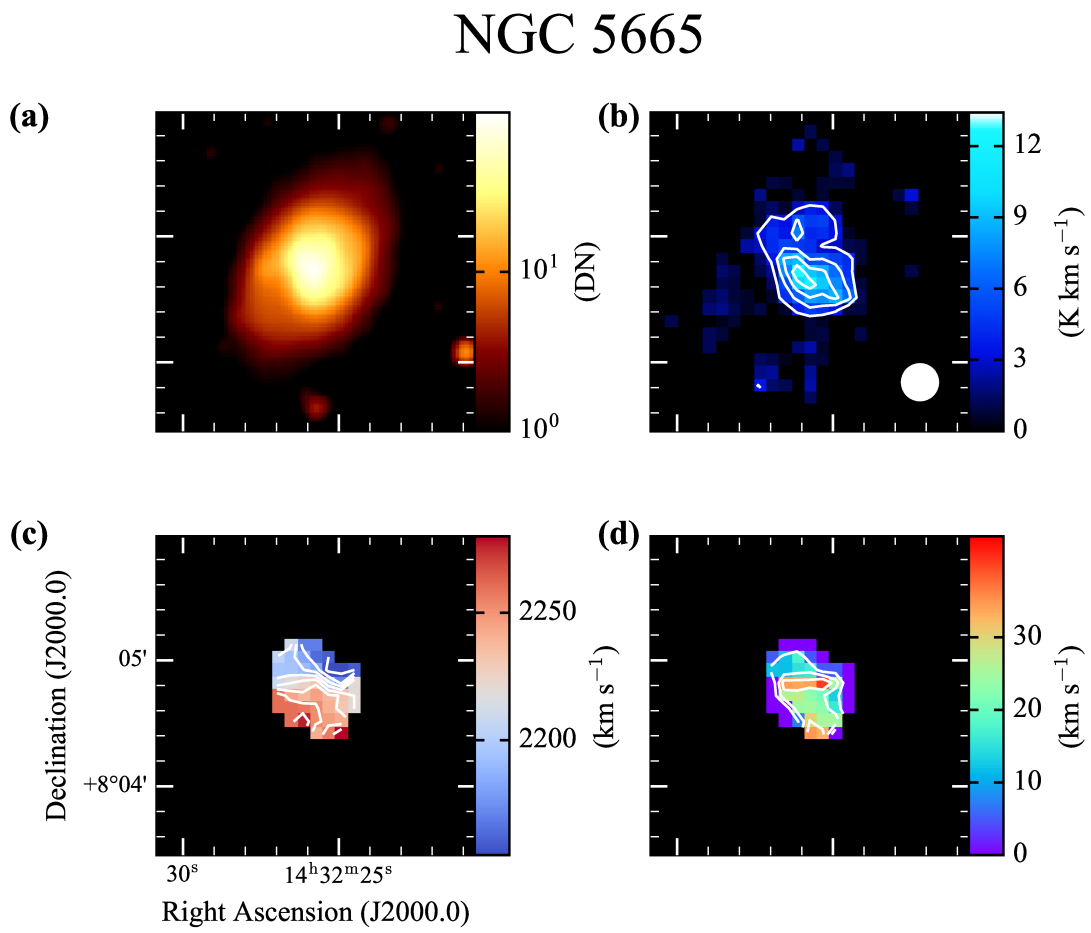

Supplementary fig. 104. Same as figure 12, but for NGC 5665. The contours are plotted at 25 %, 45 %, 65 %, and 85 % of the maximum intensity of $12.71\,\mathrm{K\,km\,s^{-1}}$ in (b), in steps of $15\,\mathrm{km\,s^{-1}}$ in (c), and in steps of $10\,\mathrm{km\,s^{-1}}$ in (d).

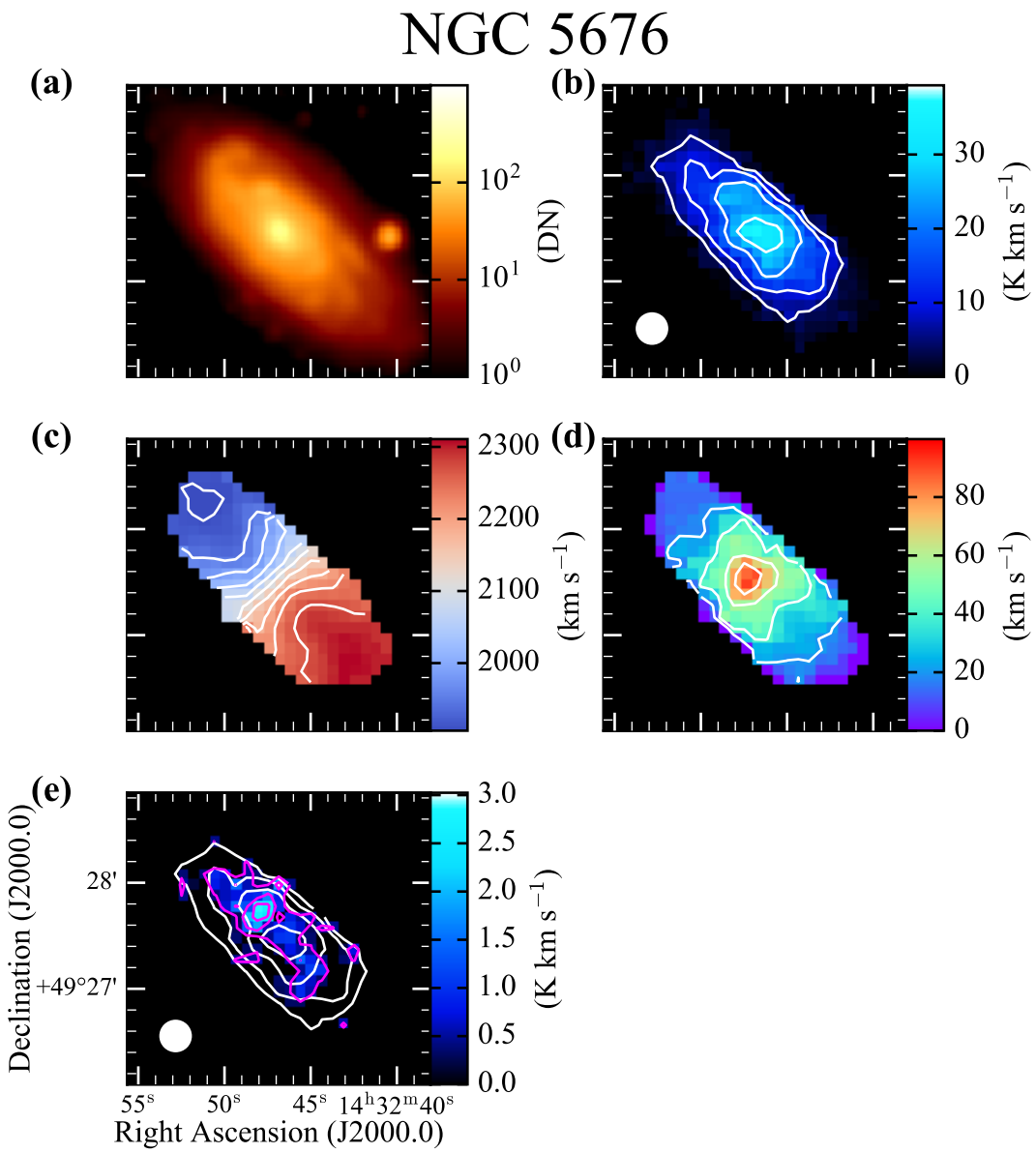

Supplementary fig. 105. Same as figure 12, but for NGC 5676. The contours are plotted at 15 %, 30 %, 55 %, and 80 % of the maximum intensity of 36.60 K km s^{-1} in (b) and (e) (*white*), in steps of 40 km s^{-1} in (c), in steps of 20 km s^{-1} in (d), and at 15 %, 50 %, and 85 % of the maximum intensity of 2.88 K km s^{-1} in (e) (*magenta*).

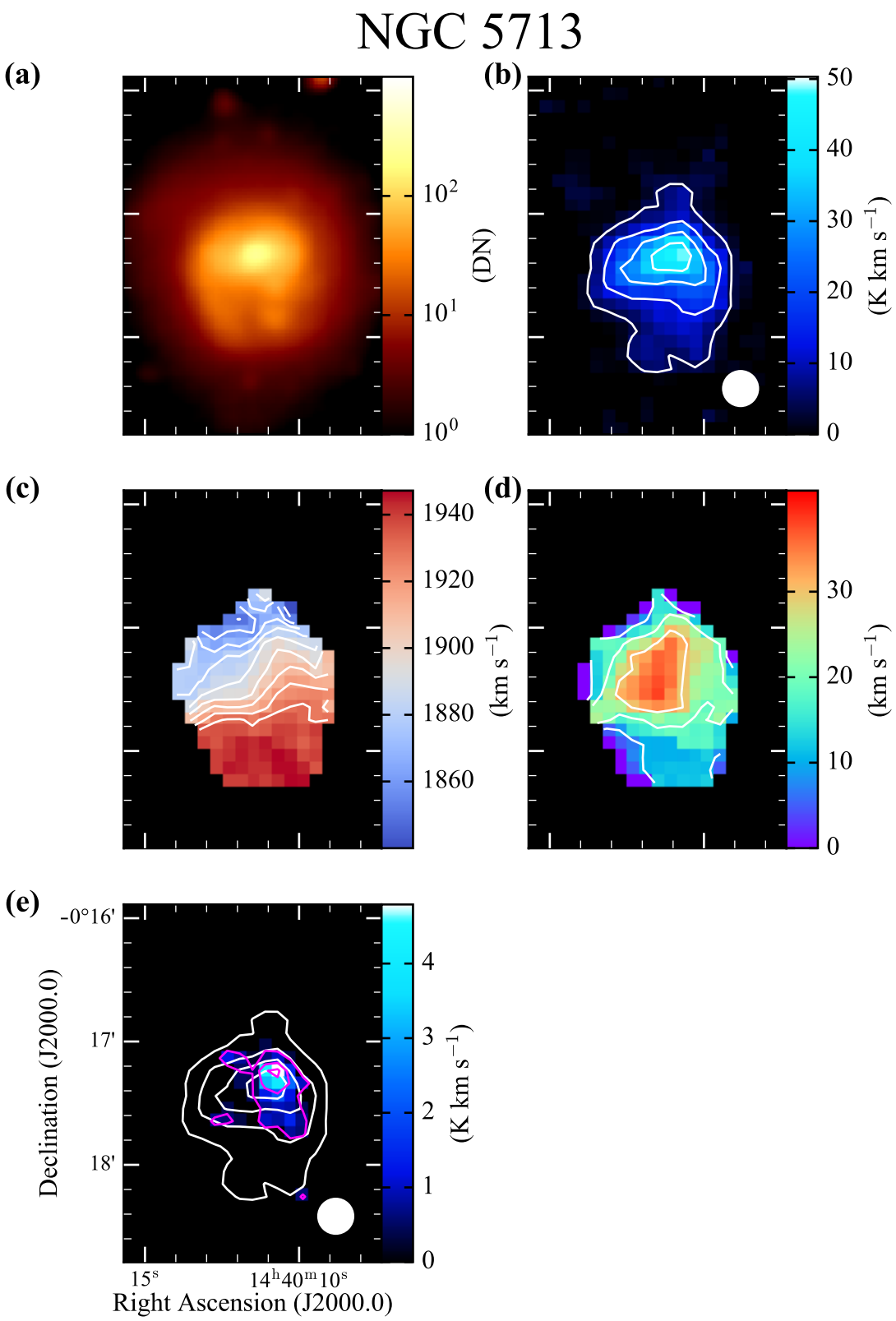

Supplementary fig. 106. Same as figure 12, but for NGC 5713. The contours are plotted at 10 %, 30 %, 55 %, and 80 % of the maximum intensity of $48.57\,\mathrm{K\,km\,s^{-1}}$ in (b) and (e) (*white*), in steps of $10\,\mathrm{km\,s^{-1}}$ in (c) and (d), and at 10 %, 50 %, and 90 % of the maximum intensity of $4.96\,\mathrm{K\,km\,s^{-1}}$ in (e) (*magenta*).

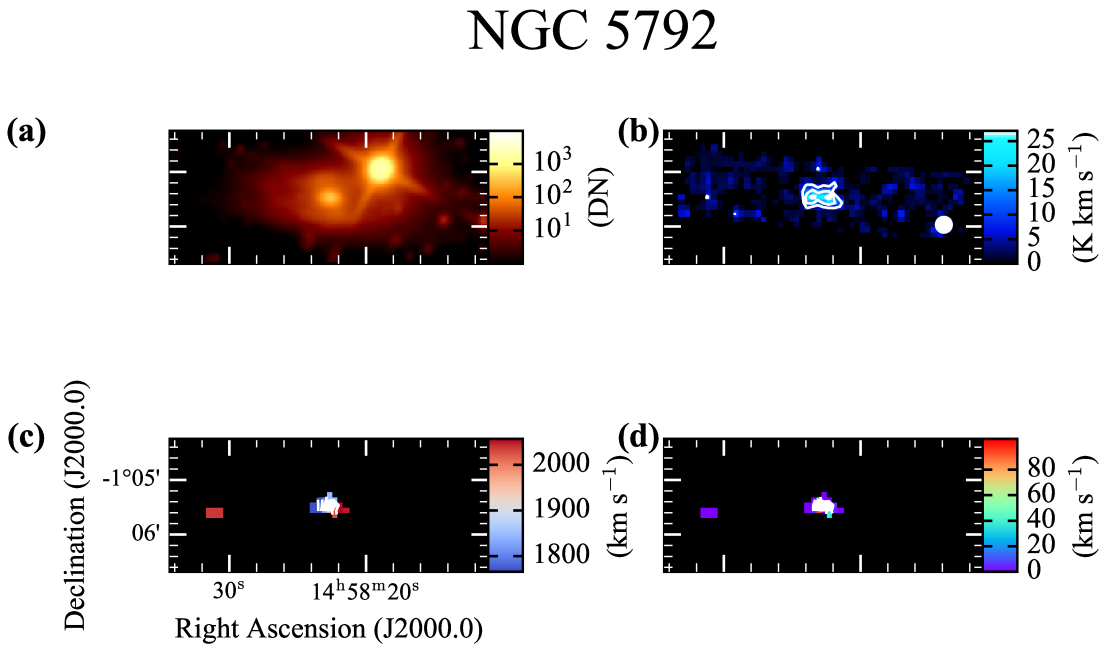

Supplementary fig. 107. Same as figure 12, but for NGC 5792. The contours are plotted at 30 %, 60 %, and 90 % of the maximum intensity of $27.76\,\mathrm{K\,km\,s^{-1}}$ in (b), in steps of $30\,\mathrm{km\,s^{-1}}$ in (c), and in steps of $20\,\mathrm{km\,s^{-1}}$ in (d).

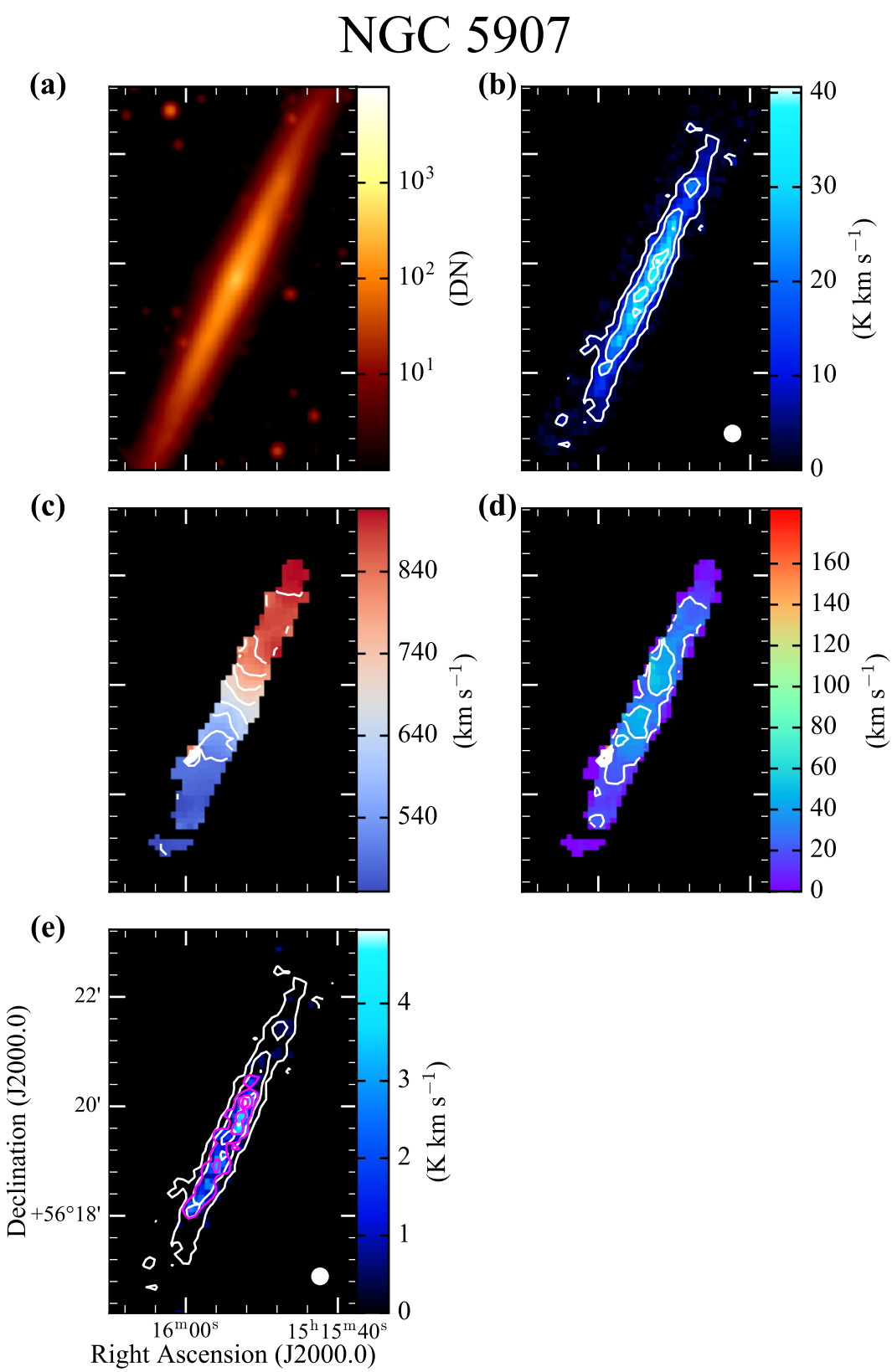

Supplementary fig. 108. Same as figure 12, but for NGC 5907. The contours are plotted at 10 %, 40 %, and 80 % of the maximum intensity of $40.49\,\mathrm{K\,km\,s^{-1}}$ in (b) and (e) (*white*), in steps of $50\,\mathrm{km\,s^{-1}}$ in (c), in steps of $20\,\mathrm{km\,s^{-1}}$ in (d), and at 10 %, 40 %, and 70 % of the maximum intensity of $7.05\,\mathrm{K\,km\,s^{-1}}$ in (e) (*magenta*).

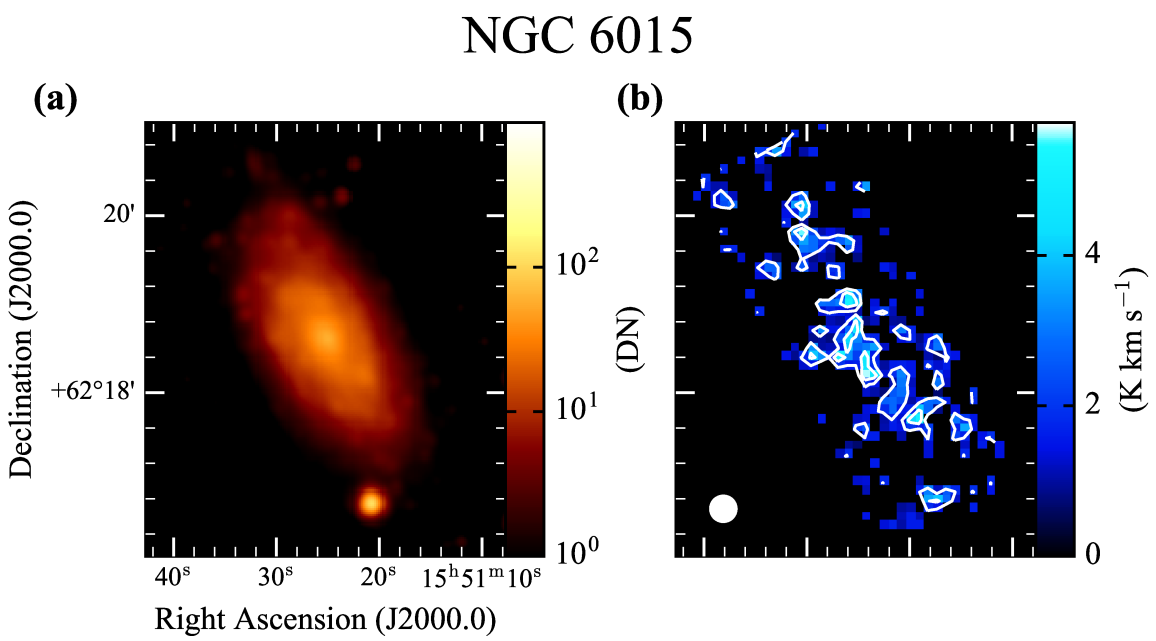

Supplementary fig. 109. Same as figure 12, but for NGC 6015. The contours are plotted at 30 % and 65 % of the maximum intensity of $5.66\,\mathrm{K\,km\,s^{-1}}$ in (b).

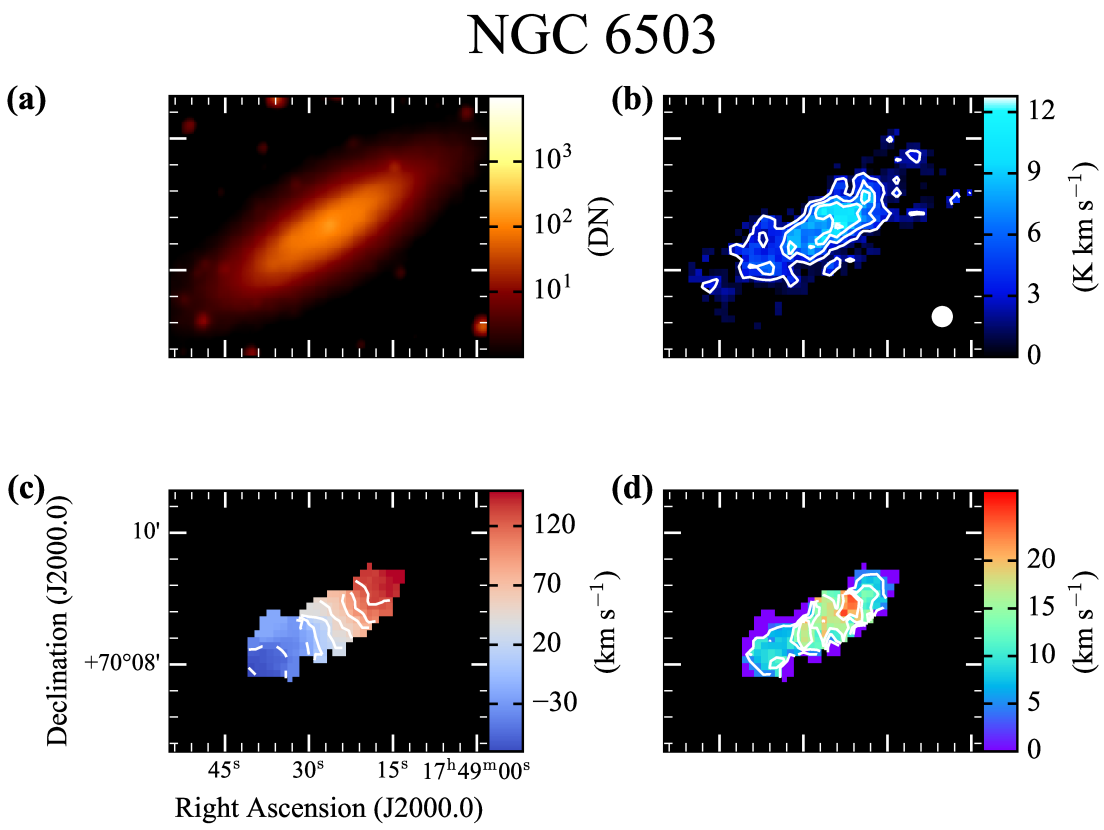

Supplementary fig. 110. Same as figure 12, but for NGC 6503. The contours are plotted at 20 %, 45 %, 70 %, and 95 % of the maximum intensity of $12.52\,\mathrm{K\,km\,s^{-1}}$ in (b), in steps of $25\,\mathrm{km\,s^{-1}}$ in (c), and in steps of $5\,\mathrm{km\,s^{-1}}$ in (d).

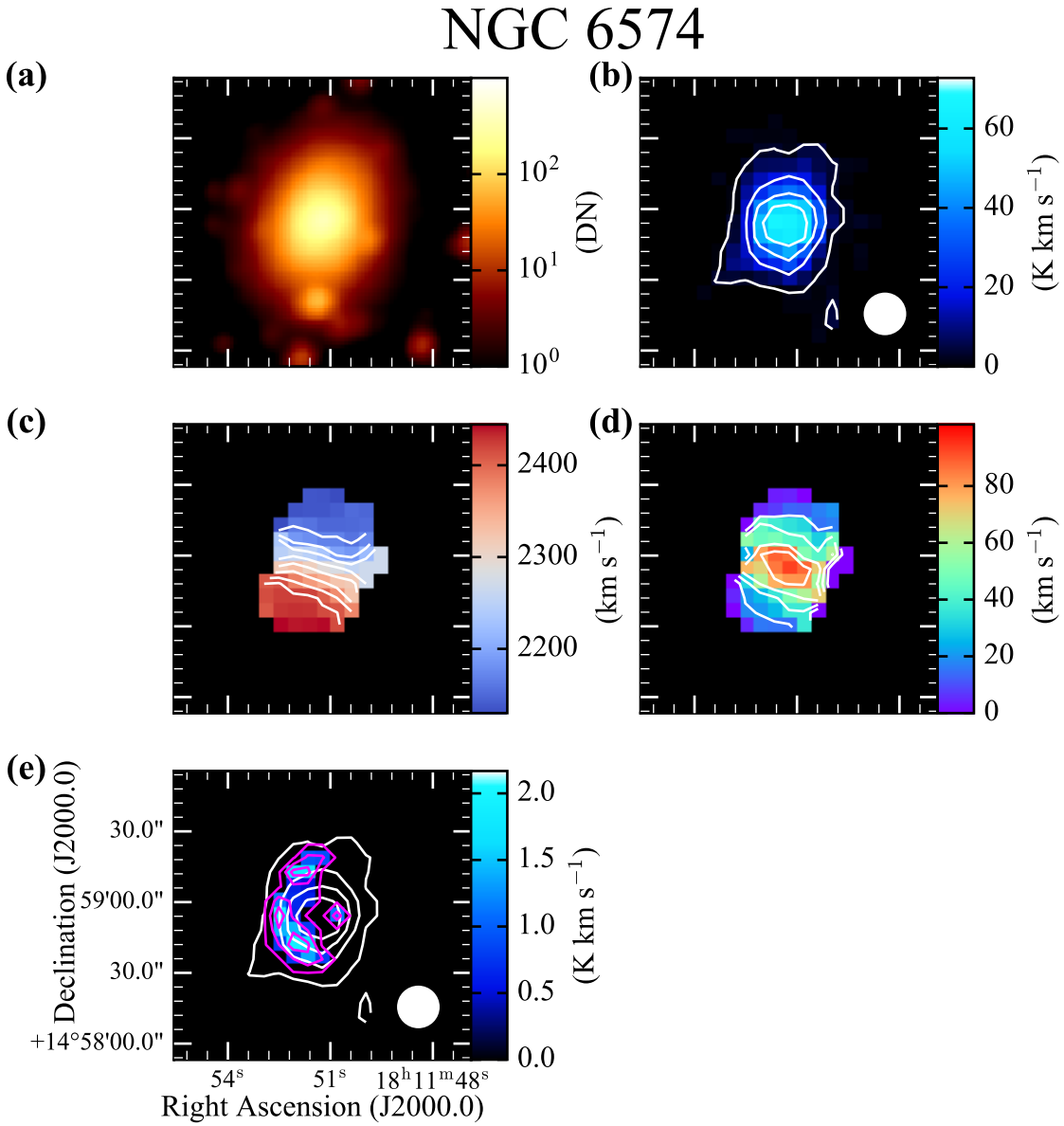

Supplementary fig. 111. Same as figure 12, but for NGC 6574. The contours are plotted at 5 %, 30 %, 55 %, and 80 % of the maximum intensity of 66.75 K km s^{-1} in (b) and (e) (*white*), in steps of 35 km s^{-1} in (c), in steps of 20 km s^{-1} in (d), and at 5 %, 40 %, and 75 % of the maximum intensity of 2.02 K km s^{-1} in (e) (*magenta*).

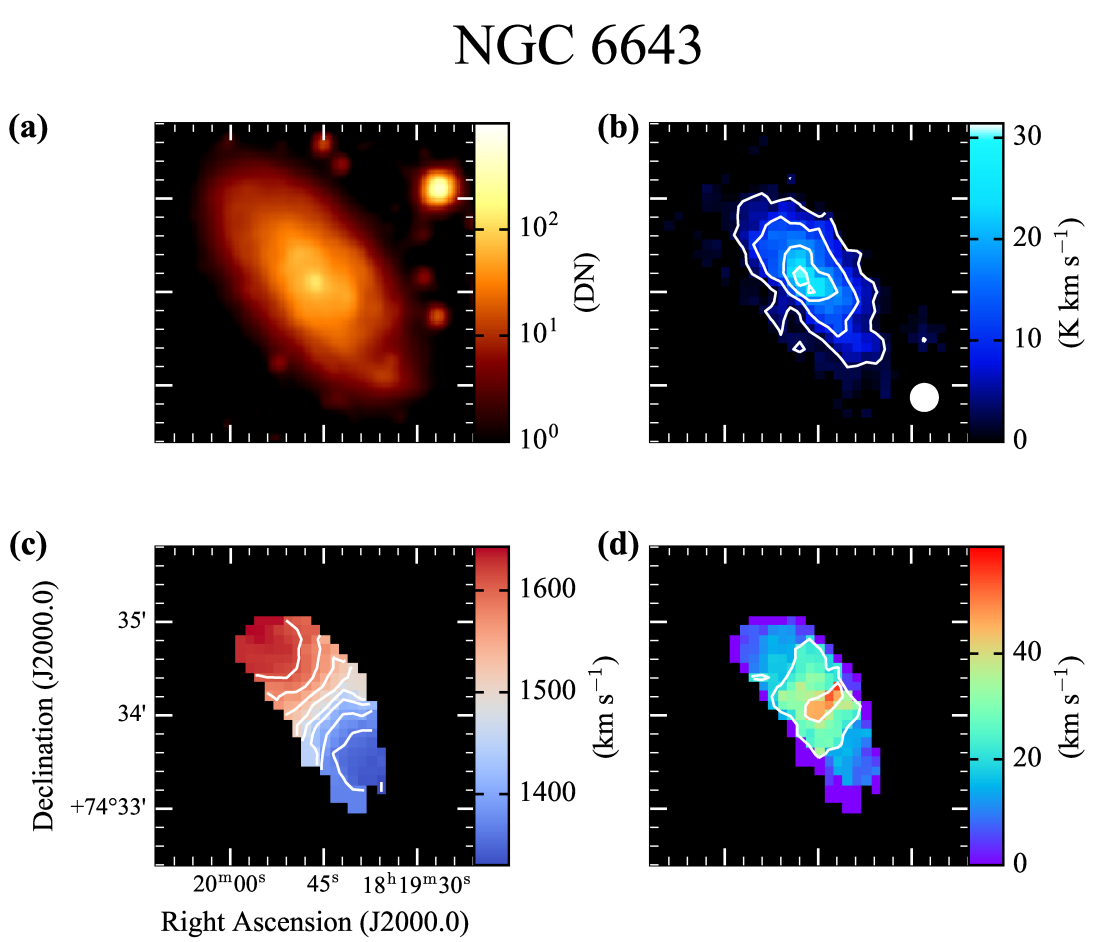

Supplementary fig. 112. Same as figure 12, but for NGC 6643. The contours are plotted at 10 %, 35 %, 60 %, and 85 % of the maximum intensity of $30.31\,\mathrm{K\,km\,s^{-1}}$ in (b), in steps of $35\,\mathrm{km\,s^{-1}}$ in (c), and in steps of $20\,\mathrm{km\,s^{-1}}$ in (d).

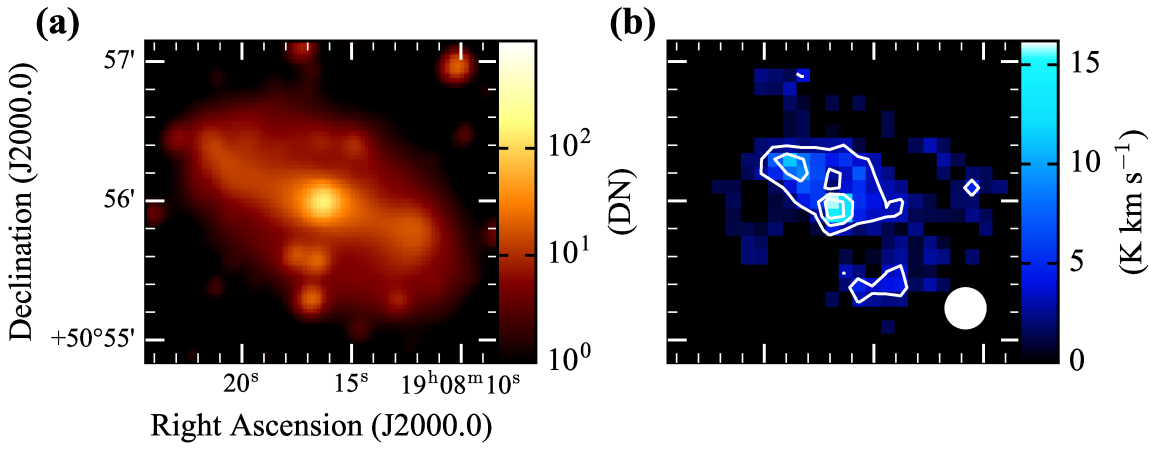

Supplementary fig. 113. Same as figure 12, but for NGC 6764. The contours are plotted at 20 %, 50 %, and 80 % of the maximum intensity of $15.90\,\mathrm{K\,km\,s^{-1}}$ in (b).

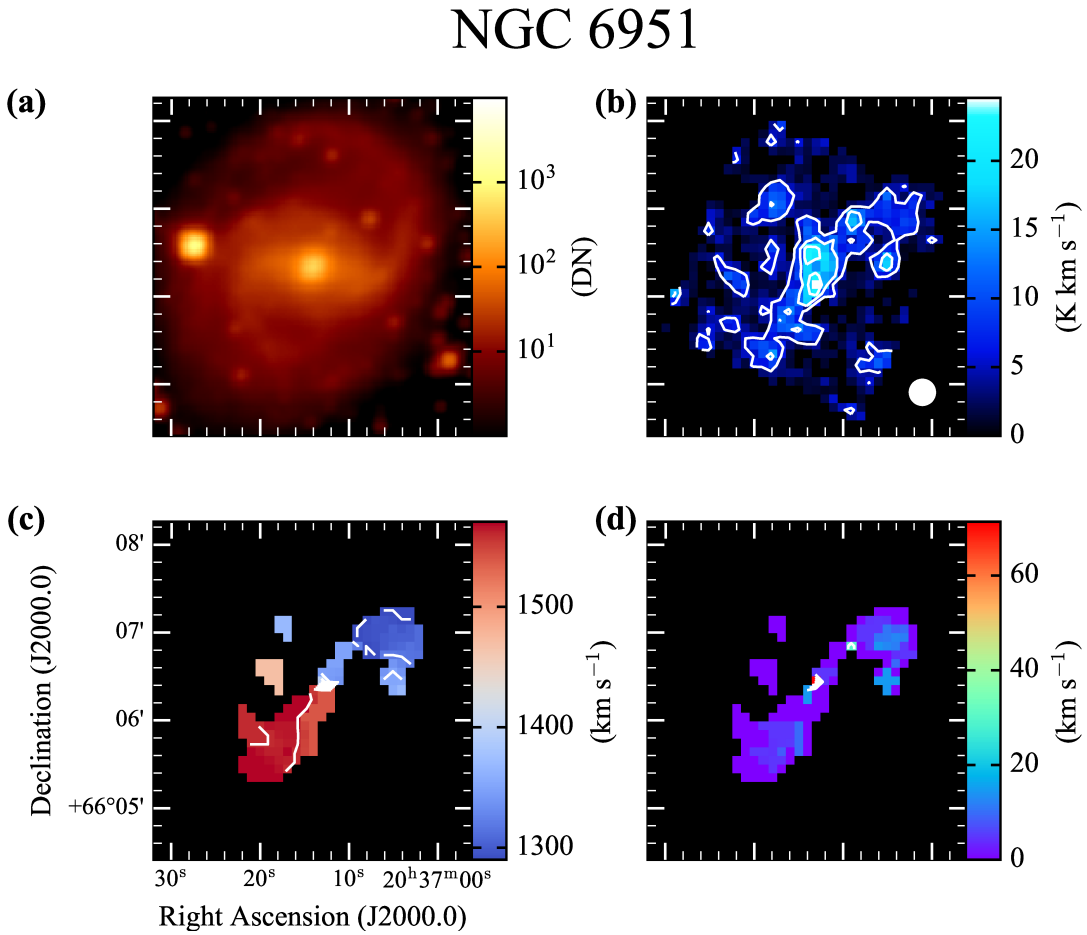

Supplementary fig. 114. Same as figure 12, but for NGC 6951. The contours are plotted at 20 %, 45 %, 70 %, and 95 % of the maximum intensity of 27.52 K km s^{-1} in (b), in steps of 30 km s^{-1} in (c), and in steps of 20 km s^{-1} in (d).

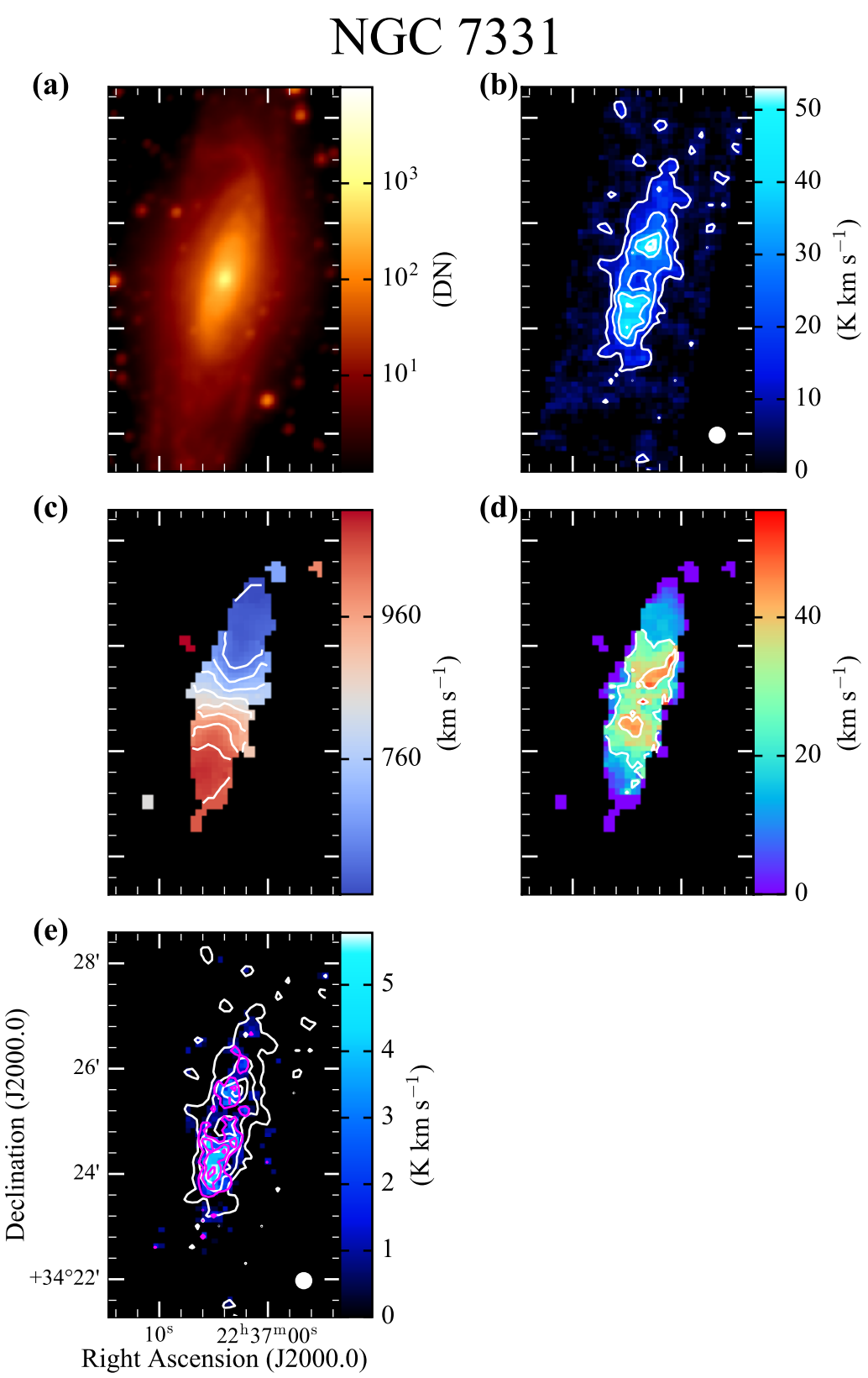

Supplementary fig. 115. Same as figure 12, but for NGC 7331. The contours are plotted at 15 %, 40 %, 65 %, and 90 % of the maximum intensity of 53.43 K km s^{-1} in (b) and (e) (*white*), in steps of 60 km s^{-1} in (c), in steps of 20 km s^{-1} in (d), and at 20 %, 55 %, and 90 % of the maximum intensity of 6.12 K km s^{-1} in (e) (*magenta*).

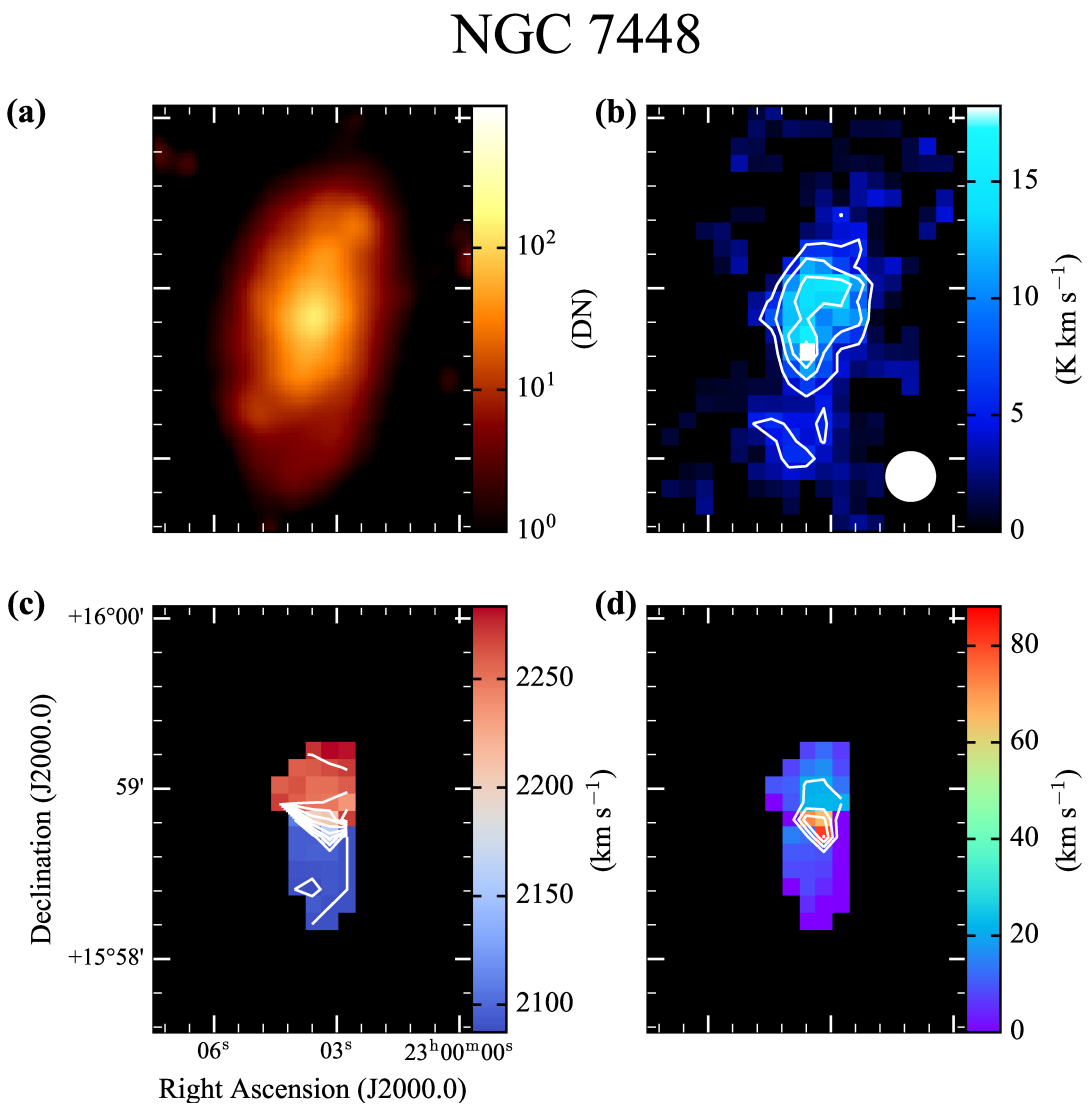

Supplementary fig. 116. Same as figure 12, but for NGC 7448. The contours are plotted at 25 %, 45 %, 65 %, and 85 % of the maximum intensity of $20.01\,\mathrm{K\,km\,s^{-1}}$ in (b) and in steps of $20\,\mathrm{km\,s^{-1}}$ in (c) and (d).

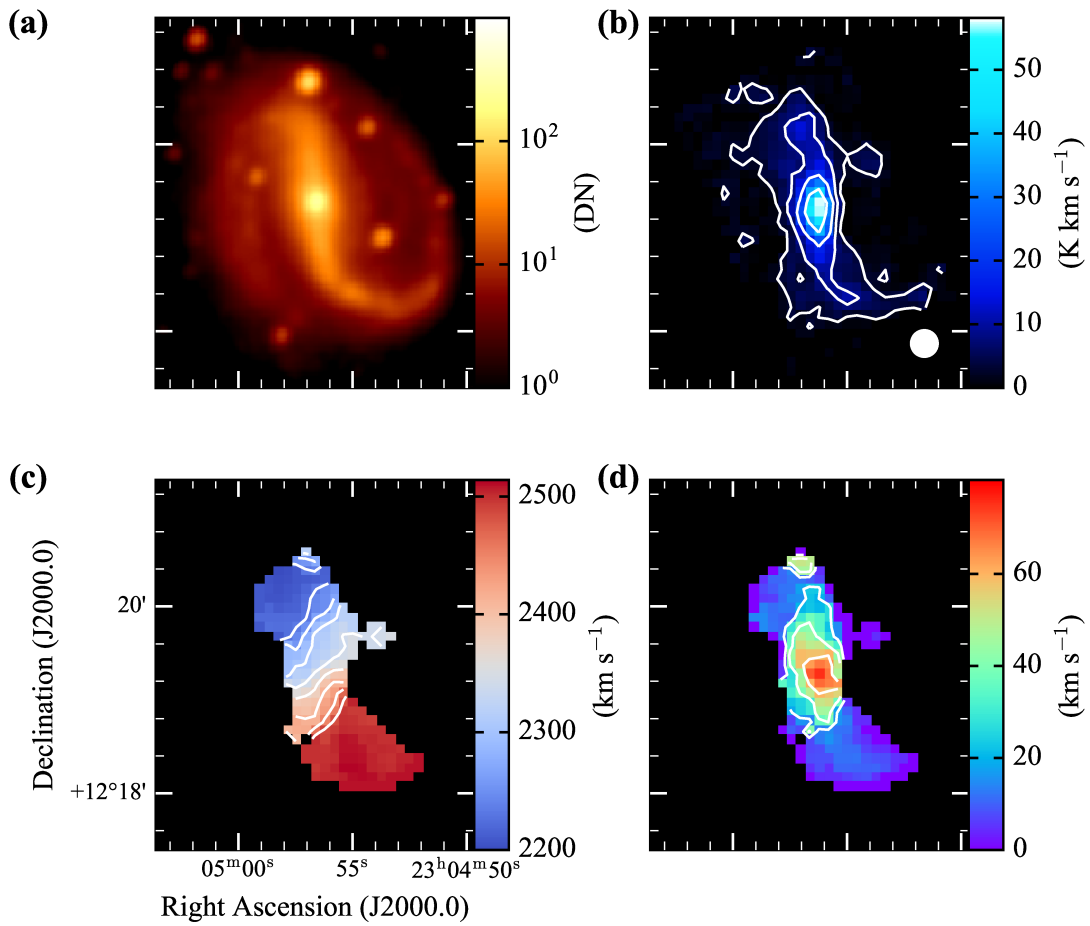

Supplementary fig. 117. Same as figure 12, but for NGC 7479. The contours are plotted at 5 %, 15 %, 35 %, and 65 % of the maximum intensity of 57.72 K km s^{-1} in (b), in steps of 35 km s^{-1} in (c), and in steps of 20 km s^{-1} in (d).

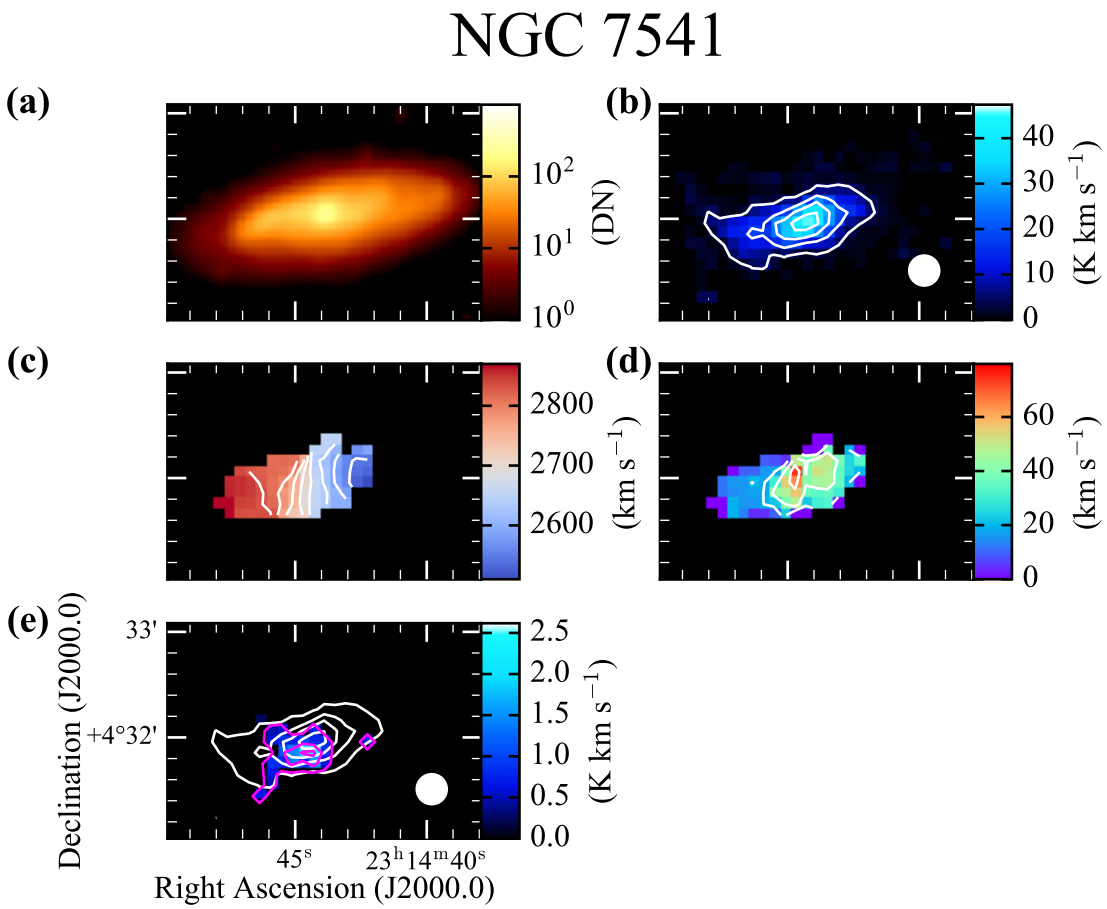

Supplementary fig. 118. Same as figure 12, but for NGC 7541. The contours are plotted at 10 %, 35 %, 60 %, and 85 % of the maximum intensity of 45.56 K km s^{-1} in (b) and (e) (*white*), in steps of 40 km s^{-1} in (c), in steps of 20 km s^{-1} in (d), and at 10 %, 50 %, and 90 % of the maximum intensity of 2.46 K km s^{-1} in (e) (*magenta*).

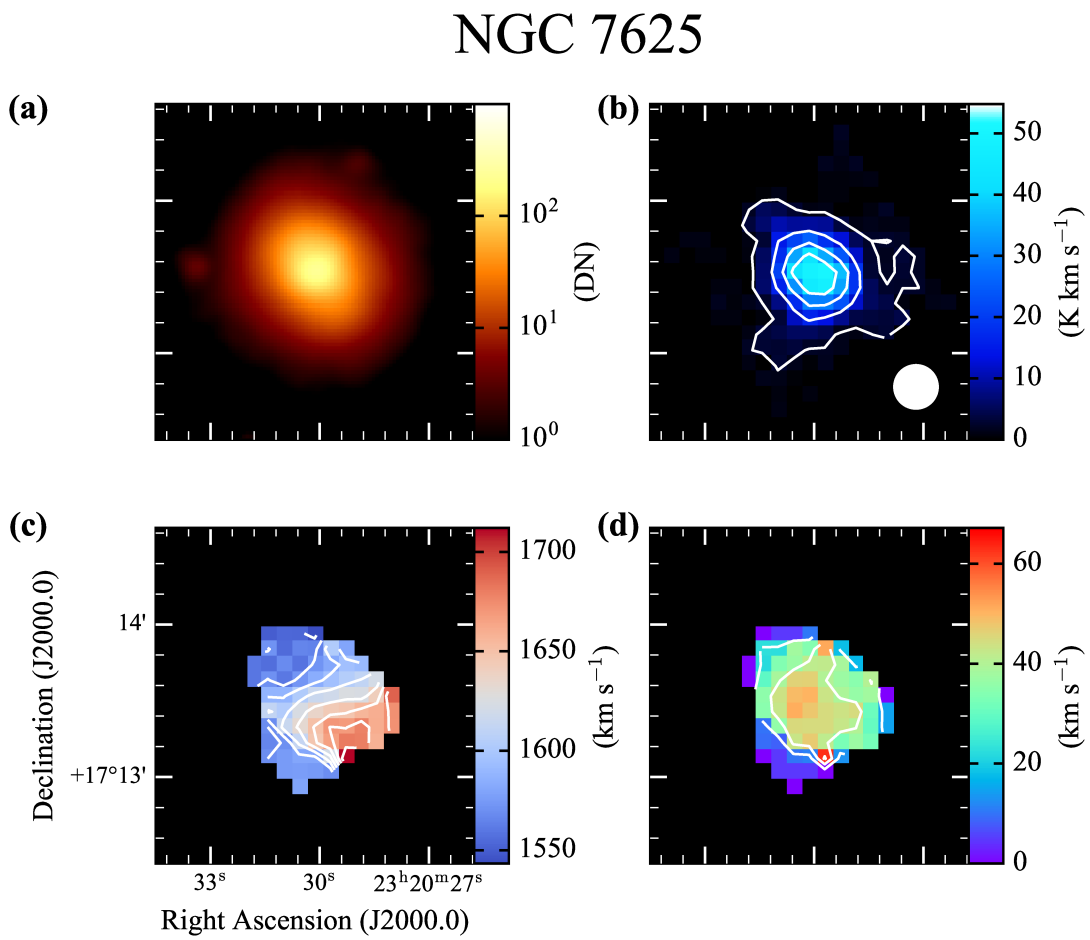

Supplementary fig. 119. Same as figure 12, but for NGC 7625. The contours are plotted at 5 %, 30 %, 55 %, and 80 % of the maximum intensity of $50.54\,\mathrm{K\,km\,s^{-1}}$ in (b) and in steps of $20\,\mathrm{km\,s^{-1}}$ in (c) and (d).

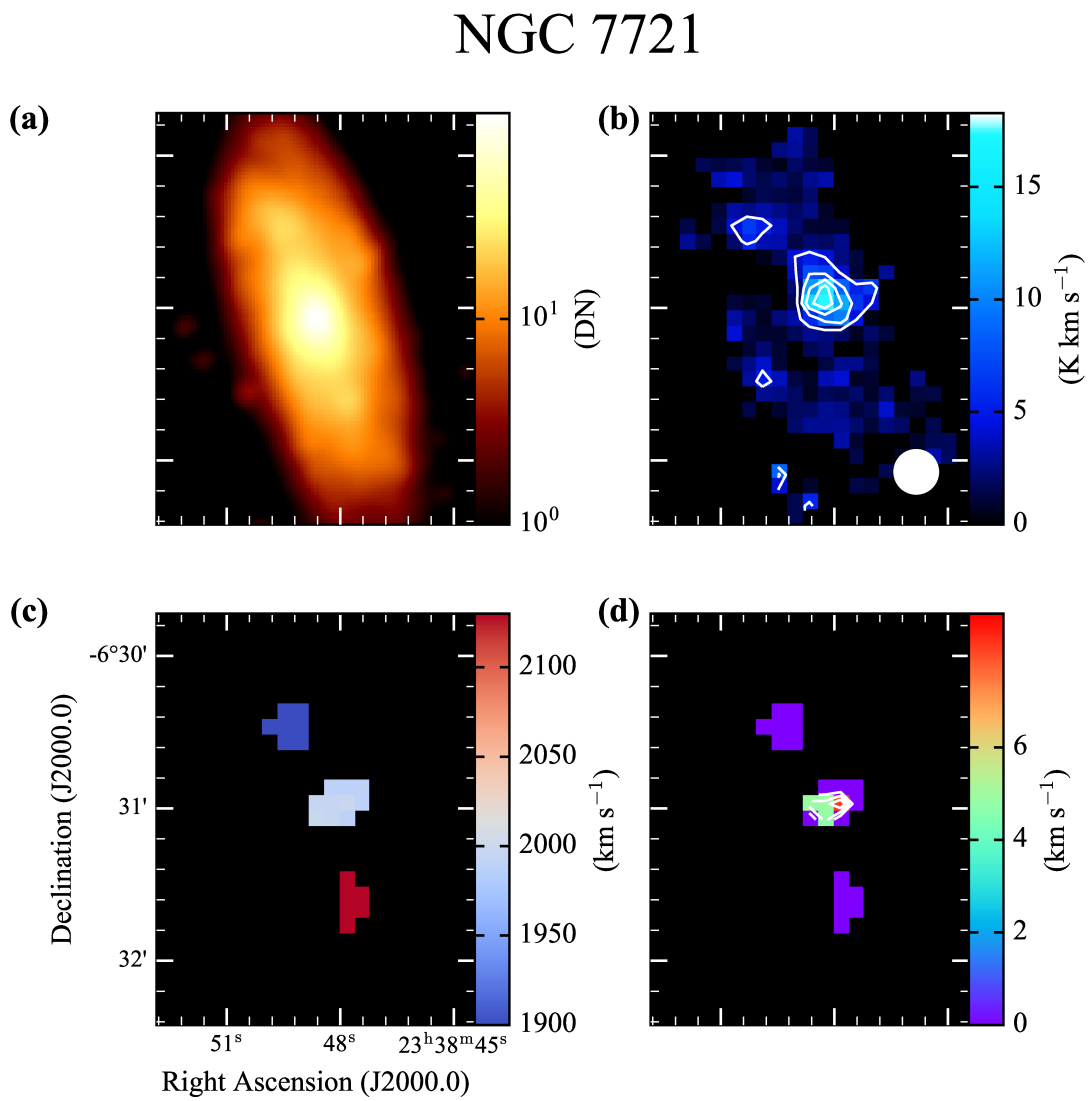

Supplementary fig. 120. Same as figure 12, but for NGC 7721. The contours are plotted at 25 %, 45 %, 65 %, and 85 % of the maximum intensity of 17.42 K km s^{-1} in (b), in steps of 25 km s^{-1} in (c), and in steps of 2 km s^{-1} in (d).

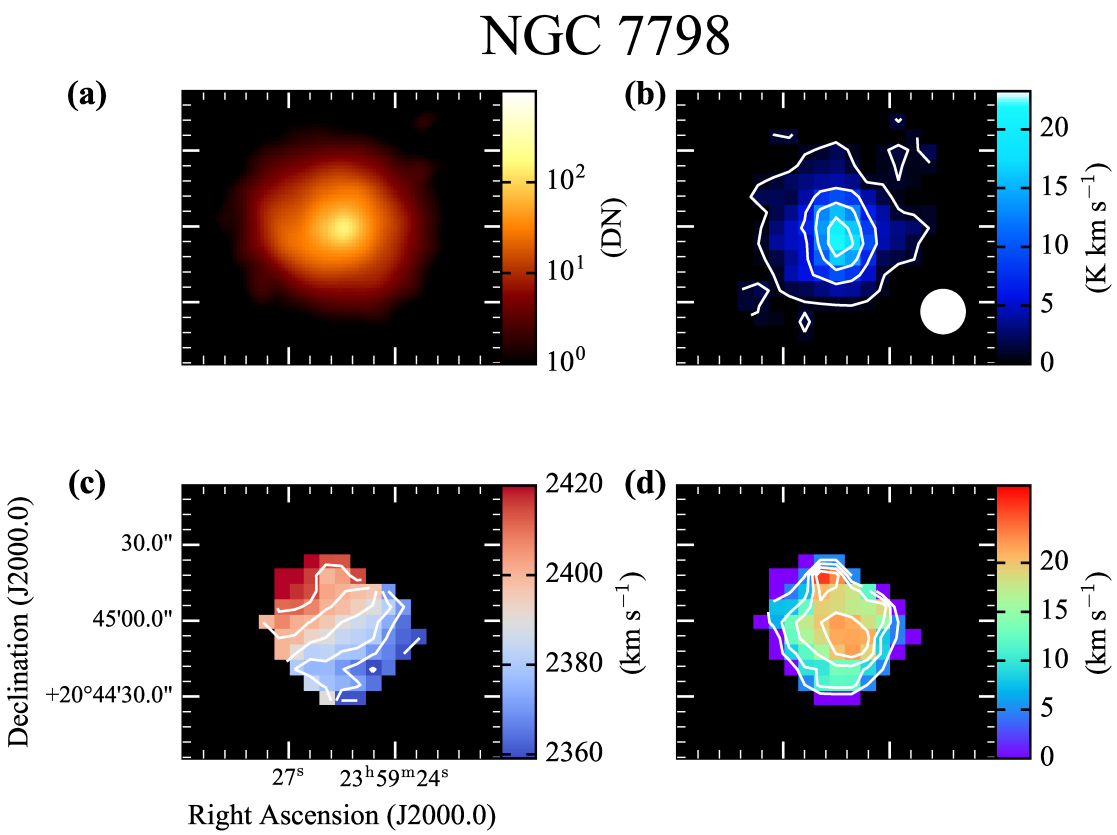

Supplementary fig. 121. Same as figure 12, but for NGC 7798. The contours are plotted at 5 %, 30 %, 55 %, and 80 % of the maximum intensity of $21.67\,\mathrm{K\,km\,s^{-1}}$ in (b), in steps of $10\,\mathrm{km\,s^{-1}}$ in (c), and in steps of $5\,\mathrm{km\,s^{-1}}$ in (d).

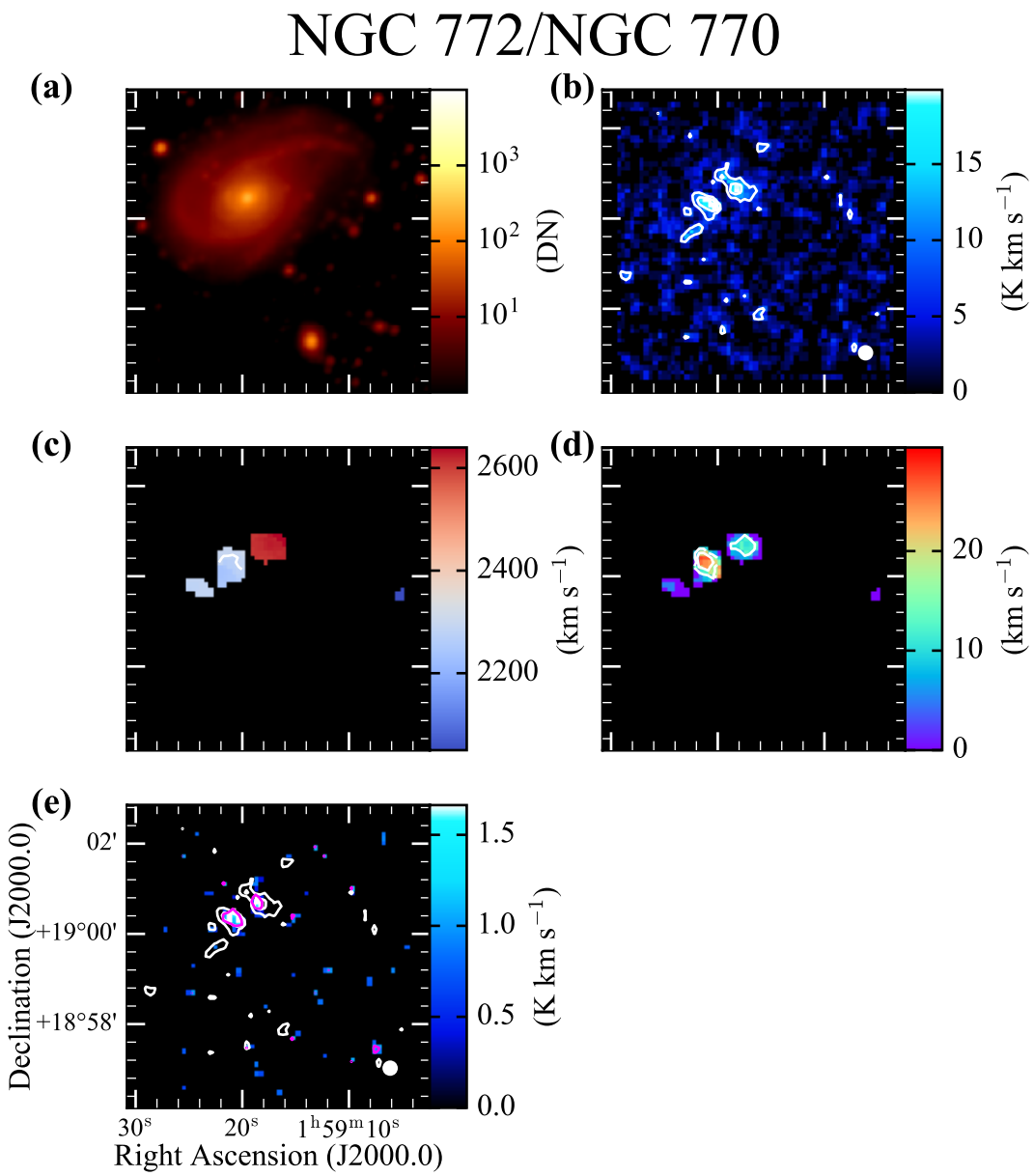

Supplementary fig. 122. Same as figure 12, but for NGC 772 / NGC 770 pair. The upper galaxy is NGC 772 and the lower and smaller one is NGC 770. The contours are plotted at 30 % and 60 % of the maximum intensity of $25.23\,\mathrm{K\,km\,s^{-1}}$ in (b) and (e) (*white*), in steps of $60\,\mathrm{km\,s^{-1}}$ in (c), in steps of $10\,\mathrm{km\,s^{-1}}$ in (d), and at 35 % of the maximum intensity of $2.78\,\mathrm{K\,km\,s^{-1}}$ in (e) (*magenta*).

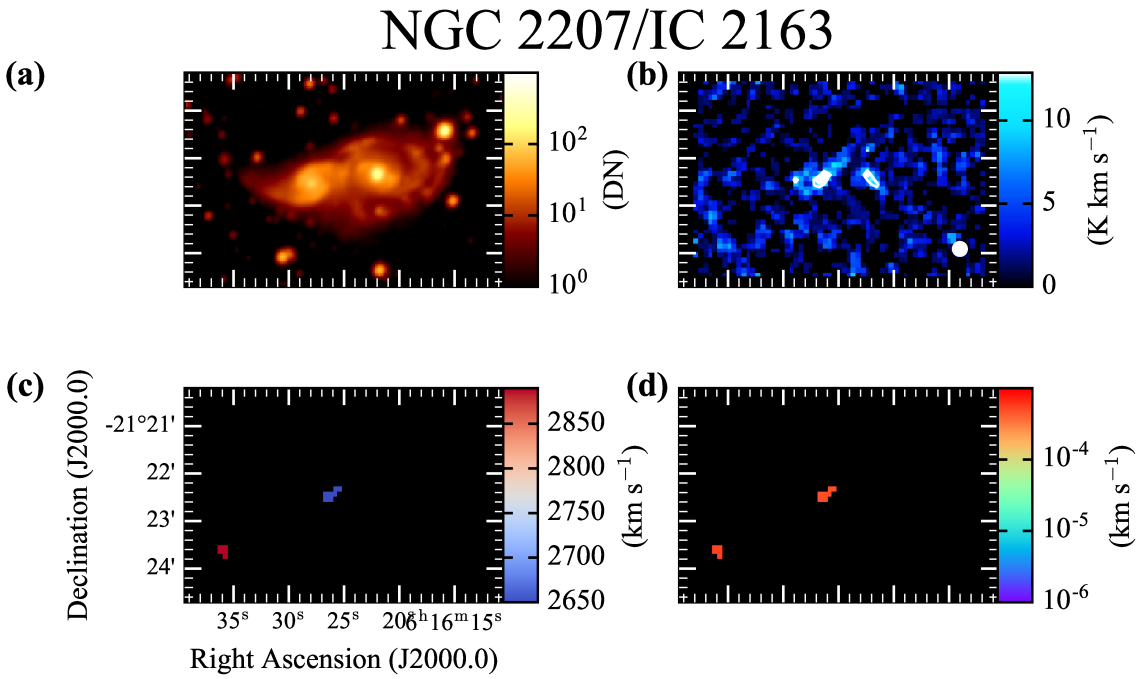

Supplementary fig. 123. Same as figure 12, but for NGC 2207 / IC 2163 pair. The right galaxy is NGC 2207 and the left one is IC 2163. The contours are plotted at 50 %, 65 %, 80 %, and 95 % of the maximum intensity of $19.48\,\mathrm{K\,km\,s^{-1}}$ in (b).

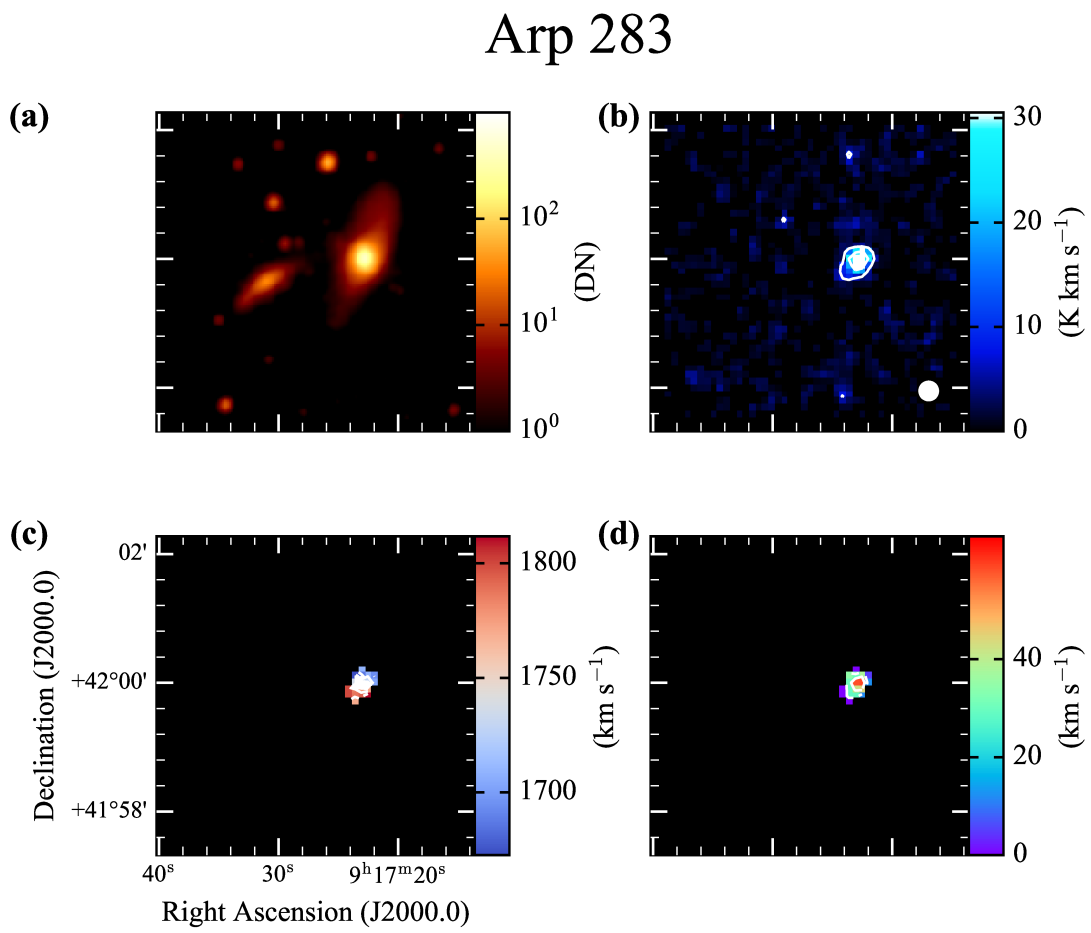

Supplementary fig. 124. Same as figure 12, but for Arp 283. The right galaxy is NGC 2798 and the left one is NGC 2799. The contours are plotted at 15 % and 55 % of the maximum intensity of $50.08\,\mathrm{K\,km\,s^{-1}}$ in (b), in steps of $15\,\mathrm{km\,s^{-1}}$ in (c), and in steps of $20\,\mathrm{km\,s^{-1}}$ in (d).

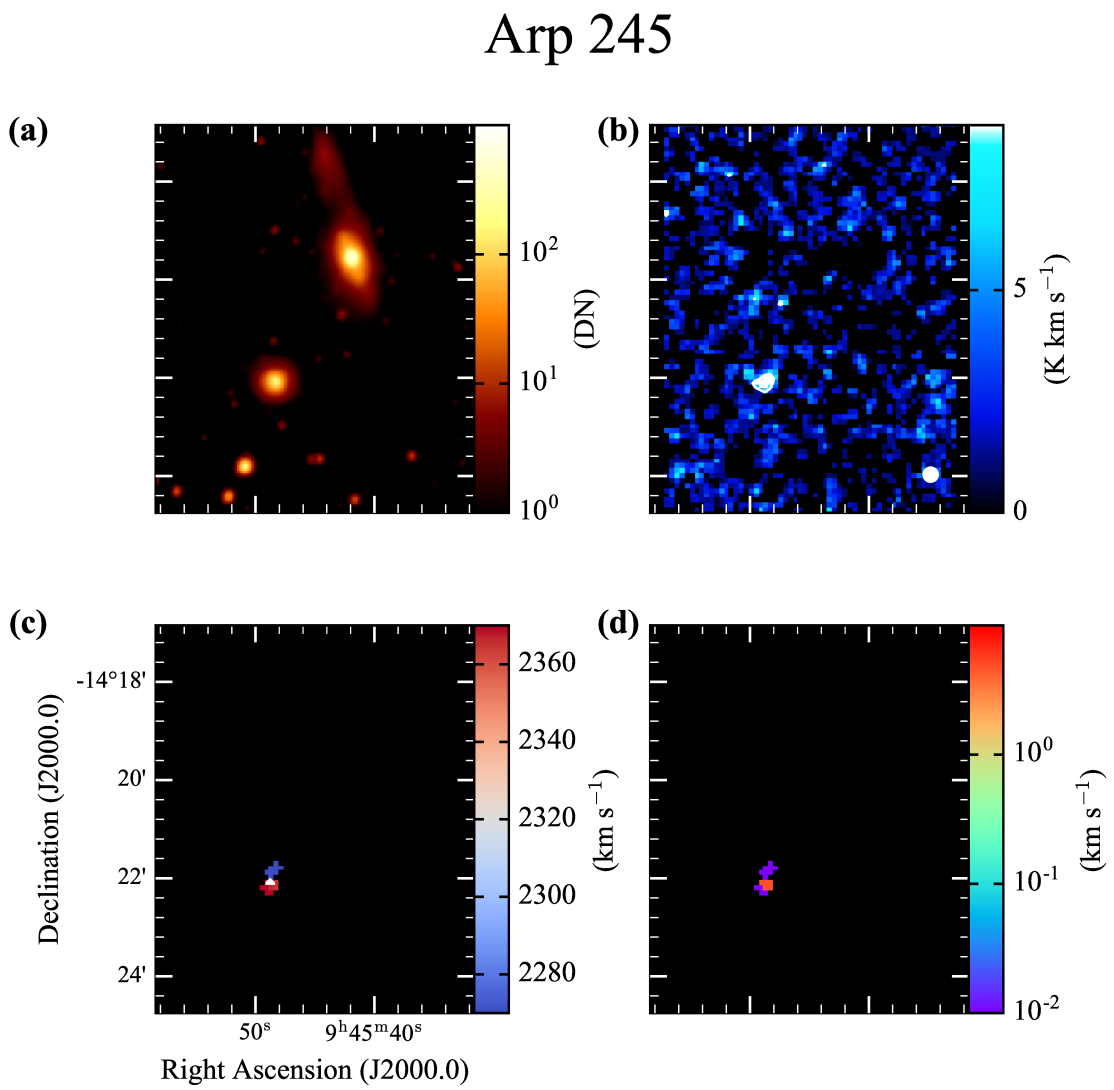

Supplementary fig. 125. Same as figure 12, but for Arp 245. The upper galaxy is NGC 2992 and the lower one is NGC 2993. The contours are plotted at 35 % of the maximum intensity of $21.24\,\mathrm{K\,km\,s^{-1}}$ in (b).

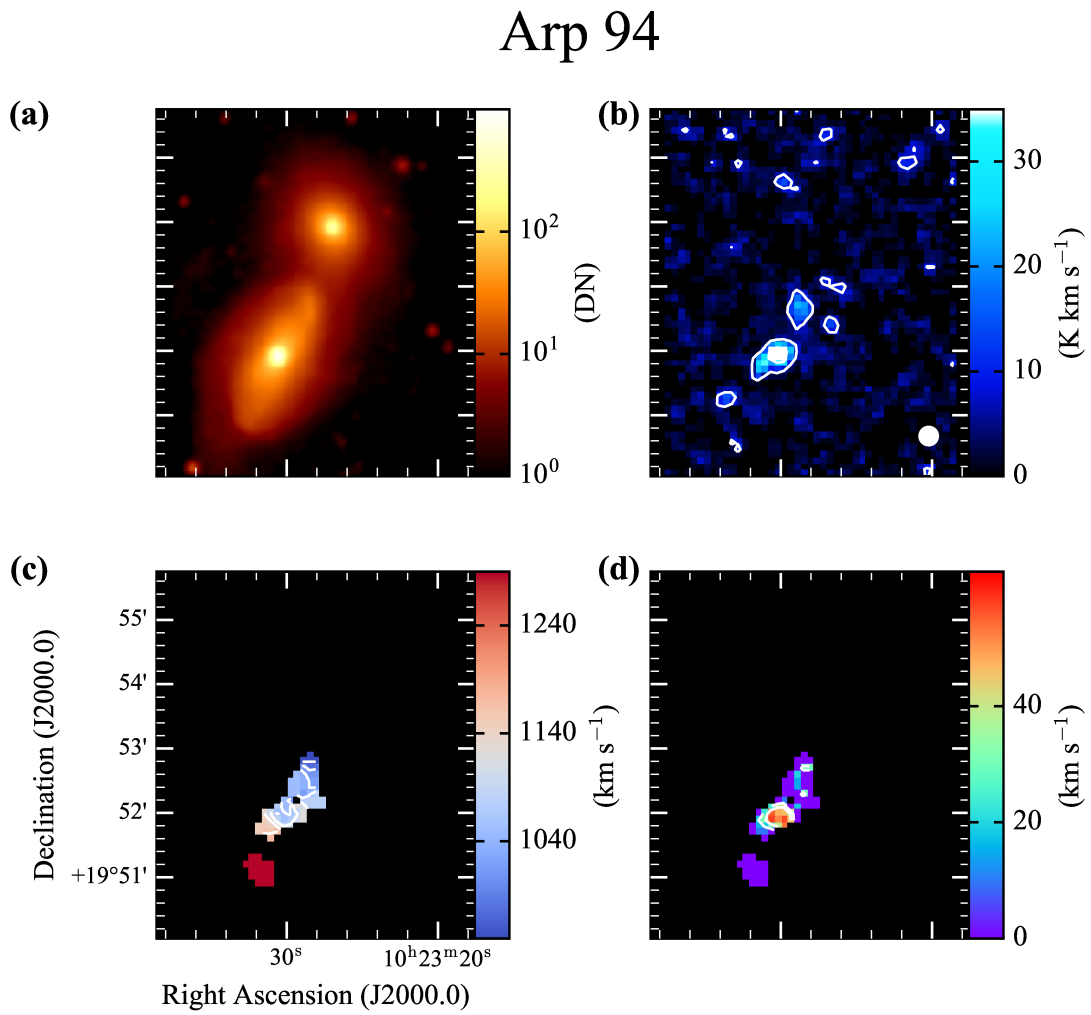

Supplementary fig. 126. Same as figure 12, but for Arp 94. The upper galaxy is NGC 3226 and the lower one is NGC 3227. The contours are plotted at 15 % and 65 % of the maximum intensity of $54.22\,\mathrm{K\,km\,s^{-1}}$ in (b), in steps of $35\,\mathrm{km\,s^{-1}}$ in (c), and in steps of $20\,\mathrm{km\,s^{-1}}$ in (d).

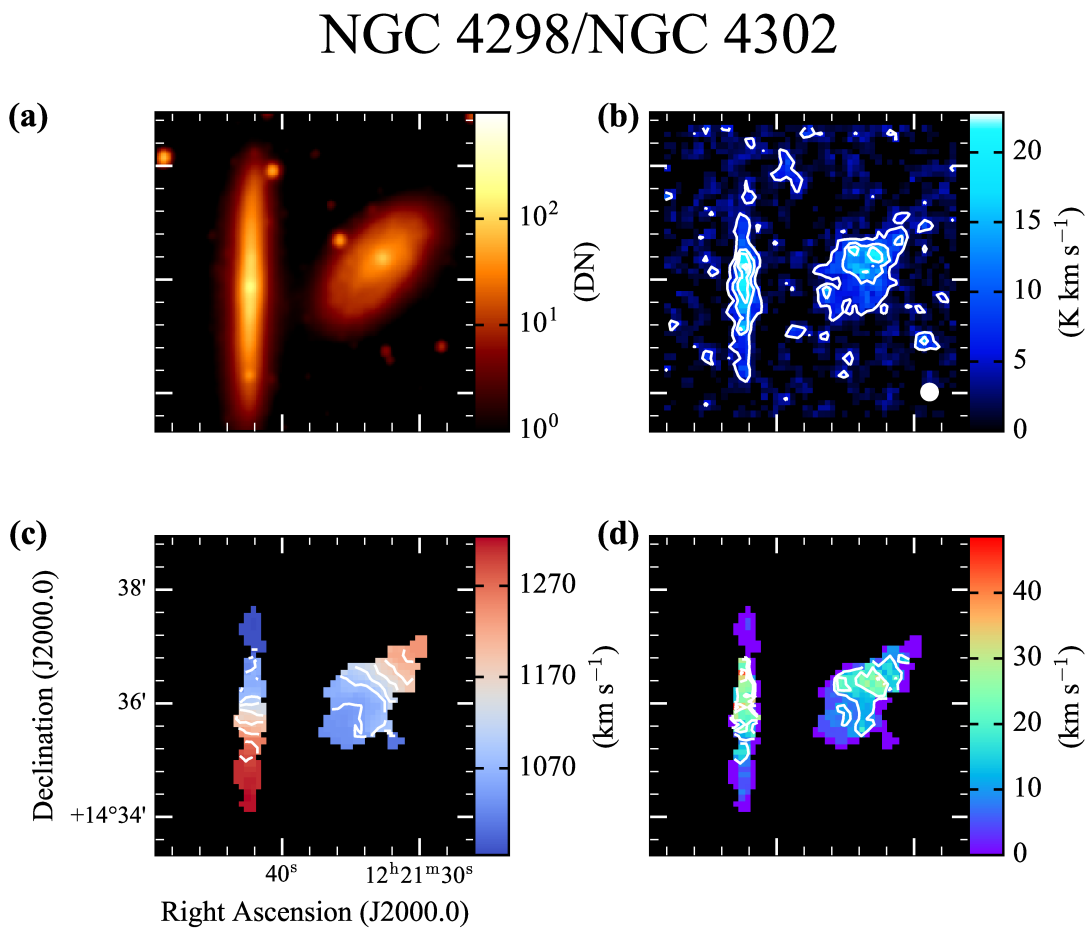

Supplementary fig. 127. Same as figure 12, but for NGC 4298 / NGC 4302 pair. The right galaxy is NGC 4298 and the left one is NGC 4302. The contours are plotted at 20 %, 45 %, 70 %, and 95 % of the maximum intensity of $24.42\,\mathrm{K\,km\,s^{-1}}$ in (b), in steps of $35\,\mathrm{km\,s^{-1}}$ in (c), and in steps of $10\,\mathrm{km\,s^{-1}}$ in (d).

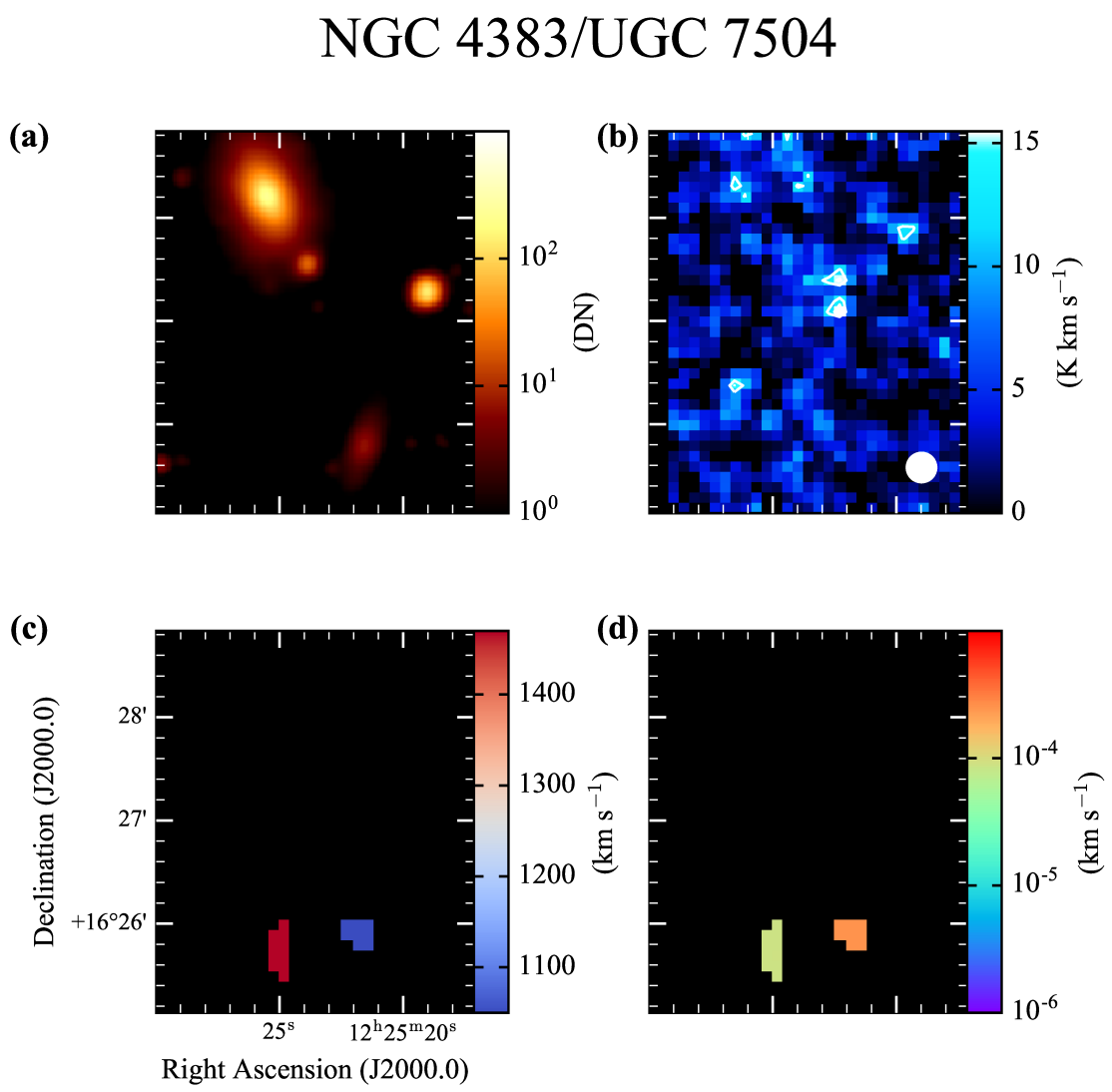

Supplementary fig. 128. Same as figure 12, but for NGC 4383 / UGC 7504 pair. The lower dim galaxy is UGC 7504 and the upper left one is NGC 4383. The contours are plotted at 65 % and 85 % of the maximum intensity of $17.27\,\mathrm{K\,km\,s^{-1}}$ in (b).

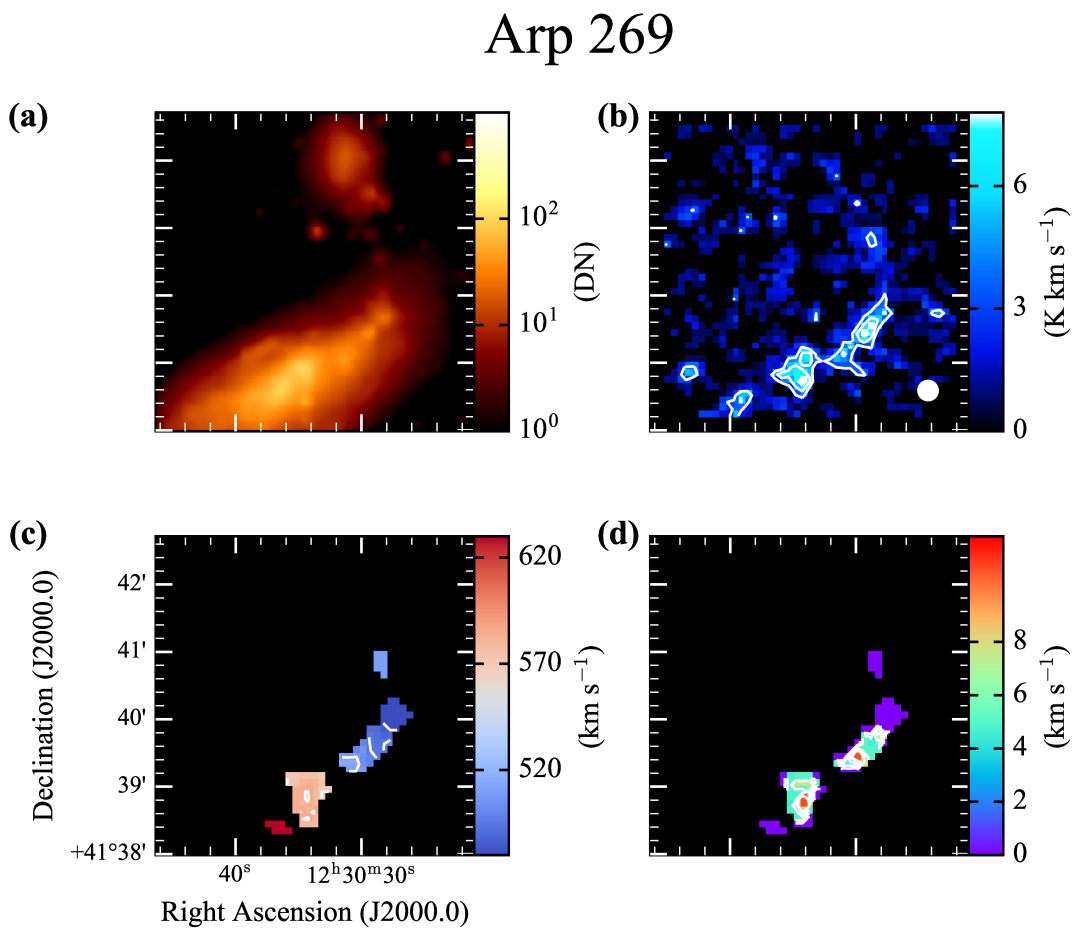

Supplementary fig. 129. Same as figure 12, but for Arp 269. The upper galaxy is NGC 4485 and the lower one is NGC 4490. The contours are plotted at 35 %, 60 %, and 85 % of the maximum intensity of $9.29\,\mathrm{K\,km\,s^{-1}}$ in (b), in steps of $15\,\mathrm{km\,s^{-1}}$ in (c), and in steps of $2\,\mathrm{km\,s^{-1}}$ in (d).

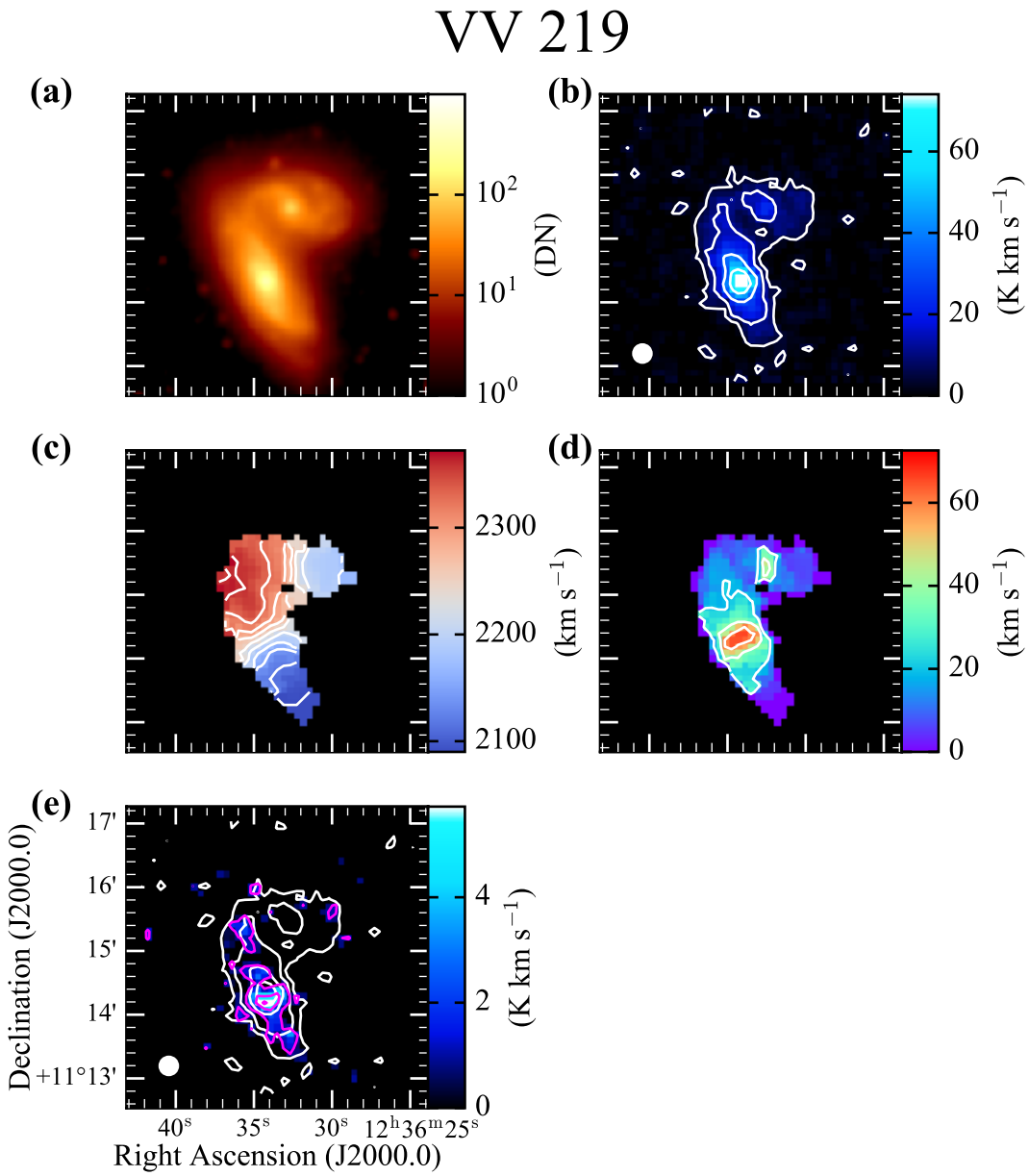

Supplementary fig. 130. Same as figure 12, but for VV 219. The upper galaxy is NGC 4567 and the lower one is NGC 4568. The contours are plotted at 5 %, 15 %, 40 %, and 70 % of the maximum intensity of $84.04\,\mathrm{K\,km\,s^{-1}}$ in (b) and (e) (*white*), in steps of $30\,\mathrm{km\,s^{-1}}$ in (c), in steps of $20\,\mathrm{km\,s^{-1}}$ in (d), and at 10 %, 50 %, and 90 % of the maximum intensity of $9.63\,\mathrm{K\,km\,s^{-1}}$ in (e) (*magenta*).

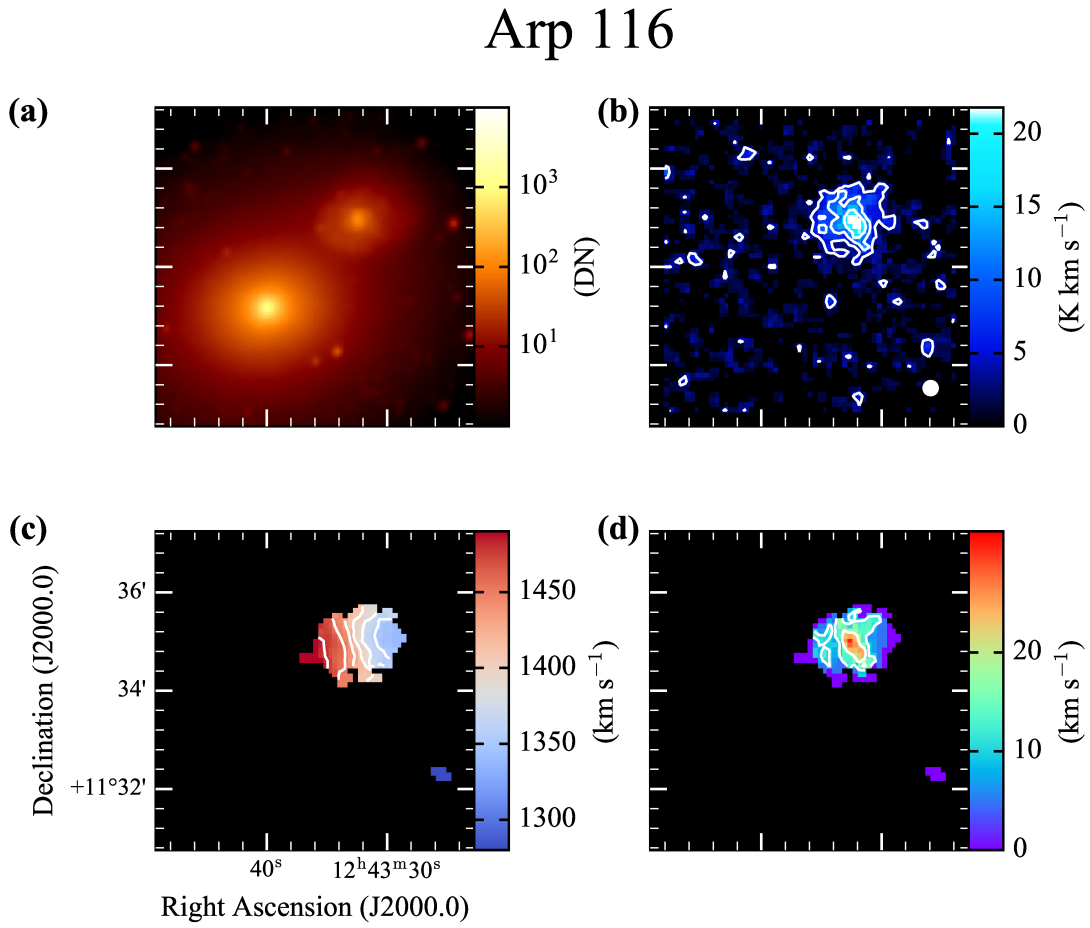

Supplementary fig. 131. Same as figure 12, but for Arp 116. The right galaxy is NGC 4647 and the left one is NGC 4649. The contours are plotted at 15 %, 35 %, and 60 % of the maximum intensity of $27.40\,\mathrm{K\,km\,s^{-1}}$ in (b), in steps of $25\,\mathrm{km\,s^{-1}}$ in (c), and in steps of $10\,\mathrm{km\,s^{-1}}$ in (d).

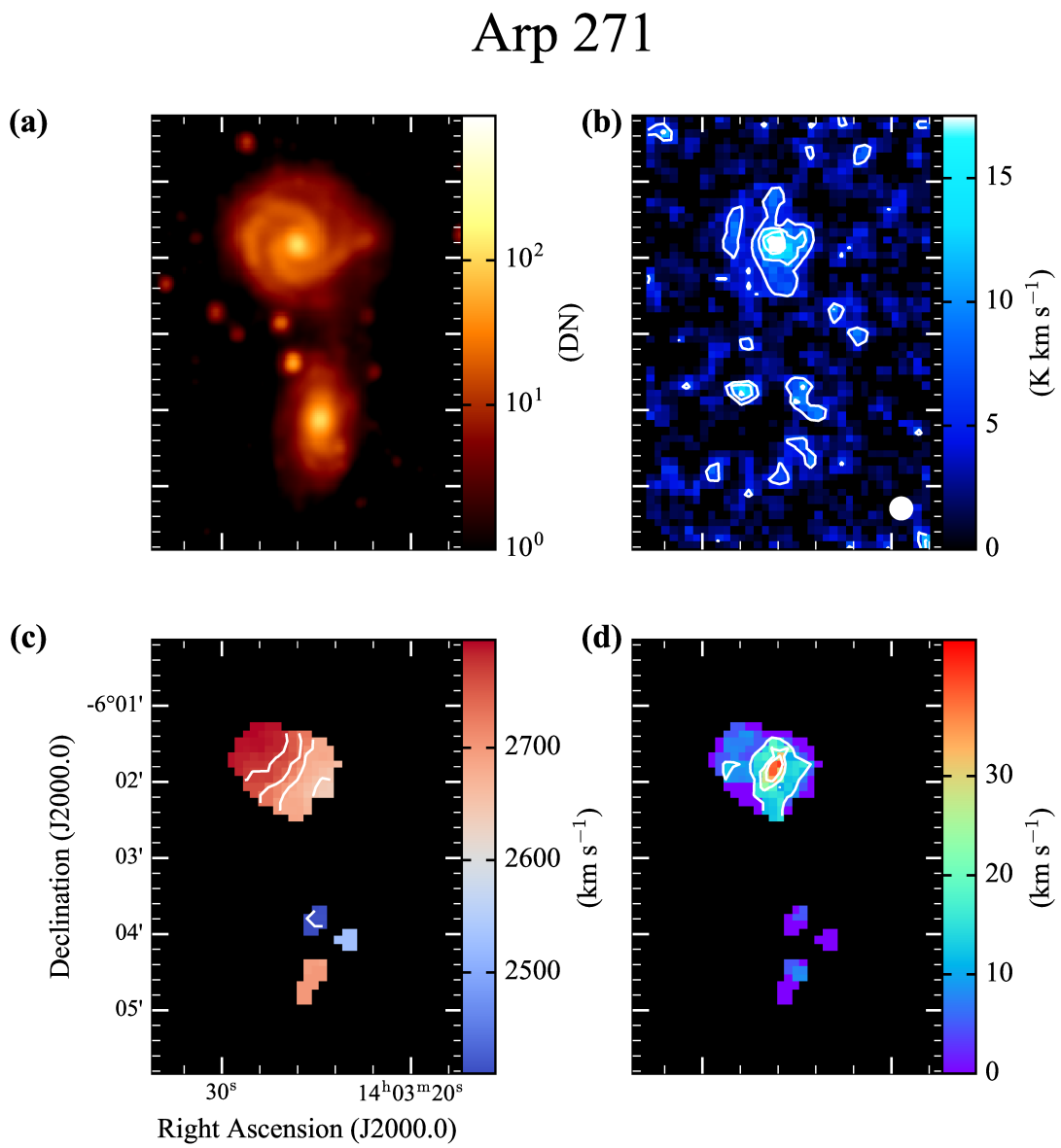

Supplementary fig. 132. Same as figure 12, but for Arp 271. The lower galaxy is NGC 5426 and the upper one is NGC 5427. The contours are plotted at 25 %, 45 %, 65 % and 85 % of the maximum intensity of $22.68\,\mathrm{K\,km\,s^{-1}}$ in (b), in steps of $40\,\mathrm{km\,s^{-1}}$ in (c), and in steps of $10\,\mathrm{km\,s^{-1}}$ in (d).

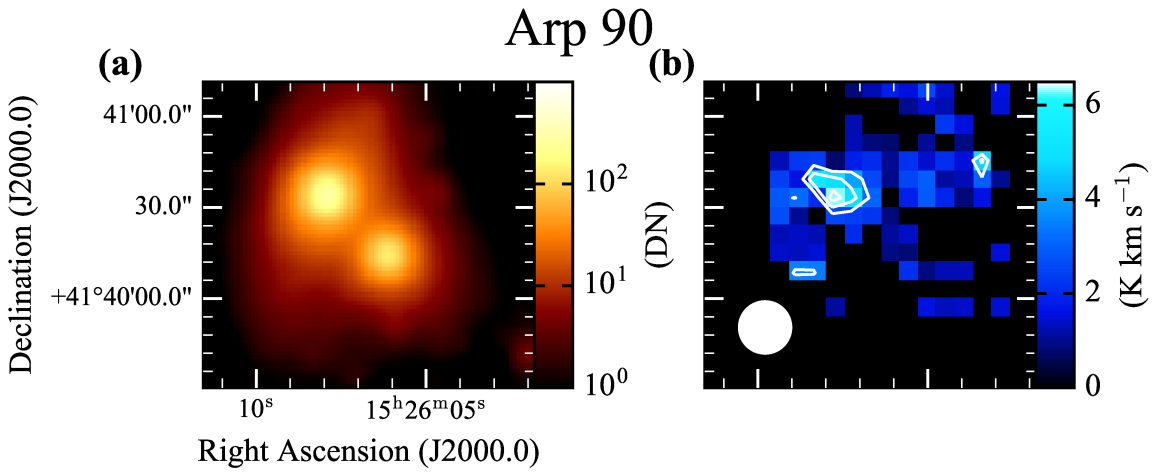

Supplementary fig. 133. Same as figure 12, but for Arp 90. The right galaxy is NGC 5929 and the left one is NGC 5930. The contours are plotted at 50 %, 70 % and 90 % of the maximum intensity of $6.34\,\mathrm{K\,km\,s^{-1}}$ in (b).

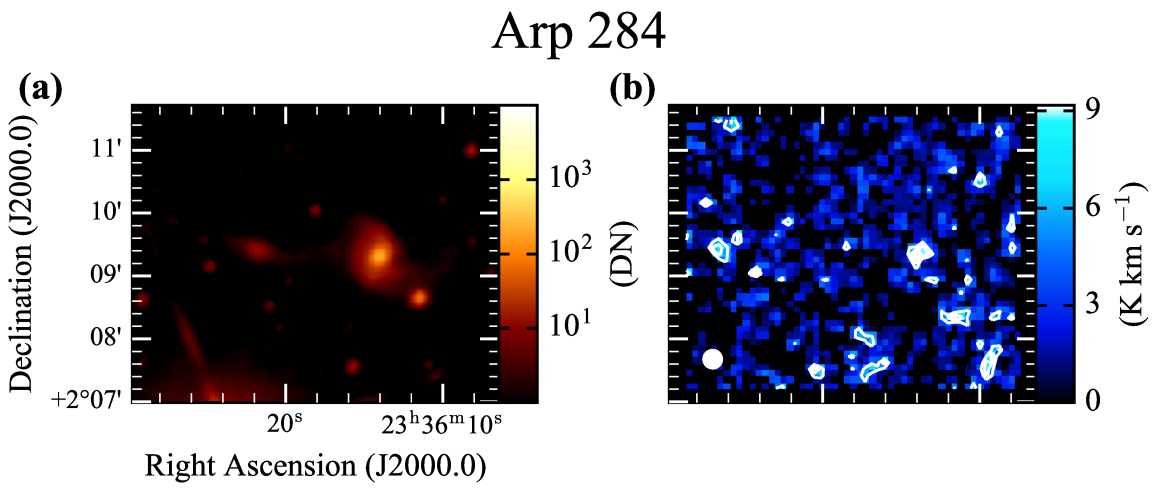

Supplementary fig. 134. Same as figure 12, but for Arp 284. The right galaxy is NGC 7714 and the left dim one is NGC 7715. The contours are plotted at 40 %, 60 % and 80 % of the maximum intensity of $11.67\,\mathrm{K\,km\,s^{-1}}$ in (b).